A Climate Modelling Primer

A Climate Modelling Primer, Third Edition. K. McGuffie and A. Henderson-Sellers.
 ISBN: 0-470-85750-1 (HB); 0-470-85751-X (PB)

A Climate Modelling Primer

THIRD EDITION

Kendal McGuffie

University of Technology, Sydney, Australia

and

Ann Henderson-Sellers

ANSTO Environment, Australia

John Wiley & Sons, Ltd

John Wiley & Sons Ltd, The Atrium, Southern Gate, Chichester,
West Sussex PO19 8SQ, England

Telephone (+44) 1243 779777

Email (for orders and customer service enquiries): cs-books@wiley.co.uk
Visit our Home Page on www.wileyeurope.com or www.wiley.com

Other Wiley Editorial Offices

John Wiley & Sons Inc., 111 River Street, Hoboken, NJ 07030, USA

Jossey-Bass, 989 Market Street, San Francisco, CA 94103-1741, USA

Wiley-VCH Verlag GmbH, Boschstr. 12, D-69469 Weinheim, Germany

John Wiley & Sons Australia Ltd, 33 Park Road, Milton, Queensland 4064, Australia

John Wiley & Sons (Asia) Pte Ltd, 2 Clementi Loop #02-01, Jin Xing Distripark, Singapore 129809

John Wiley & Sons Canada Ltd, 22 Worcester Road, Etobicoke, Ontario, Canada M9W 1L1

Wiley also publishes its books in a variety of electronic formats. Some content that appears in print may not be available in electronic books.

Library of Congress Cataloging-in-Publication Data

McGuffie, Kendal.
A climate modelling primer / Kendal McGuffie.– 3rd ed.
p. cm.
Includes bibliographical references and index.
ISBN 0-470-85750-1 (cloth) – ISBN 0-470-85751-X (pbk. : alk. paper)
1. Climatology–Mathematical models. I. Title.
QC981.M482 2005
551.6′01′1–dc22
2004016112

British Library Cataloguing in Publication Data
A catalogue record for this book is available from the British Library

ISBN 0-470-85750-1 (HB)
ISBN 0-470-85751-X (PB)

Typeset in 10/12pt Times by SNP Best-set Typesetter Ltd., Hong Kong
Printed and bound in Great Britain by TJ International Ltd, Padstow, Cornwall

This book is printed on acid-free paper responsibly manufactured from sustainable forestry in which at least two trees are planted for each one used for paper production.

TO

James E. Lovelock

who has shown us all the vitality of simple models

Contents

Preface

This littel child his littel book lernynge
As he sat in the schole at his prymer

Chaucer, *Prioress's Tale*, 1386

According to the *Oxford English Dictionary*, a primer serves as the first means of instruction or 'a prayer-book or devotional manual for the use of the laity'. Our motivation for the first edition of this book was the lack of a single work that provided a good introduction for those unfamiliar with the field. Although a number of excellent 'climate modelling' books have appeared since the 'Primer' was first published in 1987, the need for a book for those who are not meteorologists by training remains. This third edition of *A Climate Modelling Primer* follows closely the format of the previous editions but contains substantial updates where they were required. The figures have been redrawn and updated and much new material has been added relating to current issues in the climate modelling community. Few pages have escaped the red pen. The book assumes basic high-school mathematics but, in all cases, it can be read without following the mathematical development. You should be able to skip forward over more detailed treatments without prejudice to later sections. Throughout the book, we have tried to underline the importance of simple models of the climate system. With these, it is possible to gain an understanding of the relative importance of different forcing effects. These simple models are also invaluable in testing and extending the concepts upon which more complex models are based.

At its beginning, the science of climate modelling was dominated by atmospheric physicists and no one without a sound training in fluid dynamics, radiative transfer or numerical analysis could hope or expect to make a contribution. After forty or so years, the climate modelling community has embraced oceanographers, ecologists, geographers, remote sensers and glaciologists to provide expertise appropriate to the rapidly expanding domain of the models. The requirement for policy advice has meant that economists, planners, sociologists, demographers and even politicians need to know about climate models. This second group needs to understand the credibility of the different model types and how to apply (and when not to apply) the output from these models. It is for all these people that this book is intended.

We have included a list of reading at the end of each chapter. These reading lists are intended as a jumping-off point into the climate modelling literature providing more detailed discussion of the material in the particular chapter. In the years since the second edition was published, the role of the World Wide Web has grown enormously. It would be unwise to attempt an Internet directory of climate modelling, since the medium is so dynamic. Each chapter has a few Internet links that will lead you out into the world of climate modelling, we hope, better prepared by having read this book than you would otherwise have been. The extensive bibliography from the last edition (which includes references cited in tables and figures) has moved, with additions, to the Primer CD. For this third edition, we have introduced, including recommendations from friends, a collection of 'classics' of the climate modelling literature.

Since the Intergovernmental Panel on Climate Change (IPCC) process began in the late 1980s, a great deal of attention has been focused on the application of climate models to studying the sensitivity of climate to enhanced levels of greenhouse gases. We have elected to avoid a detailed discussion of these simulations. The interested reader should refer to the exhaustive treatment of the science of 'enhanced greenhouse' modelling given in the Intergovernmental Panel on Climate Change reports.

With the continuing development of computer technology, it is possible for anyone with a desktop computer to run, and learn from, a range of climate models and join the climate modelling community (e.g. http://www.climateprediction.net). We have included on the Primer CD a number of different climate models, most of which are quite accessible to the intended audience of this book, together with links to, and information about, models suitable for the most adventurous reader.

We are only too keenly aware of the simplifications that we have made in our explanations. Yet again, we beg the indulgence of climate modellers who see that sometimes our explanations and analogies are not completely rigorous. This book was not really intended for you.

Finally, climate modelling can be great fun. Tackled fully, it is a broad and demanding science, and to participate you will need to learn new techniques and approaches. We hope you enjoy reading about climate modelling. We recommend it as a way of learning about the biogeophysical environment and the human activities that affect it, as a pastime and as a career.

KENDAL McGUFFIE AND ANN HENDERSON-SELLERS
Boulder, Colorado, 2004

Acknowledgements

Very many friends and colleagues provided input to the development of the first two editions of this book and we would like to thank them again. For this edition, very special thanks are due to Graham Cogley, who maintained his sense of humour as he read the entire manuscript and provided an extensive set of valuable suggestions and feedback. Marc Peterson provided valuable input in updating Chapter 5. The process of developing this book has also benefited from comments on the final draft provided by (in alphabetical order) Gab Abramowitz, Roger Barry, Danny Harvey, Parviz Irannejad, David Karoly, Jade Soddell, Ros Taplin, Maria Tsukernik, Dick Wetherald, Liang Yang and Huqiang Zhang. Thank you also to those who took the effort to write and tell us about mistakes or omissions in earlier editions of the book. Your attention to detail and feedback is appreciated.

The Twentieth-Century Classics in Appendix A were compiled with the help of suggestions from (in alphabetical order) Meinrat Andreae, Roger Barry, André Berger, Tom Chase, Ulrich Cubasch, Bob Dickinson, Larry Gates, Jim Hansen, Mike McCracken, Jerry Meehl, John Mitchell, Dave Randall, Steve Schneider, Ian Simmonds, Susan Solomon, Warren Washington, Dick Wetherald, Tom Wigley and John Zillman. We are particularly grateful to Nick Connolly for testing and evaluating the Primer CD.

As always, we'd be pleased to hear of any further corrections (via email to Kendal.McGuffie@uts.edu.au). We completed much of the work for this edition while AHS was a visiting fellow at the Cooperative Institute for Research in Environmental Sciences (CIRES) at the University of Colorado, and KMcG was a visitor in the National Snow and Ice Data Center (NSIDC), both as the guests of Professor Roger Barry. Thanks to the staff at NSIDC and CIRES for their hospitality.

Finally, we, again, offer a huge thank you to Brian for continuing positive support, massive efforts in typing and reading, for help and advice and for saving this edition from the 'pot of not water'.

CHAPTER 1

Climate

Back in nineteen twenty seven
I had a little farm and I called it heaven
Prices up and the rain come down
I hauled my crops all into town
Got the money . . . bought clothes and groceries . . .
Fed the kids . . . and raised a big family

But the rain quit and the wind got high
Black old dust storm filled the sky
I traded my farm for a Ford machine
Poured it full of this gas-i-line
And started . . . rocking and a-rolling
Deserts and mountains . . . to California

(*Talking Dust Bowl Blues*, Woody Guthrie)

1.1 THE COMPONENTS OF CLIMATE

The term 'climate' has a very wide variety of meanings. To a geologist or geomorphologist, the 'climate' is an external agent which forces many phenomena of interest. For an archaeologist, the 'climate' of an earlier time might have been a crucial influence upon the people being studied, or might have been of little socio-economic significance, yet still so strong an environmental feature that it has left a 'signature' that can be interpreted. An agriculturalist probably sees the 'climate' as the background 'norm' upon which year-to-year and day-to-day weather is imposed, while the average person may speak of moving to a location with a 'better climate'. To many of us, 'climate' often first suggests temperature, although rainfall and humidity may also come to mind. When we think of climatic change it used to be in the time frame of glacial periods. Recently, however, most of us have become aware of the shorter-term impact upon the climate of increasing atmospheric carbon dioxide and other trace greenhouse gases.

The climate is both a forcing agent and a feature liable to be disturbed. It can fluctuate on relatively short time-scales, producing for example the droughts that dev-

A Climate Modelling Primer, Third Edition. K. McGuffie and A. Henderson-Sellers.
 ISBN: 0-470-85750-1 (HB); 0-470-85751-X (PB)

astated West Africa in the 1970s and 1980s and, over much longer times, giving rise to glacial epochs. The climate is perceived in terms of the features of the entire climate system which most readily or most usefully characterize the phenomenon of interest. All of these characteristics of the climate are depicted in Figure 1.1. The three axes themselves are fundamental but the intervals are arbitrary and many more could be included.

A single satisfactory definition of climate is probably unobtainable because the climate system encompasses so many variables and so many time- and space-scales. One definition might be 'all of the statistics describing the atmosphere and ocean determined over an agreed time interval (seasons, decades or longer), computed for the globe or possibly for a selected region'. This definition is broad, but it does serve to emphasize that higher-order statistics, such as variance (variability), can often be more useful in characterizing a climatic state than just the mean (average). The definition also permits further description of a climatic change as the difference between two climatic states, and a climatic anomaly as the difference between a climatic state

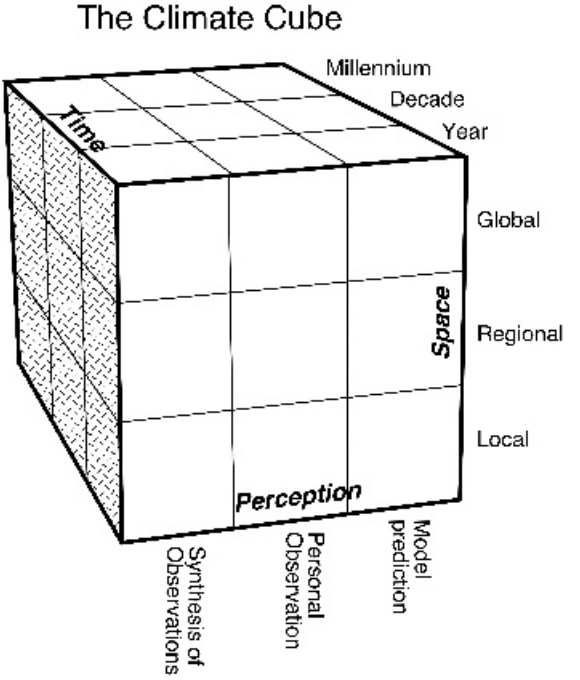

Figure 1.1 The climate cube. Climate can be viewed as existing in at least three domains: time, space and human perception. The divisions of these domains depicted here are arbitrary – a great many more could be suggested. Historically, individual disciplines have been concerned with single 'cells'. The extent of the climate system and the importance of interactions between domains are now well recognized

and the mean state. The variations of the system arise from interactions between different parts of the climate system and from external forcings. Although the greatest variations are due to changes in the phase of water (i.e. frozen, liquid or vapour), the constituents of the atmosphere and ocean and the characteristics of the continental surface can also change, giving rise to a need for consideration of atmospheric chemistry, ocean biogeochemistry and land-surface exchanges.

Introduction and outline of the book

In this book, we have set out to introduce and describe the way in which the climate is modelled. The climate models we will discuss are those developed using physically-based formulations of the processes that make up the climate system. We are concerned with explaining the approaches and methods employed by climate modellers and shall not focus directly on meteorology, socio-economic impacts of climatic changes or palaeoclimatic reconstruction, although all of these disciplines and many others will be drawn upon in our descriptions.

In this chapter, we identify the components of the climate system and the nature of their interactions, as well as describing briefly some of the motivations of climate modellers. Chapter 2 contains a history of climate modelling and provides an introduction to all the types of models to be discussed in subsequent chapters. The other chapters are concerned with different model types, their development and applications. Throughout, we have taken climate models to be predictive descriptions of regional- to global-scale phenomena; hence empirically based 'models' such as crop prediction equations and water resource management codes have not been included. The reason for this limitation is not that such models are uninteresting, but rather that they have grown from well-identified fields and thus background literature can be readily obtained elsewhere. Climate modelling in the sense in which we use the term, on the other hand, has developed from a wide variety of sources in a somewhat haphazard manner and consequently there is little accessible background to which the uninitiated can refer.

In one sense, the book develops the background material required for understanding of the most complex type of climate model, the fully coupled climate system model, by illustrating principles in other, simpler, model types. Thus, it is necessary to introduce the concept of energy balance, especially planetary radiation balance, before one-dimensional energy balance models (Chapter 3) can be understood. In Chapter 4, models that intentionally consider only a few of the important processes of the climate system are examined. These simpler models are used to gain a deeper understanding of the nature of feedbacks and forcings within the climate system as well as providing a foundation for impact assessment. These models, which have enjoyed a significant renaissance in the last ten years, are now widely known as Earth System Models of Intermediate Complexity (EMICs).

By Chapter 5, the reader should be well prepared to understand the way in which radiative forcing, ocean and atmosphere dynamics, biological processes and

chemical changes are included in coupled three-dimensional models of the climate system. In Chapter 6, we explore some of the technical issues faced by climate modellers and look at how models are tested and their results evaluated. We also address how these results can be integrated with impact assessments in the development of social and economic policies.

Twentieth-century Classics (in Appendix A) is not an exhaustive list of references (which can be found on the accompanying Primer CD), but rather an introduction to the seminal works of the climate modelling literature. We have chosen these classics, with the help of a few friends. Appendix B contains a glossary of terms that may be new to readers unfamiliar with climatology/meteorology. As we have used this glossary for definitions rather than interrupt the main thread of the text, reference to it is recommended. The Primer CD (described in Appendix C) contains source code for a range of model types contributed by their developers. These will allow readers to make their own climate simulations ranging from global glaciations to increased CO_2 experiments. A set of simulations from a global climate model also permits analysis of the results of a land-use change experiment. Also on the CD, movies illustrate some of the techniques used to analyse and display the results from a range of climate models.

Throughout the book, an effort will be made to underline the importance of simpler models in understanding the complex interactions between various components of the climate system. Complex models are only one, particularly sophisticated, method of studying climate. They are not necessarily the best tools; simple models are often used in conjunction with, or sometimes even to the exclusion of, more complex and apparently more complete models. The literature contains many fascinating examples of very simple models being used to demonstrate failures and illustrate processes in much more complex systems.

Last, but by no means least, any introduction to climate modelling must stress the crucial role played by computers. Without the recent growth in computational power and the reduction in computing costs, most of the developments in climate modelling that have taken place over the last four decades could not have happened. We have intentionally emphasized computing tools over mathematical skills in the description of the simplest type of climate model, the energy balance model (EBM), in Chapter 3. In that chapter, the steps required to construct a simple EBM are described, and the Primer CD includes example EBMs and source code.

It is estimated that a fully coupled ocean–atmosphere general circulation model (OAGCM) takes about 25–30 person-years to code, and the code requires continual updating as new ideas are implemented and as advances in computer science are accommodated. Most modellers who currently perform experiments with the most complex of models modify only particular components of the models. The size of and detail in these models means that only through a sharing of effort can progress be made. As the models have become increasingly complex, increased application of the principles of software engineering has become an essential part of the process and has made it easier to upgrade and exchange parts of the models. Host computers and model physics develop in parallel.

The climate system

The climate system was defined, in a document produced by the Global Atmospheric Research Programme (GARP) of the World Meteorological Organization in 1975, as being composed of the atmosphere, hydrosphere, cryosphere, land surface and biosphere. In 1992, the United Nations' Framework Convention on Climate Change (FCCC) defined the climate system as 'the totality of the atmosphere, hydrosphere, biosphere and geosphere and their interactions'. These definitions are similar, but the emphasis on interactions, both in the definition and in the literature, has grown in the thirty years since 1975. Figure 1.2 shows a schematic representation of the climate system components which climate modellers must consider. It complements Figure 1.1 by emphasizing components and processes rather than the space- and

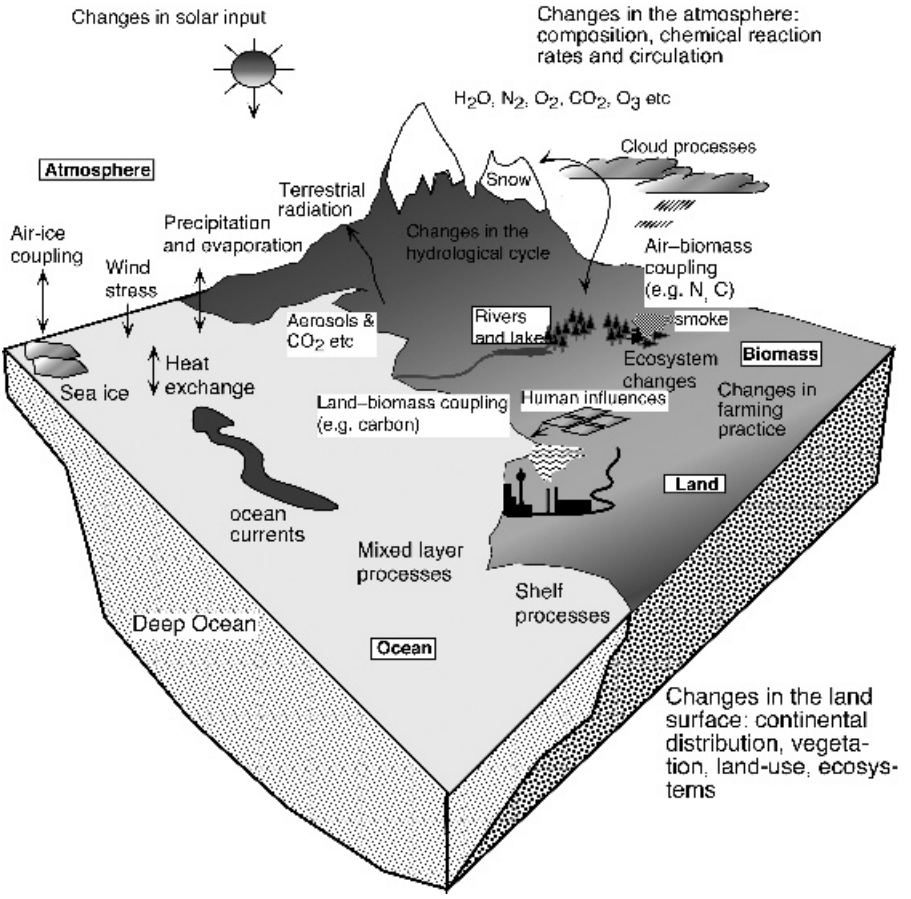

Figure 1.2 A schematic illustration of the components and interactions in the climate system (modified from Houghton *et al*., 1996)

time-scales. The order of the components of the climate enumerated in 1975 is also a rough indicator of the historical order in which these elements were considered and, to some extent, the (increasing) magnitude of their time-scales.

The first modelled component was the atmosphere, which, because of its low density and ease of movement, is the most 'nervous' of the climatic subsystems. These early models developed directly from weather prediction models. Precipitation was included early but many aspects of clouds (such as cloud liquid water and the effects of different cloud droplet sizes) are still difficult to incorporate successfully, and linking the major part of the hydrosphere, the oceans, into climate models had to wait for adequate computer resources. This was partly because the critical space- and time-scales of the ocean and atmosphere subsystems differ, but also because the coupling between the subsystems is strongly latitude-dependent. In the tropics, the systems are closely coupled, especially through temperature (Figure 1.3). In mid-latitudes the coupling is weak, predominantly via momentum transfer, whereas in high latitudes, there is a tighter coupling, primarily through salinity, which is closely involved in the formation of sea ice and oceanic deep water. Biochemical processes controlling the exchange of carbon dioxide between atmosphere and ocean also vary as a function of geographical location.

The cryosphere (frozen water) was first incorporated into climate models in the description of simple EBMs, in which the high albedo of the ice and snow dominated the radiative exchanges. The insulating effect of the cryosphere is at least as

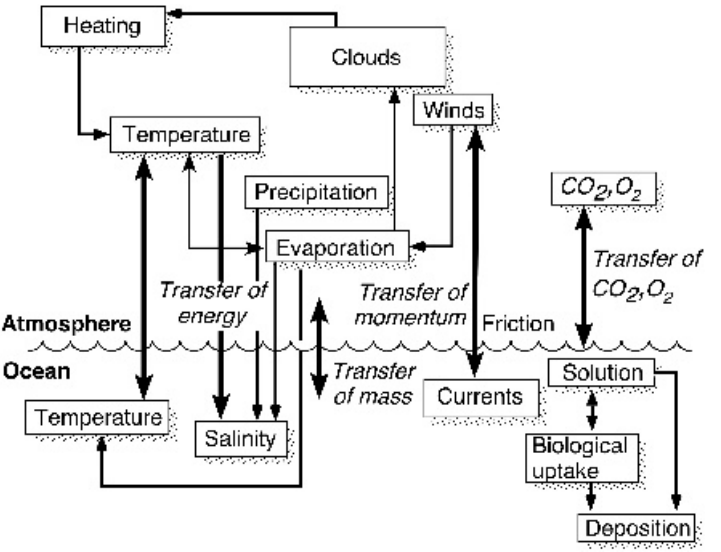

Figure 1.3 A representation of the major coupling mechanisms between the atmosphere and ocean subsystems. The relative importance of these coupling mechanisms varies with latitude. The feedback between atmospheric temperature and oceanic salinity is interesting because it is strong only in the sense of the atmosphere forcing the ocean

important as its albedo effect: sea ice decouples the ocean from the overlying atmosphere, and snow has a similar, but smaller, effect on land, causing considerable changes in separated subsystems.

Scientists concerned with land-surface processes had described the climate as both an agent and a feature of change for over a century before climate modellers began serious consideration of their theories. The importance of the biosphere has been underlined by the climate impacts resulting from atmospheric carbon dioxide levels dependent upon oceanic and terrestrial biota. Modern studies incorporate the state of the ecology on the continental surface and the growth of marine biota.

The stratospheric 'ozone hole', first identified over Antarctica in 1985, was the catalyst for incorporating atmospheric chemistry into climate models. Inclusion of these rapidly changing subsystems is still in its early stages, but it is already clear that Earth system models need to incorporate atmospheric and marine chemistry and transient changes in the world's biota. The human component of the climate system, manifested particularly in trace gas and aerosol emissions and land use change, is perhaps its most difficult and challenging aspect. Human activities have only recently begun to be parameterized in climate and 'integrated assessment' models.

In this rather clumsy fashion and from mixed parentage, the discipline of climate modelling has evolved. Climate modellers have discovered that the system that they had summarized so neatly in 1975 is exceedingly complex, containing links and feedbacks which are highly non-linear and hence difficult to identify and reproduce.

1.2 CLIMATE CHANGE ASSESSMENT

Today, the atmosphere of planet Earth is undergoing changes unprecedented in human history and, although changes as large as those we are witnessing now have occurred in the geological past, relatively few have happened with the speed that characterizes today's climate changes. Concentrations of greenhouse gases are increasing, stratospheric ozone has been depleted and the changing chemical composition of the atmosphere may be reducing its ability to cleanse itself through oxidation. These global changes threaten the balance of climatic conditions under which life evolved and is sustained. Temperatures are rising, ultraviolet radiation is increasing at the surface, and air pollutant levels are increasing. Many of these changes can be traced to industrialization, deforestation and other activities of a human population that is itself increasing at a very rapid rate.

Over the last fifteen or so years, with increased awareness of the potential impacts of changes in atmospheric concentrations of trace gases and aerosols, there has been an evolving demand from policymakers for the results of climate models. In 1988, the United Nations Environment Programme (UNEP) and the World Meteorological Organization (WMO) established the Intergovernmental Panel on Climate Change (IPCC). The IPCC was directed to produce assessments of available scientific information on climate change, written in such a way as to address the needs of policymakers and non-specialists. The First Scientific Assessment was published

in 1990 in three volumes encompassing science, impacts and response. There was a scientific update in 1992 and two further volumes were produced as input to the First Conference of the Parties to the FCCC in March 1995. The Second Scientific Assessment followed in 1996; the Third Assessment was published in 2001 and the Fourth Assessment Report is due to be concluded and published in 2007. Around 700 researchers contributed to the Third Assessment and another 700 reviewed it.

An important result of the IPCC's assessment of climate forecasts has been to focus interest on climatic reconstruction. The longest available record of proxy-based Northern Hemisphere temperatures spans the period from 200 to 2000 AD (Figure 1.4). The proxies employed in making these detailed reconstructions include tree rings, corals, ice cores and written records of events such as floods, droughts, cold spells and even the blossoming of trees. Reconstructions have been made for longer times for the Northern Hemisphere because more data exist. These long records, even recognizing their measures of uncertainty, underline the fact that twenty-first century temperatures are warmer than any experienced over at least the last 1800 years.

The IPCC process aims to determine the current level of confidence in our understanding of the forcings and mechanisms of climate change, to find out how trust-

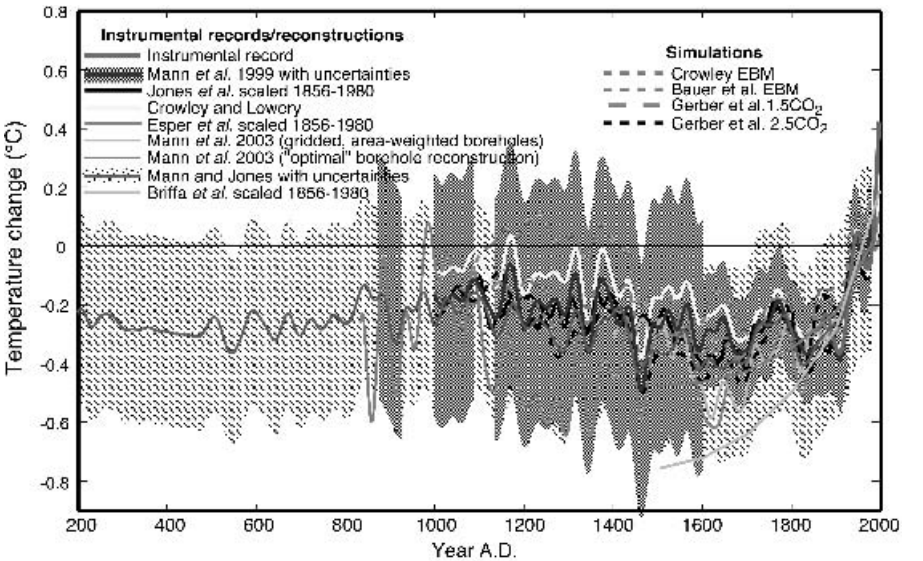

Figure 1.4 Comparison of Northern Hemisphere temperature reconstructions with model simulations of Northern Hemisphere mean temperature changes over the past millennium based on radiative forcing histories. Also shown are two independent reconstructions of warm season extra-tropical continental Northern Hemisphere temperatures and an extension back through the past 2000 years based on eight long reconstructions. All reconstructions have been scaled to the period 1856–1980 and are shown with respect to the 1961–1990 based period. This is a slightly modified version of the figure that appeared in *EOS* Vol. 84, courtesy of Michael Mann. Reproduced by permission of the American Geophysical Union from Mann *et al.* (2003), *EOS* **84**, 256–257

worthy the assessments are, and to ask whether we can yet unequivocally identify human-induced climate change. Through an exhaustive review process, the IPCC aims to provide assessments which discuss climate change on a global scale and represent international consensus of current understanding. Throughout the process, the goal is to include only information which has been subjected to rigorous review, although this is balanced by a desire to include the latest information in order that the best possible assessment can be made. These two competing desires mean that the development of the IPCC documents is an extremely time-consuming process, but ensure that the final result is a powerfully strong statement of the state of current knowledge of the climate system. The IPCC assessment covers three areas, which are handled by three working groups. For the Third Assessment Report, published in 2001, Working Group I dealt with the scientific basis of climate modelling, climate observations and climate predictions, Working Group II dealt with issues relating to the impacts of, adaptations to, and vulnerability to climate change while Working Group III reported on mitigation, i.e. actions to reduce climate change.

1.2.1 The scientific perspective

It is generally accepted that physically-based computer modelling offers the most effective means of answering questions requiring predictions of the future climate and of potential impacts of climatic changes. Although there have been great advances made in such modelling over the past 40–50 years, even the most sophisticated models are still far removed in complexity from the full climate system. Further advances are possible, but they need to be associated with increased understanding of the nature of interactions within the real climate system and translated to those within models. Perturbations caused by everything from industrial aerosols to volcanoes, from solar luminosity to climatically induced variation in surface character must be considered. Modelling in such a widely ranging subject is a formidable task and it requires co-operation between many disciplines if reliable conclusions are to be drawn.

Available computing power has increased greatly over the past 40–50 years (Figure 1.5a). Meteorological and climate research establishments have some of the fastest and most powerful computers available. This continuing increase has meant that climate models have expanded in terms of complexity, resolution and in potential simulation time. As computing capabilities have evolved, the components of the Earth system that can be included and coupled have increased, and will continue to increase in number (Figure 1.5b). Multi-decadal simulations, with full diurnal and seasonal cycles and fully coupled ocean and sea ice, are now expected in climate experiments, and transient changes in, for example, the atmospheric greenhouse gases and aerosol loading now replace the previous equilibrium simulations. As our knowledge increases, more aspects of the climate system will be incorporated into climate models, the resolution and length of integrations will further increase and additional components will be incorporated.

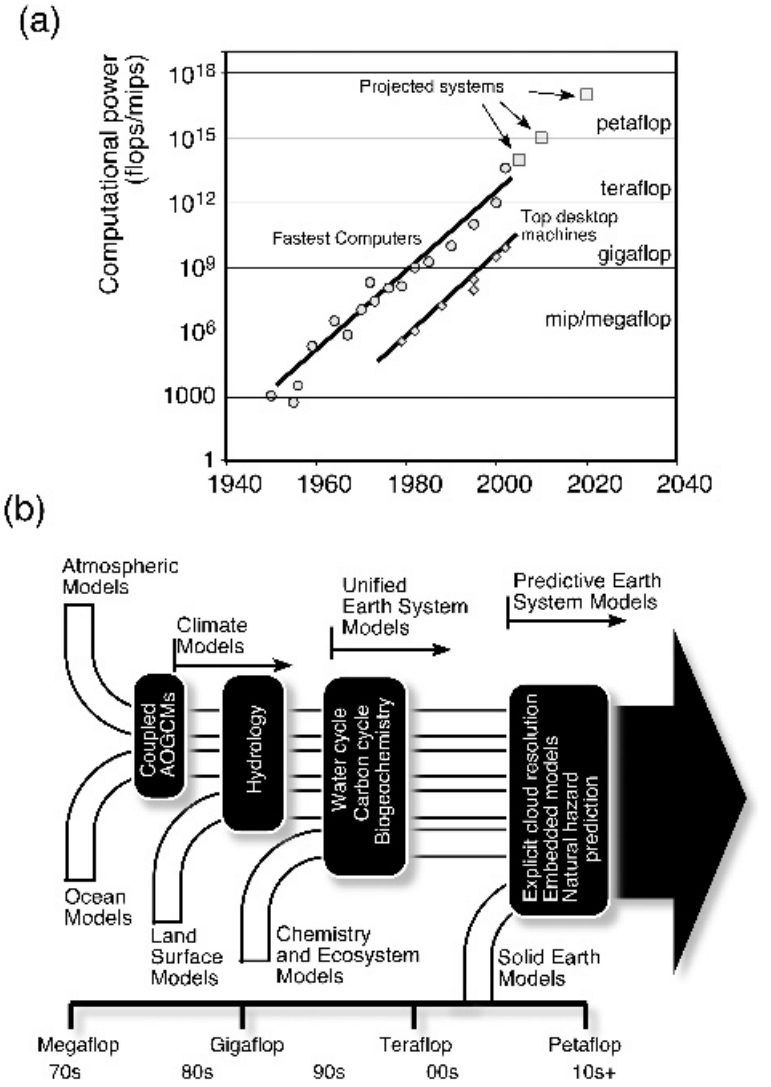

Figure 1.5 (a) Peak performance of the most powerful computers between 1953 and 2003. The power is given in millions of instructions per second (MIPS) up to 1975 and in millions of floating point operations per second (MFLOPS) since then. Note that the vertical scale is logarithmic and supercomputer performance shows no signs of levelling off. System performance has been hypothesized to continue on this trend to 2020. (b) Schematic of the interdependency of computer power and model capability. As well as increased resolution, modellers have progressively coupled more models to create today's unified Earth system models. Foreseeable advances in computer technology will allow simulations with even more sophisticated Earth system models to be constructed

The general trend that, as computer power increases, so do the complexity, resolution and length of climate model simulations is moderated by different contributing specialist groups. For example, biospheric modellers have tended to favour increasing the number of components in their submodels, while the ocean modellers have driven the resolution of their submodels higher. Spatial and temporal resolution compatibility is critical to effective and integrative coupling. Indeed, the drive towards fully coupled ocean–atmosphere biogeochemical models has seen computational demand reach new heights. New model and software engineering designs, offering better numerical representation of the climate system, promise to challenge the fastest computers for years to come. However, it would be a mistake to think that the only measure of success of a climate model is the resolution or the speed of computation achieved. The purpose of the climate models is to gain insight into the climate system and its interactions. While improved resolution and faster computers are very helpful, there are many other modelling avenues to be explored which can aid our understanding of climate.

Figure 1.6 shows the performance of a group of coupled ocean–atmosphere models that participated in CMIP, the Coupled Model Intercomparison Project. Superimposed is the envelope of atmosphere-only performance for models between 1974 and 1984. There has been considerable improvement in model simulation of observed characteristics of the climate system over the last 20 years. Certainly, some of this improvement has come with faster computers, as they have helped to increase the possible size and complexity of models, but simple models have also played a role. Simple models may be sufficient to answer particular, well-specified problems and provide insight that might otherwise be hidden by the complexity of a larger model.

Whether its predictions are correct, for the right reasons, is the ultimate test of any model. Weather forecast models can be tested over a period of a few hours to a few days, but models of climate are required to predict decades to centuries in advance or to simulate periods of the Earth's history for which validation data are scant. Importantly, climate model 'predictions' offer only a general case of the response since the model climate loses its association with the initial conditions within a few weeks. Hence, testing of single simulations is virtually meaningless and ensembles of results are needed to characterize the climate. Despite the limitations placed by chaos theory on our ability to predict the *exact* state of the atmosphere beyond about 10–15 days into the future, there is good reason to believe that our ability to predict the nature of the ensemble state (the climate) is not impaired.

A useful analogy might be with a gambler, who sees the chaotic processes of the roulette wheel as unpredictable. The casino owner, however, knows the boundary conditions set by the structure and layout of the wheel and the rules of the game, which mean that the casino exists in a winning 'climate'. A more meteorological illustration would be that we are generally comfortable with the notion of making predictions based on known constraints or a statistical envelope when deciding where to take our annual holiday. We know that certain times of year and certain locations will be acceptable to us (either delightfully sunny or enjoyably snowy),

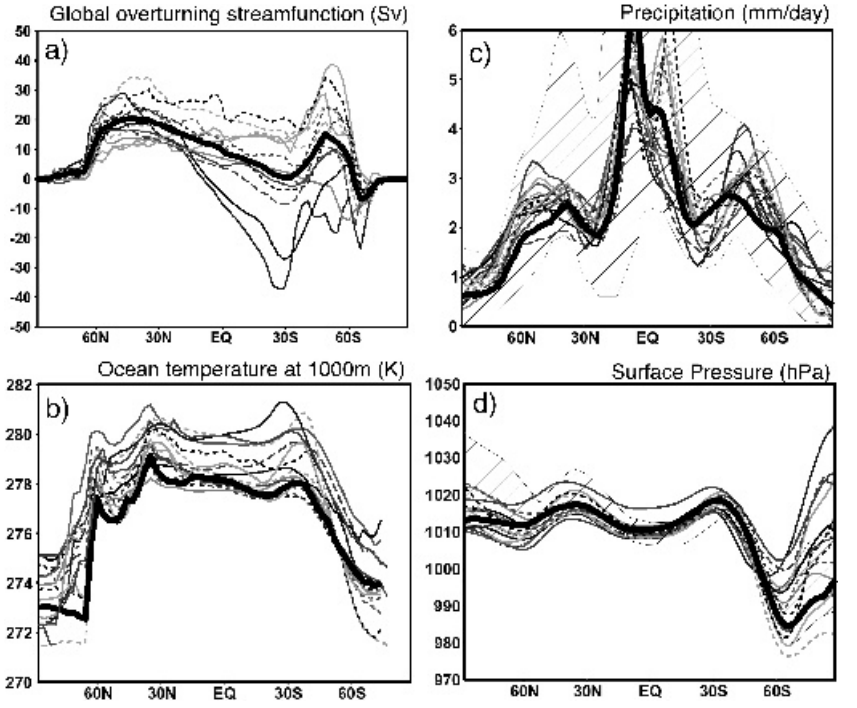

Figure 1.6 Model performance from the Coupled Model Intercomparison Project (CMIP) for selected ocean and atmosphere variables. Solid line indicates observations in the case of (b), (c) and (d) and model mean for (a). An envelope of performance for earlier atmospheric models (hatched) is shown in (c) and (d) from Gates (1985), illustrating the change in model performance over the intervening years. Reprinted from *Global and Planetary Change*, **37**, Covey *et al.*, pp. 103–133. Copyright 2003, with permission from Elsevier

but we cannot guarantee the exact nature of each day of the holiday. The weather depends on the exact state of the atmosphere within a week or so of the beginning of the holiday, rather than the overarching constraints of, for example, seasonal conditions and ocean surface temperature, which are largely similar from one year to the next.

The climate models discussed in this book cover a wide range of space- and time-scales. These different types of climate models attract interest from many different disciplines. Long-period modelling may attract glaciologists, geologists or geophysicists. For example, even simple models can predict the effect on mean temperatures of volcanic eruptions such as Mount Pinatubo quite successfully on seasonal or longer time-scales, so we can have confidence that climate predictions are not obfuscated by the same chaotic processes that trouble weather forecasts. Atmospheric chemists, dealing with complex reactions that typically have very short time-scales, are successfully incorporating these processes into three-dimensional climate models. Implications of solar-system-scale phenomena attract planetary

physicists and astronomers, while social and economic scientists are interested in the human component of the climate system. In this book, we will attempt to show how these contributions fit together and jointly enhance the science of climate modelling.

1.2.2 The human perspective

Any changes in climate, whatever the cause, may impact human activities. Crop-yield models have been used to quantify how food production depends on the weather. It might therefore be postulated, for example, that a change in climate could lead to consistently low or high yields in a particular area, which, in turn, may lead to a human response in terms of a change in agricultural practice. Such simple postulates can be misleading, since they conceal several problems that are inherent in relating climate change to human impact. These concern the nature of climatic changes themselves, the strength of the relationship between climate changes and human response and the availability of (past) climatic and sociological data for evaluation.

It is possible to think of climatic changes as being represented by changes in the long-term mean values of a particular climatic variable. Superimposed on this changing mean value will be decadal fluctuations and year-to-year variations. Such short-period variations may, of course, be influenced by the change in the mean. On the human time-scale, changes in the mean value are likely to be so slow as to be almost imperceptible. For example, the changes over the last few decades can only be detected by careful analysis of instrument records. Much more noticeable will be variability, expressed, for example, as a 'run of bad winters'. Any human response will depend on such a perception, whether consciously or subconsciously. A 'large' climate change may not lead to any response, whereas a much smaller change in a particular feature, expressed as a perceived change in variability, may have a profound impact on human activity. Detection, for example, of climate change in response to increasing atmospheric trace greenhouse gases is very difficult in the early stages if only one response is monitored. For this reason, 'fingerprint' methods have been proposed which monitor a set of small changes in a number of variables and require prespecified thresholds in all of them to be passed before a signal can be established.

Any attempt to establish the impact of past climatic changes must use historical information. Pre-instrumental historical records are qualitative and selective and emphasize information about unusual conditions which were perceived as having an impact. Consequently, they can tell us less about normal conditions than about abnormal ones. A great deal, therefore, needs to be inferred about the historical climate and its variability before any suggestions regarding its impacts can be made. Even if a change occurs which potentially has a significant impact on human activity, a societal response will not necessarily follow. Any response to a climate change is governed by a host of non-climatic factors which need to be considered. Clear, and particularly direct, links between climate change and human activity are often

difficult to establish. This problem of 'attribution' to human-produced greenhouse gas increases following detection of global warming is currently a similarly vexed issue.

It has also been suggested that as cold, damp winter conditions prevailed in some northern mid-latitudes during the Little Ice Age (*c.* 1450–1850), grain storage became impossible and famine susceptibility increased. However, population pressure and plague could have been equally important in creating the problems of this period, or could have exacerbated climatic stress. Indeed, trying to estimate widespread effects of the decrease of about 1K in mid-latitude temperatures during the Little Ice Age (see Figure 1.4) is not especially valuable since additional factors, such as the incidence of late spring frosts or destructive winds near harvest time, about which we have little or no information, may have been more significant.

Such an effect is typically seen on a local scale. One well documented example occurred in the Lammermuir Hills in Scotland. Careful study of the records of farming and settlement in this area gives credence to the suggestion that, in marginal regions, human response to climatic deterioration is identifiable. The combined isopleths of 1050 degree days plus 60 mm potential water surplus (at the end of the summer), which represents the approximate 'cultivation limit', expanded and moved downslope during the cooling period and were restored towards the end of the Little Ice Age. In the centre of an agricultural region, farming practices will be well adjusted to that particular climate and year-to-year variations will pose little threat. As the margins are approached, however, variability will become more significant. Here, overall production will be low, so that little surplus can be stored against the poor years that climate variability will inevitably bring. If a climate change occurs which alters the frequency of the poor years, some human response is very likely to follow.

The definition of marginality, of course, depends upon the climatic regime and agricultural practices considered. Three areas are shown in Figure 1.7 using different climatic indices for marginality. Northern Europe is divided into agriculturally marginal and submarginal areas. The limits are given by a combined index which is a function of the number of months with a mean monthly temperature above 10°C and the excess of precipitation over evapotranspiration, if any, in the summer months. The region of marginal cultivation identified for the USA is based upon total rainfall in the period April–September rather than upon the combination of temperature and rainfall used for northern Europe. For Australia three zones of marginality, for different climate regimes and agricultural enterprises, are shown in Figure 1.7c. Here, the limits are based on temperature and precipitation values and their ranges. The changes of these limits with time indicate the eastward encroachment of aridity and the establishment of new marginal areas.

In human terms, marginality of climate can include less obvious measures than temperature and precipitation. Today, many of the world's glaciers appear to be in retreat (Figure 1.8). Although the general picture of widespread retreat is defied in a few places in Norway and New Zealand, where some glaciers are growing, the impacts of the widespread deglaciation are likely to be profound. Among the more unexpected of these is the anticipated massive reduction in tourism revenue in

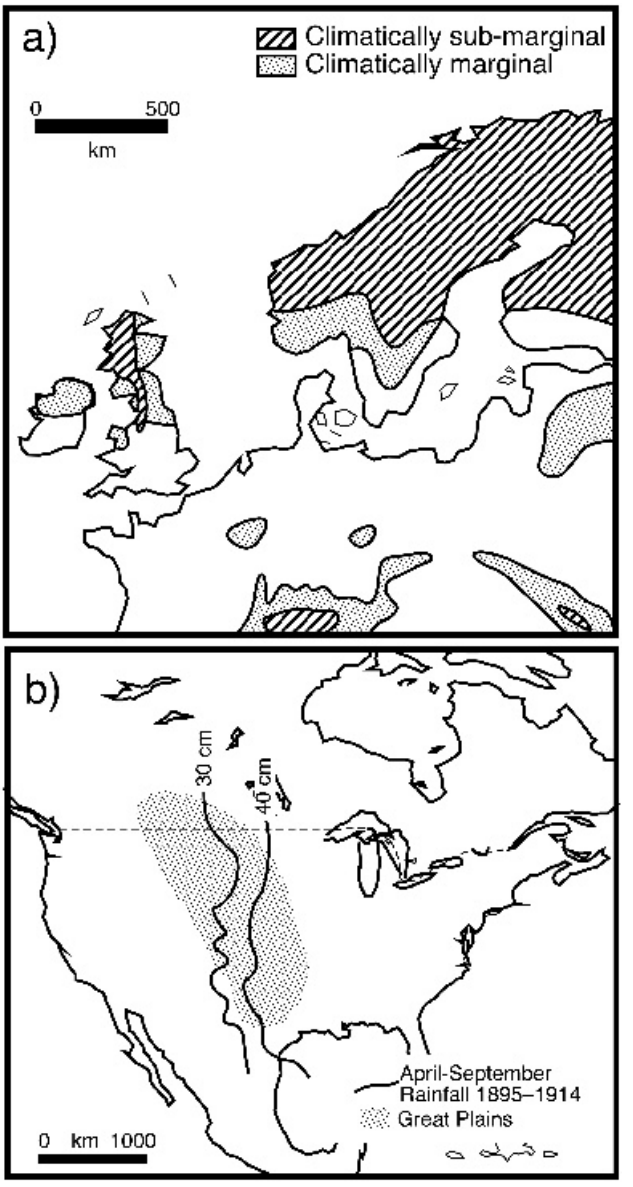

Figure 1.7 Climatologically marginal land in (a) northern Europe, (b) the Great Plains of the USA, and (c) eastern Australia. In (c) the shifts in climatic belts between 1881–1910 and 1911–1940 are seen (reproduced by permission from various sources including Gentilli, 1971, Elsevier Science Publications)

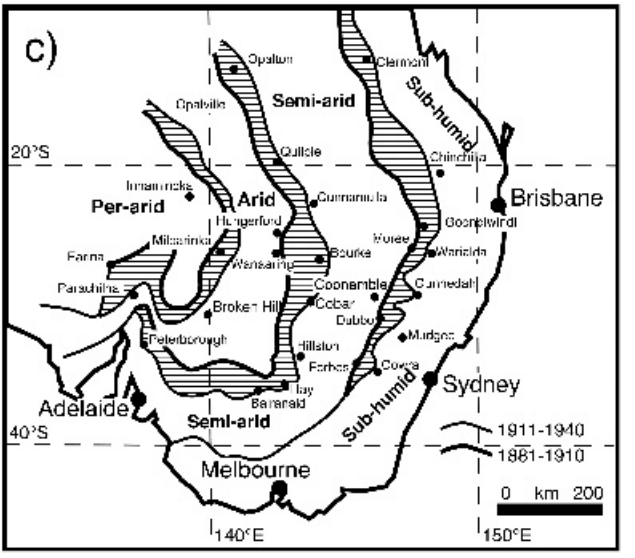

Figure 1.7 *Continued*

Tanzania as the world's most equatorial glacier, on Mount Kilimanjaro, continues disappearing: more than 80 per cent has vanished in the last 80 years. A large and negative impact is anticipated in central Asia where water for economic development currently comes from melting glaciers. Similarly, European Alpine glaciers feeding river-based hydroelectric plants are projected to be halved in number by the end of this century. From a climatic perspective, these retreating ice masses can offer new scientific and historical insights. For example, the remarkable finding of the 5000-year-old Oetzal 'ice man' in the European Alps, where radiocarbon dating indicates exposure of surfaces which have been hidden for thousands of years, has given us great insights into the life of humans in Europe at that time.

Sea-level changes have accompanied all the ice ages (lowering) and are predicted as global warming occurs (rising). As more than 100 million people live within 1 m of mean sea level, any rise threatens islands (sometimes whole nations), deltas and other low-lying coasts. As well as the danger to people and their infrastructure (homes, beaches and ports), sea-level rise inundates coastal wetlands, killing plants and rendering animals homeless. Today, we can measure and forecast sea-level rise, although these two tools do not, presently, give identical results. The best estimate of sea-level rise over the past century is closer to 2 mm/year than the 1 mm/year predicted from the thermal expansion (about 0.6 mm/year) and melting of continental glaciers (about 0.3 mm/year). Proposed solutions to this mystery include: overestimation by tide-gauges due to excessively large thermal expansions in coastal waters, a contribution from the massive glaciers of Greenland and Antarctica

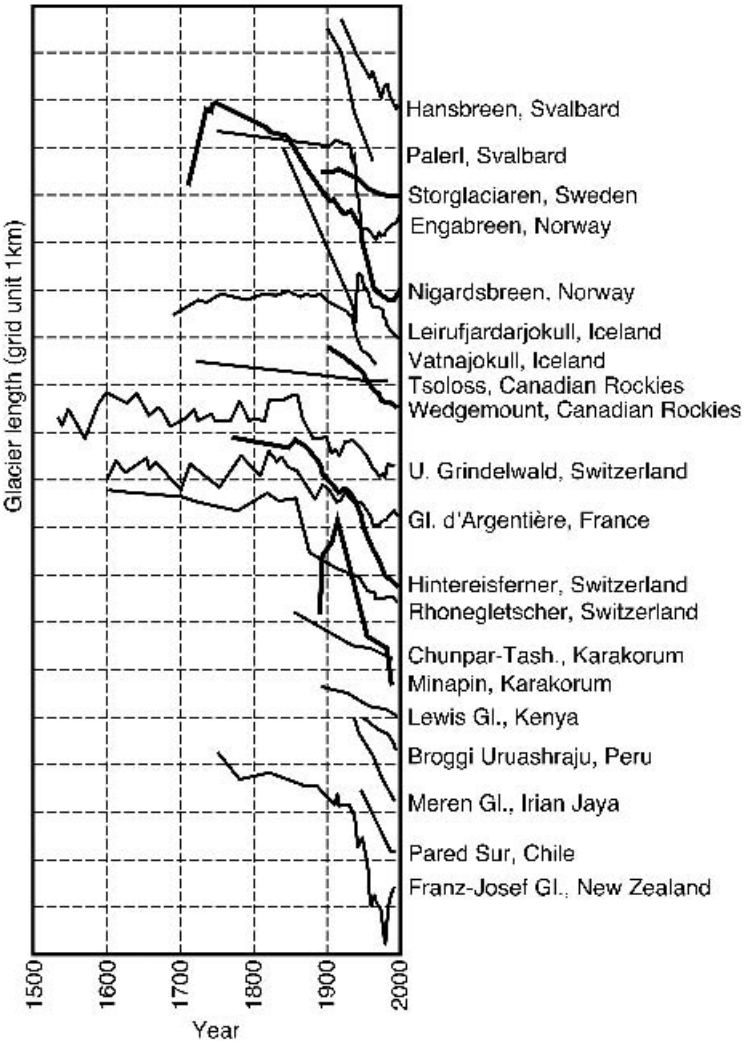

Figure 1.8 A collection of 20 glacier-length records from different parts of the world. Curves have been translated along the vertical axis to make them fit in one frame. Data are from the World Glacier Monitoring Service (http://www.geo.unizh.ch/wgms/) with some additions from unpublished sources. Reproduced with permission of the IPCC from Houghton *et al.* (2001)

(generally supposed to have had a zero net impact during the twentieth century) or an under-estimate of the two known and agreed sources. This climatic puzzle is of great importance and will be aided by improvements in models.

Evidence is also now emerging of how some animals are responding to climate changes over recent times. The timing of many animal activities such as breeding

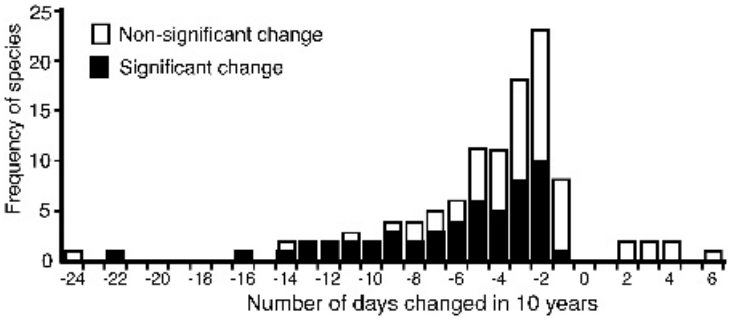

Figure 1.9 Changes in time of occurrence of events associated with various species of birds in North America. For most species, events are occurring earlier in the spring (indicated by the negative value on the *x*-axis). Over 80 per cent of species studied were shown to exhibit changes (such as nesting, hatching and arrival) consistent with global warming. Reproduced with permission from Root *et al.* (2003), *Nature* **421**, 57–60. Copyright 2003, Nature Publishing Group

is closely related to temperature and, through the study of large numbers of sample groups and species, it is possible to summarize the effect of climate change on these animals. A notable example is the North American common murre (common guillemot), found to be nesting progressively earlier each year, with a trend of over 24 days earlier per decade. A study in 2002 (Figure 1.9) found that, of all the species that exhibited changes, 80 per cent were changing in the direction expected for global warming, and, for those species with changes in the spring, the average result was 5.2 days earlier per decade.

Future human responses to climatic change are likely to involve complex webs of decisions. We will examine the modelling of the climatic part of these problems. Consideration of the nature of the interaction of elements of the climate system is an important, but by no means the only, prerequisite to consideration of potential human response. The remainder of this chapter is devoted to a description of the characteristics of the climate system of interest to modellers. Chapters 4 and 6 return to the challenge of trying to simulate integrated socio-economic interactions and biogeochemical climate processes.

1.2.3 Isotopes and climate

Stable and radioactive isotopes offer capabilities to climate scientists that have only recently begun to be exploited in climate modelling. For example, hydrogen, the simplest element, occurs in three isotopic forms: ^{1}H ('common' hydrogen – one proton in the nucleus), ^{2}H (deuterium – one proton, one neutron, also written as D) and ^{3}H (tritium – one proton, two neutrons). The abundances of these isotopes underline the dominance, 99.98%, of ^{1}H, with 0.015% occurring as the other stable isotope, deuterium, and only 0.005% as tritium, which is radioactive, decaying with a half-life of 12.4 years.

All elements are described by the number of protons (Z) in their nucleus. Combining the number of protons with the number of neutrons (N) gives the mass number (A) of the element. A single element can have different isotopes with different mass numbers because there can be different numbers of neutrons in the nucleus. The three hydrogen isotopes all with the same number of protons (one) and of electrons (one) share the same gross chemical properties. Each can bond with another hydrogen atom and an oxygen atom to form a water molecule, H_2O, for example. However, the behaviour of the heavier water molecules, termed isotopologues (e.g., $^{1}H^{2}H^{16}O$ and $^{1}H^{3}H^{16}O$), differs from the commonly occurring compound ($^{1}H^{1}H^{16}O$) in ways that can illuminate aspects of climate.

Stable isotopes offer tracking and process measurement capabilities. For example, the 'heavy' water isotope ($^{1}H^{2}H^{16}O$) binds more strongly to other water molecules and so requires more kinetic energy than its common cousin ($^{1}H^{1}H^{16}O$) to evaporate and rather less to condense. As a consequence, water vapour above an open water surface, such as an ocean, will contain relatively fewer 'heavy' water molecules than the ocean itself. As the moist air mass moves across a continent, the 'heavy' water molecules will tend to precipitate out more readily, further depleting the water vapour of 'heavy' water. This type of stable isotopic depletion has been applied to many aspects of climate science from measuring the biospheric recycling of water in the Amazon Basin to determining the global temperature fluctuations during ice ages. In high latitudes and high elevations where temperatures are cooler, fewer 'heavy' water molecules condense into droplets or ice crystals so that the precipitation becomes increasingly depleted in 'heavy' water as temperatures decrease. Of course, it is also possible to form still heavier water molecules such as $HD^{18}O$ but these are too rare to be of use in climate studies. The relationships are roughly linear in temperature, with ^{18}O decreasing by 0.7‰ (parts per thousand) with each 1°C decrease and the D amount in precipitation decreasing by about 5.6‰ for each 1°C temperature decrease.

Radioisotopes are used to date events and to count the passage of time by the metronomic 'tick' of their radioactive decay. For example, the inert but radioactive gas radon-222 (the longest lived of around 30 different radon isotopes) has a half-life of only 3.8 days, decaying to an isotope of lead (Pb-210). Radon is produced in the Earth's crust and is released into the atmosphere through the soil. If an air mass began a trajectory from a mid-continent (Figure 1.10) with 1 microgramme of radon, this would have decayed to 0.5 microgrammes in 3.8 days, to 0.25 microgrammes in 7.6 days and so on. This predictable decay offers an extremely useful method of timing a myriad of processes including validating atmospheric transport models. In climate science, radioisotopes have been applied to dating events ranging from the first occurrence of water on Earth (very close to the planet's origin 4.5 billion years ago) to accurately pinpointing the growth of tree-rings using the 1960s' atomic bomb radioactive carbon (^{14}C) signature in the wood, and timing the circulation of the deep ocean by tracking the penetration of 'bomb tritium'.

Table 1.1 lists the stable and radioactive isotopes most commonly used in global climate research. In the following chapters, some of the powerful climatic applica-

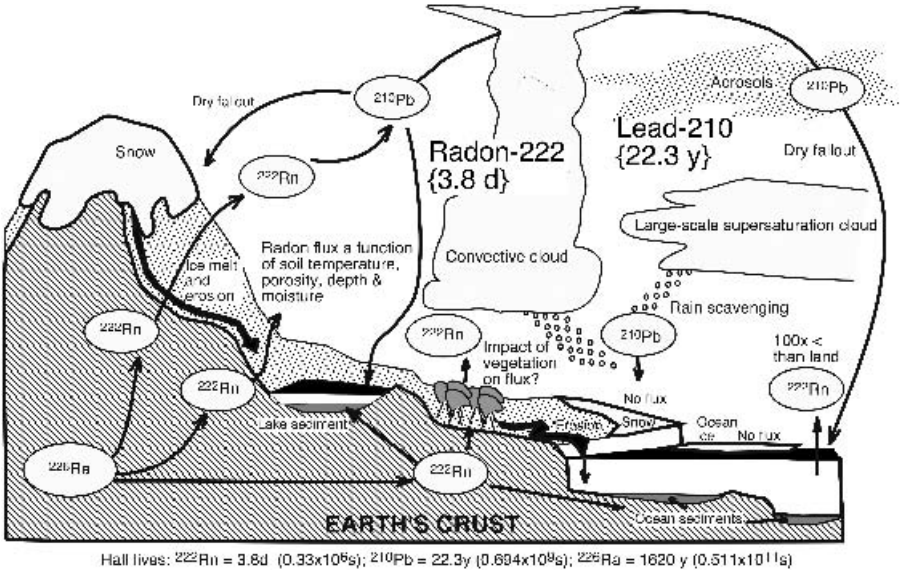

Figure 1.10 Illustration of the pathways of radon through the Earth system. Radon, a product of the natural decay of radium in the Earth's crust, is released into the atmosphere mainly through the soil and decays to ^{210}Pb with a half-life of 3.8 days

Table 1.1 Isotopes used in climate research and climate modelling

Element	*Isotope*	*Abundance* (%)
Hydrogen	^{1}H	99.985
	^{2}H (deuterium)	0.015
	^{3}H (tritium)	–*
Carbon	^{12}C	98.89
	^{13}C	1.11
	^{14}C	–*
Oxygen	^{16}O	99.759
	^{17}O	0.037
	^{18}O	0.204
Radon	^{222}Rn	–*

* Radioactive isotopes

tions of isotopic tools will be noted and their relevance to climate modelling described.

Possibly the most impressive exploitation of isotopic measurements in modern climate science is the use of hydrogen-2 (^{2}H or deuterium D) and oxygen-18 (^{18}O) found in long ice cores taken from Antarctica and Greenland. The Vostok, Antarc-

tica ice core record now extends back almost half a million years (Figure 1.11). In this core, deuterium is used as a proxy record of the local temperatures and the ^{18}O follows fluctuations in continental ice volume. The deuterium (^{2}H) is derived from the water melted from the ice itself and so represents the 'heavy' water content of precipitation as it once fell, as snow, on to the frozen glacier surface. In contrast, the ^{18}O record comes from oxygen gas (O_2) trapped in air pockets in the ice core.

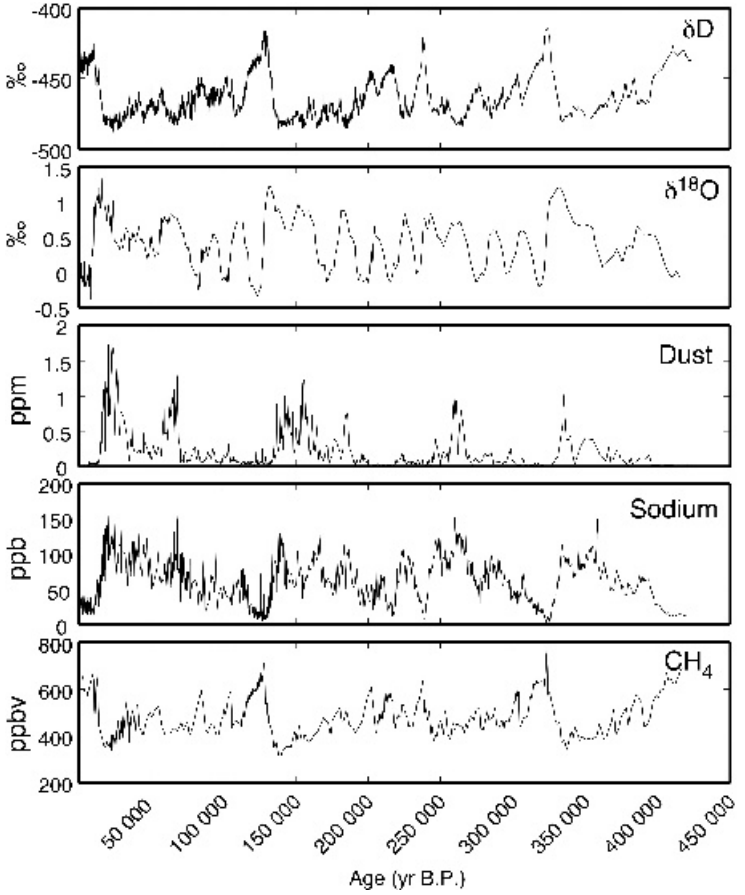

Figure 1.11 The climate of the past 420 000 years is revealed in this analysis of ice cores from Antarctica. Isotopes of hydrogen and oxygen are proxies for local temperature and ice volume, while the levels of dust, sodium and methane reveal the nature of the environment around the ice sheets. δ values for ^{18}O and D represent the deviation in parts per thousand from a standard sample of ocean water (plotted using data from Petit *et al.*, 2001, Vostok Ice Core Data for 420 000 Years, IGBP PAGES/World Data Center for Paleoclimatology Data Contribution Series #2001-076. NOAA/NGDC Paleoclimatology Program, Boulder, CO, USA)

From these pockets, it is also possible to measure greenhouse gas concentrations such as CO_2 and CH_4.

During ice ages, very large quantities of water are locked into continental glaciers. This increased ice volume has the effect of enriching the remaining ocean water in ^{18}O because so much of the more readily evaporated 'light' water has been removed. The oxygen in the atmosphere is the result of the long-term balance between production primarily by photosynthesis and removal mostly by respiration. The isotopic composition of atmospheric O_2 is controlled by biological processes, especially marine biotic photosynthesis which produces an ^{18}O characterization of atmospheric O_2 close to that of seawater. Thus, ^{18}O enriched ice core air occurs in glacial periods and a similar signal, arising from the same source, is also seen in the oxygen isotopic record in deep sea foraminifera.

1.3 CLIMATE FORCINGS

The climate system is a dynamic system in transient balance. This concept, which is vitally important in climate modelling, is easy to visualize, for instance, in terms of vehicle movements. The heart of New York City, Manhattan Island, experiences a very large vehicular influx each morning and an equally large outflux in the evening. Over time periods greater than a few days, Manhattan has an (approximate) vehicular balance, while over time periods of a few hours there are large negative and positive fluxes of vehicles. If the authorities were either (i) to close all bridges and tunnels on only the east side of the island, or (ii) to close all the car parks and refuse to allow street parking, the fluxes of vehicles would alter considerably and the net flux budget would change in this part of the New York subsystem.

Fluxes are thus seen to be vectors (they are the movement of some quantity, from one place to another, and the direction of flow is important) and net fluxes differ considerably as a function of the time period considered. Also different budgets, the result of the net fluxes, are established when the imposed disturbance changes. The most important fluxes in the climate system are fluxes of radiant (solar and heat) energy, together with fluxes of mass, especially water and, to a lesser extent, carbon, nitrogen, etc.

A climate forcing is a change imposed on the planetary energy balance that, typically, causes a change in global temperature. Forcings imposed on the climate system may be considered as falling into two separate categories. External forcings are caused by variations in agents outside the climate system such as solar radiation fluctuations. On the other hand, internal forcing, such as that due to volcanic eruptions, ice-sheet changes, CO_2 increases and deforestation are variations in components of the climate system. Longer-term internal forcings occurring as a result of continental drift and mountain-building have an effect, and changes in the polarity of the Earth's magnetic field may also influence the upper atmosphere and thus, perhaps, the whole climate.

1.3.1 External causes of climatic change

Milankovitch variations

The astronomical theory of climate variations, also called the *Milankovitch theory*, is an attempt to relate climatic variations to the changing parameters of the Earth's orbit around the Sun. The orbit of the Earth is an ellipse around the Sun, which lies at one of the foci. There are several different ways in which the orbital configuration can affect the received radiation and thus possibly the climate. They are (Figure 1.12): (i) changes in eccentricity, (ii) changes in obliquity and (iii) changes in orbital precession. The Earth's orbit becomes more eccentric (elliptical) and then more circular in a pseudo-cyclic way, completing the cycle in about 110 000 years. The mean annual incident flux varies as a function of the eccentricity of the orbit, E. For a larger value of E, there is a smaller incident annual flux. The current value of E is 0.017. In the last 5 million years, it has varied from 0.000483 to 0.060791, resulting in changes in the incident flux of +0.014% to –0.170% from the current value (~0.19 W m^{-2} and ~2.3 W m^{-2} respectively).

The obliquity, or the tilt of the Earth's axis of rotation, is the angle between the Earth's axis and the plane of the ecliptic (the plane in which the Earth and other bodies of the solar system orbit the Sun). This tilt varies from about 22° to 24.5°, with a period of about 40 000 years. The current value is 23.5°. Seasonal variations depend upon the obliquity: if the obliquity is large, so is the range of seasonality. Although the total received radiation is not altered, a greater seasonal variation in received flux is accompanied by a smaller meridional gradient in the annual radiation.

Owing to gravitational interaction with the other planets, primarily Jupiter, the perihelion (the point of the Earth's elliptical orbit closest to the Sun) moves in space so that the ellipse is moved around in space. This orbital precession will cause a progressive change in the time of the equinoxes. These changes occur in such a way that two main periodicities are apparent: 23 000 years and 18 800 years. This change, like that of obliquity, does not alter the total radiation received but does affect its temporal and spatial distribution. For example, perihelion is currently on 5 January, in the middle of the Northern Hemisphere winter, but 11 000–15 000 years from now it will occur in July. At the present-day value of eccentricity there is a range of ~6% in the solar radiation incident at the top of the atmosphere between perihelion and aphelion (i.e. 1411 to 1329 W m^{-2}).

Spectral analysis of long-term temperature data, such as the records in Figure 1.11, has shown the existence of cycles with periods of ~20 000, ~40 000 and ~100 000 years (Figure 1.13). These correspond closely with the Milankovitch cycles. The strongest signal in the observational data, however, is the 100 000-year cycle. This cycle corresponds to that of eccentricity variations in the Earth's orbit but eccentricity variations produce the smallest insolation changes. Hence, the mechanisms by which the Milankovitch cycles modify climate are far from clear. For example,

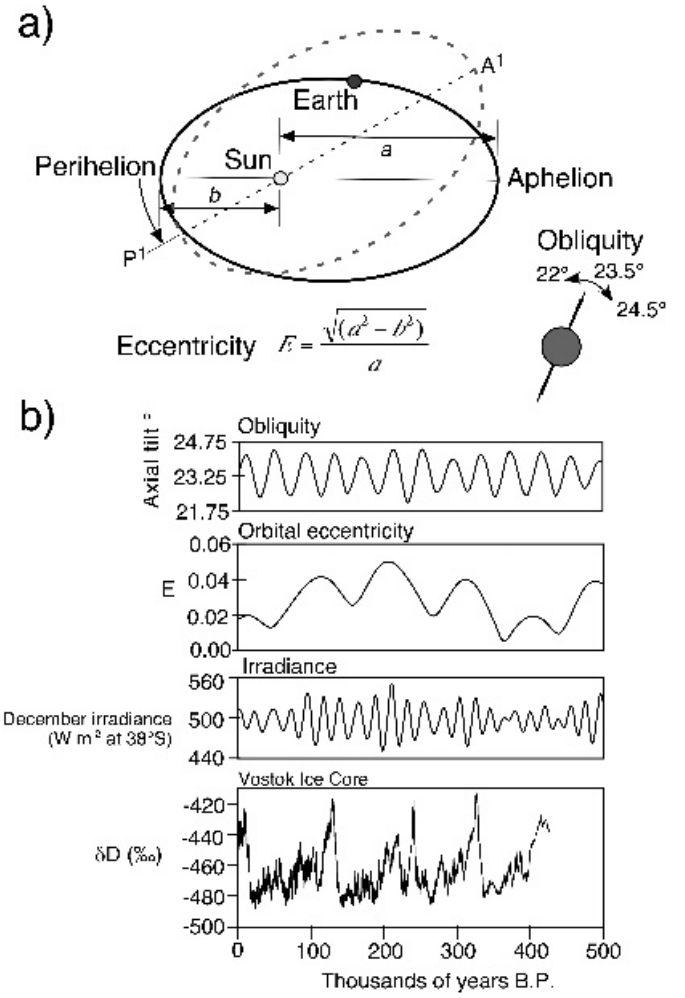

Figure 1.12 (a) Schematic diagram showing the variations in the three orbital components: obliquity (axial tilt), orbital eccentricity and precession of the perihelion. (b) Variations in these three components over the last 500 000 years together with δD proxy temperature record from the Vostok Ice Core (cf. Figure 1.11)

modelling results have suggested that the present configuration of the land masses in the Northern Hemisphere may favour rapid development of ice caps when conditions favour cool Northern Hemisphere summers. While the Milankovitch forcing offers an interesting 'explanation' for long-term, cyclic climatic changes, the energy distributions within spectral analyses of climate and of orbital variations are different and only recently have models begun to produce observed temperature changes

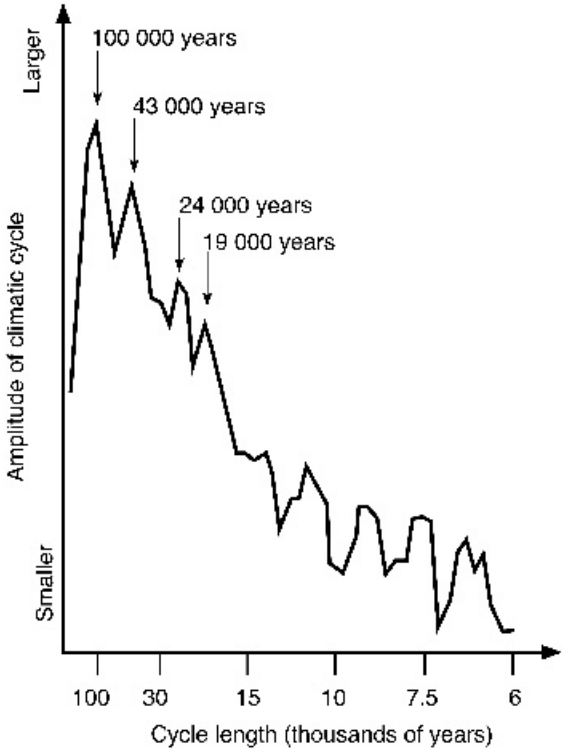

Figure 1.13 A spectrum of climatic variations over the last 500 000 years. The graph shows the importance of the climatic cycles of 100 000 years (eccentricity); 43 000 years (obliquity); and 24 000 and 19 000 years (precession of the location of the perihelion). The curve is constructed from an isotopic record of two Indian Ocean cores (reproduced from Imbrie and Imbrie (1979) by permission of Macmillan, London and Basingstoke)

from observed forcing. Almost certainly, these external changes trigger large feedback effects in the climate system which are yet to be fully understood.

Solar activity

Variations in the climate during historical times have been linked with the sunspot cycle, which is a second possible cause of solar-produced climatic change. This cycle occurs with a 22-year periodicity: the 'Hale' double sunspot cycle. The overall amplitude of the cycles seems to increase slowly and then fall rapidly with a period of 80–100 years. There also appears to be a quasi-cyclic fluctuation of the order of 180 years. No mechanistic link between sunspot activity and surface conditions on the Earth has yet been demonstrated and simple correlations between climate and sunspots usually fail when global conditions are considered.

Solar activity modulates the radiation received by the Earth because it produces dark areas (sunspots) and bright areas (faculae) that respectively deplete and enhance emitted solar radiation. It is possible to reconstruct historical solar forcings using contemporary measurements and proxies of solar activity to extend the record back to the 1600s. The Little Ice Age has been linked to the 'Maunder minimum' in sunspots, although it should be noted that the actual period of the Little Ice Age seems to vary according to the geographical area (cf. Figure 1.4) from which data are taken. Recent studies have suggested that changes in the energy output from the Sun between the Maunder minimum (*c.* 1645–1715) and the 1980s were likely to be 0.4% ± 0.2%. The magnitude of this forcing is very much less than the forcing due to enhanced CO_2 over that time, but short-term variability associated with the solar cycle is comparable with short-term greenhouse forcing this century.

Other external factors

Collisions of comets with the Earth and very large meteoritic impacts have also been proposed as causes of climatic fluctuations, as have possible but highly speculative interactions of the solar system with the galactic medium through which it travels. Many of the disturbances that meteoritic impacts would cause, such as an increase in stratospheric and tropospheric aerosols, are similar to disturbances internal to the system, described below. It is sometimes difficult to draw a clear boundary between external and natural (i.e. not human-induced) internal forcings. The distinction really depends upon the time- and space-scales encompassed in the definition of climate. Here, we take the modern view of climate as a significant part of Earth system science.

1.3.2 Internal factors: human-induced changes

Today's climate concerns centre on the possible impacts of human activities, which could operate on the relatively short time-scales necessary to create noticeable changes within the next century. These include the emissions of greenhouse gases and aerosols, changes in land-use and the depletion of stratospheric ozone. The only natural effects that are thought likely to be important on similar time-scales are volcanic activity and, possibly, oscillations in the deep ocean circulation.

Greenhouse gases

The increased concentration of a number of greenhouse gases in the atmosphere is well documented and simulating its potential effect is widely reported in the climate modelling literature, especially through the IPCC. Apart from water vapour, over which we have no control, CO_2 is the major component of both the natural greenhouse effect and of the greenhouse warming which is projected to occur as a result of continued burning of fossil fuels. The magnitude of the warming and the relative impacts on different regions of the world will depend on the nature of the feedbacks

within the climate system. The 'greenhouse warming' literature is so widespread that we opt not to review it here.

The magnitudes of the forcings that act to perturb the climate system as determined by the IPCC Third Scientific Assessment in 2001 are shown in Figure 1.14a. There is significant uncertainty in the magnitude of many of these forcings, but it is worth noting that the combined effect of cloud and aerosol forcings is potentially comparable to the forcing due to carbon dioxide, but in the opposite direction. Figure 1.14b shows a 1981 assessment which compares the effect of many other internal and external forcing agents.

Tropospheric aerosols and clouds

The influence of volcanic aerosols on climate has long been recognized, but the influence of tropospheric aerosols associated with industrial pollution and fossil fuel and biomass burning has only recently been identified and, to some extent, quantified. Solid sulphate particles result from the oxidation of SO_2 emitted when fossil fuels are burned. Other industrial processes and natural and human-initiated biomass burning and soil erosion also contribute droplets and particulate material, both termed aerosols, to the troposphere. These aerosols are localized and have two effects on the climate system. The direct effect of most aerosols is to reflect some solar radiation back into space and so act to cool the affected area, although some particulates, such as soot, are dark in colour and have the opposite effect, causing local warming. The magnitude of the cooling or warming depends on the nature of the aerosols and their distribution in the atmosphere.

There is also an important indirect effect of tropospheric aerosols. They act as additional cloud condensation nuclei and cause more, smaller, drops to form in clouds, increasing the reflectivity of the clouds, further cooling the planet (negative forcing in Figure 1.14a). The effect of changes in cloud character can have complex repercussions, since the clouds also affect the amount of radiation which escapes from the Earth's system. The indirect effect is much harder to evaluate than the direct effect, but both are believed to lead to cooling, and there is evidence that they are of comparable magnitude.

Stratospheric ozone

The discovery of the ozone hole in 1985 and, more recently, a similar, but less intense, ozone depletion over the Arctic has focused attention on the need for interactive chemical submodels in global climate models. The twentieth century ozone destruction is due to the disturbance of the natural balance of destruction and production which previously existed in the stratosphere. Paul Crutzen, Mario Molina and Sherwood Rowland were awarded the 1995 Nobel prize for chemistry for their role in identifying the threat to stratospheric ozone from anthropogenic compounds.

The presence of free chlorine atoms in the stratosphere can now be traced to the photochemical disruption of chlorofluorocarbons (CFCs) and hydrochlorofluorocarbons (HCFCs) when these inert gases migrate from the troposphere.

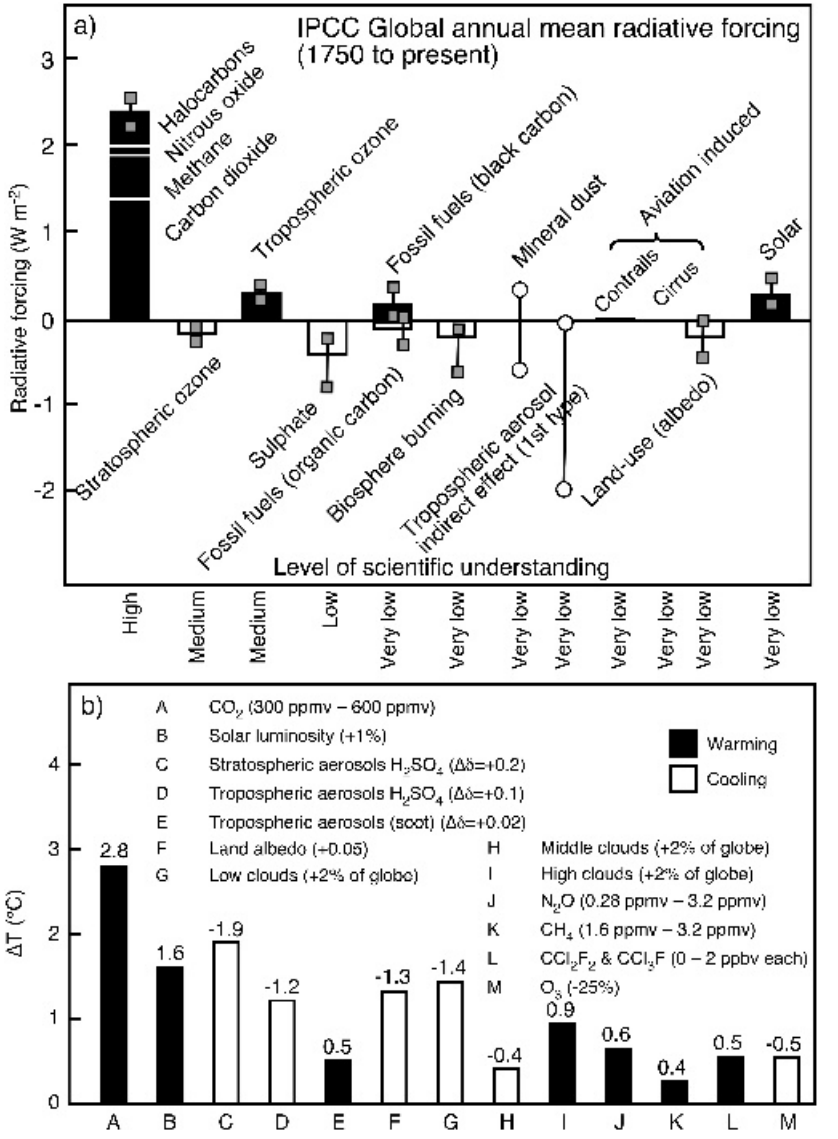

Figure 1.14 (a) Radiative forcings (annual mean) from 1750 to 2001 from the IPCC Third Assessment Report with uncertainties and estimates of the level of scientific understanding (reproduced with permission of the IPCC from Houghton *et al.*, 2001). (b) Similar estimates based on the results of a one-dimensional radiative convective model (1DRC) from Hansen *et al.* (1981)

Chlorine is the principal cause of the disturbance in ozone chemistry which produces the stratospheric polar ozone holes. Although the build-up of CFCs, at least, in the atmosphere has levelled off as a result of the Vienna Convention and the Montreal Protocol, the very long lifetimes of these gases means that they will persist in the atmosphere for hundreds of years.

The particular reactions which act to accelerate the ozone destruction rely on the presence of free chlorine atoms and a solid surface, provided by stratospheric ice clouds. Suitable conditions exist over the Antarctic continent during the winter and to a lesser extent over the Arctic Ocean in winter. It is possible that, in addition to the role played by ice crystals in the chemistry of the ozone breakdown, volcanic aerosols may also provide a suitable surface upon which the chemistry can take place.

Since CFCs, HCFCs and the hydrofluorocarbons (HFCs) that are replacing them are radiatively active (they are much more effective greenhouse gases, molecule for molecule, than CO_2), they also act to change the atmospheric temperature and this alters the rate of the chemical reactions. CFCs that remain in the troposphere are effective absorbers of infrared radiation, which would otherwise escape to space. These gases therefore act to enhance the atmospheric greenhouse and to provide a warming influence for the planet. The radiative effect of the reduced stratospheric ozone is to cool the planet. The enhanced levels of tropospheric ozone that have been observed result in a warming (Figure 1.14a).

Land-surface changes

Humans are now recognized as dominant agents in regional-scale changes of the character of the Earth's surface. These include desertification, re- and deforestation, urbanization and major river, lake and dam engineering. Climate modellers have investigated the climatic effect of such changes on the nature of the Earth's continental surface.

Desertification is a problem affecting millions of people. The sparse vegetation natural to arid and semi-arid areas can be easily removed as a result of relatively minor changes in the climate or by direct influence of human activity such as overgrazing or poor agricultural practices. Removal of vegetation and exposure of bare soil increase albedo and decrease soil water storage, because of increased runoff. Less moisture available at the surface means decreased latent heat flux, leading to an increase in surface temperature. On the other hand, the increased albedo produces a net radiative loss. In climate model calculations, the latter effect appears to dominate and the radiation deficit causes large-scale subsidence. In this descending air, cloud and precipitation formation would be impossible and aridity would increase. The result of a relevant model simulation is shown in Figure 1.15a. This global simulation involves a surface albedo change for a group of semi-arid areas. It can be seen that an increase in surface albedo does seem to decrease rainfall. Use of a global model emphasizes that all parts of the climate system are interlinked. Although this particular model includes many simplifications, the results are

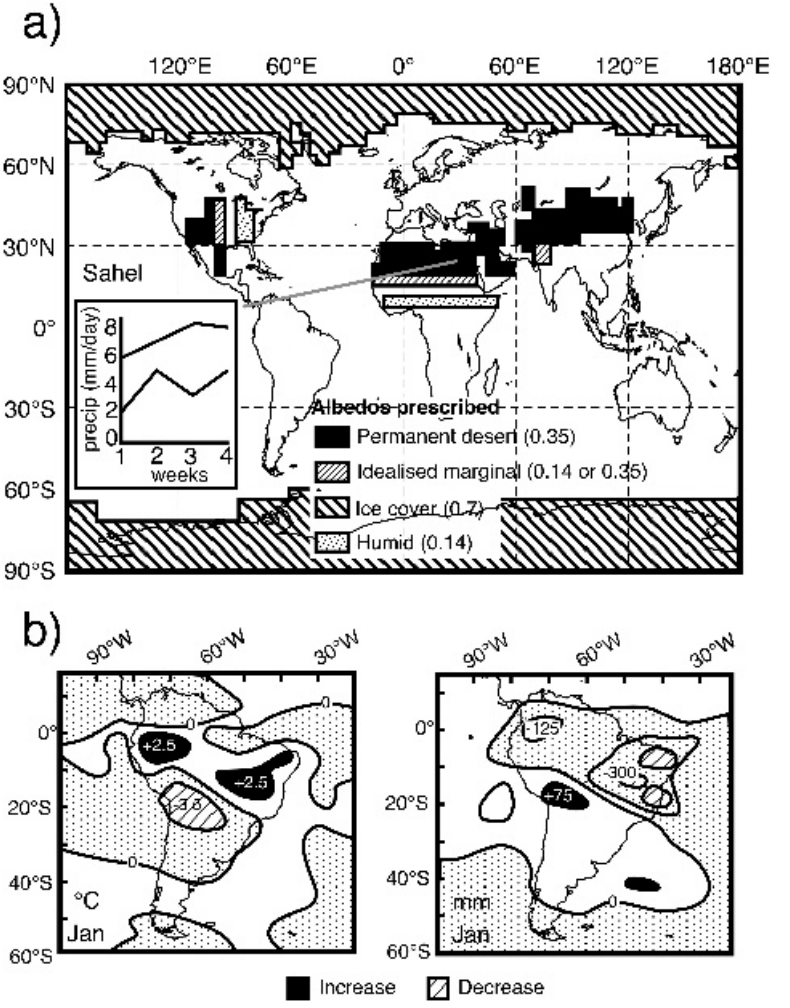

Figure 1.15 (a) The distribution of areas for which albedo changes were made in a set of experiments, originally conducted by Charney (1975), designed to examine desertification. The inset graph shows the rainfall resulting from increasing the surface albedo from 0.14 to 0.35 in the Sahel region when free evaporation was permitted (redrawn by permission from Henderson-Sellers and Wilson (1983) *Rev. Geophys. Space Phys.* **21**, 1743–1778. Copyright by the American Geophysical Union). (b) Simulated temperature (left) and precipitation (right) changes following replacement of the Amazon tropical moist forest by scrub grassland in a GCM. These are five-year means from the end of a six-year deforestation experiment. Areas of significant increase or decrease (using Student's *t*) are shown

illustrative of the types of surface-induced climatic effects that are currently captured by models.

At present around 30 per cent of the land surface of the Earth is forested and about 10 per cent is cultivated. However, the amount of forest, particularly in the tropics, is rapidly being reduced while reforestation is prevalent in mid-latitudes. As a consequence, the surface characteristics of large areas are being greatly modified. Modellers have attempted to examine the climatic effects of forest planting and clearance. The change in surface character can be especially noticeable when forests are replaced by cropland. One area that is undergoing deforestation is the Amazon Basin in South America. The important change in deforestation is in the surface hydrological characteristics since the evapotranspiration from a forested area can be many times greater than from adjacent open ground. Most climate model simulations of Amazonian deforestation show a reduction in moisture recycling (because of the lack of the moist forest canopy) which reduces precipitation markedly (Figure 1.15b). However, the available global model experiments do not agree on whether an increase in surface temperature occurs. The largest impacts are the local and regional effects on the climate, which could exacerbate the effects of soil impoverishment and reduced biodiversity accompanying the deforestation. It has proved possible to detect impacts resulting from tropical deforestation propagating to the global scale by increasing the length of the integrations to improve the statistics.

1.3.3 Internal factors: natural changes

Volcanic eruptions

Volcanoes influence climate by projecting large quantities of particulates and gases into the atmosphere. Volcanic eruptions can thereby produce measurable temperature anomalies of at least a few tenths of a degree. The major climatic contribution of volcanoes is from stratospheric H_2SO_4 droplets. The effect of the injected aerosol upon the radiation balance and whether heating or cooling ensues will depend largely on the height of injection into the atmosphere. If the aerosol absorbs in the visible part of the spectrum, energy is transferred directly to the atmosphere. If the aerosol absorbs and emits in the infrared, the greenhouse effect is increased.

Most eruptions inject particulates into the troposphere at heights between 5 and 8 km. These are rapidly removed either by gravitational fall-out or rain-out and the resultant climatic effect is minimal. More violent eruptions hurl debris into the upper troposphere or even into the lower stratosphere (15–25 km) (e.g. Mount Agung in 1963, El Chichón in 1982 and Mount Pinatubo in 1991). Eruptions such as these are much less frequent but are likely to have more extensive climatic effects. The aerosols have a long residence time in the stratosphere: of the order of a year for aerosols of radii 2–5 μm but as long as 12 years for smaller aerosols of radii 0.5–1.0 μm. Mount Pinatubo injected around 20 million tonnes of SO_2 to heights of 25 km. As it was dispersed by the stratospheric winds, the SO_2 was photochemically transformed into sulphate aerosols. These non-absorbing aerosols increase the

albedo of the atmosphere and reduce the amount of solar radiation that reaches the surface.

Immediately following an eruption the stratosphere is dominated by dust particles which scatter radiation of wavelengths up to 10 μm roughly ten times as efficiently as normal stratospheric aerosols. The 'clear sky' optical thickness can rise to 0.1 (20 times the normal value) after large eruptions, but these dust particles fall out very quickly. Sulphate production is increased a few months later and a further increase in the visible scattering occurs along with a slight increase in the infrared absorption. These changes will affect the atmospheric heating rates. The enhanced absorption of visible radiation is typically not sufficient to compensate for enhanced cooling by reflection and by emission of infrared radiation. The aerosols generated by the eruption of Mount Pinatubo in 1991 have been estimated to have resulted in a forcing of the climate system of around $-0.4\,\mathrm{W\,m^{-2}}$ with a resultant temporary global cooling of about 0.5°C. Since the eruption of Mount Pinatubo occurred at a time when the global observing network was extraordinarily well equipped to gather appropriate data, it prompted enormous advances in our knowledge of the effects of volcanic eruptions on atmospheric processes.

Model simulations suggest that radiative effects will, overall, produce a global cooling when large-scale volcanic eruptions occur. Figure 1.16 shows results of a simulation in which an attempt was made to include the effects of volcanic eruptions in a future climate simulation of the effects of increasing greenhouse gases. The simulation was performed in 1987 and assumed a volcanic eruption in 1995. The figure was updated with observed temperatures in 2000. The observed tempera-

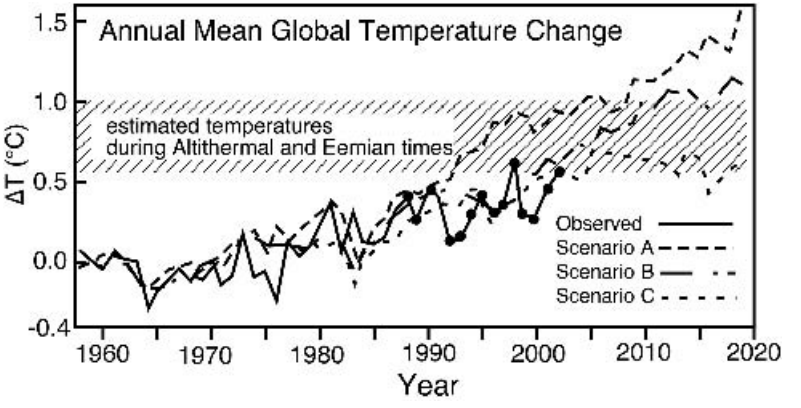

Figure 1.16 Global surface air temperature computed with the GISS model in 1987 (Hansen *et al.*, 1999) and observed surface air temperature (with dotted continuation). Model scenario A assumes exponential growth in greenhouse gases and no large volcanic eruptions; scenario B assumes linear greenhouse gas growth; and scenario C includes simulated volcanic eruptions in 1995 and 2015. In fact, a large eruption (Mount Pinatubo) occurred in 1991 and its impact can be seen in the observed temperatures. Reprinted from *General Circulation Model Development*, edited by D. Randall. Copyright 2000, with permission from Elsevier

ture anomaly resulting from Mount Pinatubo (in 1991, not 1995) is clearly seen in the observed curve, slightly leading the modelled anomaly. The results of the 1987 'prediction' agree well with the magnitude of the observed temperature anomalies. The effects on the atmosphere of eruptions like Mount Pinatubo are very short-lived compared to the time needed to influence the heat storage of the oceans. Hence, temperature anomalies do not persist, nor are they likely to initiate significant long-term climatic changes.

Ocean circulation changes

The ocean is one of the main constituents of the climate system. The bulk of the energy absorbed by the climate system is absorbed at the ocean surface and its huge thermal capacity and its ability to circulate this energy over long time-scales mean that its role in the climate system is powerful and complex. The circulation of the ocean combines three components: surface currents driven by the winds, deep currents driven by gradients of temperature and salinity, and tides driven by the gravitational effects of the Moon and Sun. These forces interact in a non-linear way to produce a complex system of motion we know as the global ocean circulation. Winds interact with regions of coastal upwelling to produce localized changes in sea-surface temperature, but perhaps the most significant changes in the ocean circulation are tied to phenomena with much longer time-scales. The circulation of the global ocean is dominated by what is termed the deep water circulation over time-scales of tens to thousands of years (Figure 1.17). There are two deep water sources active today: the North Atlantic Deep Water (NADW) and the Antarctic Bottom Water (AABW).

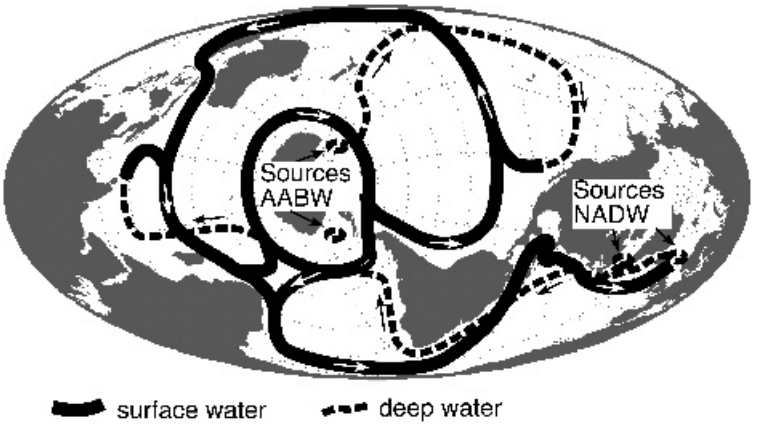

Figure 1.17 Schematic illustration of the thermohaline circulation of the ocean, commonly termed the 'ocean conveyor belt'. The four main sources of deep ocean water, which lie off the Greenland and Antarctic coasts, form North Atlantic Deep Water (NADW) and Antarctic Bottom Water (AABW) respectively. These cold and dense waters circulate the globe first near the ocean floor and later as near-surface flows

These water masses, although both are cold and dense, have different characteristics. The slightly warmer, southward flowing NADW lies above the more dense and colder northward flowing AABW, producing the characteristic layering observed in the deep ocean. The circulation of the ocean deep water can be simplified to illustrate the principal aspects of the system. The warm surface currents flow towards regions of deep water formation, namely the Labrador and Greenland Seas in the Northern Hemisphere and the Ross and Weddell Seas in the Southern.

The natural variability of the ocean circulation is an important factor for climate. The ocean circulation varies on glacial time-scales, over which the circulation is known to change markedly, and on interannual time-scales over which the El Niño Southern Oscillation (ENSO) phenomenon is important. Modellers have recently achieved some success in developing predictive models of ENSO events in the Equatorial Pacific on seasonal time-scales using spatially restricted ocean models, but the reliable prediction of El Niño events remains a challenge for the future. Over longer time-scales the ocean circulation changes markedly as changes occur in the distribution of land, either as a result of sea-level changes during periods of glaciation, or on much longer time-scales as the continents move across the Earth's surface.

Another challenge which faces ocean scientists is trying to explain the sudden changes that occur in circulation patterns. For example, in the North Atlantic, the relative warmth of Europe (palms in Western Scotland) in our present era is attributable to the formation of North Atlantic Deep Water (NADW) discussed above, which maintains the flow of warm surface water from the south. However, geological evidence from mid-Atlantic ocean drilling shows that NADW production has varied greatly over the last 25 000 years, seeming to be tied closely to stages of the last glaciation. Although the mechanisms that trigger changes in NADW production are not yet fully understood, computer models of the ocean circulation have been shown to support multiple equilibria for the Atlantic thermohaline circulation. This suggests that the ocean may respond abruptly to small perturbations in the hydrological cycle.

As our understanding of the ocean circulation has increased, in part due to the availability of high-resolution ocean circulation models, other areas of interest have emerged in relation to ocean circulation. It has been suggested that periods of aridity in East Africa between 5 million and 2.5 million years ago, which may have been the catalyst that drove our ancestors from the forests to the savannah, can be related to Indian Ocean cooling caused by narrowing of the Indonesian seaway. Such links are difficult to validate as yet, but new techniques in the analysis of Mg/Ca ratios in foraminifera offer some promise for reconstruction of the local temperature record.

Compilations of tropical sea-surface and bottom-water temperatures derived from isotopic analysis of sediment cores from the ocean floor have shown that tropical sea-surface temperatures have varied very little over the last 140 million years while the bottom-water temperatures have decreased by more than 10 K since the Cretaceous period, when the distribution of continents was different from today and the poles were significantly warmer than today. Maintaining these high, deep ocean

temperatures suggests a thermohaline conveyor quite different from today with much higher rates of overturning at the poles. The exact means by which such temperatures could have occurred and what effects the changes that caused them had on other components of the climate are questions which models are being used to answer.

1.4 CLIMATE FEEDBACKS AND SENSITIVITY

In the broadest sense, a feedback occurs when a portion of the output from the action of a system is added to the input and subsequently alters the output. The result of such a loop system can either be an amplification of the process or a dampening. These feedbacks are labelled positive and negative respectively. Positive feedbacks enhance a perturbation whereas negative feedbacks oppose a perturbation (Figure 1.18).

The importance of the direction of a feedback can be simply illustrated by considering the impact of self-image on diet. Someone slightly overweight who eats for consolation can become depressed by their increased food intake and so eat more and rapidly become enmeshed in a detrimental positive feedback effect. On the other hand, perception of a different kind can be used to illustrate negative feedback. As a city grows there is a tendency for immigration but the additional influx of industry, cars and people is often detrimental to the environment so that it may be balanced, or even exceeded, by an outflux of wealthier inhabitants, with a potentially

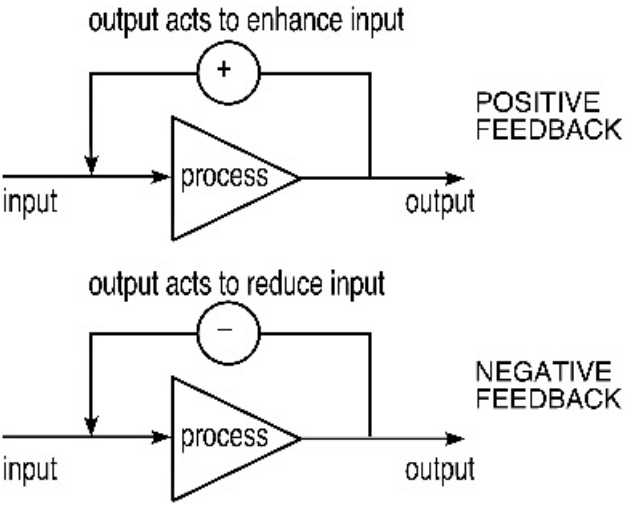

Figure 1.18 Types of feedback. Feedback processes can be classified as positive or negative. In positive feedback a portion of the output is fed back to the input and acts to further stimulate the process. In the case of negative feedback, the portion of the output is subtracted from the input and acts to dampen the process

negative impact on the central city's economy. In this section, some of the feedback mechanisms inherent in the climate system are described.

1.4.1 The ice-albedo feedback mechanism

If some external or internal perturbation acts to decrease the global surface temperature, then the formation of additional areas of snow and ice is likely. These cryospheric elements are bright and white, reflecting almost all the solar radiation incident upon them. Their albedo (ratio of reflected to incident radiation) is therefore high. The surface albedo, and probably the planetary albedo (the reflectivity of the whole atmosphere plus surface system as seen from 'outside' the planet), increase. Thus, a greater amount of solar radiation is reflected away from the planet and temperatures decrease further. A further increase in snow and ice results from this decreased temperature and the process continues. This positive feedback mechanism is known as the ice-albedo feedback mechanism. Of course, this mechanism is also positive if the initial perturbation causes an increase in global surface temperatures. With higher temperatures, the areas of snow and ice are likely to be reduced, thus reducing the albedo and leading to further enhancement of temperatures. The existence of clouds over regions of snow and ice can greatly modify the shortwave feedbacks associated with the cryosphere. The presence of a snow or ice surface also affects the temperature structure of the atmosphere, introducing feedbacks associated with longwave radiation.

1.4.2 The water vapour 'greenhouse'

Another positive feedback mechanism occurs with the increase of atmospheric water vapour as temperatures are raised. Many atmospheric gases contribute to the greenhouse warming of the surface as a result of their absorption of infrared radiation emitted from the surface. The dominant greenhouse gas in the Earth's atmosphere is water vapour, although carbon dioxide and other trace gases, such as methane and chlorofluorocarbons, are becoming increasingly important. The additional greenhouse effect of the extra water vapour enhances the temperature increase. Similarly, if temperatures fall, there will be less water vapour in the atmosphere and the greenhouse effect is reduced.

1.4.3 Cloud feedbacks

To establish even the direction of the feedback associated with clouds is difficult, since they are both highly reflective (thus contributing to the albedo) and composed of water and water vapour (thus contributing to the greenhouse effect, because of their control of the longwave radiation). It has been suggested that for low- and middle-level clouds the albedo effect will dominate over the greenhouse effect, so that increased cloudiness will result in an overall cooling. On the other hand, cirrus clouds which are fairly transparent at visible wavelengths have a smaller impact

upon the albedo so that their overall effect is to warm the system by enhancing the greenhouse effect.

Cloud feedback is, however, not this straightforward. There are dynamical and thermodynamical factors to be considered (Figure 1.19a) so that it is uncertain whether an increased temperature will lead to increased or decreased cloud cover (as opposed to cloud amounts). Although it is generally agreed that increased temperatures will cause higher rates of evaporation and hence make more water vapour available for cloud formation, the form these additional clouds will take is much less certain. For the same 'volume' of new cloud, an increased dominance of cumuliform clouds probably reduces the percentage of the surface covered by clouds. More stratiform clouds, on the other hand, would increase the area covered (Figure 1.19b). Thus, using the simplest reasoning, it might be claimed that an increase in cumuliform clouds implies positive feedback, whereas an increase in stratiform clouds implies a negative feedback.

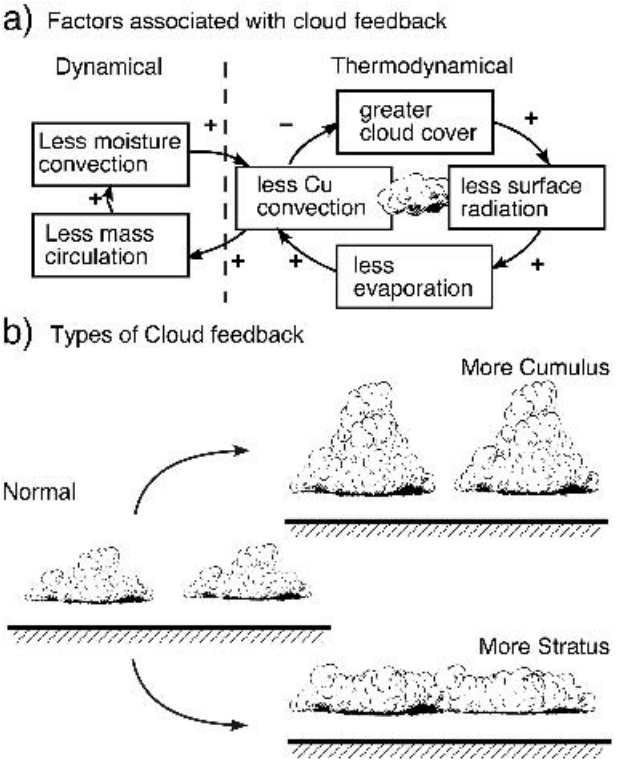

Figure 1.19 (a) Specific examples of dynamical and thermodynamical feedbacks and their directions in the case of a change in the amount of cumulus convection. (b) The exact nature of an increase in cloud amount is unclear. The cloud could either be more extensive vertically or more extensive horizontally

Another unknown factor about how clouds change in response to a climate perturbation is their height of formation. The situation is further complicated by the lack of understanding of how the radiative properties of clouds may change. The sizes of the droplets in a cloud have an important influence on how the clouds interact with radiation and the amount of water in the clouds also changes the way the clouds interact with the radiation. Clouds with larger drops have a lower albedo than clouds composed of smaller drops, but have the same amount of liquid water (usually described in terms of the 'liquid water path'). Successful modelling of cloud liquid water must account for the competing effects of changing drop size and liquid water path, which will ultimately affect the nature of the interaction with solar and terrestrial radiation streams.

1.4.4 Combining feedback effects

Since more than one feedback effect is likely to operate within the climate system in response to any given perturbation, it is important to understand the way in which these feedbacks are combined. For example, consider a system in which a change of surface temperature of magnitude ΔT is introduced. Given no internal feedbacks, then this temperature increment will represent the change in the surface temperature. If feedbacks occur, then there will be an additional surface temperature change and the new value of the surface temperature change will be

$$\Delta T_{final} = \Delta T + \Delta T_{feedbacks} \tag{1.1}$$

where $\Delta T_{feedbacks}$ can be either positive or negative. The value of ΔT_{final} (i.e. whether it is large or small) is usually related to the perturbation which caused it by a measure of the sensitivity of the climate system to disturbance. There are a number of such sensitivity parameters in the climate modelling literature. An early measure of a model's sensitivity was termed the β parameter, where β is equal to the ratio of the calculated surface temperature change to an incremental change in the prescribed incident solar radiation. More recently Equation (1.1) has been rewritten in terms of a feedback factor, f, so that

$$\Delta T_{final} = f\Delta T \tag{1.2}$$

This feedback factor has, in turn, been related to the amplification or gain, g, of the system which is defined, using the analogy of gain in an electronic system, by

$$f = 1/(1-g) \tag{1.3}$$

The f factor is neither additive nor multiplicative and is thus not especially useful mathematically. Gain factors, g, are additive but depend, as does the β parameter, on knowing the present climate system albedo or outgoing fluxes. A much more convenient climate sensitivity parameter is given in terms of a perturbation in the global

surface temperature ΔT which occurs in response to an externally prescribed change in the net radiative flux crossing the tropopause, ΔQ,

$$C[\delta(\Delta T)/\delta t] + \lambda \Delta T = \Delta Q \tag{1.4}$$

Here $\lambda \Delta T$ is the net radiation change at the tropopause resulting from the internal dynamics of the climate system, t is time, and C represents the system heat capacity.

Although Equation (1.4) represents an extreme simplification of the system it is useful in interpreting and summarizing the sensitivity of more complex climate models. A convenient reference value for λ is the value λ_B which λ would have if the Earth were a simple black body with its present-day albedo,

$$\lambda_B = 4\sigma T_e^3 = 3.75 \text{ W m}^{-2} \text{ K}^{-1} \tag{1.5}$$

where σ is the Stefan–Boltzmann constant and T_e is the Earth's effective temperature, both of which are defined in the glossary and explained in Chapter 3. The overall climate system sensitivity parameter λ_{TOTAL} is composed of the summation of λ_B and all contributing feedback factors λ_i such that, for example,

$$\lambda_{TOTAL} = \lambda_B + \lambda_{water\ vapour} + \lambda_{ice\ albedo} \tag{1.6}$$

Thus for a given system heat capacity a positive value of feedback factors (λ_i) implies stability, or negative feedback, and a negative value (rather confusingly) implies positive feedback and possibly growing instability. It is worth noting that, as discussed in relation to the ice-albedo feedback, the feedback factors are not necessarily independent. To establish the resulting temperature change, the value of ΔQ for the perturbation considered is divided by the value of λ_{TOTAL}. The relationship (derived directly from Equation (1.4) for the case of zero heat capacity, C) that $\Delta T = \Delta Q/\lambda$ has given rise to another definition of a feedback factor as $1/\lambda$ or λ'. It is this sensitivity parameter that has been used as a measure of the sensitivity of climate models in the IPCC assessment and in some recent Global Climate Model (GCM) intercomparisons (see Chapter 6).

For doubling atmospheric CO_2, it has been shown that $\Delta Q \approx 4.2 \text{ W m}^{-2}$. If we take $\lambda_B = 3.75 \text{ W m}^{-2} \text{ K}^{-1}$ and $\lambda_{water\ vapour} = -1.7 \text{ W m}^{-2} \text{ K}^{-1}$ and $\lambda_{ice\ albedo} = -0.6 \text{ W m}^{-2} \text{ K}^{-1}$, we have that $\lambda_{TOTAL} = 1.45 \text{ W m}^{-2} \text{ K}^{-1}$. Consequently, the globally averaged temperature rise due to doubling atmospheric CO_2 is found to be about 2.9 K, whereas if we had neglected the ice-albedo feedback the temperature increase would have been only about 2.0 K. Various estimates have been made of the feedback effects likely to be caused by changes in cloud amount and cloud type. These estimates range from λ_{cloud} is zero (i.e. the effects cancel) to results from GCMs which suggest that λ_{cloud} could be as large as $-0.8 \text{ W m}^{-2} \text{ K}^{-1}$. The addition of this feedback effect to those considered above would raise the surface temperature increase due to doubling CO_2 to about 6.5 K. This example demonstrates clearly how powerful a combination of positive feedback effects can be for the predicted surface temperature change.

Great care must be taken in interpretation of quoted values for feedback factors since, as we have seen, several different definitions are available. Three of those

used are shown in Figure 1.20 plotted as functions of the feedback factor, λ_{TOTAL}. Note the areas of the graph (and the values of the feedback factors) which represent positive and negative feedback. As the term λ is often used synonymously with λ_{TOTAL} it is important to establish which is meant by careful contextual reading.

The climatic system is clearly extremely heterogeneous. There are many subsystems which interact with one another producing feedback effects. Climate dynamics is not unique in being controlled by changing feedback effects. If we reconsider the feedbacks affecting the socio-economics of a city, mentioned earlier, it is easy to imagine a range of other feedbacks operating in either the same or the opposite direction as the negative feedback on population induced by the perception of declining environmental character. As the city grows, there are greater profits to be made in centrally located businesses (a positive feedback on population) while land prices, rents, etc. increase (a negative feedback), street crime probably increases (negative feedback) but long journey-to-work times are detrimental to family life (positive feedback). All these and many other feedback effects operate in a dynamically

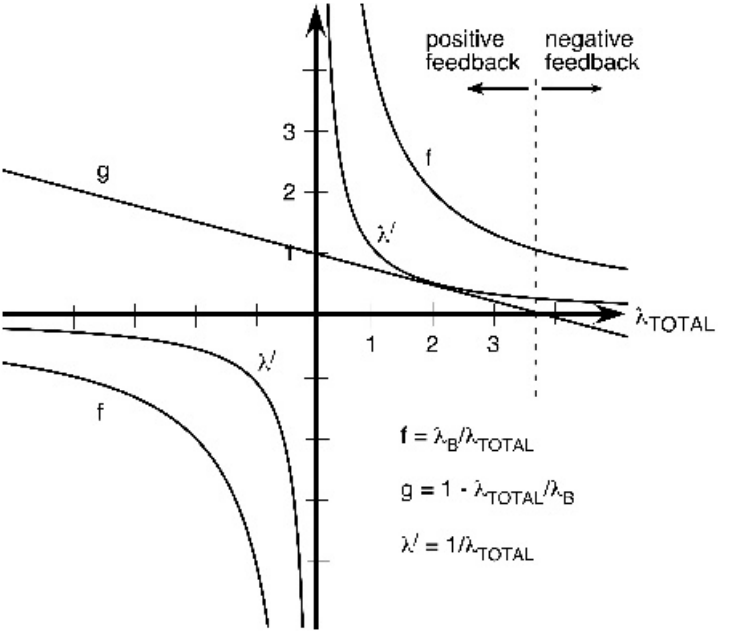

Figure 1.20 The feedback factor, *f*, the gain of the system, *g*, and a third feedback factor λ' used by the IPCC, all plotted as a function of λ_{TOTAL} (probably the most useful measure of climate system sensitivity), the sum of all the contributing λ_is; λ_B is the value of λ_{TOTAL} for zero feedback. The areas of the diagram signifying overall positive and negative climatic feedback are shown. [The older sensitivity parameter, the β parameter, not shown here, can be written as $\beta = S_o/\lambda_{TOTAL}$, where S_o is the global average incoming solar radiation (= 340 W m^{-2}: one-fourth of the solar constant). Consequently, for λ_{TOTAL} = 3.75 W m^{-2}, β = 91.33 K]

changing 'control' of the city's population size. Climatic feedbacks can be thought of as analogous to these geographical and economic controls.

Often the importance of feedback effects depends upon the time-scale of behaviour of the subsystems they affect and so the concept of time-scale of response is crucially important to all aspects of climate modelling. This time-scale is variously referred to as the equilibration time, the response time, the relaxation time or the adjustment time. It is a measure of the time the subsystem takes to re-equilibrate following a small perturbation to it. A short equilibration time-scale indicates that the subsystem responds very quickly to perturbations and can therefore be viewed as being quasi-instantaneously equilibrated with an adjacent subsystem with a much longer equilibration time. It is common to express equilibration times in terms of the time it would take a system or subsystem to reduce an imposed displacement to a fraction $1/e \approx 0.37$ of the displaced value, termed the e-folding time. For example, a pot of hot water removed from a stove will re-equilibrate with the room environment with an e-folding time depending upon the difference in temperature of the pot contents and the room, as well as the size and shape of the pot. A smaller temperature difference, a smaller pot or a larger surface-to-volume ratio of the container will result in relatively shorter e-folding times.

Subsystems which respond only very slowly have long e-folding times. A fundamental response time in climate modelling is the thermal response time. Table 1.2 lists equilibration times for a range of subsystems of the climate system. The longest equilibration times are those for the deep ocean, the glaciers and ice sheets (hundreds to thousands of years), while the remaining elements of the climate system have equilibration times ranging from days to years.

Table 1.2 Equilibration times for several subsystems of the climate system

Climatic domain	*Seconds*	*Equivalent*
Atmosphere		
Free	10^6	10 days
Boundary layer	10^5	24 hours
Ocean		
Mixed layer	10^6–10^7	Months to years
Deep	10^{10}	300 years
Sea ice	10^6–10^{10}	Days to 100s of years
Continents		
Snow and surface ice layer	10^5	24 hours
Lakes and rivers	10^6	10 days
Soil/vegetation	10^6–10^{10}	10 days to 100s of years
Mountain glaciers	10^{10}	300 years
Ice sheets	10^{11}	3000 years
Earth's mantle	10^{15}	30 million years

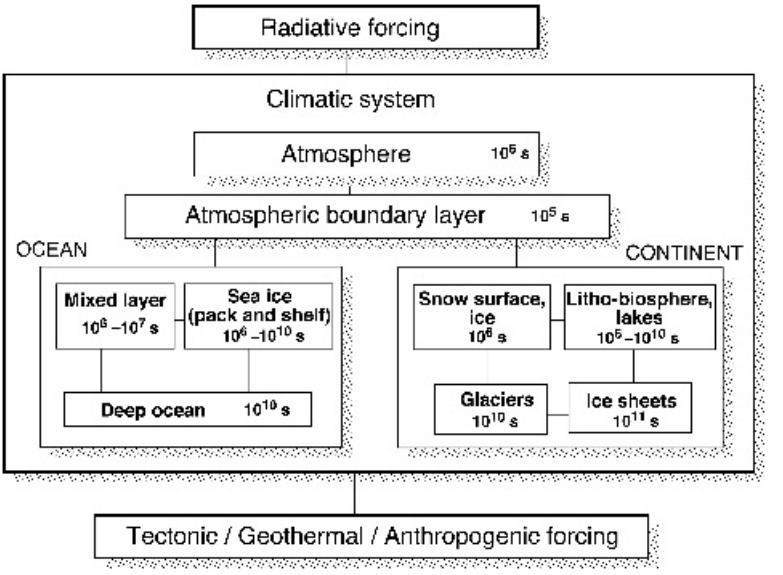

Figure 1.21 A schematic representation of the domains of the climate system showing estimated equilibration times (reproduced by permission of Academic Press from Saltzman, 1983)

Thus, the climatic system can be pictured as in Figure 1.21 not only in terms of subsystems and their directions and types of interactions but also in terms of approximate equilibration times. The very long equilibration time of the deep ocean poses a particularly difficult problem for climate modellers. The methods by which the short response time of the atmospheric features can be linked to the much slower response time of the ocean system are discussed in Chapter 5. Some elements of the cryosphere, which have long response times, have not, so far, been included in the parameterizations of GCMs but are already important components of the Earth Models of Intermediate Complexity (EMICs) discussed in Chapter 4.

Clearly, modelling of climatic feedbacks (i.e. the processes and interactions) will be crucial to the results of the modelling experiment, as the inclusion or exclusion of a feedback mechanism could radically alter the results. Understanding feedbacks can only come through careful examination of the action of likely perturbations and the relative equilibration times of various parts of the climate system. The very wide range of time-scales in the climate system is reflected in the wide range of climate model types described in this book.

1.5 RANGE OF QUESTIONS FOR CLIMATE MODELLING

The type of question asked by climate modellers has changed over time. In the early years of climate modelling the question was, ‘Can the model capture the fundamental characteristics of the atmosphere?’ so that particular attention was paid to adequately

reproducing the atmospheric time mean state. Over the last forty or so years, climate models of all types have been applied to questions that are strictly demands for predictions: for example, 'What is the impact on the climate of doubling, tripling or quadrupling atmospheric CO_2?', 'Will removing the tropical forests of the world affect the climate at locations distant from the deforested area?' and 'Is the North Atlantic ocean circulation likely to change rapidly?'. As will become clear in the rest of this book, many 'predictions' have been made with models that have not yet been fully tested. Sensitivity testing, intercomparison and careful evaluation of climate models have only become widespread since the models have been shown to be doing a good basic job.

The next stage in the evolution of climate modelling seems likely to be an attempt to answer still more difficult questions about the climate system. One such question which could not even be considered by modellers until they felt confident of their predictions of greenhouse warming is the likely social and economic implications of this future climate change.

The rest of this book is intended to give the reader a basic understanding of the types and complexity of climate models. We have not tried to answer specific questions such as those outlined above or to describe, in detail, particular models or experiments. In writing this primer, our aim has been to help those new to climate modelling to a quicker and fuller understanding of the available literature.

RECOMMENDED READING

Charney, J.G. (1975) Dynamics of deserts and drought in the Sahel. *Quart. J. Roy. Met. Soc.* **101**, 193–202.

Covey, C., Rao, K.M.A., Lambert, S. and Taylor, K.E. (2003) *Intercomparison of present and future climates simulated by Coupled Ocean–Atmosphere GCMs*. PCMDI Report No. 66, UCRL-ID-140325 [Available from http://www-pcmdi.llnl.gov].

Dansgaard, W. (1964) Stable isotopes in precipitation. *Tellus* **16**, 436–468.

Dickinson, R.E. (1985) Climate sensitivity. In S. Manabe (ed.) *Issues in Atmospheric and Oceanic Modelling, Part A, Climate Dynamics*. Advances in Geophysics, Vol. 28, Academic Press, New York, pp. 99–129.

Ferraro, R., Sato, T., Brasseur, G., Deluca, C. and Guilyardi, E. (2003) Modeling the Earth System: Critical computational technologies that enable us to predict our planet's future [available online from http://www.esmf.ucar.edu/main_site/esmf_pub.html].

Gat, J. (1996) Oxygen and hydrogen in the hydrologic cycle. *Ann. Rev. Earth Plan. Sci.* **24**, 225–262.

GARP (1975) The physical basis of climate and climate modelling. GARP Publication Series No. 16, WMO/ICSU, Geneva.

Gentilli, J. (ed.) (1971) Climates of Australia and New Zealand. *World Survey of Climatology.* Elsevier, Amsterdam, 405 pp.

Hansen, J.E. and Takahashi, T. (eds) (1984) *Climate Processes and Climate Sensitivity*. Geophysical Monograph 29, Maurice Ewing Vol. 5, American Geophysical Union, Washington DC, 368 pp.

Hansen, J.E., Lacis, A., Ruedy, R., Sato, M. and Wilson, H. (1993) How sensitive is the world's climate? *Nat. Geog. Res. Exp.* **9**, 142–158.

Hansen, J.E., Ruedy, R., Lacis, A., Sato, M., Nazarenko, L., Tausnev, N., Tegen, I. and Koch, D. (2000) Climate modelling in the global warming debate. In D.A. Randall (ed.) *General*

Circulation Model Development: Past, Present and Future. Academic Press, San Diego, 807 pp.

Harvey, L.D.D. (1999) *Global Warming: The Hard Science*. Prentice Hall, Englewood Cliffs, 408 pp.

Hays, J.D., Imbrie, J. and Shackleton, N.J. (1976) Variations in the Earth's orbit: Pacemaker of the ice ages. *Science* **194**, 1121–1132.

Henderson-Sellers, A. (ed.) (1995) *Future Climates of the World: A Modelling Perspective*. World Survey of Climatology Series, Vol. 16, Elsevier, Dordrecht, Holland, 568 pp.

Houghton, J.T. (ed.) (1984) *The Global Climate*. Cambridge University Press, Cambridge, 233 pp.

Houghton, J.T., Ding, Y., Griggs, D.J., Noguer, M., van der Linden, P.J. and Xiaosu, D. (eds) (2001) *Climate Change 2001: The Scientific Basis, Contribution of Working Group I to the Third Assessment Report of the Intergovernmental Panel on Climate Change (IPCC)*. Cambridge University Press, Cambridge, UK, 944 pp.

Imbrie, J. and Imbrie, K.P. (1979) *Ice Ages: Solving the Mystery.* Macmillan, London, 224 pp.

Manabe, S. (ed.) (1985) *Issues in Atmospheric and Oceanic Modelling, Part A, Climate Dynamics*. Advances in Geophysics, Vol. 28, Academic Press, New York, 591 pp.

Mann, M., Bradley, R.S., Briffa, K., Jones, P., Osborn, T., Crawley, T., Hughes, M., Oppenheimer, M., Overpeck, J., Rutherford, S., Trenberth, K. and Wigley, T. (2003) On past temperatures and anomalous late-20th century warmth. *EOS Transactions of the American Geophysical Union*, **84**, July 2003, 256–257.

McCarthy, J.J., Canziani, O.F., Leary, N.A., Dokken D.J. and White K.S. (eds) (2001) *Climate Change 2001: Impacts, Adaptation & Vulnerability, Contribution of Working Group II to the Third Assessment Report of the Intergovernmental Panel on Climate Change (IPCC)*. Cambridge University Press, Cambridge, UK, 1000 pp.

Metz, B., Davidson, O., Swart, R. and Pan, J. (eds) (2001) *Climate Change 2001: Mitigation Contribution of Working Group III to the Third Assessment Report of the Intergovernmental Panel on Climate Change (IPCC)*. Cambridge University Press, Cambridge, UK, 700 pp.

Peixoto, J.P. and Oort, A.H. (1991) *Physics of Climate*. American Institute of Physics, Washington, D.C., 520 pp.

Petit, J.R., Jouzel, J., Raynaud, D., Barkov, N.I., Barnola, J-M., Basile, I., Bender, M., Chappellaz, J., Davis, M., Delaygue, G., Delmotte, M., Kotlyakov, V.M., Legrand, M., Lipenkov, V.Y., Lorius, C., Pépin, L., Ritz, C., Saltzman, E. and Stienvard, M. (1999) Climate and atmospheric history of the past 420 000 years from the Vostok ice core, Antarctica. *Nature* **399**, 429–436.

Root, T.T., Price, J.T., Hall, K.R., Schneider, S.H., Rosenzweig, C. and Pounds, A. (2003) Fingerprints of global warming on wild animals and plants. *Nature* **421**, 57–60.

Schlesinger, M.E. (ed.) (1988) *Physically Based Modelling of Climate and Climatic Change: Parts 1 and 2*. NATO ASI Series C: No 243, Kluwer Academic Publishers, Dordrecht, 990 pp.

Trenberth, K.E. (1992) *Climate System Modelling*. Cambridge University Press, Cambridge, 600 pp.

Wang, W-C. and Isaksen, I.S. (1995) *Atmospheric Ozone as a Climate Gas: General Circulation Model Simulations*. NATO ASI Series I: Vol. 32, Springer, New York, 459 pp.

Washington, W.M. and Parkinson, C.L. (2004) *An Introduction to Three-Dimensional Climate Modelling*. University Science Books, Mill Valley, California.

Web resources

http://www.ipcc.ch	The Intergovernmental Panel on Climate Change
http://www.wmo.ch	The World Meteorological Organization (including the World Climate Programme)
http://www.cpc.ncep.noaa.gov/	US National Weather Service Climate Prediction Centre
http://www.usgcrp.gov/	The United States Global Change Research Program
http://www.ncdc.noaa.gov/	The United States National Climate Data Center
http://www.clivar.org/	CLIVAR: An International Research Programme on Climate Variability and Predictability
http://www.meted.ucar.edu/topics_climate.php	Climate pages at the UCAR COMET program
http://www.giss.nasa.gov/research/forcings/ceq_presentation.pdf	Can we defuse the global warming time bomb?
http://www.gfdl.noaa.gov/~rw/GREENHOUSE-HISTORY.html	Greenhouse Warming Research – Past, Present and Future

CHAPTER 2

A History of and Introduction to Climate Models

The mathematical problem is not yet defined: there are more unknowns than equations.

C. G. Rossby (1946)

2.1 INTRODUCING CLIMATE MODELLING

Any climate model is an attempt to represent the many processes that produce climate. The objective is to understand these processes and to predict the effects of changes and interactions. This characterization is accomplished by describing the climate system in terms of basic physical, chemical and biological principles. Hence, a numerical model can be considered as being comprised of a series of equations expressing these laws. Climate models can be slow and costly to use, even on the fastest computer, and the results can only be approximations.

The need for simplification

For several reasons, a model must be a simplification of the real world. The processes of the climate system are not fully understood, although they are known to be complex. Rossby was alluding to this problem in the quotation at the start of this chapter. Furthermore, the components of the climate system interact with each other, producing feedbacks (Section 1.4), so that any solution of the governing equations must involve a great deal of computation. The solutions that are produced start from some initialized state and investigate the effects of changes in a particular component of the climate system. The boundary conditions, for example the solar radiation, sea-surface temperatures or vegetation distribution in the case of the atmosphere, or the bathymetry and atmospheric wind field in the case of the ocean, are set from observational data or other simulations. These data are rarely complete or of adequate accuracy to specify completely the environmental conditions, so that there is inherent uncertainty in the results.

A Climate Modelling Primer, Third Edition. K. McGuffie and A. Henderson-Sellers.
 ISBN: 0-470-85750-1 (HB); 0-470-85751-X (PB)

Today's large-scale coupled climate system models, designed to simulate the climate of the planet, take into account the whole climate system (see Figure 1.2). All of the interactions between the components must be integrated in order to develop such a model. This presents great problems because the various interactions operate on different time-scales. For example, the effects of changes in deep water formation in the ocean may be very important when considering climate averaged over decades to centuries, while local changes in wind direction may be unimportant on this time-scale. If, on the other hand, monthly time-scales are of concern, the relative importance would be reversed.

Early global models were of the atmosphere alone and were initially used to generate average conditions for January and July. This was usually done by maintaining forcing appropriate to one particular month and running the model for hundreds of days. These models typically did not include the diurnal cycle and were termed 'perpetual January' or 'perpetual July' (depending on forcing). This is not to imply that a particular January in the period for which a climate model prediction is made would have these conditions, only that the conditions apply to an average January. The latest climate models now include many components, most importantly the ocean and atmosphere, and are now routinely run for hundreds of years with diurnally varying radiation and for multi-year seasonal cycles, and these are used to produce 'climate' averages. The availability of faster computers has introduced the idea of 'ensemble runs'. In such experiments, the modellers carefully perturb initial conditions for each of a collection of model runs, producing an ensemble set. It is always implied that any 'new' climate predicted will have variation about the mean, just as with the present climate. Such experiments help place limits on the variation in climate. This is important when the results of global-scale models are used to estimate the possible impact of climatic change in a local or regional area, or in detection of a climatic change.

The simplifications that must be made in the laws governing climatic processes can be approached in several ways. Consequently, numerous different global-scale climate models are available. In general, two sets of simplifications need to be made. The first involves the processes themselves. It is usually possible to treat in detail some of the processes, specifying their governing equations fairly fully. However, other processes must be treated in an approximate way, either because of our lack of exact information, lack of understanding or because there are still inadequate computer resources to deal with them. For example, it might be decided to treat the radiation processes in great detail, but only approximate the horizontal energy flows associated with regional-scale winds. The approximation may be approached either by using available observational data, the empirical approach, or through specification of the physical laws involved, the theoretical (or conceptual) approach.

Resolution in time and space

The second set of simplifications involves the resolution of the model in both time and space (see Figure 1.1). While it is generally assumed that finer spatial resolu-

tions produce more reliable results, constraints of both data availability and computational time may dictate that a model may have to have, for example, latitudinally averaged values as the basic input. In addition, too fine a resolution may be inappropriate because processes acting on a smaller scale than the model is designed to resolve may be inadvertently incorporated. Similar considerations are involved in the choice of temporal resolution. Most computational procedures require a 'timestep' approach to calculations. The processes are allowed to act for a certain length of time and the new conditions are calculated. The process is then repeated using these new values. This continues until the conditions at the required time have been established. Timestepping is a natural consequence of there not being a steady-state solution to the model equations. Although accuracy potentially increases as the timestep size decreases, there are constraints imposed by data, computational capacity and the design of the model. The time and space resolutions of the model are also linked, as will be explained in Chapter 5.

Although models are designed to aid in predicting future climates, performance can only be tested against the past or present climate. Usually when a model is developed, an initial objective is to test the sensitivity of the model and to ascertain how well its results compare with the present climate. Thereafter it may be used to simulate past climates, not only to see how well it performs but also to gain insight into the causes and features of these climates. Although such past climates are by no means well known, this comparison provides a very useful step in establishing the validity of the modelling approach. After such tests, the model may be used to gain insight into possible future climates.

2.2 TYPES OF CLIMATE MODELS

The important components to be considered in constructing or understanding a model of the climate system are:

1. *Radiation* – the way in which the input and absorption of solar radiation by the atmosphere or ocean and the emission of infrared radiation are handled;
2. *Dynamics* – the movement of energy around the globe by winds and ocean currents (specifically from low to high latitudes) and vertical movements (e.g. small-scale turbulence, convection and deep-water formation);
3. *Surface processes* – inclusion of the effects of sea and land ice, snow, vegetation and the resultant change in albedo, emissivity and surface–atmosphere energy and moisture interchanges;
4. *Chemistry* – the chemical composition of the atmosphere and the interactions with other components (e.g. carbon exchanges between ocean, land and atmosphere);
5. *Resolution in both time and space* – the timestep of the model and the horizontal and vertical scales resolved.

The relative importance of these processes and the theoretical (as opposed to empirical) basis for parameterizations employed in their incorporation can be discussed

using the climate modelling pyramid (Figure 2.1). The edges represent the basic elements of the models, with complexity shown increasing upwards. Around the base of the pyramid are the simpler climate models which incorporate only one primary process. There are four basic types of model.

1. Energy balance models (EBMs) are zero- or one-dimensional models predicting the surface (strictly the sea-level) temperature as a function of the energy balance of the Earth. Simplified relationships are used to calculate the terms contributing to the energy balance in each latitude zone in the one-dimensional case.
2. One-dimensional models such as radiative–convective (RC) models and single column models (SCMs) focus on processes in the vertical. RC models compute the (usually global average) temperature profile by explicit modelling of radiative processes and a 'convective adjustment' which re-establishes a predetermined lapse rate. SCMs are single columns 'extracted' from a three-dimensional model and include all the processes that would be modelled in the three-dimensional version but without any of the horizontal energy transfers.
3. Dimensionally constrained models now take a wide variety of forms. The oldest are the statistical dynamical (SD) models, which deal explicitly with surface processes and dynamics in a zonally averaged framework and have a vertically resolved atmosphere. These models have been the starting point for the incorporation of reaction chemistry in global models and are still used in some Earth Models of Intermediate Complexity (EMICs).
4. Global circulation models (GCMs). The three-dimensional nature of the atmosphere and ocean is incorporated. These models can exist as fully coupled ocean–atmosphere models or 'coupled climate system models' or, for testing and evaluation, as independent ocean or atmospheric circulation models. These models attempt to simulate as many processes as possible and produce a three-dimensional picture of the time evolution of the state of the ocean and atmosphere. Vertical resolution is typically much finer than horizontal resolution but, even so, the number of layers is usually much less than the number of columns.

The vertical axis in Figure 2.1 shows increasing complexity (i.e. more processes included and linked together) and also indicates increasing resolution: models appearing higher up the pyramid tend to have higher spatial and temporal resolutions.

There is ambiguity concerning the expansion of GCM. Two possible terms are the more recent 'global climate model' and the older 'general circulation model'. The latter also refers to a weather forecast model so that in climate studies GCM is understood to mean 'general circulation climate model'. A further distinction has historically been drawn between oceanic general circulation models and atmospheric general circulation models by terming them OGCMs and AGCMs. As the pyramid is ascended, more processes are integrated to develop a coupled ocean–atmosphere global model (OAGCM or CGCM). It has been suggested that, as processes that are currently fixed come to be incorporated into GCMs, the coupling will be more complete, say including changing biomes (an AOBGCM) or changes in atmospheric,

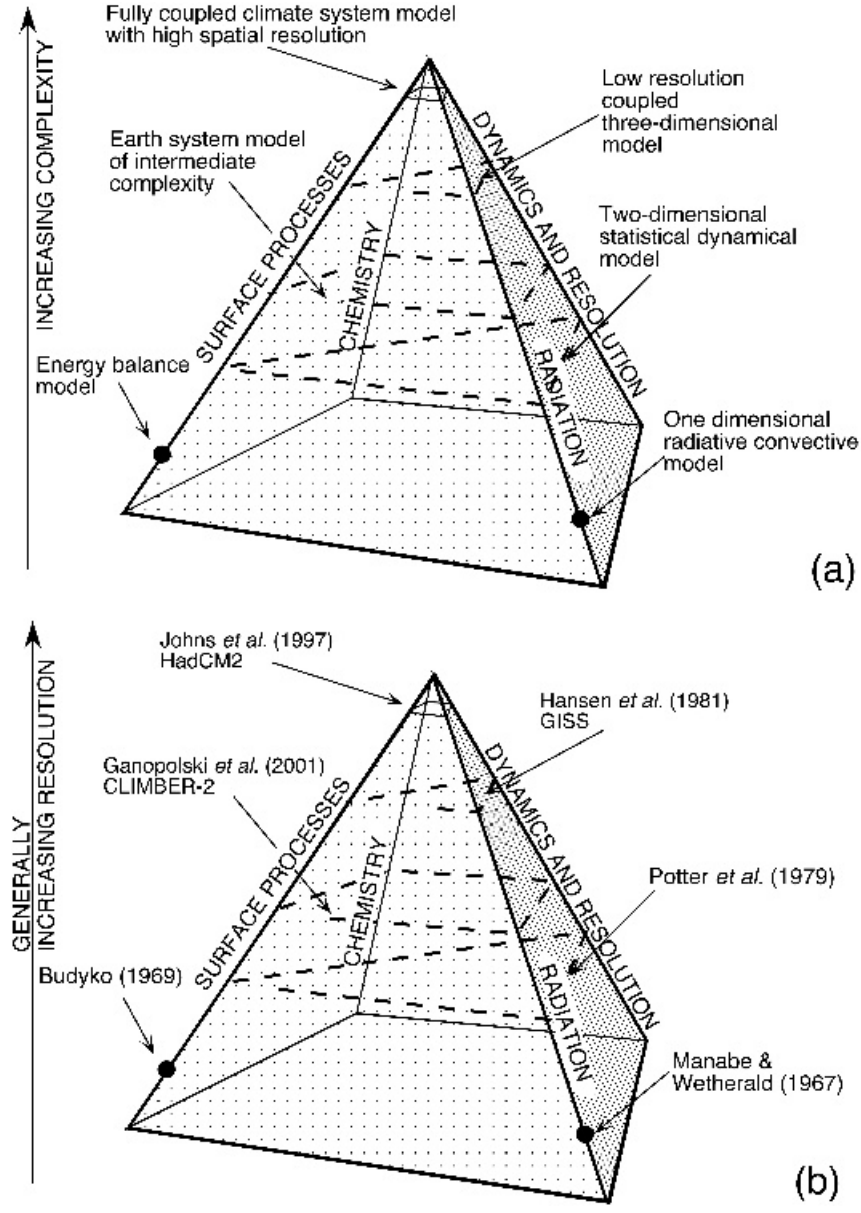

Figure 2.1 The climate modelling pyramid. The position of a model on the pyramid indicates the complexity with which the four primary processes (dynamics, radiation, surface and oceans and chemistry) interact. Progression up the pyramid leads to greater interaction between each primary process. The vertical axis is not intended to be quantitative. (a) The position of various model types; (b) Examples from the literature and their positions on the pyramid

ocean and even soil chemistry. Such models are becoming known as 'coupled climate system models' or 'Earth system models'. From being the only components in GCMs, the atmosphere and ocean are now parts of modular software packages designed to tackle a wide variety of problems. In this book, the generic term 'GCM' is used to mean a complex three-dimensional model of the atmosphere and ocean incorporating other components and used for climate simulation. As in the broader literature, the particular meaning will be clear from the context.

2.2.1 Energy balance climate models

These models have been instrumental in increasing our understanding of the climate system and in the development of new parameterizations and methods of evaluating sensitivity for more complex and realistic models. This type of model can be readily programmed and implemented on most small computers and the inherent simplicity of EBMs combined with the ease of interpreting results make them ideal instructional tools. They are widely used to investigate the sensitivity of the climate system to external changes and to interpret the results of more complex models. Energy balance models are discussed more fully in Chapter 3 and codes are included on the Primer CD (see Appendix C).

Energy balance models are generally one-dimensional, the dimension in which they vary being latitude. Vertical variations are ignored and the models are used with surface temperature as the predicted variable. Since the energy balance is allowed to vary from latitude to latitude, a horizontal energy transfer term must be introduced, so that the basic equation for the energy balance at each latitude, ϕ, is

$$C_m[\Delta T(\phi)/\Delta t] = R{\downarrow}(\phi) - R{\uparrow}(\phi) + \text{net transport into zone } \phi \qquad (2.1)$$

where C_m is the heat capacity of the system and can be thought of as the system's 'thermal inertia' and $R{\downarrow}$ and $R{\uparrow}$ are the incoming and outgoing radiation fluxes respectively.

The radiation fluxes at the Earth's surface must be parameterized with care since conditions in the vertical are not considered in this type of model. To a large extent the effects of vertical temperature changes are treated implicitly. In a clear atmosphere, convective effects tend to ensure that the lapse rate remains fairly constant. However, cloud amount depends only weakly on surface temperature, so that cloud albedo is only partially incorporated in the model. In particular, clouds in regions of high temperatures, such as the intertropical convergence zone, are ignored in the parameterization of albedos in EBMs.

Atmospheric dynamics are not modelled in an EBM; rather it is assumed that a 'diffusion' approximation is adequate for including heat transport. This approximation relates energy flow directly to the latitudinal temperature gradient. This flow is usually expressed as being proportional to the deviation of the zonal temperature, T, from the global mean, $\overline{T}$. When using the model for annual average calculations, the surface albedo can be regarded as constant for a given latitude. This type of model, however, can also be used for seasonal calculations. In this case, it is usual

to allow the albedo to vary with temperature to simulate the effects of changes in sea ice and snow extent.

Early EBMs were originally found to be stable only for small perturbations away from present-day conditions. For instance, they predicted the existence of an ice-covered state for the Earth for only slight reductions in the present solar constant. This result prompted studies of the sensitivity of various climate model types to perturbations (see Section 2.4).

2.2.2 One-dimensional radiative–convective climate models

One-dimensional RC models represent an alternative approach to relatively simple modelling of the climate and they also occur at the bottom of the modelling pyramid (Figure 2.1). In this case the 'one dimension' in the name refers to altitude. One-dimensional RC models are designed with an emphasis on the global average surface temperature, although temperatures at various levels in the atmosphere can be obtained.

The main emphasis in these models is on the explicit calculation of the fluxes of solar and terrestrial radiation (the radiation streams). Given an initially isothermal atmosphere, the heating rates for a number of layers in the atmosphere are calculated, although the cloud amount, optical properties and the albedo of the surface generally need to be specified. The temperature change in each layer which results from an imbalance between the net radiation at the top and bottom of the layer is calculated. At the end of each timestep a revised radiative temperature profile is produced. If the calculated lapse rate exceeds some predetermined 'critical' lapse rate, the atmosphere is presumed to be convectively unstable. An amount of vertical mixing, sufficient to re-establish the prescribed lapse rate, is carried out and the model proceeds to calculate the next radiative timestep. This procedure continues until convective readjustment is no longer required and the net fluxes for each layer approach zero. One-dimensional RC models operate under the constraints that at the top of the atmosphere there must be a balance of shortwave and longwave fluxes and that surface energy gained by radiation equals that lost by convection. However, they vary in the way they incorporate the critical lapse rate. Some use the dry adiabatic lapse rate, some the saturated one, while many use a value of $6.5\,\mathrm{K\,km^{-1}}$, which is the value in an observed standard atmospheric profile. Similarly, different humidity and cloud formulations are possible.

Radiative–convective models (discussed more fully in Chapter 4) can be constructed either as equilibrium models or in a time-dependent form. FORTRAN code for the latter type is included on the Primer CD – see Appendix C. These models can also be given an additional dimension and applied to zonally averaged conditions, by including a description of the horizontal energy transport. The main use of radiative–convective models is to study the effects of changing atmospheric composition and to investigate the likely relative influences of different external and internal forcings. They are the basis for the 'column' models that have recently begun to be used to evaluate aspects of the parameterizations of the atmospheric (and

surface) 'columns' in more complex GCMs. Column models are, in effect, single columns from a GCM and include the sophisticated physics usually found in these models.

2.2.3 Dimensionally-constrained climate models

Dimensionally-constrained climate models typically represent either two horizontal dimensions or the vertical plus one horizontal dimension. The latter were originally more common, combining the latitudinal dimension of the energy balance models with the vertical one of the radiative–convective models. These models also tended to include a more realistic parameterization of the latitudinal energy transports. In such models, the general circulation is assumed to be composed mainly of a cellular flow between latitudes, which is characterized using a combination of empirical and theoretical formulations. A set of statistics summarizes the wind speeds and directions while an eddy diffusion coefficient of the type used in EBMs governs energy transport. As a consequence of this approach, these models are called 'statistical dynamical' (SD) models. These 2D SDs can be considered as the first attempts at Earth modelling with intermediate complexity – the EMICs.

EMICs are about one-third of the way up the modelling pyramid (Figure 2.1), being more complicated than the vertically or latitudinally resolved one-dimensional models. Indeed, as we shall see in Chapter 4, many EMICs now claim to represent fractionally more than two dimensions and some even represent all three but with very coarse spatial or temporal resolution. Their use has provided insight into the operation of the present climate system, for example showing that the relatively simple diffusion coefficient approach for poleward energy transports is appropriate, provided that the coefficient, as well as the transport, is allowed to vary with the latitudinal temperature gradient. Advances in the understanding of baroclinic waves were achieved from studies of the results of 2D SD models. Dimensionally-constrained models have been employed to make simulations of the chemistry of the stratosphere and mesosphere. These models typically involve the modelling of tens to hundreds of chemical species and many hundreds of different reactions, and are much more demanding of computer time than atmosphere-only 2D models. Although traditional two-dimensional models are insensitive to changes within a latitude band, a compromise (and fractionally increased dimensionality) may be obtained by considering each zone as being divided into a land and ocean part. This type of 'two-channel' approach is discussed with reference to a more complex EBM in Section 4.9.

As a result of the lack of full three-dimensional resolution and the increased availability of computer resources enabling many more people to run GCMs, two-dimensional SD models have been largely superseded for consideration of the effect of perturbations on the present climate and for purposes such as IPCC. However, use of this type of model has blossomed recently in applications involving socio-economic change and climate assessments. These modern dimensionally-

constrained models, the EMICs, proudly abandon physical dimensions specifically to incorporate human systems, their impacts and susceptibilities.

2.2.4 General circulation models

The aim of GCMs is the calculation of the full three-dimensional character of the atmosphere or ocean (Figure 2.2). The solution of a series of equations (Table 2.1)

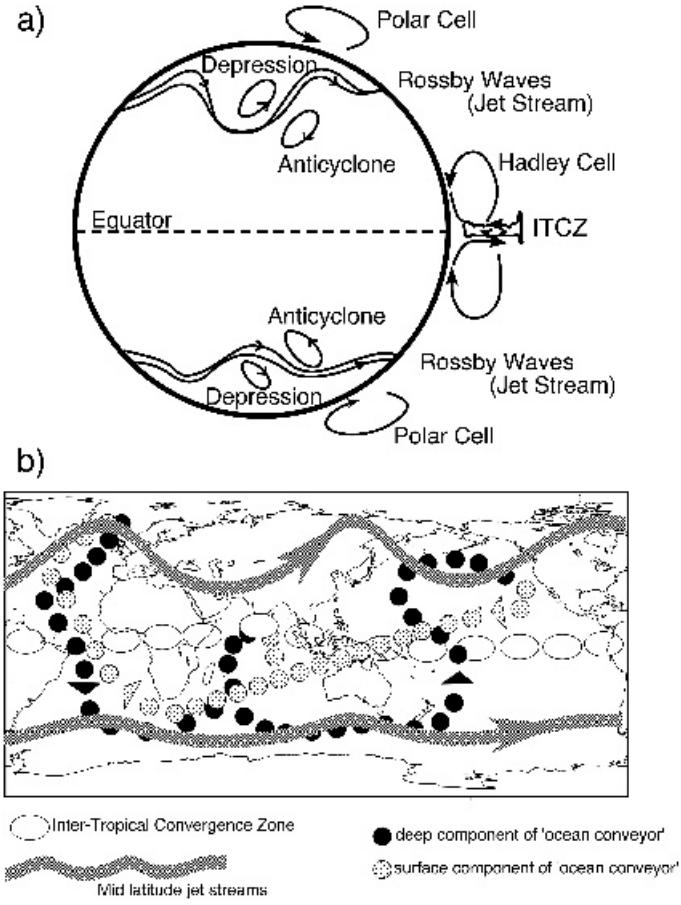

Figure 2.2 Illustration of the main features of the atmospheric (a) atmospheric and oceanic (b) circulation. The atmospheric circulation is determined primarily by the net radiation budgets (excess in the tropics and deficit near the poles) and the rotation of the Earth (especially the Rossby waves). The thermohaline circulation of the ocean (lines of shaded circles), often referred to as the 'ocean conveyor belt', results in the movement of water throughout the major ocean basins of the world over periods of hundreds to thousands of years. The black circles show the deep ocean conveyor, and the grey the surface component (see also Figure 1.17)

Table 2.1 Fundamental equations solved in GCMs

1. *Conservation of energy* (the first law of thermodynamics)
   i.e. Input energy = increase in internal energy plus work done
2. *Conservation of momentum* (Newton's second law of motion)
   i.e. Force = mass × acceleration
3. *Conservation of mass* (the continuity equation)
   i.e. The sum of the gradients of the product of density and flow-speed in the three orthogonal directions is zero. This must be applied to air and moisture for the atmosphere and to water and salt for the oceans, but can also be applied to other atmospheric and oceanic 'tracers' such as cloud liquid water.
4. *Ideal gas law* (an approximation to the equation of state – atmosphere only)
   i.e. Pressure × volume is proportional to absolute temperature × density

that describe the movement of energy, momentum and various tracers (e.g. water vapour in the atmosphere and salt in the oceans) and the conservation of mass is therefore required. Generally the equations are solved to give the mass movement (i.e. wind field or ocean currents) at the next timestep, but models must also include processes such as cloud and sea ice formation and heat, moisture and salt transport. The first step in obtaining a solution is to specify the atmospheric and oceanic conditions at a number of 'grid points', obtained by dividing the Earth's surface into a series of rectangles, so that a traditionally regular grid results (Figure 2.3). Conditions are specified at each grid point for the surface and several layers in the atmosphere and ocean. The resulting set of coupled non-linear equations is then solved at each grid point using numerical techniques. Various techniques are available, but all use a timestep approach.

Although GCMs formulated in this way have the potential to closely approach the real oceanic and atmospheric situation, at present there are a number of practical and theoretical limitations. The prime practical consideration is of the time needed for the calculations. For example, one particular low-resolution AGCM requires around 48 Mbytes of memory, whereas a more recent, higher resolution, version of the model requires over 160 Mbytes. Much of this stored information must be accessed and updated at each model timestep and this places a strain on the resources of even the largest and fastest computers (cf. Figure 1.5). Since the accuracy of the model partly depends on the spatial resolution of the grid points and the length of the timestep, a compromise must be made between the resolution desired, the length of integration and the computational facilities available. At present, atmospheric grid points are typically spaced between 2° and 5° of latitude and longitude apart and timesteps of approximately 20–30 minutes are used. Vertical resolution is obtained by dividing the atmosphere into between six and fifty levels, with about twenty levels being typical.

The ocean is a three-dimensional fluid that must be modelled using the same principles as for the atmosphere. As well as acting as a thermal 'fly-wheel' for the climate

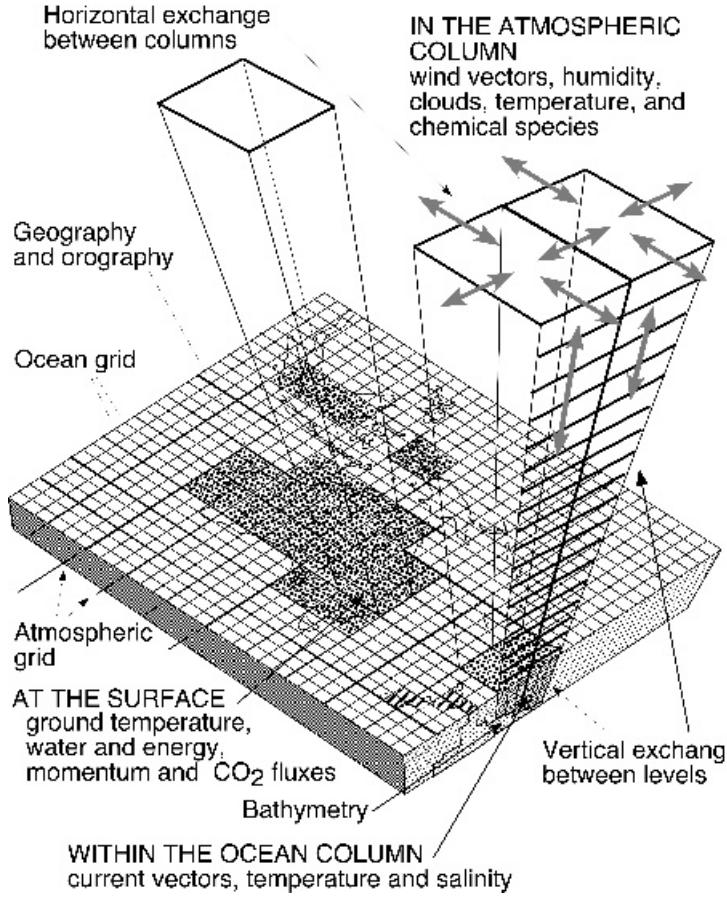

Figure 2.3 Illustration of the basic characteristics of a three-dimensional climate model, showing the manner in which the atmosphere and ocean are split into columns. Both atmosphere and ocean are modelled as a set of interacting columns distributed across the Earth's surface. The resolutions of the atmosphere and ocean models are usually different

system, the ocean also plays a central role in the carbon cycle, accounting for approximately half of the carbon absorbed from the atmosphere every year. The dynamics of the ocean are governed by the amount of radiation available at the surface and by the wind stresses imposed by the atmosphere. Ocean modellers must also track the salt in the ocean. Evaporation, precipitation, sea ice formation and river discharge affect the salinity of the ocean, which in turn affects the density of the water. The flow of ocean currents is also constrained by the positions and shapes of the continents (Figure 2.2). Ocean GCMs calculate the temporal evolution of oceanic variables (velocity, temperature and salinity) on a three-dimensional grid of

points spanning the global ocean domain. Although early climate model simulations incorporated only very simple models of the ocean, which do not explicitly include ocean dynamics, the incorporation of a dynamic ocean is now an essential part of any state-of-the-art climate model.

Modelling a full three-dimensional ocean is made difficult by the fact that the scale of motions in the oceans is much smaller than in the atmosphere (ocean eddies are around 10–50 km compared to around 1000 km for atmospheric eddies) and that the ocean also takes very much longer to respond to external changes (cf. Table 1.2). The deep water circulation of the ocean (Figure 2.2) can take hundreds or even thousands of years to complete. Ocean models that include these dynamic processes are now routinely coupled with atmospheric GCMs to provide our most detailed models of the climate system. The formation of oceanic deep water is closely coupled to the formation and growth of sea ice, so that representative ocean dynamics demands effective modelling of the dynamics and thermodynamics of sea ice. Modelling groups are continuously faced with the problem of dealing with a complex, interacting and diverse collection of models, demanding new skills and approaches.

Originally, computational constraints dictated that global circulation models could only run for very short periods. For the atmosphere this meant only simulating a particular month or season, rather than a full seasonal cycle, although now all models include a seasonal cycle and most include a diurnal cycle. For the oceans, restrictions of computer power meant that the models were used before they had fully equilibrated. This could result in the 'drift' of the ocean climate away from present-day conditions, which was often corrected by applying adjusting fluxes at the ocean surface to compensate for systematic errors which persist at equilibrium. This was a particular problem for early coupled OAGCMs, but most modern coupled models have overcome this problem. The importance of removing such arbitrary adjustments and of including realistic time-dependent phenomena is now well established, and modellers have striven to include increasing numbers of these phenomena as well as using the increased computer power to provide higher resolution and better physics (cf. Figure 2.1).

It is important to identify the very different aims of those developing and using GCMs as compared to the designers of numerical weather forecast models. The latter are prediction tools, while GCMs can represent only probable conditions. For this reason, many GCM integrations must be performed and their results averaged to generate an ensemble before a climate prediction can be made.

Computational constraints lead to problems of a more theoretical nature. With a coarse grid spacing, small-scale atmospheric motions (termed sub-gridscale), such as thundercloud formation, cannot be modelled, however important they may be for real atmospheric dynamics. Fine grid models can be used for weather prediction because the integration time is short. In contrast, climate models must mostly rely on some form of parameterization of sub-gridscale processes (see Section 5.2.4). Some progress has been made in incorporating cloud-resolving models into GCMs and this is discussed in Chapter 5.

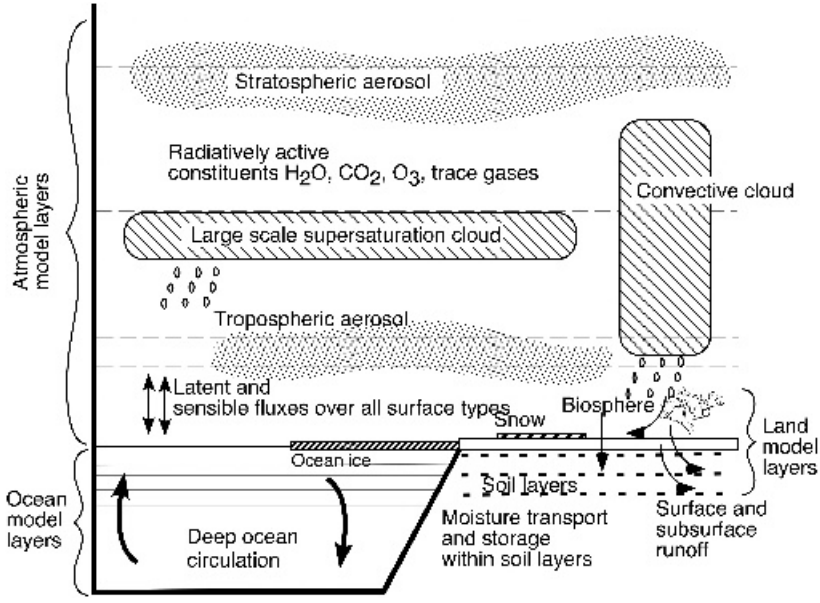

Figure 2.4 Schematic illustration of the processes in a single column of a global circulation climate model. In most models, two types of cloud are treated. In this example, soil moisture is modelled in a number of layers, and tropospheric and stratospheric aerosols are included. (Reproduced with permission from Hansen *et al*. (1983), *Mon. Wea. Rev.*, **111**, 609–662

Some of the processes usually incorporated into global circulation climate models are shown in Figure 2.4. Within the atmosphere, modellers adopt an approach similar to that used for the RC models in calculating heating rates (although they are often computationally simpler), but also often include cloud formation processes as part of the convection and consider in detail the effects of horizontal transport. Ocean models must take into account how the radiation from the atmosphere is absorbed in the upper layers of the ocean in an analogous manner along with the factors that affect the ocean salinity. The interaction between the land or ocean surface and the near-surface layer of the atmosphere, however, must be parameterized. Detailed consideration of these transfer processes is computationally too demanding for explicit inclusion. Commonly, the surface fluxes of momentum, sensible heat and moisture are taken to be proportional to the product of the surface wind speed and the gradient of the property away from the surface. More detailed aspects of ocean and atmospheric circulation models will be considered in Chapter 5.

2.2.5 Stable isotopes and interactive biogeochemistry

The many roles of the biosphere of importance to the climate include the exchange of carbon and other elements; the transfer of moisture from the soil into the atmosphere; modification of the albedo, which changes the amount of radiation absorbed

by the climate system; and modification of the surface roughness, which alters the exchange of momentum. The interactive nature of the plant life of the planet has only fairly recently been included in climate models. The first approach was to delineate geographic boundaries of biomes (species characterized by similar climate demands) using simple predictors available from GCMs such as temperature, precipitation and possibly sunshine or cloudiness. Attempts made to evaluate these methods included using palaeo-reconstructions of vegetation cover during past epochs. Recently, modellers have included ecological succession models into their GCMs and have been able to make sub-gridscale features of the terrestrial biosphere interactive. These interactive biosphere models are still in their infancy but are beginning to provide useful predictions of responses of the biosphere to climate including the issue of possible future CO_2 fertilization of the biosphere. Tracking various isotopes in the water cycle has illuminated diverse aspects of bio-climate modelling and model validation.

Isotopic measurements have been used to illuminate aspects of the water and chemical budgets of the Amazon Basin. The Amazon drains around one-third of the continental area of South America generating a massive discharge totalling about 20 per cent of the freshwater influx to the world's oceans. Understanding such an important source of non-saline water is critical for the ocean's climate, but the Amazon puzzled mid-twentieth century climate scientists. It was known that the basin-average Amazon precipitation is about $2200\,\mathrm{mm\,yr^{-1}}$ (which, multiplying by the basin's area of $6.5 \times 10^6\,\mathrm{km^2}$, implies a total water influx to the basin of $\sim 14 \times 10^{12}\,\mathrm{m^3\,yr^{-1}}$) but the Amazon's ultimate water discharge to the sea is 'only' $6 \times 10^{12}\,\mathrm{m^3\,yr^{-1}}$ – still a massive flow. So, something happens to $8 \times 10^{12}\,\mathrm{m^3}$ of water every year in the Amazon system. This mystery of the almost 60 per cent of rainfall that does not run to the sea was solved in the 1970s using measurements of the stable isotopes of water.

The dominant atmospheric flow over the Amazon is along the equator from east to west. Water evaporates from the equatorial Atlantic and this moist air is carried by the trade winds up-river to the Andes. Precipitation falls as the air passes over the land and is lifted towards the mountains (Figure 2.5a). If this were as simple as depicted, all the precipitation would appear as river discharge instead of 60 per cent being 'lost'. Also the rainfall would display a straightforward decrease in heavy water isotopes, $^1HD^{16}O$ and $^1H_2{}^{18}O$, because these form precipitation more readily than the common and lighter water molecule $^1H_2{}^{16}O$. Measurements of D and ^{18}O enrichments do show fairly steady decreases inland over all continents but, in the Amazon, the slopes are much shallower than anywhere else. It seems that some of the 'heavy' rain falling in the Amazon re-enters the atmosphere. Efficient recycling of moisture re-inserts heavier isotopes (as well as normal water) back into the atmosphere, and this is the reason that the depletions of D and ^{18}O measured in Amazon rainfall reduce more slowly inland than in other continents (Figure 2.5b). This means that most evaporation is not from water bodies such as lakes and the river itself, because these would preferentially evaporate light isotopes. The majority of the Amazon's water recycling must be transpiration through plants or re-evaporation of

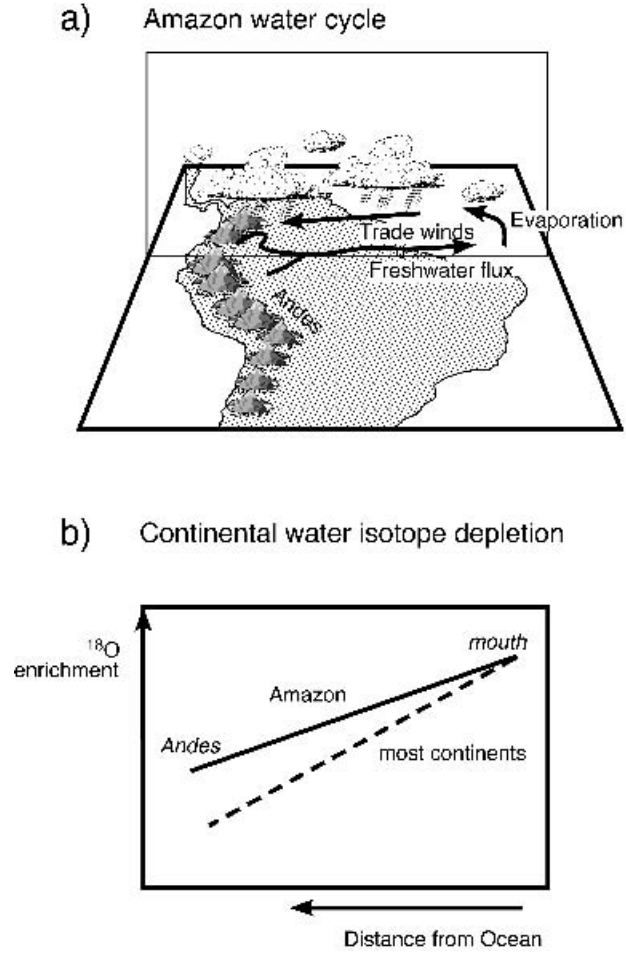

Figure 2.5 (a) Schematic illustration of the water cycle in the Amazon Basin. The Andes Mountains provide an effective barrier to moisture from the Pacific Ocean, meaning that moisture in the upper basin is transported from the Atlantic Ocean and is returned to the ocean by the river. (b) The progressive recycling of moisture by non-fractionating processes (transpiration and canopy evaporation) as it travels from the mouth to the Andes means that the gradient of heavy isotope enrichment is less than for other, less heavily vegetated continents

water caught on foliage: both are non-fractionating processes i.e. they do not distinguish between light and heavy isotopes.

The isotopic measurements showed that the Amazon Basin recycles about half its water. Specifically, the central Amazon has a water recycling time of about 5.5 days and, during this period, about half of all rainfall is re-evaporated or transpired and, of this, around 50 per cent falls again as precipitation. This moisture recycling within

the Amazon Basin leads to a seasonally averaged downward gradient of only 1.5‰ per 1000 km in ^{18}O going inland on an east to west transect as compared with 2.0‰ decrease observed for other continents. So, the puzzle of the missing Amazonian water was really an illusion. The river outflow really equals the available water but it is counted as precipitation many times.

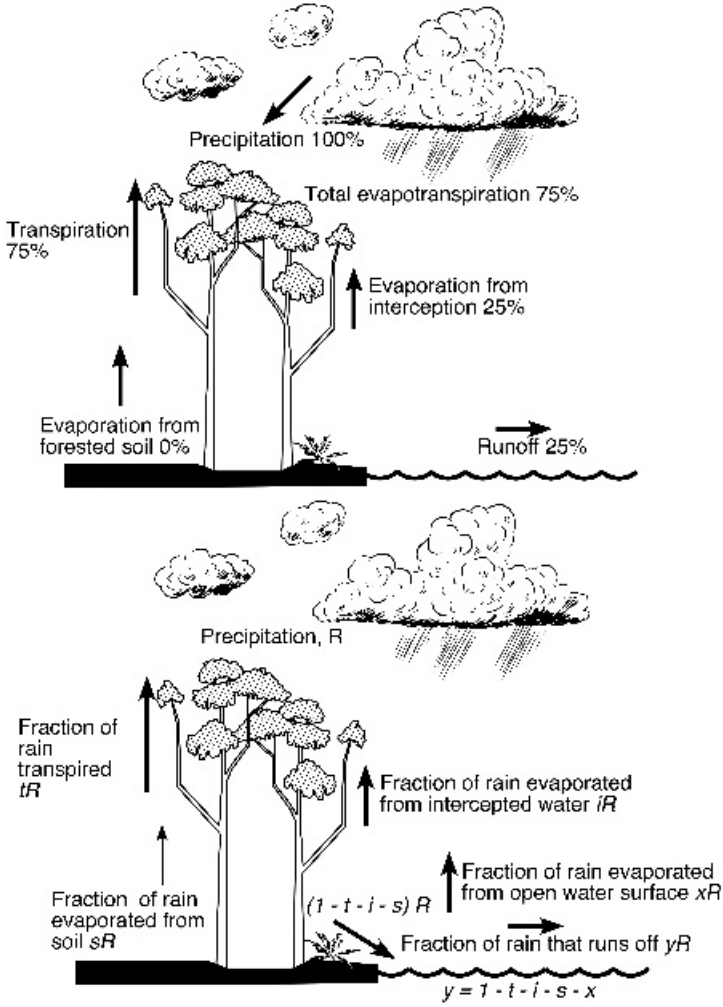

Figure 2.6 The hydrological cycle of the Amazon forest from a traditional viewpoint (top) and from an isotopic viewpoint (lower). In an isotopic view, the moisture fluxes must be differentiated into fractionating (separates heavier and lighter isotopes) and non-fractionating (no preferential separation) processes. This fractionation can be seen in the values of the fractions (y, t, i, s and x) of total rainfall (R). Typical values for y are between 0.25 and 0.35 and in the Amazon $t + i >> s + x$ because non-fractionating processes dominate (resulting in the gradient shown in Figure 2.5b)

This isotopic dimension focused attention on the importance of the biosphere in this major basin's hydrology around the time that GCMs acquired the ability to simulate some aspects of land–atmosphere interactions. The challenge for GCMs, to simulate the partition of Amazonian rainfall into appropriate proportions of evaporation, transpiration and runoff so that the gross basin hydrology is correct (i.e. only one-third of the rain going into runoff) and so that the isotopic recycling occurs through non-fractionating processes, remains today. The different representations of the relative proportions of runoff, re-evaporation from the canopy, transpiration and other evaporative components (Figure 2.6) may account for the range of temperature sensitivities among the large number of GCM simulations of Amazonian deforestation (see Figure 1.15b). GCMs have only recently begun to include open water elements such as lakes and rivers and, as yet, very few track isotopic ratios.

The stable isotopes of carbon (^{13}C and ^{12}C) have also begun to be incorporated into some biospheric components of GCMs. This inclusion is to try to improve understanding of the substantial year-to-year variation in the annual increase in atmospheric carbon dioxide despite the relatively constant input due to fossil fuel emissions. Interannual variations in the uptake of carbon by the biosphere are, very likely, responsible for this observed variation. The biosphere, particularly in heavily forested regions such as the Amazon, responds strongly to seasonal and interannual variations in the environment. The isotopic fractionation of stable carbon isotopes in various processes in the biosphere provides a means of studying the seasonal and interannual variations in biospheric activity. The $^{13}C/^{12}C$ ratio in plant material provides information about the physiological characteristics of the plant over the time the carbon was fixed and, together with atmospheric measurements of isotopes in CO_2, biospheric activity can thus be quantified.

2.3 HISTORY OF CLIMATE MODELLING

As climate models are readily described in terms of an hierarchy (e.g. Figure 2.1), it is often assumed that the simpler models were the first to be developed, with the more complex GCMs being developed most recently. This is not the case. Norman Phillips performed the classic global circulation computations in the mid-1950s. His model was limited as he had only 5 kilobytes of computer memory available (barely enough to store the textual information on this page) but it was successful. His model atmosphere was a cylindrical sheet to avoid complex geometry, with heating at the bottom and cooling at the top. His results demonstrated that it was possible to simulate the motion of the atmosphere on monthly and longer time-scales. This experiment led directly to the first atmospheric general circulation climate models (as we know them) being developed in the early 1960s, concurrently with the first RC models. Energy balance climate models, as they are currently known, were not described in the literature until 1969, and the first discussion of two-dimensional SD models was in 1970. The latter metamorphosed into EMICs in the 1990s and now represent the fastest evolving model group.

The first atmospheric general circulation climate models were derived directly from numerical models of the atmosphere designed for short-term weather forecasting. These had been developed during the 1950s and, around 1960, ideas were being formulated for longer period integrations of these numerical weather prediction schemes. It is in fact rather difficult to identify the transition point in many modelling groups. For example, Syukuro Manabe joined the National Oceanic and Atmospheric Administration's Geophysical Fluid Dynamics Laboratory (GFDL) in the USA in 1959 to collaborate in the numerical weather prediction efforts, and was to go on to become one of the world leaders in the climate modelling community. Scientists concerned with extending numerical prediction schemes to encompass hemispheric or global domains were also studying the radiative and thermal equilibrium of the Earth–atmosphere system. It was these studies that prompted the design of the RC models, which were once again spearheaded by Manabe, the first of these being published in 1961.

Other workers, such as Julián Adem, also expanded the domain of numerical weather prediction schemes in order to derive global climate models. The low-resolution thermodynamic model first described by Adem in 1965 is an interesting type of climate model, since it lies part-way towards the apex of the climate modelling pyramid (Figure 2.1) although the methodology is simpler in nature than that of an atmospheric GCM. Similar in basic composition to an EBM, Adem's model includes, in a highly parameterized way, many dynamic, radiative and surface features and feedback effects, giving it a higher position on the modelling pyramid.

Mikhail Budyko and William Sellers published descriptions of two very similar EBMs within a couple of months of each other in 1969. These models did not depend upon the concepts already established in numerical weather prediction schemes, but attempted to simulate the essentials of the climate system in a simpler way. The EBMs drew upon observational data derived from descriptive climatology, suggesting that major climatic zones are roughly latitudinal. As a consequence of the intrinsically simpler parameterization schemes employed in EBMs, they could be applied to longer time-scale changes than the atmospheric GCMs of the time. It was the work by Budyko and Sellers, in which the possibility of alternative stable climatic states for the Earth was identified, that prompted much of the interest in simulation of geological time-scale climatic change. Concurrently with these developments, RC models, usually globally averaged, were being applied to questions of atmospheric disturbance including the impact of volcanic eruptions and the possible effects of increasing atmospheric CO_2.

The desire to improve numerical weather forecasting abilities also prompted the fourth type of climate model, the SD model. A primary goal for dynamical climatologists was seen to be the need to account for the observed state of averaged atmospheric motion, temperature and moisture on timescales shorter than seasonal but longer than those characteristic of mid-latitude cyclones. One group of climate modellers preferred to design relatively simple low-resolution SD models to be used to illuminate the nature of the interaction between forced stationary longwaves and travelling weather systems. Much of this work was spearheaded in the early 1970s

by John Green. Theoretical study of large-scale atmospheric eddies and their transfer properties combined with observational work led to the parameterizations employed in two-dimensional climate models.

By 1980, this diverse range of climate models seemed to be in danger of being overshadowed by one type: the atmospheric GCM. Although single-minded individuals persevered with the development of simpler models, considerable funding and almost all the computational power used by climate modellers was being consumed by atmospheric GCMs. However, by the mid- to late 1980s, a series of occurrences of apparently correct results being generated for the wrong reason by these highly non-linear and highly complex models prompted many modelling groups to move backward, in an hierarchical sense, in order to try to isolate essential processes responsible for the results that are observed from more comprehensive models. When only the most topical (e.g. doubled CO_2) model experiments are considered, the trend has been for GCM experiments to replace simpler modelling efforts. For example, in 1980–81, from a total of 27 estimates of the global temperature change due to CO_2 doubling, only seven were made by GCMs. By 1993–4, GCMs produced 10 out of 14 estimates published. The IPCC science working group has underlined the value of results from simple models such as the 'box' models (described in Chapter 3) while its impacts and responses groups have spawned many EMICs (see Chapter 4). The strategy of intentionally utilizing an hierarchy of models was originally proposed in the 1980s by scientists such as Stephen Schneider at the US National Center for Atmospheric Research. More recently, the soundness of an hierarchy of climate modelling tools has been championed by Tom Wigley.

In 1969, Kirk Bryan at GFDL developed the ocean model that has become the basis for most current ocean GCMs. The model has been modified and has become widely known as the Bryan–Cox–Semtner model. Albert Semtner and Robert Chervin constructed a model version which is 'eddy resolving' and as a consequence pushed the simulations to higher and higher resolution (currently 1/6 degree). Others have chosen to implement the model in non-eddy resolving form and have been able to run the model at 2° resolution for direct coupling with an atmospheric model.

Even though this three-dimensional ocean model dates back to the late 1960s, most global climate models treated the oceans in much simpler ways until the early 1990s. The original GCMs used fixed ocean temperatures based on observed averaged monthly or seasonal values. This 'swamp' model allows the ocean to act only as an unlimited source of moisture. Naturally, it is very difficult in such a model to disturb the climate away from present-day conditions when such large areas of the globe remain unchanged. Following this, in the late 1980s, computation of the heat storage of the mixed layer of the ocean (approximately 70–100 m) was the most common approach. In this model the lower deep ocean layer acts only as an infinite source and sink for water. The mixed layer approach is appropriate for time-scales $\leq$30 years, beyond which the transfer of heat to lower levels becomes significant. The mixed layer model does not include the transport of heat by ocean currents. GCMs with mixed layer models either needed to specify ocean heat transports to

each grid square as a function of season, or make do with poor simulation of the ocean surface temperature in many areas.

The nature of climate model experiments has changed considerably as climate model complexity has increased. Early modellers were restricted to short 'experiment' and 'control' integrations, where the effects of a perturbation could be viewed in isolation. The inclusion of interactive oceans, biosphere, aerosols and clouds together with historical volcanic and solar forcings has led to the development of more complex experimental strategies. For example, early GCM experiments studying the effect of increased CO_2 were based on equilibrium experiments, where a model was allowed to equilibrate with the enhanced forcing. Modellers then subtracted the mean 'experiment' climate from the mean 'control' climate to determine the effect of the imposed change in CO_2. However, in the real world, climate forcings such as volcanic aerosols, solar variability, CO_2 and land-surface changes are transient, and different components of the model will react with different time-scales. Modellers must now focus on this aspect of the climate system and develop transient forcing datasets to be applied to their model.

The desire to make climate models more realistic has led to the involvement of many disciplines in the framework of climate modelling and hence to the realization that no one discipline can assume constancy in the variables prescribed by the others. Joseph Smagorinsky, who pioneered much of the early development in numerical weather prediction and steered the course of one of the flagships of climate modelling, NOAA's Geophysical Fluid Dynamics Laboratory, when commenting on the exponential growth in climate modelling research, noted that at the international conference on numerical weather prediction held in Stockholm in June 1957, which might be considered the first international gathering of climate modellers, the world's expertise comprised about 40 people, all loosely describable as physicists. In 2001, the IPCC Third Assessment Report (Working Group I alone) comprised hundreds of contributors and authors. A complete list of all who might term themselves climate modellers would today number tens of thousands and encompass a wide variety of disciplines. Interdisciplinary ventures have led to both rapid growth in insight and near-catastrophic blunders. Also, increasing complexity in narrowly defined areas such as land-surface climatology has forced upon modellers the recognition that other characteristics of their models, such as the diurnal cycle of precipitation, are being poorly predicted. The inclusion of more complex parameterizations of various subsystems, for example sea ice, is of little value if the atmospheric forcing in polar regions is inadequate. The tuning process that accompanies the addition of new model components might, in this situation, soak up these errors. Modellers must maintain an holistic view of their model.

2.4 SENSITIVITY OF CLIMATE MODELS

An important stage in the development of climate models is a series of sensitivity tests. Modellers examine the behaviour of their modelled climate system by altering one component and studying the effect of this change on the model's climate.

Equilibrium climatic states

As an example of a change in an internal variable we can consider the variation in the albedo, α, as a function of the mean global temperature in an EBM. Above a certain temperature, T_g, the planet is ice-free and the value of the albedo is independent of temperature. As it becomes colder we expect the albedo to increase as a direct result of increases in ice and snow cover. Eventually the Earth becomes completely ice-covered, at temperature T_i, and further cooling will produce no further albedo change. This could be expressed in the form

$$\begin{aligned} \alpha(T) &= \alpha_i && \text{for } T \le T_i \\ \alpha(T) &= \alpha_g && \text{for } T \ge T_g \\ \alpha(T) &= \alpha_g + b(T_g - T) && \text{for } T_i < T < T_g \end{aligned} \tag{2.2}$$

where b is the rate of change of α as the temperature decreases. T_i is usually assumed to be 273 K but may range between 263 and 283 K. If we are concerned with equilibrium conditions (i.e. when the left-hand side of Equation (2.1) is zero) we can calculate $R\uparrow$ for a series of temperatures and $R\downarrow$ for a series of albedos and show the results graphically. The points of intersection of the curves occur when emitted and absorbed radiation fluxes balance (i.e. $R\downarrow = R\uparrow$) which represent the equilibrium situations (Figure 2.7). Any slight imbalances between the fraction of the incident solar radiation, S, absorbed, $S(1 - \alpha(T))$, and the emitted longwave flux at the top of the atmosphere, approximated by $\varepsilon\sigma T^4$ where ε is the emissivity, lead to a

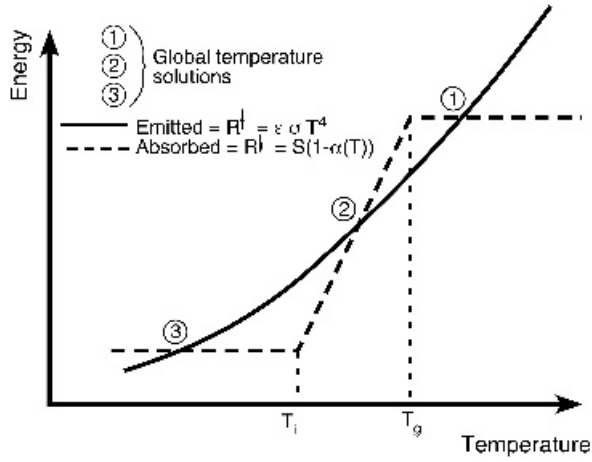

Figure 2.7 The three equilibrium temperature solutions for a zero-dimensional global climate model are shown at the intersection between the curves of emitted infrared radiation $R\uparrow$ and absorbed solar radiation $R\downarrow$. They are: (1) an ice-free Earth; (2) an Earth with some ice; (3) a completely ice-covered Earth (reproduced with permission from Crafoord and Källén (1978), *J. Atmos. Sci.*, **35**, 1123–1125

change in the temperature of the system at the rate $\Delta T/\Delta t$, the changes serving to return the temperature to an equilibrium state. However, there are three equilibrium solutions, as shown in Figure 2.7: an ice-free Earth (1), a completely glaciated (or 'Snowball') Earth (3) and an Earth with some ice (2) (e.g. the present situation of the planet). All are possible.

Stability of model results

Great care must be taken in choosing the constants for any parameterization scheme in any model. If values have been determined solely from empirical evidence, it may be that they are appropriate only for the present day, with the result that the model is likely to be constrained to predict the present-day situation and thus the less likely it is to be able to respond realistically to perturbations.

For 'external stability', we can test the response of the model to perturbations in the solar constant, since this is a convenient method of exploring climate model structure. Figure 2.8 shows the way in which $\overline{T}$ changes as the total incident radiation, μS, changes. Reduction of the solar constant to some critical value ($\mu_c S$) means that the number of solutions is reduced from two to one. Below $\mu_c S$, no solution is possible. This point is termed the bifurcation point. For values of incoming radiation, μS, less than $\mu_c S$, temperatures are so low that the albedo, $\alpha(T, \phi)$, becomes very close to or equal to 1 and thus it is impossible to regain energy balance. However, if some limit is put on how high the albedo may become, as is usually the case, e.g. $\alpha \leq 0.75$, the solution becomes what might be described as an ice-covered Earth.

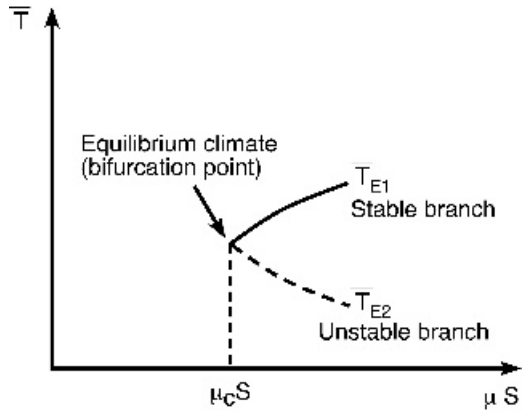

Figure 2.8 The equilibrium climate bifurcation point. For values of the solar luminosity given by μS where μ is a fractional premultiplier of the solar constant S, such that $\mu S > \mu_c S$, there are two solutions, whereas below this critical value no solutions exist. Changes in solar radiation lead to either a stable or an unstable equilibrium climate, illustrated here by the two equilibrium branches

'Internal stability' concerns the response of each branch in Figure 2.8 to perturbations from equilibrium which are created by internal factors. To determine if temperatures will return to equilibrium after the perturbation, we can use a time-dependent formulation and postulate a new value for $\overline{T}$ that is close to the equilibrium climate already calculated at that level of μS. This change can be computed iteratively until it is determined whether the values do regain the original $\overline{T}$ solution. If it is regained, then the solution is said to be internally stable. In Figure 2.8, only the top branch is stable because the model preserves $\overline{T}$ as proportional to μS. Using this method, it is possible to determine whether the model is transitive or intransitive, these terms being defined in Figure 2.9. The identification of almost intransitivity, also defined in Figure 2.9, is not possible in this manner.

Equilibrium conditions and transitivity of climate systems

Such a simple model has some very obvious limitations. However, it not only shows one means of analysing the results of climate models, it also indicates some of the more general problems associated with the solutions; in particular, the question of whether or not all three equilibrium states identified are 'stable' and capable of persisting for long periods of time. Many non-linear systems, even ones that are far simpler than the climate system, have a characteristic behaviour termed almost intransitivity. This behaviour is illustrated in Figure 2.9. If two different initial states of a system evolve to a single resultant state as time passes, the system is termed a transitive system. State A for this transitive system would then be considered the solution or normal state and all perturbed situations would be expected to evolve to

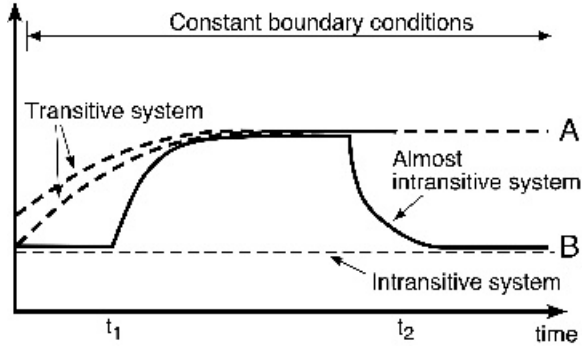

Figure 2.9 The behaviour of three types of climate system: transitive, intransitive and almost intransitive with respect to the initial state. In a transitive system, two different initial states evolve into the same resultant state, A. An intransitive system exhibits the 'opposite' behaviour, with more than one alternative resultant state. The characteristic of an almost intransitive state is that it mimics transitive behaviour for an indeterminate length of time and then 'flips' to an alternative resultant state (reproduced by permission of National Academies Press, 1975)

it. At the other extreme, an intransitive system has at least two equally acceptable solution states (A and B), depending on the initial state.

Difficulty arises when a system exhibits behaviour which mimics transitivity for some time, then flips to the alternative state for another (variable) length of time and then flips back again to the initial state and so on. In such an almost intransitive system it is impossible to determine which is the normal state, since either of two states can continue for a long period of time, to be followed by a quite rapid and perhaps unpredictable change to the other. At present, geological and historical data are not detailed enough to determine for certain which of these system types is typical of the Earth's climate. In the case of the Earth, the alternative climate need not be so catastrophic as complete glaciation or the cessation of all deep ocean circulation. It is easy to see that, should the climate turn out to be almost intransitive, successful climate modelling will be extremely difficult. Current studies of the climate as a chaotic system have focused on determining the characteristics of a climate attractor. The behaviour of the simple model of Edward Lorenz (Figure 2.10) has been used as an example of such an attractor, but no definitive conclusions have been reached on the nature of this attractor (if it exists) and no clear statements can be made regarding the transitivity of the climate system.

Measures of climate model sensitivity

The magnitude and direction of the sensitivity of any climate model to a known forcing are important characteristics. Although the term 'sensitivity' has recently

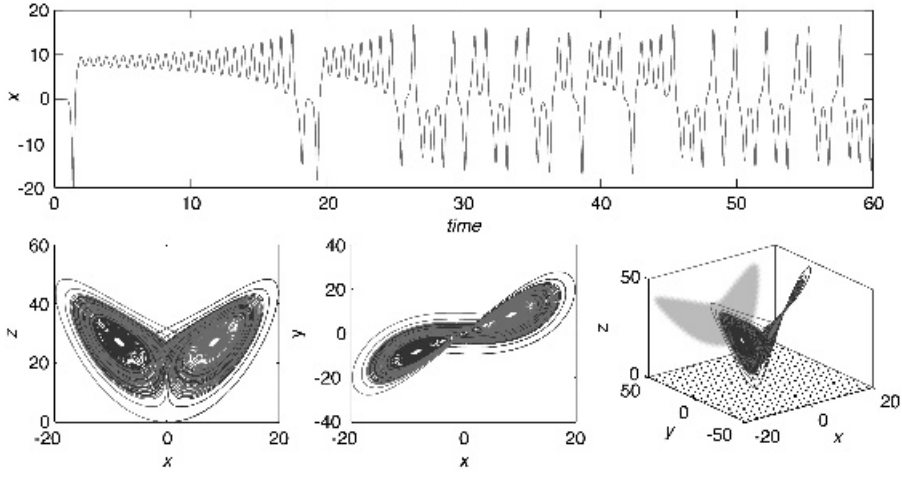

Figure 2.10 The 'Lorenz Butterfly'. A Poincaré section, showing the 'climate attractor' for the simple climate model constructed by Edward Lorenz in the 1960s. The system is characterized by three variables (x, y and z), which pinpoint the state of the system in a three-dimensional space. The apparently disordered behaviour of the system indicated in the graph in the top left conceals the structure which is apparent when the system is examined in three dimensions. Since the system never repeats itself exactly, the track never crosses itself

acquired mystique, the concept is straightforward. Most people, if pricked by a pin, exhibit a sensitivity and demonstrate this by a recognizable and quantifiable response. This response, although not identical in all subjects (a child might cry, while an adult would not), is readily differentiable from the generalized response to being hit by a flying cricket ball or baseball. The direction of both responses is generally negative and the magnitudes differ. The same is true for climate models.

Ideally, a climate model to be used for prediction should exhibit sensitivities that are commensurate with equivalent observable responses. However, this is not easy to check. Thus, for us to have confidence in model predictions of temperature increases in response to doubling or quadrupling of CO_2, we would like to know whether models of Venus, which has a massive greenhouse, are correct, or whether models of the Earth can correctly hindcast past periods when CO_2 and other greenhouse gas concentrations were much higher than today. Even for the single situation of doubled CO_2, there is a range of different measures of climate (and climate model) sensitivity including:

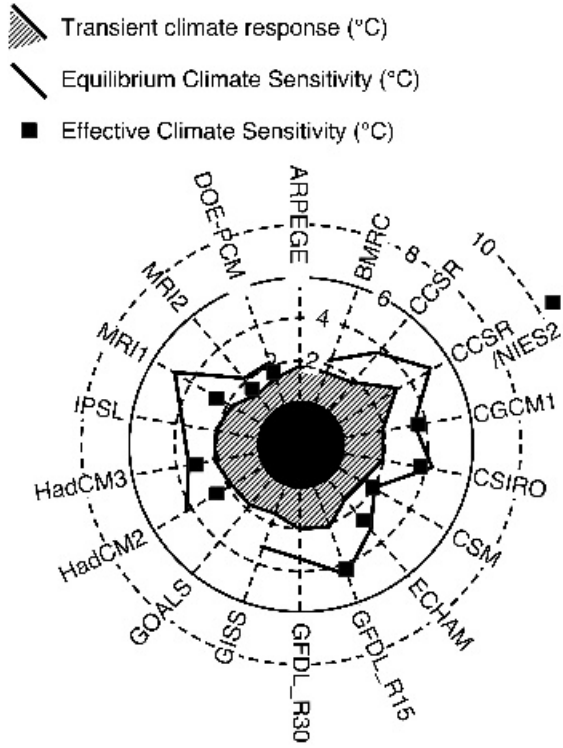

Figure 2.11 The three segments of the circle contain three different measures of modelled climate sensitivity derived for the IPCC Third Assessment Report. These sensitivities (shown by the length of the radial lines) are: (i) transient climate response; (ii) equilibrium climate sensitivity and (iii) effective climate sensitivity. Within segment measures are comparable but between segment comparisons are not valid (created from Table 9.1 from IPCC TAR WGI)

- transient climate response;
- equilibrium climate sensitivity (mixed layer ocean);
- effective climate sensitivity (deep ocean); and
- equivalent climate sensitivity.

These are illustrated in Figure 2.11 to describe the climate change predictions included in the IPCC Third Assessment Report. Different modellers choose different sensitivity measures and the result is a scatter of estimates that must be fed to policymakers.

Climate sensitivity measures can take many other forms, some of which were discussed in Chapter 1. Many modellers now prefer to evaluate models by reviewing their simulation of the twentieth-century climate. Sensitivity measures can be contrived that evaluate regional responsiveness to known forcings, such as the extent of the monsoonal activity or variations in seasonal snow cover.

Usually, the greatest confidence tends to be placed in climate models that exhibit sensitivities most like those observed. However, even this, apparently reasonable, view may produce excessive confidence because of the rather narrow climatic experiences during the observable record.

2.5 PARAMETERIZATION OF CLIMATIC PROCESSES

The climate system is a physical/chemical/biological system possessing infinite degrees of freedom. Any attempt to model such a highly complex system is fraught with dangers. It is (unfortunately) necessary to represent a distinct part, or more usually many distinct parts, of the complete system by imprecise or semi-empirical mathematical expressions. Worse still is the need to neglect completely many parts of the complete and highly complex system. This process of neglect/semi-empirical or imprecise representation is termed parameterization. Parameterization can take many forms. The simplest form is the null parameterization where a process, or a group of processes, is ignored. The decision to neglect these can only be made after a detailed consideration of their importance relative to other processes being modelled. Unnecessary computing time should not be spent on processes that can be adequately represented in some simpler way, or on processes that have relatively little effect on the climate at the scale of the model. Processes treated in this way are always candidates for improvement in later versions of the model.

Climatological specification, usually by prescribing observed averages, is a form of parameterization widely used in most types of model. In the 1970s, it was not uncommon to specify oceanic temperatures (with a seasonal variation) and in some of these models the clouds were also specified. When considering climate sensitivity experiments, it is important to recognize all such prescriptions because feedback features of the climate system will have been suppressed. Even today, most models specify the land-surface characteristics and few models permit the soil or vegetation to change in response to climate forcing. Only slightly less hazardous than this is the procedure by which processes are parameterized by relating them to present-day

observations: the constants or functions describing the relationship between variables are 'tuned' to obtain agreement. It is important that physically unrelated processes are not tuned together by this method. For example, the association of gradients in two different variables need not mean that the two are physically related. At best, this procedure presumes that constants and relationships appropriate to today's climate will still be applicable should some aspect of the climate alter.

The most advanced parameterizations have a theoretical justification. For instance, in some two-dimensional zonally averaged dynamical models, the fluxes of heat and momentum are parameterized via baroclinic theory (in which the eddy fluxes are related to the latitudinal temperature gradient). The parameterization of radiative transfer in clear skies is another example. To a good approximation, the atmosphere is like a set of parallel sheets of air with different properties. All that needs to be known is the vertical variation of temperature and humidity. Unfortunately, these parameterizations can lead to problems of uneven weighting because another process of equal importance cannot be adequately treated. In the case of heat and momentum transport by eddies, the contribution to these fluxes from stationary waves forced primarily by the orography and the land/ocean thermal contrast cannot be so easily considered. In radiation schemes, since clouds are three-dimensional and horizontal interactions are important, the parameterization of cloudy sky processes is not as advanced as for clear skies.

Interactions in the climate system

The interactions between processes in any model of the climate are crucially important. Wiring diagrams which show all these interactions are often used to illustrate the complexity of incorporating them all adequately. A most important concept in climate modelling is that the relative importance of processes and the way that different processes interlink is a strong function of the time-scale being modelled. The whole concept of parameterization is subsumed by this assertion. Establishing whether a system is likely to be sensitive to the parameterization used for a particular process often depends upon the response time of that feature as compared with other 'interactive' features. It is pointless to invoke a highly complex, or exceedingly simplistic, parameterization if it has been constructed for a time-scale different from that of the other processes and linkages in the model. The adage 'choosing horses for courses' is fundamental to the art of climate modelling.

As the climate system depends upon scales of motion and interactions ranging from molecular to planetary, and from time-scales of nanoseconds to geological eras, parameterizations are a necessary part of the modelling process. A decision is generally made very early in model construction about the range of space- and time-scales which will be modelled explicitly. Figure 2.12 illustrates the difficulty faced by all climate modellers. The constraints of computer time and costs and data availability restrict the prognostic (or predictive) mode. Outside this range there are 'frozen' boundary conditions and 'random variability'. Thus the two examples shown in Figure 2.12 illustrate the range of prognostic computations for (i) an Earth

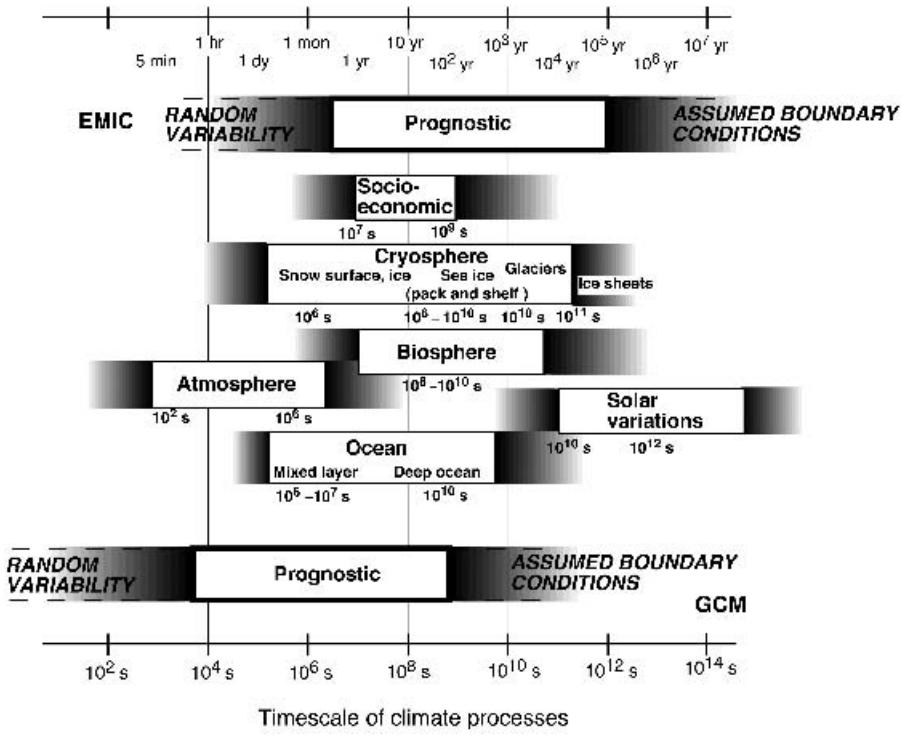

Figure 2.12 The importance of different temporal scales changes as a function of the type of model. The domain in which the model simulates the behaviour of the system is called 'prognosis'. It is expected that processes which fluctuate very rapidly compared with the prognostic time-scales will contribute only small random variability to the model predictions, while processes which fluctuate very slowly compared with the prognostic time-scale can be assumed to be constant. Two types of model are illustrated: an EMIC and a coupled ocean atmosphere general circulation model

System Model of Intermediate Complexity (EMIC, see Chapter 4), and (ii) a GCM focused on examining the effects of greenhouse gases on climate. In both cases, longer time-scales than those of concern to the modeller are considered as invariant and shorter time-scales are neglected as being random fluctuations, the details of which are of too short a period to be of interest.

Parameterizations must be mutually consistent. For instance, if two processes produce feedback effects of opposite sign, it is important that one process is not considered in the other's absence. An example is the effect that clouds have on the radiative heating of the atmosphere. Longwave radiation causes a comparatively rapid cooling at the cloud top, whereas the absorption of solar radiation results in heating. To consider the effect of clouds on only one of the two radiation fields may be worse than neglecting the effect of clouds entirely.

Figure 2.13 portrays an hierarchical averaging scheme for the climate system. The averaging processes are described in terms of a single variable, which could be as simple a component of the climate system as temperature, but could alternatively be, for example, representative of the carbon budget. There are two averaging subsystems in the lower part of the diagram, the one on the right-hand side being based on an initial averaging of the mean state in the vertical, followed by zonal and/or meridional averaging, while the one on the left-hand side is averaged first around latitude zones.

A traditional view of the averaging diagram in Figure 2.13 would be that the simplest approximations to the climate system (models) lie at the bottom of the diagram (*cf.* the base of the climate modelling pyramid: Figure 2.1) with increasing resolution being synonymous with increasing (and perhaps more desirable) complexity on ascent through the diagram. The apex of this diagram would be presumably that radiative and diffusive processes would be described at the molecular level in GCMs. Clearly such an ultimate goal is absurd, although it sometimes seems to be consistent with the desire for increasing complexity in a few GCM modelling groups. An alternative view might be that some of the more sophisticated lower-resolution SD models might contain the maximum information currently available/verifiable for very long-term integration periods. These would, therefore, be adequate and appropriate models since the climate system over long time-scales would be deemed to be insensitive to higher-resolution features. Thus, the key element in any model is the method of parameterization, whereby processes that cannot be treated explicitly

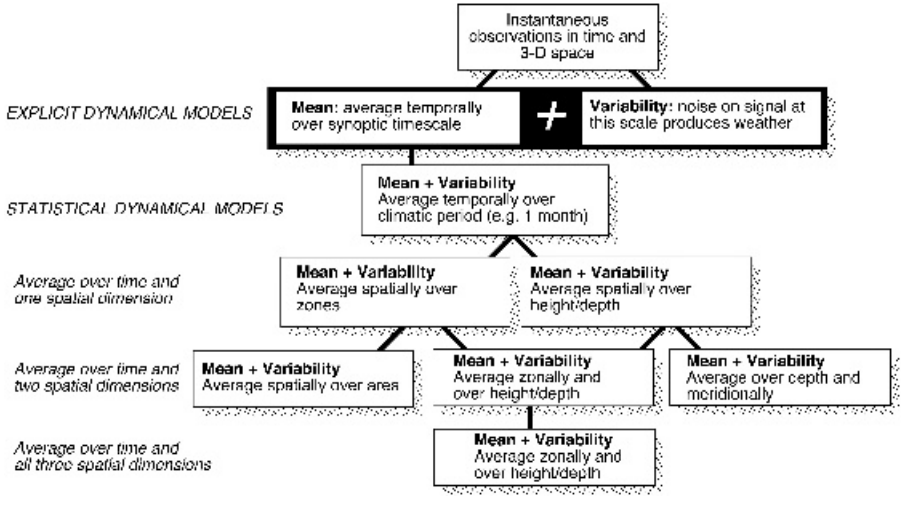

Figure 2.13 An hierarchical scheme for the averaging of climatological variables. In the lower half of the figure the representations of the climate system on the right-hand side involve averaging first over the atmospheric column, whereas the representations on the left-hand side involve zonal averaging first (adapted from Saltzman, 1978)

are instead related to variables that are considered directly in the model. An example is in EBMs where only the surface temperature is calculated explicitly. Since poleward transport of heat by atmospheric motions is important, this transport has to be parameterized in some way relating to the surface temperature, such as the latitudinal temperature gradient. In GCMs, those processes that operate on scales too small to be resolved by the model (sub-gridscale processes), like convective clouds, can, and do, exert influence on the atmosphere and must be parameterized in terms of available model variables.

The need for observations

All climate models need observed values for part of their input, especially in order to specify the boundary conditions, and all require observational data with which to compare their results. Some variables, such as surface pressure, are available worldwide and pose only the problem of evaluating the accuracy of the observed dataset. Others, however, are sparse in either time or space. Knowledge of sea ice extent is largely dependent on satellite observations, so that there is only a short observational record and, although satellites offer information on extent and concentration of sea ice, there is little they can say about ice thickness. Thus it is difficult to compare such observations with any long-term average values obtained from models. As modellers include ever more sophisticated components of the climate system in their experiments, there is a growing need for information on other parameters for validation of models. One particular example is 'soil moisture'. The term could mean all the water in a soil column (which might, technically, include large reserves of groundwater not accessed by the biosphere) or might be limited to the amount of water accessible to the biosphere (possibly termed 'available soil water'). There is no consistent definition between different modelling groups and no validation set comparable to traditional observations of pressure and temperature. There is still much to be done in the field of model validation.

2.6 SIMULATION OF THE FULL, INTERACTING CLIMATE SYSTEM: ONE GOAL OF MODELLING

Despite their limitations, coupled climate system models (*cf.* Section 2.2.4) represent the most complete type of climate model currently available. They illustrate the tremendous advances in our understanding of the atmosphere and ocean and our ability to model them over the 40–50 years since the first numerical climate models were produced. They do not yet, however, incorporate all aspects of the climate system and are therefore not at the apex of the pyramid in Figure 2.1. Indeed, it seems reasonable to suppose that the apex is unattainable. There will always be more features to include in the model. These models can, however, provide a great deal of information about the present climate and the possible effects of future perturbations. That these predictions are often contradictory is inevitable, given our incomplete knowledge of present conditions and developing understanding of the

controlling processes and interactions. If a model is built on sound theoretical principles, incorporates rational, and balanced, parameterization schemes, accounts for the major processes acting in the climate system and has been adequately tested against the available data, its results should be treated with respect. The results provide at least an indication of the possible future climate conditions created by a perturbation in the forces controlling our present climate.

The rest of the book is structured so that the concepts upon which full three-dimensional models are based are introduced sequentially. Chapter 3 underlines the fundamental basis of climate modelling: the energy balance. Chapter 4 describes models which operate with intermediate complexity, often by reducing the problem to one or two dimensions, and which help to provide insight into the operation of the full climate system over protracted periods or pay particular attention to specific aspects.

The overt goal of the text is therefore clear: we are aiming towards Chapters 5 and 6 in which the big players, the coupled atmosphere–ocean models, are explained and the process of evaluating and using climate model results is described. The other equally valid and important goal is less obvious. Throughout the book we have tried to choose examples to illustrate and enhance understanding of the mechanisms controlling the climate, their complexities, time- and space-scales and interactions. Both goals are worthy of considerable effort.

RECOMMENDED READING

Adem, J. (1965) Experiments aiming at monthly and seasonal numerical weather prediction. *Mon. Wea. Rev.* **93**, 495–503.

Adem, J. (1979) Low resolution thermodynamic grid models. *Dyn. Atmos. Ocean.* **3**, 433–451.

Bourke, W., McAvaney, B., Puri, K. and Thurling, R. (1977) Global modelling of atmospheric flow by spectral methods. In J. Chang (ed.) *Methods in Computational Physics*, **17**, Academic Press, New York, pp. 267–324.

Bryan, K. (1969) A numerical method for the study of the world ocean. *J. Comput. Phys.* **4**, 347–376.

Budyko, M.I. (1969) The effect of solar radiation variations on the climate of the Earth. *Tellus* **21**, 611–619.

Garcia, R.R., Stordal, F., Solomon, S. and Kiehl, J.T. (1992) A new numerical model of the middle atmosphere, 1, dynamics and transport of tropospheric source gases. *J. Geophys. Res.* **97**, 12967–12991.

Gates, W.L. (1979) The effect of the ocean on the atmospheric general circulation. *Dyn. Atmos. Ocean.* **3**, 95–109.

Green, J.S.A. (1970) Transfer properties of the large-scale eddies and the general circulation of the atmosphere. *Quart. J. Roy. Meteor. Soc.* **96**, 157–185.

Hansen, J.E., Johnson, D., Lacis, A.A., Lebedeff, S., Lee, P., Rind, D. and Russell, G. (1981) Climate impact of increasing atmospheric CO_2. *Science* **213**, 957–1001.

Hasselmann, K. (1976) Stochastic climate models, Part 1. Theory. *Tellus* **28**, 473–485.

Held, I.M. and Suarez, M.J. (1978) A two-level primitive equation model designed for climate sensitivity experiments. *J. Atmos. Sci.* **35**, 206–229.

MacKay, R.M. and Khalil, M.A.K. (1994) Climate simulations using the GCRC 2-D zonally averaged statistical dynamical climate model. *Chemosphere* **29**, 2651–2683.

Manabe, S. and Bryan, K. (1969) Climate calculations with a combined ocean atmosphere model. *J. Atmos. Sci.* **26**, 786–789.
Manabe, S. and Möller, F. (1961) On the radiative equilibrium and heat balance of the atmosphere. *Mon. Wea. Rev.* **89**, 503–532.
Manabe, S. and Strickler, R.F. (1964) Thermal equilibrium of the atmosphere with a convective adjustment. *J. Atmos. Sci.* **21**, 361–385.
Potter, G.L., Ellsaesser, H.W., MacCracken, M.C. and Mitchell, C.S. (1981) Climate change and cloud feedback: the possible radiative effects of latitudinal redistribution. *J. Atmos. Sci.* **38**, 489–493.
Randall, D.A. (ed.) (2000) *General Circulation Model Development: Past, Present and Future.* International Geophysics Series, Vol. 70, Academic Press, San Diego, California, 807 pp.
Saltzman, B. (1978) A survey of statistical dynamical models of terrestrial climate. *Advances in Geophysics* **20**, 183–304.
Semtner, A.J. (1995) Modelling ocean circulation. *Science* **269**, 1379–1385.
Shine, K.P. and Henderson-Sellers, A. (1983) Modelling climate and the nature of climate models: a review. *J. Climatol.* **3**, 81–94.
Smagorinsky, J. (1983) The beginnings of numerical weather prediction and general circulation modeling: early recollections. In B. Saltzman (ed.) *Theory of Climate*. Academic Press, New York, pp. 3–38.
Smith, N.R. (1993) Ocean modelling in a global observing system. *Rev. Geophys.* **31**, 281–317.
Stone, P.H. (1973) The effects of large-scale eddies on climatic change. *J. Atmos. Sci.* **30**, 521–529.
Thompson, S.L. and Schneider, S.H. (1979) A seasonal zonal energy balance climate model with an interactive lower layer. *J. Geophys. Res.* **84**, 2401–2414.
US National Academy of Sciences (1975) *Understanding Climatic Change: A Program for Action.* Washington, DC, 239 pp.
Washington, W.M., Semtner, A.J. Jr, Meehl, G.A., Knight, D.J. and Mayer, T.A. (1980) A general circulation experiment with a coupled atmosphere–ocean and sea ice model. *J. Phys. Oceanogr.* **10**, 1887–1908.

Web resources

http://www.met-office.gov.uk/research/hadleycentre/	UK Meteorological Office: Hadley Centre
http://www.giss.nasa.gov/	NASA Goddard Institute for Space Studies
http://www.gfdl.gov/	The Geophysical Fluid Dynamics Laboratory
http://www.cgd.ucar.edu	US National Center for Atmospheric Research
http://www.cccma.bc.ec.gc.ca/eng_index.shtml	Canadian Centre for Climate Modelling and Analysis
http://www.dkrz.de/	Deutsches Klimarechenzentrum GmbH
http://www.bom.gov.au/bmrc/	Australian Bureau of Meteorology Research Centre

http://ugamp.nerc.ac.uk/	UK Universities Global Atmospheric Modelling Programme
http://www.mri-jma.go.jp/	Japanese Meteorological Agency: Meteorological Research Institute
http://www.climateprediction.net/	Climate Prediction.net
http://www.lmd.jussieu.fr/	Laboratoire de Météorologie Dynamique du CNRS
http://www.aip.org/history/climate/GCM.htm	The American Institute of Physics History of GCMs
http://www.cdc.noaa.gov/cdc/reanalysis/	NCEP/NCAR Reanalysis
http://www.cru.uea.ac.uk/cru/data	Climatic Research Unit, University of East Anglia, UK
http://nsidc.org/data/index.html	US National Snow and Ice Data Center

CHAPTER 3

Energy Balance Models

The more it snows,
(Tiddely pom),
The more it goes,
(Tiddely pom),
The more it goes,
(Tiddely pom),
On snowing . . .

From *The House at Pooh Corner*, by A.A. Milne (1928). Reproduced by permission of Methuen Children's Books, McClelland and Stewart, Toronto and E.P. Dutton, a division of NAL Penguin Inc.

3.1 BALANCING THE PLANETARY RADIATION BUDGET

There is an excellent book by E.A. Abbott, first published in 1884, which describes a world called 'Flatland', inhabited by two-dimensional beings and, finally, visited by a strange three-dimensional object: a sphere. The sphere passes through Flatland and is perceived by the inhabitants as being only a series of discs of changing radius. This glimpse of the three-dimensional 'reality' is impossible for most Flatlanders to comprehend. Climate modellers, on the other hand, are only too painfully aware of the multi-dimensional nature of the climate system. Those who design and work with one- and two-dimensional models are not uncomprehending of the missing dimensions but have chosen to use a simpler model type. They have two main reasons: (i) these models are simpler and therefore cheaper to integrate on computers and thus can be used for much longer or very many more integrations than full three-dimensional models and, (ii) being simpler, the models therefore represent particular features of the climate system more simply because other confusing features are removed. Thus modellers, unlike Flatlanders, recognize complexity and intentionally seek to reduce it. In this chapter, we explore some of their reasons and results.

Balancing the planetary radiation budget offers a first, simple approximation to a model of the Earth's climate. The radiation fluxes and the equator-to-pole energy

A Climate Modelling Primer, Third Edition. K. McGuffie and A. Henderson-Sellers.
 ISBN: 0-470-85750-1 (HB); 0-470-85751-X (PB)

transport are the fundamental processes of the climate system incorporated in EBMs. Originally, interest was stimulated by the independent results of Budyko and of Sellers in 1969. While many of the questions raised by these studies have since been answered, these models remain interesting tools for studying climate. This chapter describes how EBMs are constructed and outlines how these models have been used both to study and to illustrate characteristic components of the climate system.

3.2 THE STRUCTURE OF ENERGY BALANCE MODELS

The simplest method of considering the climate system of the Earth, and indeed of any planet, is in terms of its global energy balance. Viewing the Earth from outside, one observes an amount of radiation input which is balanced (in the long term) by an amount of radiation output. Since over 70 per cent of the energy which drives the climate system is first absorbed at the surface, the surface albedo will be predominant in controlling energy input to the climate system. The output of energy will be controlled by the temperature of the Earth but also by the transparency of the atmosphere to this outgoing thermal radiation. An EBM can take two very simple forms. The first form, the zero-dimensional model, considers the Earth as a single point in space having a global mean effective temperature, T_e. The second form of the EBM considers the temperature as being latitudinally resolved. Figure 3.1 illustrates these two approaches.

3.2.1 Zero-dimensional EBMs

In the first case shown in Figure 3.1, the climate can be simulated by considering the radiation balance. The total energy received from the Sun per unit time is $\pi R^2 S$ where R is the radius of the Earth. The total area of the Earth is, however, $4\pi R^2$. Therefore the time-averaged energy input rate is $S/4$ over the whole Earth. Hence,

$$(1-\alpha)S/4 = \sigma T_e^4 \tag{3.1}$$

where α is the planetary or system albedo, S is the solar constant ($1370\,\mathrm{W\,m^{-2}}$) and σ is the Stefan–Boltzmann constant. If the atmosphere of the planet contains gases which absorb thermal radiation then the surface temperature, T_s, will be greater than the effective temperature, T_e. The increment ΔT is known as the *greenhouse increment* and depends upon the efficiency of the infrared absorption. Thus the surface temperature can be calculated if ΔT is known since

$$T_S = T_e + \Delta T \tag{3.2}$$

For the Earth, the greenhouse increment due to the present atmosphere is about $\Delta T = 33\,\mathrm{K}$ and hence combining Equations (3.1) and (3.2) gives, for $\alpha = 0.3$, $T_s = 288\,\mathrm{K}$. (Note that the only prognostic variable in an EBM is the temperature, characterized as a surface temperature.)

If the planetary features were different, for example if the solar luminosity were $S = 2619\,\mathrm{W\,m^{-2}}$ and $\alpha = 0.7$, then $T_e = 242\,\mathrm{K}$. These are the values appropriate to

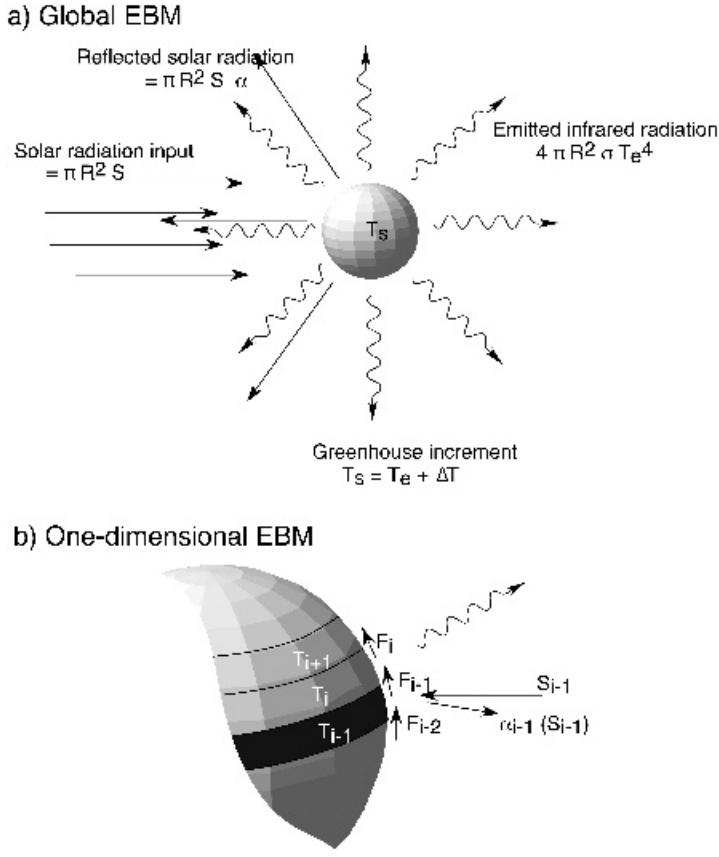

Figure 3.1 Energy transfers in (a) a global EBM and (b) a zonal EBM

the planet Venus which, while being closer to the Sun and hence enjoying greater incident solar radiation, is almost completely cloud-covered and thus has a very high planetary albedo. The albedo dominates the radiation balance, resulting in an effective temperature which is slightly lower than the Earth's T_e value of 255 K. However, the atmosphere of Venus is extremely dense and composed almost entirely of carbon dioxide. Hence, there is a very much greater greenhouse effect on Venus. The surface temperature of Venus has been found by spacecraft to be ~730 K and, although it is now believed that not all of this ΔT is due to greenhouse absorbers, they certainly contribute substantially. The other major contributor to surface heating on Venus is adiabatic warming in large regions of descending air (not included in EBMs).

In a simple EBM, the incoming and outgoing energy for the globe are balanced and a single climatic variable (the surface temperature, T) is calculated, i.e. T is the dependent variable for which the 'climate equations' are solved. The rate of change of temperature, T, with time, t, is caused by a difference between the top-of-the-

atmosphere (or planetary) net incoming, $R\downarrow$, and net outgoing, $R\uparrow$, radiative fluxes (per unit area):

$$mc\Delta T/\Delta t = (R\downarrow - R\uparrow)A_E \tag{3.3}$$

where A_E is the area of the Earth, c is the specific heat capacity of the system and m is the mass of the system.

This is a very general equation with a variety of uses. If, for example, the system we wish to model is an outdoor swimming pool, we can calculate the rate of temperature change in timesteps of 1 day from Equation (3.3). Suppose the pool has surface dimensions 30×10 m, is well mixed and is 2 m deep. Since 4200 J of energy are needed to raise the temperature of 1 kg of water by 1 K (4200 J kg^{-1} K^{-1} is the specific heat capacity of water), and 1 m^3 of water has a mass of 1000 kg, the pool has a total heat capacity equal to 2.52×10^9 J K^{-1}. If we assume that the difference between the absorbed radiation and the emitted radiation from the pool ($R\downarrow - R\uparrow$) is 20 W m^{-2} for 24 hours, then the difference in energy content of the pool for each 24-hour timestep is $20 \times 30 \times 10 \times 24 \times 60 \times 60$ J. Then, from Equation (3.3)

$$2.52 \times 10^9 \Delta T = 20 \times 30 \times 10 \times 24 \times 60 \times 60$$

Therefore,

$$\Delta T(\text{in one day}) = \frac{5.184 \times 10^8}{2.52 \times 10^9} \approx 0.2\text{K} \tag{3.4}$$

Thus, at this rate, it would take about a month to raise the temperature of the pool water by 6 K.

On the Earth, the value of c is largely determined by the oceans. The specific heat (J kg^{-1} K^{-1}) for water is around four times that for air and the mass of the ocean is also much greater than that of the atmosphere. For instance, if we assume that the energy is absorbed in the first 70 m of the ocean (the average global depth of the top or mixed layer) and that approximately 70 per cent of the Earth's surface is covered by oceans, then the value for C (the total heat capacity) comes from

$$C = 0.7\rho_w c_w d A_E = 1.05 \times 10^{23}\,\text{J K}^{-1} \tag{3.5}$$

where ρ_w is the density of water, c_w the specific heat capacity of water, d is the depth of the mixed layer and A_E is the Earth's surface area.

For our simple EBM of the Earth, the energy emitted, $R\uparrow$, can be estimated using the Stefan–Boltzmann law and the surface temperature, T. This value must be corrected to take into account the infrared transmissivity of the atmosphere τ_a, since $R\uparrow$ is the planetary flux. Therefore we can write

$$R\uparrow \approx \varepsilon\sigma T^4 \tau_a \tag{3.6}$$

The absorbed energy, $R\downarrow$, is a function of the solar flux, S, and the planetary albedo such that $R\downarrow = (1 - \alpha)S/4$. Equation (3.3) therefore becomes

$$\frac{\Delta T}{\Delta t} = \frac{1}{C}\left\{\frac{S}{4}(1-\alpha) - \varepsilon\tau_a\sigma T^4\right\} \tag{3.7}$$

This equation can be used to ascertain the equilibrium climatic state by setting $\Delta T/\Delta t = 0$. This use is complementary to the timestep mode described above. The result represents an 'ultimate' or equilibrium solution of the equation when the change in temperature has ceased. In this case

$$(1-\alpha)\frac{S}{4} = \varepsilon\tau_a\sigma T^4 \tag{3.8}$$

Using values of $S = 1370\,\mathrm{W\,m^{-2}}$, $\alpha = 0.3$, $\varepsilon\tau_a = 0.62$ and $\sigma = 5.67 \times 10^{-8}\,\mathrm{W\,m^{-2}\,K^{-4}}$ gives a surface temperature of 287 K, which is in good agreement with the globally averaged surface temperature today.

An alternative use of Equation (3.7) is similar to the calculation of the swimming-pool warming rate made above. Here, a timestep calculation of the change in T is made. This could be a response to an 'external' forcing agent, such as a change in solar flux or in the heat capacity of the oceans resulting from changes in their depth or area. Alternatively, the response could be determined by an 'interactive' climate calculation when one of the internal variables (e.g. α) alters.

3.2.2 One-dimensional EBMs

In the case where we consider each latitude zone independently,

$$S_i(1-\alpha(T_i)) = R\uparrow(T_i) + F(T_i) \tag{3.9}$$

where T_i represents $T_s(i)$, the surface temperature of zone i. Note that we now have an additional term $F(T_i)$ which refers to the loss of energy by a latitude zone to its colder neighbour or neighbours. So far, we have ignored any storage by the system since we have been considering the climate on time-scales where the net loss or gain of stored energy is small. Any stored energy would simply appear as an additional term, $Q(T_i)$, on the right-hand side of Equation (3.9).

Since the zero-dimensional model (Equation (3.8)) is a simplification of Equation (3.9), further discussion will consider the latitudinally resolved model and look in detail at the role of the terms involved.

Each of the terms in Equation (3.9) is a function of the predicted variable T_i. The surface albedo is influenced by temperature in that it is increased drastically when ice and snow are able to form. The radiation emitted to space is proportional to T^4 although, over the temperature range of interest (~250–300 K), this dependence can be considered linear. The horizontal flux out of the zone is a function of the difference between the zonal temperature and the global mean temperature. The albedo is described by a simple step function such that

$$\alpha_i \equiv \alpha(T_i)\begin{cases} = 0.6 & T_i \le T_c \\ = 0.3 & T_i > T_c \end{cases} \tag{3.10}$$

which represents the albedo increasing at the snowline; T_c, the temperature at the snowline, is typically between −10°C and 0°C. Because of the relatively small range of temperatures involved, radiation leaving the top of the latitude zone can be approximated by

$$R_i \equiv R\uparrow(T_i) = A + BT_i \tag{3.11}$$

where A and B are empirically determined constants designed to account for the greenhouse effect of clouds, water vapour and CO_2. The rate of transport of energy can be represented as being proportional to the difference between the zonal temperature and the global mean temperature by

$$F_i \equiv F(T_i) = k_t(T_i - \overline{T}) \tag{3.12}$$

where k_t is an empirical constant.

Incorporation of Equations (3.11) and (3.12) into Equation (3.9) forms an equation which can be rearranged to give

$$T_i = \frac{S_i(1-\alpha_i) + k_t\overline{T} - A}{B + k_t} \tag{3.13}$$

Given a first-guess temperature distribution and by devising an appropriate weighting scheme to distribute the solar radiation over the globe (because of the tilt of the Earth's axis, a simple cosine distribution with latitude does not work in the annual mean), successive applications of this equation will eventually yield an equilibrium solution. An alternative course of action is to explicitly calculate the time evolution of the model climate by including a term representing the thermal capacity of the system. The former method results in computationally faster results but the latter allows for more experimentation. Such models are relatively simple to construct on a personal computer in an accessible programming language, as is illustrated in Section 3.4.

3.3 PARAMETERIZING THE CLIMATE SYSTEM FOR ENERGY BALANCE MODELS

The model described above illustrates the basic principles of energy balance climate modelling. In this section we shall consider further each of the parameterization schemes and how they are developed.

As mentioned in Chapter 2, the first EBMs were found to be alarmingly sensitive to changes in the solar constant. Small reductions in solar constant appeared to cause catastrophic and irreversible glaciations of the entire planet. Such an effect, although extreme, suggests that such models might be utilized in studying large-scale glaciation cycles. This is indeed the case, but some preparation and background work on the mechanisms in the model must be undertaken before glaciation cycles can be simulated.

Albedo

The albedo parameterization in EBMs is based simply on the surface albedo being greater when the temperature is low enough to allow snow and ice formation. Two simple parameterizations are that the albedo increases instantaneously to an ice-covered value (Equation (3.10)), and a description, which might seem more appropriate, that the albedo increases linearly over a temperature interval within which the Earth can be said to be becoming increasingly snow-covered.

$$\begin{aligned} \alpha(T_i) &= b(\phi) - 0.009T_i \qquad T_i < 283\text{K} \\ \alpha(T_i) &= b(\phi) - 0.009 \times 283 \quad T_i \geq 283\text{K} \end{aligned} \tag{3.14}$$

Using empirical constants, $b(\phi)$, allows for the inclusion of a latitudinal variation of ice-free albedo which is not affected by temperature. The change in planetary albedo at the poles can then be made to be around half of that at the equator when the ice-free surface is replaced with an ice-covered one. This allows for the higher albedo of the ice-free ocean and enhanced atmospheric scattering, which occurs at the low solar elevations near the poles. The sensitivity is reduced by a factor of two but remains too high to explain a paradox termed the 'faint Sun–warm early Earth paradox'. This conundrum stems from the inference that, although the solar luminosity was only about 70 per cent of its present value during the first aeon of the Earth's history, the surface of the Earth seems not to have been glaciated to the extent which would be suggested by these EBM calculations (i.e. although little evidence exists for the period from 3.5 to 4.5 thousand million years ago, there is none to suggest a global glaciation).

The explanation for the apparent gross instability of the Earth's climate system to small perturbations in solar constant lies in the close coupling in the parameterizations of the temperature and planetary albedo. This strong dependency is, perhaps, not a good representation of the real system since, although the surface albedo is certainly influenced by temperature, the planetary albedo is affected by the presence of clouds and is also a function of latitude. For example, as latitude increases, the effect on the planetary albedo of adding more snow or ice tends to decrease.

The fundamental flaw in this albedo parameterization is the assumption of a very strong connection between the planetary albedo and the surface albedo. Clouds are responsible for the reflection of 70–80 per cent of the radiation that is reflected by the Earth. There is no clear relationship between surface temperature and cloudiness, which further reduces the connection between surface temperature and planetary albedo. In our parameterization of the albedo described above, by considering only the effect of ice and snow cover, it would appear at first glance that clouds have been ignored in the formulation of EBMs. This might be acceptable because the effect of an increase in cloudiness on the amount of absorbed solar radiation is approximately countered by the effect of clouds in retaining a greater proportion of emitted infrared radiation.

Outgoing infrared radiation

The Earth is constantly emitting radiation. Some of this radiation is absorbed by the atmosphere and re-emitted back to the ground. Parameterizations will involve some method of accounting for this greenhouse effect. One formulation is to match outgoing longwave radiation to surface temperature and to devise a linear relationship between the two. This was the method included in Equation (3.11). An alternative formulation is to modify the black body flux by some factor that accounts for the reduction in outgoing longwave radiation by the atmosphere, e.g.

$$R_i = \sigma T_i^4 [1 - m_i \tanh(19 T_i^6 \times 10^{-16})] \tag{3.15}$$

where m_i is the factor representing the atmospheric opacity. This formulation was derived empirically by Sellers. Parameterizations of infrared radiation in EBMs follow one or other of these structures.

Heat transport

The simplest form of heat transport which may be incorporated into an EBM is that of Equation (3.12). Here the flux out of a latitude zone is equal to some constant multiplied by the difference between the average temperature of the zone and the global mean temperature. A more complex method is to consider each of the transporting mechanisms separately, with the flux divergence being given by

$$\mathrm{div}(F) = \frac{1}{\cos\phi} \frac{\partial}{\partial y} [\cos\phi (F_o + F_a + F_q)] \tag{3.16}$$

where ϕ is latitude, y is the distance in the poleward direction and the three terms on the right represent transports due to ocean, atmosphere and latent heat:

$$\begin{aligned} F_o &= -\rho c_w K_o \frac{\partial T}{\partial y} \\ F_a &= -\rho c_a K_a \frac{\partial T}{\partial y} + \rho c_a \langle v \rangle T \\ F_q &= -\rho_w L_w K_q \frac{\partial q(T)}{\partial y} + \rho_w L_w \langle v \rangle T \end{aligned} \tag{3.17}$$

where K_o, K_a and K_q are all functions of latitude, $q(T)$ is the water vapour mixing ratio, $\langle v \rangle$ is the zonally averaged wind speed, ρ is the density, c the specific heat capacity and L the latent heat coefficient; subscripts a and w refer to air and water respectively. More realistic parameterizations might be expected to be more complicated. There are the two basically different methods of incorporating the div(F) term: the Newtonian form developed by Budyko (Equation (3.12)) or the eddy diffusive mixing form developed by Sellers (Equations (3.16) and (3.17)). The choice is, as is often the case in climate modelling, to weigh the extra detail offered by Sellers against the decreased computational time of Budyko's method.

3.4 BASIC MODELS

3.4.1 A BASIC EBM

This type of climate model is a useful teaching/learning tool. The program shown in Figure 3.2 was originally written for undergraduate use at the University of Liverpool in the early 1980s. It has been updated for desktop computers and rewritten into other languages but fundamentally the calculations are the same as they were in 1983. The program is available on the Primer CD that accompanies this book. The original source code is also included as a plain text file on the Primer CD.

The formulation of the EBM has been kept as simple as possible. The equations are those described in Section 3.2. The albedo parameterization is a simple 'on-off' step function based on a specified temperature threshold (see Equation (3.10)). The emitted longwave radiation is a linear function of the zonal surface temperature (see Equation (3.11)) and the transport term is given by Equation (3.12). The following sections contain a brief summary of the model presented in Figure 3.2 and suggest some exercises which demonstrate the model's behaviour.

Description of the EBM

The model is governed by the equation originally devised by both Sellers and Budyko in 1969:

$$\text{(Shortwave in)} = \text{(Transport out)} + \text{(Longwave out)} \tag{3.18}$$

which is formulated as

$$S(\phi)\{1-\alpha(\phi)\} = k_t\{T(\phi)-\overline{T}\} + \{A + BT(\phi)\} \tag{3.19}$$

where

k_t = the transport coefficient (here set equal to $3.81\,\mathrm{W\,m^{-2}\,^{\circ}C^{-1}}$),
$T(\phi)$ = the surface temperature at latitude ϕ,
$\overline{T}$ = the mean global surface temperature,
A and B are constants governing the longwave radiation loss (here taking values $A = 204.0\,\mathrm{W\,m^{-2}}$ and $B = 2.17\,\mathrm{W\,m^{-2}\,^{\circ}C^{-1}}$),
$S(\phi)$ = the mean annual radiation incident at latitude ϕ,
$\alpha(\phi)$ = the albedo at latitude ϕ.

Note that if the surface temperature at ϕ is less than -10°C the albedo is set to 0.62. The solar constant in the model is taken as $1370\,\mathrm{W\,m^{-2}}$.

The EBM is designed to be used to examine the sensitivity of the predicted equilibrium climate to changes in the solar constant. If the default values for the variables A, B, k_t and the albedo formulation are selected, an equilibrium climate which

```
10 '   Energy budget puzzle  1986     K.McGuffie & A.Henderson-Sellers
11 ''''''''''''''''''''''''''''''''''''''''''''''''''''''''''''''''''''''
12 '  Note that this is copyright material          '
13 '  (c) KMcG and AH-S 1986 All Rights Reserved    '
14 '  Unauthorised copying prohibited               '
15 ''''''''''''''''''''''''''''''''''''''''''''''''''''''''''''''''''''''
20 DIM S(18),ALBEDO(18),TM(18),LATZ$(18),TSTART(18),AL(18),TEMP(18)
30 DIM OL(18),ASOL(18),CLOUD(18)
40 FOR I = 1 TO 18
50 READ LATZ$(I)
60 NEXT I
70 DATA "80-90","70-80","60-70","50-60","40-50","30-40","20-30","10-20"," 0-10"
80 DATA " 0-10","10-20","20-30","30-40","40-50","50-60","60-70","70-80","80-90"
90 E$=CHR$(27):CLS
140 CALB = .5
150 IN= 3.14159/36!
160 P2=3.14159/2!
170 DEF FNR(X)=INT(100*X)/100
180 FOR LAT = 1 TO 18
190 READ S(LAT)
200 NEXT LAT
210 DATA 0.5,0.531,0.624,0.77,0.892
220 DATA 1.021,1.12,1.189,1.219
230 DATA 1.219,1.189,1.12,1.021
240 DATA .892,.77,.624,.531,.5
250 PRINT
275 COLOR 5,0
280 PRINT "*******************************************************************************"
285 COLOR 2,0
290 PRINT "               A   G L O B A L   E N E R G Y   B A L A N C E
300 PRINT "                                   M O D E L
310 PRINT "                                <<<<<<< >>>>>>>>>"
315 COLOR 5,0
320 PRINT "*******************************************************************************"
325 COLOR 2,0
330 PRINT:PRINT
370 PRINT
380 PRINT "    This model is similar to those of Budyko and Sellers.
390 PRINT "    You will be offered the opportunity to alter the
400 PRINT "    values of the parameters which control the model climate.
410 PRINT "
420 PRINT
425 COLOR 7,0
430 PRINT "
440 PRINT "              Press the space bar to continue
441 PRINT "                        Press <Escape> to abort":COLOR 3,0
442 LOCATE 23,1:PRINT " > > > > >     A C L I M A T E  M O D E L L I N G  P A C K A G E  < <
< < <"
443 LOCATE 25,1:PRINT"Copyright 1987  A. Henderson-Sellers & K. McGuffie. All Rights
Reserved.";
445 COLOR 2,0
450 GOSUB 3460
470 CLS
490 PRINT "         There are various possibilities for changing
510 PRINT "         the model climate.     You can then test the
530 PRINT "         sensitivity of this climate to changes in the
550 PRINT "         solar constant.    That you should observe the
570 PRINT "         changes due to your changing of the model
590 PRINT "         parameters is also of importance in understanding
610 PRINT "         the nature of this model.
635 COLOR 7,0
640 PRINT "         Press space to continue "
645 COLOR 3,0
650 GOSUB 3460
660 FOR I = 1 TO 18
670 READ AL(I)
680 NEXT I
690 DATA 0.5,0.3,0.1,0.08,0.08,0.2,0.2,0.05,0.05
700 DATA 0.08,0.05,0.1,0.08,0.04,0.04,0.6,0.7,0.7
710 AICE=.68
720 TCRIT=-10
```

Figure 3.2 Listing of the BASIC code for a simple EBM. This code is included (with others) on the Primer CD

```
740 Q=342.5
750 A=204
760 B=2.17
765 C=3.8
770 FOR I = 1 TO 18
780 READ CLOUD(I)
790 NEXT I
800 DATA .52,.58,.62,.63,.57,.46,.40,.42,.50
810 DATA .50,.42,.40,.46,.57,.63,.62,.58,.52
820 CLS
825 COLOR 5,0
830 PRINT "               * * * * * * * * * * * * * * * * * * * *
835 COLOR 2,0
840 PRINT "                        M A I N   M E N U
845 COLOR 5,0
850 PRINT "               * * * * * * * * * * * * * * * * * * * *
855 COLOR 2,0
870 PRINT
880 PRINT "         There are 3 main parameterization schemes within the
890 PRINT "         model.  You may make alterations to any or all of them
900 PRINT "         at any one time.  Any which you choose not to alter
910 PRINT "         will be filled by default values.
925 COLOR 6,0
930 PRINT
940 PRINT "   Choice                    Parameterization
950 PRINT "-------------------------------------------------------------------"
960 PRINT "    (1)                       Albedo & Clouds
970 PRINT "    (2)                       Latitudinal transport
980 PRINT "    (3)                       Longwave radiation to space
1000 PRINT "    (4)                       Run
1010 PRINT
1015 COLOR 7,0
1020 PRINT "   Enter the number of your choice
1030 N$=INKEY$
1040 IF N$="1" THEN 1090
1050 IF N$="2" THEN 1920
1060 IF N$="3" THEN 2120
1070 IF N$="4" THEN 2340
1080 GOTO 1030
1090 CLS
1095 COLOR 5,0
1100 PRINT "* * * * * * * * * * * * * * * * * * * * * * * * * * * * * * * * * * * * * * * * * * * * "
1105 COLOR 2,0
1110 PRINT "              P A R A M E T E R I Z A T I O N   O F
1120 PRINT "                      A L B E D O
1125 COLOR 5,0
1130 PRINT "* * * * * * * * * * * * * * * * * * * * * * * * * * * * * * * * * * * * * * * * * * * * "
1135 COLOR 2,0
1150 PRINT
1160 PRINT "         There are five things which you may alter
1170 PRINT
1175 COLOR 6,0
1180 PRINT "           1.   The temperature at which the surface "
1190 PRINT "                becomes ice covered."
1210 PRINT "           2.   The albedo of this ice covered surface
1230 PRINT "           3.   The albedo of the underlying ground.
1250 PRINT "           4.   Change the cloud amounts
1270 PRINT "           5.   Change the cloud albedo"
1290 PRINT "           6.   Return to main menu
1305 COLOR 7,0
1310 PRINT " Choose which one you want"
1320 AL$=INKEY$
1330 IF AL$="1" THEN 1400
1340 IF AL$="2" THEN 1470
1350 IF AL$="3" THEN 1580
1360 IF AL$="4" THEN 1540
1370 IF AL$="5" THEN 1560
1380 IF AL$="6" THEN 820
1390 GOTO 1320
1400 CLS
1420 PRINT
```

Figure 3.2 *Continued*

```
1425 COLOR 2,0
1430 PRINT USING"   The current value of TCRIT is ###.# deg. C";TCRIT
1440 PRINT
1445 COLOR 7,0
1450 INPUT "   What is the new value you want for TCRIT ? ",TCRIT
1460 GOTO 1090
1470 CLS
1485 COLOR 2,0
1490 PRINT USING"   The albedo of the ice is currently #.##.";AICE
1500 PRINT
1505 COLOR 7,0
1510 INPUT "   What is your new value for this albedo ? ",AICE
1520 IF AICE > .99 OR AICE < 0! THEN GOSUB 3535 :AICE=.68:GOTO 1470
1530 GOTO 1090
1540 CLS: PRINT:PRINT
1550 PRINT "   Input the new cloud amounts for all the zones":FOR LK= 1 TO 18 :PRINT "   ";
LATZ$(LK);:INPUT" cloudiness is",CLOUD(LK)
1555 NEXT LK :GOTO 1090
1556 COLOR 2,0
1560 CLS:PRINT:PRINT:PRINT:PRINT"     Cloud albedo currently is";CALB:PRINT:PRINT"       You
need to choose a new value":COLOR 7,0:PRINT:PRINT:INPUT "    New value=",CALB:IF CALB=<0 OR
CALB>=1 THEN CALB=.5:GOSUB 3535:FOR I=1 TO 700 :NEXT I:GOTO 1556
1570 GOTO 1090
1580 CLS
1590 PRINT
1595 COLOR 2,0
1600 PRINT "         The albedos look like this from north to equator "
1610 PRINT
1620 PRINT USING"        (1)         80-90  #.## ";AL(1)
1630 PRINT USING"        (2)         70-80  #.## ";AL(2)
1640 PRINT USING"        (3)         60-70  #.## ";AL(3)
1650 PRINT USING"        (4)         50-60  #.## ";AL(4)
1660 PRINT USING"        (5)         40-50  #.## ";AL(5)
1670 PRINT USING"        (6)         30-40  #.## ";AL(6)
1680 PRINT USING"        (7)         20-30  #.## ";AL(7)
1690 PRINT USING"        (8)         10-20  #.## ";AL(8)
1700 PRINT USING"        (9)          0-10  #.## ";AL(9)
1710 PRINT USING"       (10)          0-10  #.## ";AL(10)
1720 PRINT USING"       (11)         10-20  #.## ";AL(11)
1730 PRINT USING"       (12)         20-30  #.## ";AL(12)
1740 PRINT USING"       (13)         30-40  #.## ";AL(13)
1750 PRINT USING"       (14)         40-50  #.## ";AL(14)
1760 PRINT USING"       (15)         50-60  #.## ";AL(15)
1770 PRINT USING"       (16)         60-70  #.## ";AL(16)
1780 PRINT USING"       (17)         70-80  #.## ";AL(17)
1790 PRINT USING"       (18)         80-90  #.## ";AL(18)
1800 PRINT
1805 COLOR 6,0
1810 PRINT "  Which one do you want to alter ( zero for none of them )"
1820 PRINT
1825 COLOR 7,0
1830 INPUT "   Enter the number ",I
1840 IF I = 0 THEN 1090
1845 IF  I > 18 OR I < 0 THEN GOTO 1800
1850 PRINT
1855 COLOR 2,0
1860 PRINT "   The old value in band ",I," is ",AL(I)"."
1865 COLOR 7,0
1870 INPUT "   What is your new value ? ",AL(I)
1880 IF AL(I) >0! AND AL(I) < 1! GOTO 1580
1890 GOSUB 3535
1900 GOTO 1870
1920 CLS
1935 COLOR 5,0
1940 PRINT "* * * * * * * * * * * * * * * * * * * * * * * * * * * * * * * * * * * * * * * * "
1945 COLOR 2,0
1950 PRINT "                        T R A N S P O R T
1955 COLOR 5,0
1960 PRINT "* * * * * * * * * * * * * * * * * * * * * * * * * * * * * * * * * * * * * * * * "
1965 COLOR 3,0
1980 PRINT "      In this case you can alter the rate at which heat is
```

Figure 3.2 *Continued*

```
1990 PRINT "      transported around the model by varying the value of C
2000 PRINT "      in the following equation.
2015 COLOR 4,0
2020 PRINT "             Heat Flux = C x ( T(mean) - T(zone) )"
2025 COLOR 2,0
2040 PRINT "                  The current value is ",C
2055 COLOR 7,0
2060 INPUT "   What is the value you want to use ? ", C
2070 IF C >0 AND C<50 GOTO 820
2080 GOSUB 3540
2090 GOTO 2060
2100 GOTO 820
2110 PRINT
2120 CLS
2125 COLOR 5,0
2130 PRINT "* * * * * * * * * * * * * * * * * * * * * * * * * * * * * * * * * * * * * * * * * * * * "
2135 COLOR 2,0
2140 PRINT "                L O N G W A V E  L O S S  T O  S P A C E
2145 COLOR 5,0
2150 PRINT "* * * * * * * * * * * * * * * * * * * * * * * * * * * * * * * * * * * * * * * * * * * * "
2155 COLOR 2,0
2170 PRINT "         The longwave loss to space is determined by the
2180 PRINT "         following equation.
2185 COLOR 4,0
2200 PRINT "             R = A + B x T(zone) "
2205 COLOR 2,0
2220 PRINT "       Currently       A=";A
2230 PRINT "                       B=";B
2245 COLOR 7,0
2250 PRINT "   Enter  1 to change them 0 to keep them the same"
2260 R$=INKEY$
2270 IF R$="0" THEN 820
2280 IF R$="1" THEN 2300
2290 GOTO 2260
2310 INPUT " Enter new value for A   >>",A
2320 INPUT " Enter new value for B   >>",B
2330 GOTO 820
2340 CLS
2365 COLOR 2,0
2370 PRINT "    What fraction of the solar constant would you like ?"
2375 COLOR 7,0
2380 INPUT "    Your choice >",SX
2381 IF SX =< 0 OR SX > 20 THEN GOSUB 3535:GOTO 2340
2390 REM start of routine to calculate temperatures
2395 RESTORE 2430
2400 FOR LAT = 1 TO 18
2410 READ TSTART(LAT)
2420 NEXT LAT
2430 DATA -16.9,-12.3,-5.1,2.2,8.8,16.2,22.9,26.1,26.4
2440 DATA 26.4,26.1,22.9,16.2,8.8,2.2,-5.1,-12.3,-16.9
2450 F=1
2460 FOR LAT= 1 TO 18
2470 TEMP(LAT)=TSTART(LAT)
2480 NEXT LAT
2490 FOR H = 1 TO 50
2510 SOLCON=SX*1370!/4!
2520 '    Calculate albedo of zones
2530 LATICE=0
2540 FOR LAT = 1 TO 18
2550 NL=0
2560 ALBEDO(LAT)=AL(LAT)*(1-CLOUD(LAT))+CALB*CLOUD(LAT)
2570 IF TEMP (LAT) > TCRIT THEN GOTO 2800
2580 ALBEDO(LAT) = AICE
2590 IF LAT = 9 GOTO 2790
2600 IF LAT = 10 GOTO 2790
2610 IF LAT = 18 GOTO 2800
2620 IF TEMP(LAT+1)<=TCRIT GOTO 2800
2630 DP=(-TCRIT+TEMP(LAT+1))*IN/(TEMP(LAT+1)-TEMP(LAT))
2640 A2=(P2-(LAT+.5)*IN)
2650 LATICE =A2+DP
2660 IF DP > .0872564 THEN GOTO 2730
```

Figure 3.2 *Continued*

```
2670 A3=P2-(LAT+1)*IN
2680 A4=A3-IN
2690 A5=(SIN(A4)-SIN(LATICE))/(SIN(A4)-SIN(A3))
2700 NC=ALBEDO(LAT+1)*(1!-A5)+AICE*A5
2710 NL=LAT+1
2720 GOTO 2800
2730 A3=P2-LAT*IN
2740 A4=P2-(LAT-1)*IN
2750 A5= (SIN(LATICE)-SIN(A3))/(SIN(A4)-SIN(A3))
2760 NC=AICE-(AICE-ALBEDO(LAT))*A5
2770 NL=LAT
2780 GOTO 2800
2790 NL=0
2800 NEXT LAT
2810 IF ALBEDO(1) = AL(1) THEN NI = 90!/57.296
2830 SM=0
2840 FOR LAT = 1 TO 18
2850 A1=P2-(LAT-1)*IN
2860 A2=A1-IN
2870 AC=ALBEDO(LAT)
2880 IF LAT=NL THEN AC=NC
2890 SM=SM+(SIN(A1)-SIN(A2))*AC*S(LAT)
2900 NEXT LAT
2910 TX=(SOLCON*(1-SM)-A)/B
2930 FOR LAT = 1 TO 18
2940 OL(LAT)=(1-CLOUD(LAT))*(A+B*TEMP(LAT))
2950 OL(LAT)=OL(LAT)+CLOUD(LAT)*(A+B*(TEMP(LAT)-5))
2960 ASOL(LAT)=SOLCON*S(LAT)*(1-ALBEDO(LAT))
2970 TM(LAT)=TEMP(LAT)
2980 TEMP(LAT)=(SOLCON*S(LAT)*(1-ALBEDO(LAT))-A+C*TX)
2990 TEMP(LAT)=FNR(TEMP(LAT)/(C+B))
3000 NEXT LAT
3020 AM=0
3030 IC=0
3040 FOR LAT= 1 TO 18
3050 MA=ABS(TEMP(LAT)-TM(LAT))
3055 IF TEMP(LAT)>800 THEN GOSUB 4000
3060 IF MA > AM THEN AM =MA
3070 NEXT LAT
3080 IF AM < .01 THEN IC = 1
3090 IF IC = 1 GOTO 3130
3100 NEXT H
3110 GOSUB 4000
3120 END
3130 REM RESULTS
3140 CLS
3145 COLOR 12,0
3150 PRINT "                              ---- R E S U L T S ----
3155 COLOR 13,0
3160 PRINT"       Zone    Temperature     Albedo  Cloudiness  Longwave Out   Abs. Sol
3165 COLOR 3,0
3170 FOR LAT = 1 TO 18
3180 PRINT "         ";
3190 PRINT LATZ$(LAT);
3200 PRINT "     ";
3210 PRINT USING "###.#" ;TEMP(LAT);
3220 PRINT USING "      ###.##";ALBEDO(LAT);
3230 PRINT USING "   ##.##";CLOUD(LAT);
3240 PRINT USING "        ####.  ";OL(LAT);
3250 PRINT USING "         ####.  ";ASOL(LAT)
3260 NEXT LAT
3270 LATICE= FNR(LATICE*57.296)
3275 COLOR 2,0
3280 PRINT USING "  Fraction of solar constant is ##.### ";SX
3290 PRINT USING "  A=###.#  B=##.##  C=##.## Cloud alb=#.##";A,B,C,CALB
3300 PRINT USING "  Ice albedo=#.##  Changes at ###.# deg C";AICE,TCRIT
3310 COLOR 7,0 :PRINT "   Press space bar to continue";
3320 GOSUB 3460
3330 CLS
3340 PRINT
3345 COLOR 2,0
```

Figure 3.2 *Continued*

```
3350 PRINT "              Do you want to try again ?"
3370 PRINT "           (1)      Reset all parameters
3380 PRINT "           (2)      Modify current parameters
3385 PRINT "           (3)      Choose a different program
3400 RESTORE 670
3410 CH$=INKEY$
3420 IF CH$="1" GOTO 660
3430 IF CH$="2" GOTO 820
3435 IF CH$="3" THEN CHAIN"menu.bas" :END
3440 GOTO 3410
3450 END
3460 SP$=INKEY$
3470 IF SP$=" " THEN GOTO 3490
3475 IF SP$=CHR$(27) THEN CHAIN"menu"
3480 GOTO 3460
3490 RETURN
3500 FOR I=1 TO 700
3510 NEXT I
3530 RETURN
3535 COLOR 12,0
3540 PRINT "   Illegal response try again"
3545 FOR IIIJ = 1 TO 4000 :NEXT IIIJ:COLOR 7,0
3550 RETURN
4000 CLS
4010 COLOR 27,0:LOCATE 10,7:PRINT "  Non viable input parameters caused model failure"
4020 LOCATE 12,7:PRINT "  You need to moderate your values somewhat "
4025 COLOR 12,0
4030 LOCATE 20,7:PRINT "  Press the space bar to to edit your values or"
4040 LOCATE 21,7:PRINT "  or press <Escape> abort"
4050 SP$=INKEY$:IF SP$=" " THEN GOTO 820
4060 IF SP$=CHR$(27)THEN CHAIN "ebm2"
4070 GOTO 4050
5000 CLS:ON ERROR GOTO 7000:PRINT:PRINT:PRINT:PRINT"             P R I N T I N G . . . . "
5002 LPRINT "-------------------------------------------------------------------------------"
5003 LPRINT"  Energy Balance Model                          A Climate Modelling Package"
5004 LPRINT "-------------------------------------------------------------------------------"
5005 LPRINT "                            ---- R E S U L T S ----
5010 LPRINT"       Zone    Temperature     Albedo  Cloudiness  Longwave Out   Abs. Sol
5020 FOR LAT = 1 TO 18
5030 LPRINT "          ";
5040 LPRINT LATZ$(LAT);
5050 LPRINT "      ";
5060 LPRINT USING "###.#" ;TEMP(LAT);
5070 LPRINT USING "      ###.##";ALBEDO(LAT);
5080 LPRINT USING "   ##.##";CLOUD(LAT);
5090 LPRINT USING "        ####.  ";OL(LAT);
5100 LPRINT USING "         ####.  ";ASOL(LAT)
5110 NEXT LAT
5120 LPRINT USING "  Fraction of solar constant is ##.### ";SX
5130 LPRINT USING "  A=###.#  B=##.#  C=##.## Cloud alb=#.##";A,B,C,CALB
5140 LPRINT USING "  Ice albedo=#.##  Changes at ###.# deg C";AICE,TCRIT
5141 LPRINT "-------------------------------------------------------------------------------"
5142 LPRINT:LPRINT:LPRINT:LPRINT:LPRINT:LPRINT
5143 RETURN
7000 PRINT:PRINT:PRINT:COLOR 12,0:PRINT "    Either there is no printer or it isn't connected
properly":FOR III = 1 TO 15000:NEXT III:COLOR 3,0:GOTO 5143
```

Figure 3.2 *Continued*

is quite close to the present-day situation is predicted for a fraction = 1 of the solar constant. This equilibrium climate is given in Table 3.1.

Once this equilibrium value for an unchanged solar constant has been seen, the user can modify the fraction of the solar constant prescribed and note the changes in the predicted climate. More importantly, the EBM permits the user to alter the albedo formulation, the latitudinal transport and the parameters in the infrared radiation term and examine the sensitivity of the modified model. The EBM is presented here in a hemispheric form.

Table 3.1 EBM simulation display showing input parameters and resultant equilibrium climate

Parameter values set in the EBM code

$A = 204\,\mathrm{W\,m^{-2}}$, $B = 2.17\,\mathrm{W\,m^{-2}\,°C^{-1}}$, $k_t = 3.81\,\mathrm{W\,m^{-2}\,°C^{-1}}$.
Albedo ($A_c = 0.62$) below critical temperature ($T_c = -10$°C).
Fraction of solar constant = 1

Resultant equilibrium climate

Latitude	*Temp. (°C)*	*Albedo*
85	−13.5	0.62
75	−12.9	0.62
65	−4.8	0.45
55	1.8	0.40
45	8.5	0.36
35	16.0	0.31
25	22.3	0.27
15	26.9	0.25
5	27.7	0.25

EBM model code

In the program shown in Figure 3.2, an equilibrium solution is achieved by iterating the calculation of each zonal T_i of Equation (3.13). A maximum of 50 iterations is allowed in the code. The snow-free albedo of the planet has been coded as latitude-dependent. The exercises in Table 3.2 are useful examples of the types of climate simulation experiments that can be undertaken.

As well as producing single calculations, the EBM can also vary the solar constant over a range of values and plot a graph. You can use this graph to investigate the sensitivity of the model. You can also save the numbers for later analysis. The next section describes some other types of experiments that can be conducted with EBMs similar to this.

3.4.2 BASIC geophysiology

The concept of geophysiology was introduced in the early 1980s as a paradigm for the coupling of living organisms and the physical systems that make up the planet. A simple model can be used to demonstrate the concept that a set of living organisms can interact and modify their environment, to their own benefit, without consciously planning such a modification. The ‘Daisyworld’ model, developed by Andrew Watson and James Lovelock in the early 1980s, consists of a world populated by two sorts of daisies: black daisies and white daisies. Both daisies compete for the available land on the planet and grow similarly as a function of temperature but, because of their albedo, black daisies can tolerate a lower solar luminosity.

Table 3.2 Energy balance model exercises

Exercise 1	(a) Using the default values of albedo, k_t, A and B determine what decrease in the solar constant is required just to glaciate the Earth completely (ice edge at 0°N). (b) Select some other values of A, B, k_t and the albedo formulation and repeat Exercise 1(a).
Exercise 2	(a) Various authors have suggested different values for the transport coefficient, k_t. For instance, Budyko (1969) originally used $k_t = 3.81\,\mathrm{W\,m^{-2}\,°C^{-1}}$ and Warren and Schneider (1979) used $k_t = 3.74\,\mathrm{W\,m^{-2}\,°C^{-1}}$. How sensitive is the model's climate to the particular value of k_t? (b) Investigate the climate that results when using very small or very large values of k_t. How sensitive are these different climates to changes in the solar constant? Try to 'predict' how you think the model will behave before you perform the experiment.
Exercise 3	(a) Observations show that land will be totally snow-covered during winter for an annual mean surface temperature of 0°C, and oceans totally ice-covered all year for a temperature of about −13°C. The model specifies a change from land/sea to snow/ice at −10°C. Alter this 'critical' temperature and investigate the change in the climate and the climatic sensitivity to changing the solar constant. (b) The albedo over snow-covered areas can vary within the limits of 0.5–0.8 depending on vegetation type, cloud cover and snow/ice condition. Investigate the sensitivity of the simulated climate to changing the snow/ice albedo.
Exercise 4	(a) There have been many suggestions for the values of the constants A and B determining the longwave emission from the planet – some have been dependent on cloud amount. Budyko (1969) originally used $A = 202\,\mathrm{W\,m^{-2}}$ and $B = 1.45\,\mathrm{W\,m^{-2}\,°C^{-1}}$. Cess (1976) suggested $A = 212\,\mathrm{W\,m^{-2}}$ and $B = 1.6\,\mathrm{W\,m^{-2}\,°C^{-1}}$. How do these different constants influence the climate and its sensitivity? (b) Holding A constant, just vary B and investigate the effect on the climate. What does a variation of B correspond to physically?
Exercise 5	Repeat Exercise 1 with the values of A, B, k_t and the albedo formulation which you believe are 'best' (i.e. most physically realistic for the present-day climate). Once the Earth is just fully glaciated, begin to increase the fractional solar constant. Determine how much of an increase in the solar constant is required before the ice retreats from the equator. Do you understand the value?

White daisies, on the other hand, can tolerate a higher solar luminosity since they reflect more energy.

Daisyworld is an extension of the EBM idea discussed in the previous section. Instead of the albedo being simply due to the presence of reflective snow or ice cover when the temperature is below a certain threshold, the albedo now depends on how well the environment can support a species of daisy. Daisyworld was originally formulated as a zero-dimensional model, where the temperature depended, as in an

EBM, on the energy balance between outgoing and incoming radiation. Daisyworld's two species of 'daisies' (black and white) have albedos (α_b and α_w) that govern the amount of radiation absorbed. The albedo of each species therefore governs the local temperature, which in turn controls the growth rate (affecting the total area covered).

The global average planetary albedo, α_g, is determined by considering the area of the planet covered by the daisies as

$$\alpha_g = f_{bare}\alpha_{bare} + f_w\alpha_w + f_b\alpha_b \tag{3.20}$$

The fractional areas of each daisy species (f_w and f_b) evolve with time. As the local temperature changes in response to changes in solar luminosity, the growth rates of the daisies change and this feeds through to the albedo of the planet. The daisies can grow to cover the available fertile land on the planet based on a simple temperature dependence of growth rate. Growth, G_w, is greatest at a local temperature T_{opt} and drops off (at a rate dependent on the growth factor, k_g) at colder and warmer

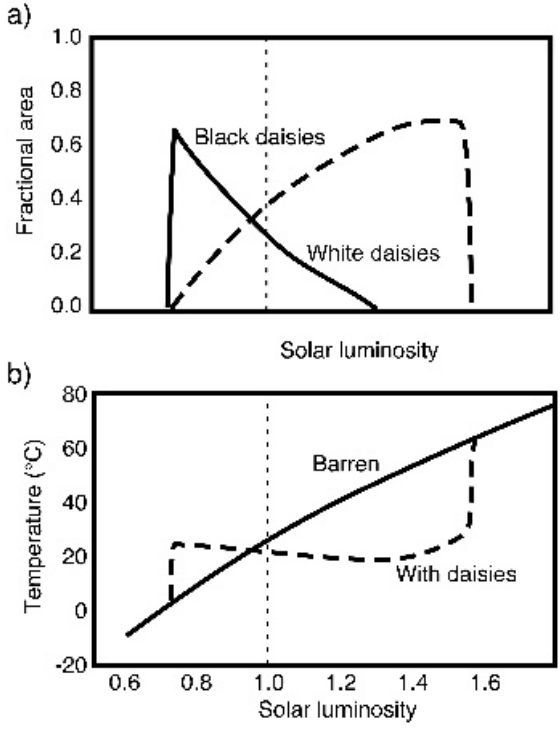

Figure 3.3 (a) Results from a simulation using the 'Daisyworld' equations showing black daisies dominating at low temperatures and white daisies at higher temperatures. (b) The daisies act to moderate the planetary temperature whereas, without the daisies, the temperature steadily increases as solar luminosity increases

temperatures

$$G_w = 1 - k_g (T_{opt} - T_w)^2 \tag{3.21}$$

When solar luminosity is low, the black daisies dominate, as they absorb more energy and can attain the optimum growing temperature at a lower luminosity. However, as solar luminosity increases, the white daisies become the dominant species. White daisies reflect more radiation and therefore are able to stay cool at these higher luminosities. As a result, the temperature of the planet is moderated as shown in Figure 3.3. As the 'Sun' increases in luminosity, much as our own Sun has brightened over the history of the Earth, the daisies keep the temperature of the planet within a few degrees of their optimum temperature.

If we consider a generalized situation with many species, what we are seeing is the daisies mutating in response to the change in boundary conditions. This model has provided a framework for the exploration of how organisms can self-regulate their environment. A version of the Daisyworld model is included on the Primer CD and you can explore the behaviour of such a model for yourself.

3.5 ENERGY BALANCE MODELS AND GLACIAL CYCLES

So far we have looked at the components and the results of EBMs. In this section, the results of some EBM experiments will be examined. In previous sections, we have ignored seasonality and, to some extent, have neglected the effect of the oceans as a heat source and sink. In this section, we will examine how EBMs have been used in climate simulation experiments. EBMs have been used extensively in the study of palaeoclimates. One common experiment is to introduce the effect of orbital (Milankovitch) variations and changed continental configurations on an EBM.

Geochemical data suggest a positive correlation between CO_2 and temperature over the last 540 million years. A notable exception to this is the Late Ordovician glaciation (around 440 million years ago) which occurred at a time when the atmospheric CO_2 content is believed to have been around fifteen times as high as it is today. Reduced solar luminosity compensated in part for this, but experiments with EBMs have shown that the configuration of the continents was such that the ice sheets could coexist with high CO_2 levels. With the benefit of the insight gained from such EBM studies, it has been possible to go on to perform more detailed calculations with a GCM, which have confirmed the hypothesis based on the EBMs. The advantage of EBMs in this kind of problem is the ease with which many different experiments can be performed. Since information on boundary conditions for model simulations is poor, the simple model offers the chance to test a range of situations before embarking on expensive calculations with a GCM.

We have already mentioned the rapid glaciation of the modelled Earth as a result of a decreased solar constant. Energy balance models incorporate the cryosphere, which is the frozen water of the Earth, as if it were a thin, high-albedo covering of the Earth's surface. The solution of the governing equation of an EBM for various

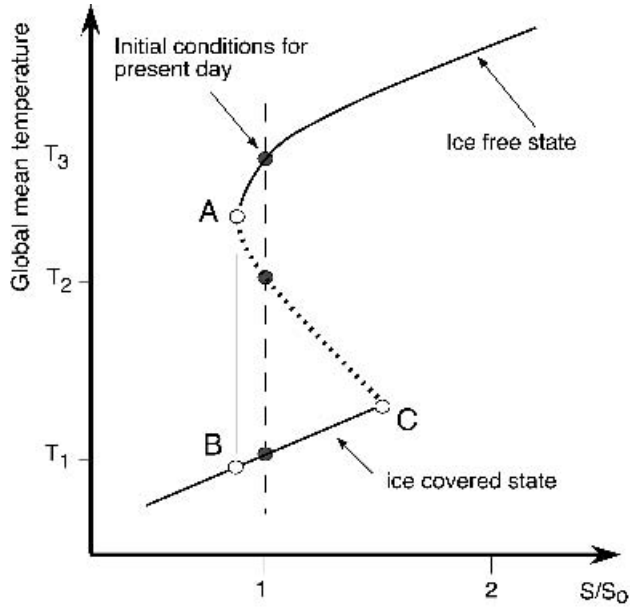

Figure 3.4 Characteristic solution of an EBM, plotted here as global mean temperature as a function of fraction of present-day solar constant. The dotted line represents a branch of the solution which, while being mathematically correct, is physically unrealistic. On this branch, increasing energy input results in a decreased temperature. More complex parameterizations within EBMs induce more complex shaped curves

values of solar constant is shown in Figure 3.4. The model in Figure 3.2 yields a similar curve. Figure 3.4 is an illustration of the solution of a simple, zero-dimensional model. It shows a fundamental characteristic of non-linear systems. A slow decrease in the solar constant from initial conditions for the present day means a gradual decrease in temperature until the point is reached (point A) where a runaway feedback loop causes total glaciation and a rapid drop in temperature (solid line to point B). When the solar constant is then increased the process is not immediately reversed; the temperature follows a different route until at a value of the solar constant greater than that of the present day (point C) temperatures rise again (dashed line). The modelled climate exhibits hysteresis.

The formulation of an EBM in 'time-dependent' form changes the nature of the interpretation of the 'unphysical' branch in Figure 3.4. This branch now represents the presence of a small, unstable ice cap. Ice caps that are smaller than some characteristic length scale are unstable, a phenomenon referred to as the small ice cap instability (SICI) or sometimes as the thin ice cap instability (TICI). The phenomenon has been proposed as a mechanism for the initiation and growth of the Greenland and Antarctic ice sheets.

3.5.1 Milankovitch cycles

Much of the response of ice sheets to climate fluctuations depends on their thermal inertia. To make effective models of ice sheets, it is necessary to consider the ice sheet as more than a simple, thin covering of ice or snow. Some modellers have developed ice sheet models that extend the simple thin ice sheet model of the EBMs to be more realistic. In contrast, most GCMs do not deal with the growth and decay of ice sheets since the time-scales over which the ice sheets change is much longer than typical GCM integrations. In current GCMs, ice sheets continually collect snow, but one of the important loss mechanisms, iceberg formation, is not included in the model because the time-scales are very long. The other important losses are by melting, which is insignificant in Antarctica today but is significant in Greenland and was important for the other Northern Hemisphere ice sheets. A more fundamental problem with modelling ice sheets is that we still know very little about the properties of the ice sheets and the way in which they change in response to climate forcing.

Figure 3.5 shows schematically two types of ice sheet. Figure 3.5a characterizes the major Northern Hemisphere ice sheets in contrast to Figure 3.5b, which depicts the type of ice sheet which forms when a land mass exists at a pole, as is the case

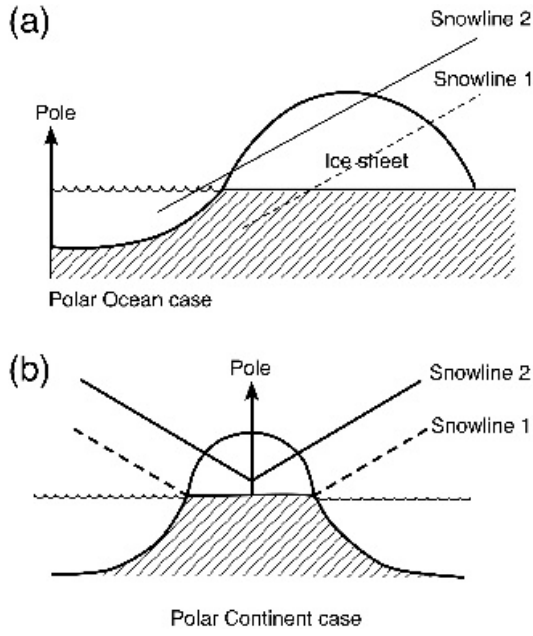

Figure 3.5 In climatological terms, there are basically two different types of ice sheet: those occurring when there is a polar ocean and those occurring when there is a polar continent. In both cases it is possible for the ice sheet to persist even when the snowline is above ground level

currently in the Southern Hemisphere. Provided the snowline is below the level of the ice or bedrock topography, then an ice sheet can exist. Once the ice sheet has acquired height, then it can be sustained even if the snowline moves above the bottom of the ice sheet (i.e. snowline 1 changes to snowline 2). Such a situation is found today in Greenland. The extent of an ice sheet is governed by the balance between net accumulation (snowfall) above the snowline and net ablation (melting and the calving of icebergs) below it, and by the compensating ice flow from accumulation area to ablation area. The ice sheet's equilibrium extent, at which ablation of mass equals accumulation of mass exactly, can be limited significantly by calving if the ice sheet spreads to reach the coastline. Otherwise the extent is limited by increased melting as the ice extends towards the equator, but there is also an important, internally-imposed negative feedback loop: as the ice sheet grows higher and colder, it creates a regional climate in which less and less moisture can be delivered by the atmosphere to the accumulation area. In effect, the ice sheet 'starves' itself. There is another, externally-imposed negative feedback in the form of the response of the solid Earth to the load of the ice sheet: the lithosphere subsides slowly, lowering the ice sheet's surface relative to the snowline and shifting its mass balance towards more ablation. These two negative feedbacks both have time-scales of the order of 10 000 years, but their interactions with each other and with the rest of the system, under the influence of the Milankovitch forcing, are extremely complex.

The distribution of accumulation and ablation, above and below the snowline respectively, gives the ice sheet its characteristic shape: a parabolic profile in the 'perfectly-plastic' approximation. Bigger ice sheets have a lower accumulation rate. Ice flow is actually viscous (strain rate proportional to the third power of stress) but this is difficult to model. The response of the solid Earth is actually a coupled response of the lithosphere and the much weaker underlying asthenosphere. The ice has a viscosity of about 10^{13} Pa s, the corresponding values being about $10^{27} \approx \infty$ for the lithosphere and 10^{21} for the asthenosphere. Future increases in computational power (Figure 1.5) will see these processes begin to be included in Earth System Models. An ice sheet model can be coupled to representations of the response of the lithosphere to ice load and to an EBM such as that described earlier in this chapter to make a combined model. Some models of this sort have been shown to exhibit internal variability. The components interact to form a temporally varying climate even without external forcing such as the Milankovitch variations (*cf.* the 'climate attractor' in Figure 2.10).

Continental ice sheets and permafrost extent typically vary on timescales of approximately 1000–10 000 years (Table 1.2), although shorter time-scale effects have been suggested. The results from detailed cryospheric EBMs as early as 1980 showed that the influence of an ice sheet on the radiation balance was small if sea ice and snow cover were already incorporated. On the other hand, the inclusion of the ice sheet height–accumulation feedback loop discussed above substantially increased climate sensitivity.

In modelling the response of ice sheets to Milankovitch variations, a range of sensitivity experiments has shown that the final outcome is highly dependent on the

values of the input parameters. By combining an ice sheet model similar to that shown in Figure 3.5a with a two-dimensional EBM, it is possible to simulate the glacial/interglacial cycles over the past 240 000 years. Although the ice sheet model simulates growth well, it is found that the observed rapid dissipation of ice sheets can only be simulated by a parameterization of the calving. In the model of an ice sheet many different factors must be incorporated, the complexity of the formulation being related to the projected use of the model.

3.5.2 Snowball Earth

The predictions of EBMs have recently become important in a climate paradox that has been termed 'Snowball Earth'. Although debate still rages about this climatic possibility, its history dates back to the 1960s. At that time, geologists discovered rocks from many parts of the Earth that exhibited the effects of an early and very large glaciation. Together, they seemed to imply that glaciers extended to, or at least occurred in, low equatorial latitudes just over 600 million years ago.

This geological evidence, although pervasive and persuasive, seems to be in direct conflict with the predictions of EBMs. As you may have discovered with the EBM in Figure 3.2 and as illustrated in Figure 3.4, once the planet is totally ice-covered (point A), temperatures drop so low that a massive increase in solar luminosity is required for defrosting. For much of the second half of the twentieth century, these EBM predictions held the geological evidence at bay: the climate models said that recovery from a global glaciation was impossible, so it could not have happened.

There were some scientists who challenged the EBM-based refutation of the evidence for global glaciation. They considered what other mechanisms might be substituted for the near doubling of solar luminosity which would be required for deglaciation but which certainly had not occurred. Their idea was that perhaps the Earth's greenhouse increment became much larger (see Equation (3.2)). Joseph Kirschvink, a geobiologist, suggested that changed atmospheric carbon dioxide levels could solve the 'Snowball Earth' puzzle. His theory recognized that if the Earth were totally ice-covered, an important part of the carbon cycle would be closed down. CO_2 would continue to be introduced into the atmosphere by volcanoes protruding through the glaciers. On the other hand, the natural sink for CO_2 over geological time-scales – the erosion of silicate rocks, creation of biocarbonates and ultimate formation of marine carbonate sediments – would cease. Thus, CO_2 would build up to very high concentrations in the atmosphere above the Snowball Earth.

Two climate modellers, Kenneth Caldeira and James Kasting, calculated that about 350 times the present-day levels of CO_2 could overcome a total glaciation. Although these amounts of CO_2 are large compared with modern greenhouse concerns of two to four times pre-industrial levels, they are by no means unachievable on geological time-scales. To accumulate 350 times the present-day CO_2, volcanoes would have to belch for a few tens of millions of years. If this is the solution, the 'Snowball Earth' is likely to have been our longest ever ice age.

Once the fundamental climate paradox had been solved, geologists were able to contribute additional and rather intriguing details to the story by noting that rocks from areas as distant as Australia, Africa, North America, China and the Arctic share a number of fascinating characteristics. The Neoproterozoic glacial deposits from the period 750 to 580 million years ago all occur topped by 'cap carbonates'. These blankets of carbonate rocks on top of the glacial evidence for Snowball Earth look like deposits that form today in warm shallow seas and also suggested a very rapid transition from glaciated land to tropical ocean. Although this conclusion is less certain, there is no evidence that significant time passed between the deposition of the Neoproterozoic glacial sediments and the 'cap carbonates' (Figure 3.6).

The second feature of the 'cap carbonates' relates to the isotopic character of the carbon locked into these rocks. To understand this involves recognizing the impact

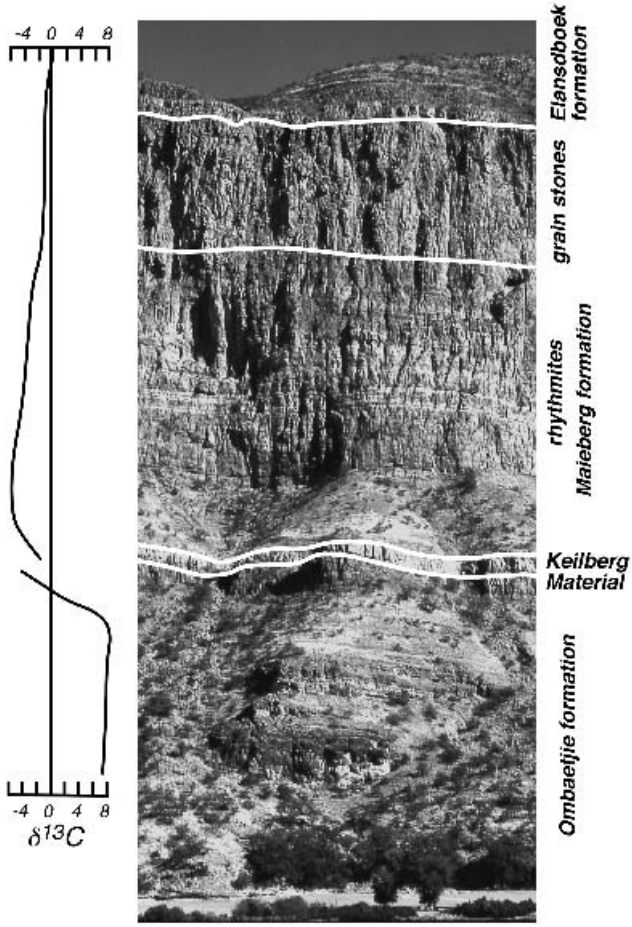

Figure 3.6 Annotated stratigraphy on the rim of the Congo platform in Namibia, the location of one of the most commonly cited pieces of evidence for 'Snowball Earth'. (Photo: Paul F. Hoffmann)

life has on the relative amounts of ^{13}C and ^{12}C, the two stable isotopes of carbon. Volcanic gases contain about 1 per cent ^{13}C while the rest is ^{12}C (Table 1.1). In an abiotic world, this same fraction of ^{13}C would appear in carbonate rocks. However, photosynthesis preferentially abstracts ^{12}C over ^{13}C because the lighter isotope requires less work. Thus, in an ocean containing marine life, carbonate rocks contain relatively more ^{13}C because the photosynthetic organisms have depleted the ^{12}C. Just below the Neoproterozoic glacial deposits, the amounts of ^{13}C drop from the expected biologically-enhanced levels to pristine volcanic amounts. These volcanic proportions of ^{13}C persist through the glacial rocks and capping carbonates, only recovering to biologically-affected levels many hundreds of metres higher in the geological column (Figure 3.6).

This stable isotope story agrees with the developing history of the 'Snowball Earth'. It could have happened in this way. A shock, perhaps due to a Milankovitch-type insolation fluctuation or a meteorite impact, decreases temperatures. As snow falls, the ice-albedo feedback effect plunges the Earth into a global glaciation, as EBMs predict. The ice locks up much of the oceans and kills most of the biosphere but volcanoes protruding through the glaciers continue to degas. The atmosphere gradually enriches in CO_2 and the glacial deposits carry its isotopic signature. After tens of millions of years, a CO_2 greenhouse hundreds of times larger than today's melts the ice and frees the planet. Responding to the massive greenhouse effect, temperatures soar and carbonate rocks form in warm oceans still carrying the volcanic-enriched greenhouse isotope signal. Finally, the biosphere rebuilds and blossoms returning carbon isotopic ratios to bio-mediated levels.

The current questions about the 'Snowball Earth' pertain to the Cambrian biological 'explosion' and the geological evidence itself. The 'freeze and bake' period depicted in the climatic sketches of the Neoproterozoic has been implicated in the previously unexplained sudden blossoming of multicellular life in the Proterozoic. Eukaryotes (multicellular organisms) had been around for almost a billion years before the Cambrian but they diversify suddenly after the period now labelled 'Snowball Earth'. This, it has been claimed, is further evidence for the global climate catastrophe.

On the other hand, Scottish geologists have recently found evidence apparently calling into question the original prompt for the Snowball theory. In their opinion, many of the Neoproterozoic glacial deposits contain sedimentary material that could only have been derived from ice floating in open water. The totality of the geological evidence has recently been reviewed comprehensively, casting further doubt on the idea of global glaciation. Once again, the Snowball Earth hypothesis may need additional evidence from global climate models before it can be fully understood and explained.

3.6 BOX MODELS – ANOTHER FORM OF ENERGY BALANCE MODEL

The concept of computing the energy budget of an area or subsystem of the climate system can be extended and modified to produce other forms of energy balance models. These models are not strictly EBMs and are often termed box models. A

very elementary box model was considered early in this chapter (Section 3.2) in the example of the solar-heated swimming pool. That model had two boxes: one 'box' being the water and the other the air overlying the pool. A more complex consideration involves a more realistic parameterization of the energy transfer between the air and the pool, and interactive variation of other elements such as the radiative forcing. Following the same formulation, a simple column EBM can be used to consider the likely effect upon global temperatures of rising levels of atmospheric CO_2.

3.6.1 Zonal box models that maximize planetary entropy

Testing and validating climate models is an ongoing challenge for modellers and those who use their predictions. The real problem is that most evaluations of climate model parameterizations are conducted for the present-day conditions on Earth. However, to be valid for predictions in changed conditions, it would be better if models could be tested against different climate regimes. One way is to use palaeoclimatic data; another is to use models to simulate climates on other planets.

Recent reconsideration of the applicability of simple EBMs to Titan, Mars and Venus has revived interest in a 30-year-old proposal. In 1975, Garth Paltridge found that he could recreate the Earth's climate best with an EBM if he maximized the entropy (the mechanical work done by the atmosphere and oceans) (Figure 3.7a). Although other researchers have confirmed his result, it was thought to be only an interesting coincidence until measurements of Titan's zonal temperatures showed that this principle also best explained this other, very different planetary climate. The concept of a fundamental 'law' that planetary climates maximize entropy is contrary to the ideas that currently govern comprehensive climate models. These models, with the many degrees of freedom offered by ocean and atmospheric processes, have tended to be built from the bottom up (i.e. component by component) to look like the present-day Earth. For distant planets, however, we have very few measurements and so simpler models, like EBMs, are more appropriate.

In 1999, Ralph Lorenz, a planetary scientist, tried to fit the parameters of a simple EBM to Titan and Mars and found that he had to choose values that maximized entropy on these planets just as Paltridge had discovered for Earth 25 years earlier. His model is like the one-dimensional EBM in Figure 3.1 except that Lorenz used only two equal area latitude zones: polar (poleward of 30°) and tropical (equatorward of 30°) (Figure 3.7b). His formulation for the heat transfer factor F^* resembles that in Equation (3.12)

$$F^* = 2D(T_t - T_p) \tag{3.22}$$

and the model is completed by noting that the planetary climate's entropy production is

$$E_P = F^*/T_p - F^*/T_t \tag{3.23}$$

For Earth, D has a value of about 0.6–1.1 $\mathrm{W\,m^{-2}\,K^{-1}}$. When EBMs have been applied to palaeo-simulations or other planets, there is a need to calculate an appropriate

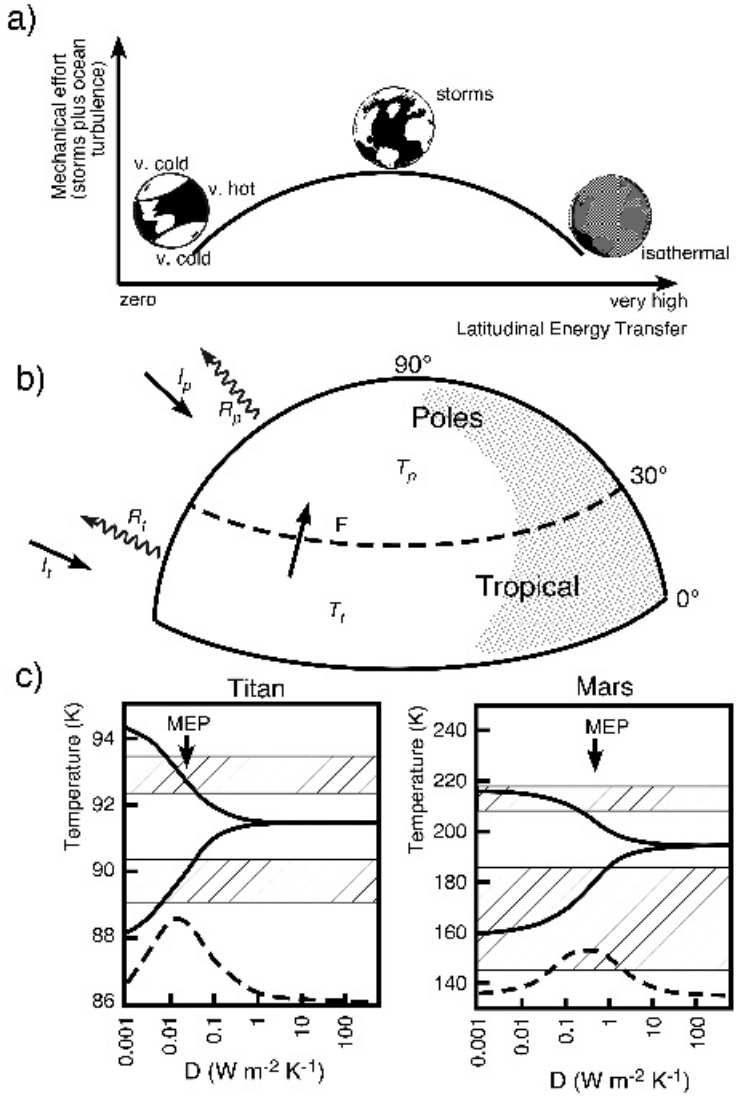

Figure 3.7 (a) The range of possible states for the Earth's atmosphere plotted in terms of latitudinal energy transfer and mechanical work done. The Earth's climate system occupies the position of maximum work midway along the energy transfer axis. (b) Schematic of a simple planetary model with two temperature zones. (c) Results from a simple model of the climate systems of Mars and Titan. The entropy production is shown by the dashed lines with the maximum entropy production (MEP) arrowed. The model temperature is shown by solid lines for 'tropical' and 'polar' regions of the model in (b): the upper solid curve is for the tropical region and the lower curve for the polar region. Observed temperature ranges for latitudes 10° to 20° and 40° to 60° are shown as shaded regions. (Part (c) reproduced by permission of the American Geophysical Union from Lorenz *et al*. (2001), *Geophys. Res. Lett.,* **28**, 415–418)

Table 3.3 Values of the meridional heat transfer coefficient (for Earth, $D = 0.6–1.1\,\mathrm{W\,m^{-2}\,K^{-1}}$)

	Conventional scaling	*Maximizing entropy*
Mars	0.001–0.01	0.45–2.0
Titan	10^2–10^4	0.01–0.04

value of D. This is usually undertaken by scaling with a range of factors such as the planetary surface pressure, the atmospheric specific heat capacity, the relative molecular mass of the atmosphere and the planetary rotation rate. Table 3.3 compares the values of D for the conventional meteorological scaling and the theory of maximizing entropy.

Lorenz's model predicts two zonal temperature curves (polar and tropical) shown in Figure 3.7c as a function of the meridional heat transfer coefficient D. Maximizing entropy for Titan gives a much better fit to the observed zonal temperatures but means that its climate system is 20 times less efficient at transferring equatorial heat than Earth even though, or possibly because, its atmosphere is four times denser. The same principle holds for Venus but in this case the atmosphere is so dense that pressure scaling and maximizing entropy production give very similar results.

The 'theory' of maximized entropy production works for the Earth now, produces the only observationally-validated simulation of Titan's latitudinal climate, improves the predictions for Mars and agrees with more conventional scaling methods for Venus. Finally, this intriguing idea might add another aspect to solving the 'Snowball Earth' paradox described earlier in this chapter. As temperatures drop, overall latitudinal energy transport decreases under a maximized entropy model. Thus, a modified EBM prediction of the 'snowball' that maximizes entropy might leave an equatorial zone of habitable temperatures.

3.6.2 A simple box model of the ocean–atmosphere

The column EBM, used as an example here, represents the ocean–atmosphere system by only four 'compartments' or 'boxes': two atmospheric (one over land, one over ocean), an oceanic mixed layer and a deeper diffusive ocean (Figure 3.8a). The heating rate of the mixed layer is calculated by assuming a constant depth in which the temperature difference, ΔT, due to some perturbation, changes in response to: (i) the change in the surface thermal forcing, ΔQ; (ii) the atmospheric feedback, expressed in terms of a climate feedback parameter, λ, and (iii) the leakage of energy permitted into the underlying waters. This energy, ΔM, acts as an upper boundary condition for the deep ocean below the mixed layer in which the turbulent diffusion coefficient, K, is assumed to be a constant. The equations describing the rates of heating in the two 'layers' are thus:

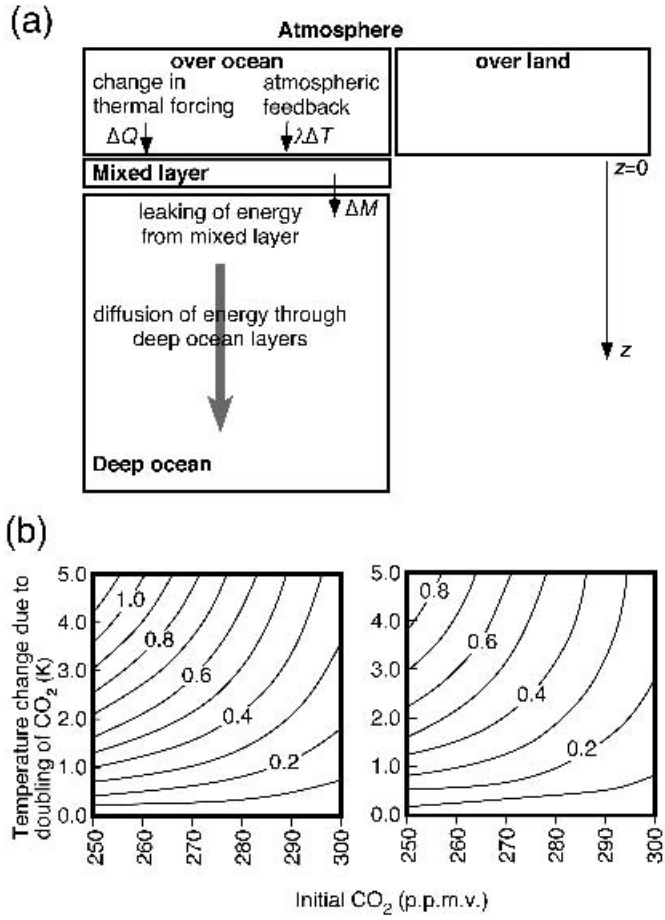

Figure 3.8 (a) Schematic diagram of a simple box-diffusion model of the atmosphere–ocean system. (b) Isolines of temperature change to 1980 (CO_2 level of 338 ppmv) as a function of the CO_2-doubling temperature change and the 1850 initial CO_2 level for two pairs of ocean diffusivity and mixed layer depth: left-hand diagram, $K = 10^{-4}\,m^2\,s^{-1}$, h = 70 m; right-hand diagram, $K = 3 \times 10^{-4}\,m^2\,s^{-1}$, $h = 100$ m. Results are based on a full numerical solution of the equations described in Wigley and Schlesinger (1985) (reproduced with permission from Wigley and Schlesinger (1985), *Nature* **315**, 649–652. Copyright 1985, Nature Publishing Group)

(i) for the mixed layer (total heat capacity C_m)

$$C_m \frac{d\Delta T}{dt} = \Delta Q - \lambda \Delta T - \Delta M \tag{3.24}$$

(ii) for the deeper waters

$$\frac{\partial \Delta T_0}{\partial t} = K \frac{\partial^2 \Delta T_0}{\partial z^2} \tag{3.25}$$

This latter equation may be evaluated at any depth, z (measured vertically downwards from zero at the interface), or calculated numerically using a vertical grid. In either case, the heat source at the top surface of the deep water is the energy 'leaking' out of the mixed layer, ΔM, which thus acts as a surface boundary condition to the lower-level differential equation (Equation (3.25)). However, a simpler parameterization can be utilized by assuming that at the interface there is continuity between the mixed-layer temperature change, ΔT, and the deeper-layer temperature change evaluated at the interfacial level, $\Delta T_o(0,t)$, i.e.

$$\Delta T_0(0,t) = \Delta T(t) \tag{3.26}$$

With this formulation, the value of ΔM can be calculated from

$$\Delta M = -\gamma \rho_w c_w K \left\{ \frac{\partial \Delta T_0}{\partial z} \right\} \Bigg|_{z=0} \tag{3.27}$$

and used in Equation (3.24). In this last equation, γ is the parameter utilized to average over land and ocean and has a value between 0.72 and 0.75, ρ_w is the density of water and c_w is its specific heat capacity.

The model described by Equations (3.24) and (3.25) can be used to evaluate different atmospheric forcings, related to possible impacts of increasing atmospheric carbon dioxide. There are two possible forms for the change, ΔQ: either an instantaneous 'jump'

$$\Delta Q = a \tag{3.28}$$

or a gradual increase

$$\Delta Q = bt \exp(\omega t) \tag{3.29}$$

where b and ω are coefficients. Using both these forms for ΔQ, it is possible to compare a full numerical solution of the model with an approximation that is gained by considering an infinitely deep ocean for which ΔM can be given by the expression

$$\Delta M = \gamma \mu \rho_w c_w h \frac{\Delta T}{(\tau_d t)^{1/2}} \tag{3.30}$$

where μ is a tuning coefficient evaluated by comparison with the numerical solution, h is the mixed layer depth and τ_d ($= \pi h^2/K$) a characteristic time for exchange between the mixed layer and the deep ocean. Substituting Equation (3.30) into Equation (3.24) results in an ordinary differential equation:

$$\gamma \frac{d\Delta T}{dt} + \Delta T \left\{ \frac{1}{\tau_f} + \frac{\mu\gamma}{(\tau_d t)^{1/2}} \right\} = \frac{\Delta Q}{\rho_w c_w h} \tag{3.31}$$

where $\tau_f = \rho_w c_w h/\lambda$. This can then be solved analytically using a prescribed functional form for ΔQ. For the two expressions, given here as Equations (3.28) and (3.29), values for the temperature increment over a period of 130 years (1850–1980)

can be deduced (Figure 3.8b) for chosen values of K and h. Here two sets of parameter values are shown. Using the CO_2 values observed for 1958 (315 ppmv) and 1980 (338 ppmv), the coefficients b and ω are easily evaluated from the equation for the increase of CO_2, which, corresponding to Equation (3.29), is

$$C(t) = C_0 \exp(B^* t \exp(\omega t)) \tag{3.32}$$

The values of the two coefficients, C_0 and B^*, are determined by choice of initial (1850) CO_2 concentrations (horizontal axis in Figure 3.8b), from which the coefficient b in Equation (3.25) can then be calculated as

$$b = \frac{B^* \Delta Q_{2x}}{\ln 2} \tag{3.33}$$

where the atmospheric forcing resulting from a doubling of CO_2, ΔQ_{2x}, is related to the chosen values for the climate feedback parameter, λ (where λ is the same as λ_{TOTAL} defined in Section 1.4.4), and the assumed value for the CO_2 doubling temperature change, ΔT_{2x} (vertical axis in Figure 3.8b).

$$\Delta Q_{2x} = \lambda \Delta T_{2x} \tag{3.34}$$

From these diagrams it is apparent that for reasonable estimates of initial (viz. 1850 baseline) carbon dioxide concentration (270 ppmv), the expected 1850 to 1980 temperature increment of the mixed layer for a wide range (0–5 K) of expected temperature increments due to a doubling of CO_2 is well in accord with observations. (Note that the observed air temperature increments must be assumed equal to the mixed layer temperature increases over the same period by assuming long-term quasi-equilibrium.) A numerical implementation of this simple box model is available on the Primer CD (see Appendix C).

3.6.3 A coupled atmosphere, land and ocean energy balance box model

It is possible to increase the level of complexity incorporated into a box model, such as that described in the previous section, so that other features can be resolved. Figure 3.9 illustrates the components of an energy balance box model that includes separate subsystems for Northern and Southern Hemisphere land, ocean mixed layer, ocean intermediate layer and deep oceans. This model separates the atmospheric response over land and ocean and incorporates polar sinking of oceanic water into the deep ocean (the formation of deep water). Despite these features, the model is essentially a box advection–diffusion model although it includes seasonally varying mixed layer depth and is forced with a seasonally varying insolation.

As with all relatively simple models, some features are prescribed. For example, hemispherically averaged cloud fraction is prescribed as a seasonally varying feature. As the land is hemispherically averaged, there is no opportunity to incorporate a temperature–surface albedo feedback in this sort of model. Despite these constraints, this simple box model can be used to investigate sensitivity to features

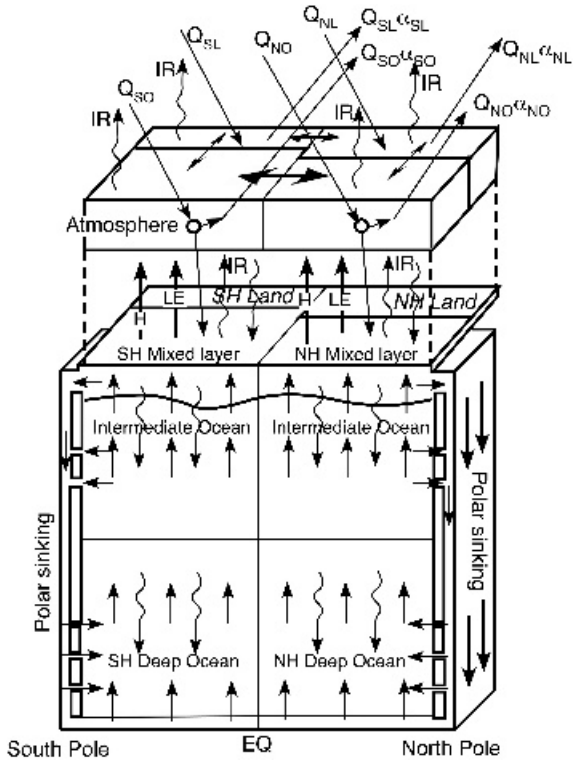

Figure 3.9 Illustration of the construction of and interactions within a complex box model of the Earth's climate system which includes hemispheric and land/ocean resolution and oceanic deep water formation (reproduced by permission of the American Geophysical Union from Harvey and Schneider (1985), *J. Geophys. Res.*, **90**, 2207–2222)

that have not yet been effectively incorporated into coupled ocean–atmosphere GCMs such as those discussed in Chapter 5. For example, the response of atmospheric and mixed layer temperatures to feedback processes involving changes in vertical diffusivity and changes in vertical velocities can be computed explicitly. Figure 3.10 shows the response of the atmospheric temperatures over the land and over the ocean, and of the oceanic mixed layer temperature of both hemispheres, following a transient CO_2 perturbation simulated by a change in the parameterization of the infrared (IR) emission to space, where

$$\text{Emitted IR} = A' + B'T + (\text{cloud term}) \tag{3.35}$$

and the transient increase in atmospheric CO_2 causes a change in A' given by

$$\Delta A'(t) = -2.88 \times 10^{-4} t^2 \tag{3.36}$$

where t is the time, in years, since 1925. Here A' and B' are empirical parameters.

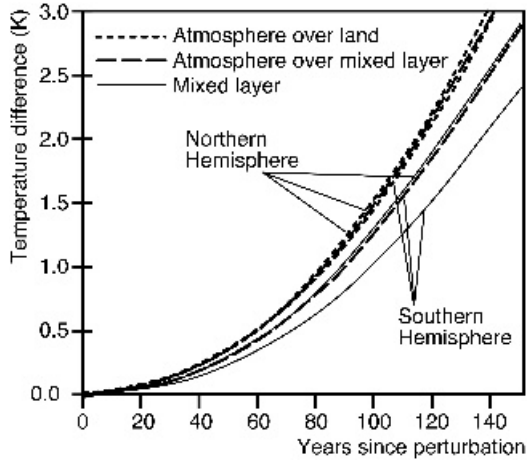

Figure 3.10 Effect of increasing CO_2 on the climate of the sophisticated box model of the climate system shown in Figure 3.9 (reproduced by permission of the American Geophysical Union from Harvey and Schneider (1985), *J. Geophys. Res.*, **90**, 2207–2222)

In this model, oceanic vertical velocities can change in perturbed climatic states. The results in Figure 3.10 follow from the velocity increase in the Northern Hemisphere and the decrease in the Southern Hemisphere. There is a faster mixed layer warming which reduces the lag of the mixed layer warming behind the atmospheric warming in the Northern Hemisphere as compared with the response in the Southern Hemisphere. These results suggest that more detailed analysis of oceanic feedback effects is required than can apparently be accomplished at present by three-dimensional coupled ocean–atmosphere models. These box models often rely on GCMs to calibrate transport and diffusion coefficients and are thus only as representative of the real climate as these GCMs. In the IPCC Second and Third Scientific Assessments, models like this were used to examine the likely thermal expansion of the oceans, considering a wider range of futures for fossil fuel usage than possible with (expensive) GCMs. Figure 3.11 shows the sea-level rise predicted for a range of futures including changing levels of tropospheric aerosols.

3.7 ENERGY BALANCE MODELS: DECEPTIVELY SIMPLE MODELS

Although they are of very simple construction, EBMs are extremely valuable tools in our study of the climate system. By forcing an EBM with random heat flux anomalies, it is possible to investigate the relationship between this ‘weather’ and variability on longer time-scales. Simple EBMs can generate useful information on decadal and longer-term variability. They can tell us about the variability and responsiveness of the cryosphere through changes in ice-sheet growth and decay, and they offer information on other ‘passive’ aspects of variability. In this chapter, we have

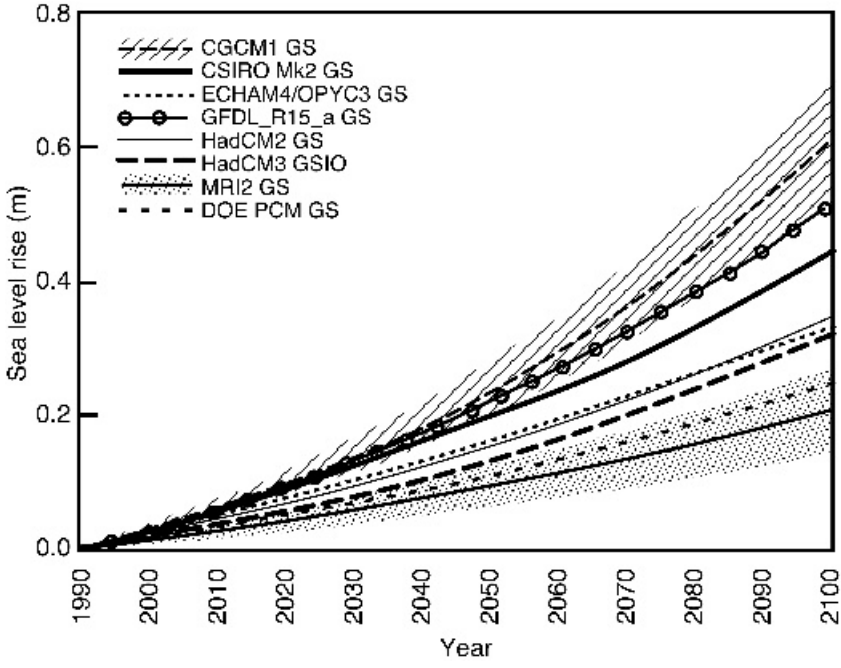

Figure 3.11 IPCC global average sea-level rise 1990 to 2100 for the IS92a scenario, including the direct effect of sulphate aerosols. Thermal expansion and land ice changes were calculated from AOGCM experiments, and contributions from changes in permafrost, the effect of sediment deposition and the long-term adjustment of the ice sheets to past climate change were added. For the models that project the largest (CGCM1) and the smallest (MRI2) sea-level change, the shaded region shows the bounds of uncertainty associated with land ice changes, permafrost changes and sediment deposition. Uncertainties are not shown for the other models. The outermost limits of the shaded regions indicate our range of uncertainty in projecting sea-level change for the IS92a scenario. (Reproduced by permission of the IPCC from Houghton *et al*., 2001)

intentionally emphasized the simple basis of EBMs – the energy fluxes into and out of the climate system as a whole (or parts of it) must balance unless there is cooling or heating. This concept is fundamental to climate modelling. It will recur in Chapter 4, where the heating rates of atmospheric layers are computed for the energy balance, and in Chapter 5, where each of the components of global climate models are seen to be driven by their energy balances.

The other topic which has been stressed in this chapter is computing. We wanted to underline that the basis of practically all climate modelling is (relatively) simple mathematical formulations and parameterizations represented in and executed by very fast computers. We have listed the full code of one EBM in Figure 3.2. The code of an atmospheric GCM written in a similar high-level language (most are currently written in FORTRAN, which is similar to BASIC) would be as thick as a sub-

stantial dictionary. More sophisticated coupled GCMs have codes whose page listings are thicker than a stack of encyclopaedias but, despite this apparent complexity, the exercises posed in this chapter could usefully be considered with reference to more complex models. Indeed, EBM-type analyses are commonly performed on the output of GCMs. It is therefore helpful to keep in mind the fundamental concepts developed in this chapter and to return, often, to the deceptively simple basis of the models described. The principle of energy balance is fundamental to the construction of physically based climate models and the concept of using models to reveal and interpret the nature of the climate system, and its behaviour is to be found throughout the remainder of this book.

RECOMMENDED READING

Abbott, E.A. (1884) *Flatland: A Romance of Many Dimensions*, (5th edn). Barnes and Noble, New York, 108 pp.

Budyko, M.I. (1969) The effect of solar radiation variations on the climate of the Earth. *Tellus* **21**, 611–619.

Cess, R.D. (1976) Climatic change, a reappraisal of atmospheric feedback mechanisms employing zonal climatology. *J. Atmos. Sci.* **33**, 1831–1843.

Hansen, J., Russell, G., Lacis, A., Fung, I., Rind, D. and Stone, P. (1985) Climatic response times: dependence on climate sensitivity and ocean mixing. *Science* **229**, 857–859.

Harvey, L.D.D. and Schneider, S.H. (1985) Transient climate response to external forcing on $100–10^4$ year time-scales. 2. Sensitivity experiments with a seasonal, hemispherically averaged, coupled atmosphere, land, and ocean energy balance model. *J. Geophys. Res.* **90**, 2207–2222.

Hyde, W.T., Crowley, T.J., Baum, S.K. and Peltier, W.R. (2000) Neoproterozoic 'Snowball Earth' simulations with a coupled climate/ice-sheet model. *Nature* **405**, 425–429.

Lee, W-H. and North, G.R. (1995) Small ice cap instability in the presence of fluctuations. *Clim. Dyn.* **11**, 242–246.

Murphy, J.M. (1995) Transient response of the Hadley Centre coupled ocean–atmosphere model to increasing carbon dioxide. Part III: Analysis of global mean response using simple models. *J. Climate* **8**, 496–514.

North, G.R., Cahalan, R.F. and Coakley, J.A. (1981) Energy balance climate models. *Rev. Geophys. Space Phys.* **19**, 91–121.

Oerlemans, J. and van der Veen, C.J. (1984) *Ice Sheets and Climate*. Reidel, Dordrecht, 217 pp.

Sellers, W.D. (1969) A global climatic model based on the energy balance of the Earth–atmosphere system. *J. Appl. Met.* **8**, 392–400.

van de Wal, R.S.W. and Oerlemans, J. (1997) Modelling the short-term response of the Greenland ice-sheet to global warming. *Clim. Dyn.* **13**, 733–744.

Walker, G. (2003) *Snowball Earth: The Story of the Great Global Catastrophe that Spawned Life as We Know It*. Random House, New York, 269 pp.

Warren, S.G. and Schneider, S.H. (1979) Seasonal simulation as a test for uncertainties in the parameterization of a Budyko–Sellers zonal climate model. *J. Atmos. Sci.* **36**, 1377–1391.

Watson, A.J. and Lovelock, J.E. (1983) Biological homeostasis of the global environment: The parable of Daisyworld. *Tellus* **35**, 284–288.

Wigley, T.M.L. and Schlesinger, M.E. (1985) Analytical solution for the effect of increasing CO_2 on global mean temperature. *Nature* **315**, 649–652.

Wigley, T.M.L. and Raper, S. (1992) Implications for climate and sea level of revised IPCC emissions scenarios. *Nature* **357**, 293–300.

Web resources

http://profhorn.meteor.wisc.edu/wxwise/museum/	The Verner E. Suomi Virtual Museum features an interactive exhibit on planetary energy balance MAGICC, and SCENGEN
http://www.cgd.ucar.edu/cas/wigley/magicc/	
http://homepages.vub.ac.be/%7Ephuybrec/eismint.html	Ice sheet model intercomprison for Greenland
http://www.geop.ubc.ca/Glaciology/modelling.html	Ice sheet modelling at University of British Columbia
http://www.ume.maine.edu/iceage/Research/Contrib/html/contrib15.html	Ice sheet modelling at the University of Maine
http://www.geo.utexas.edu/courses/387h/climate_models.htm	Hands-on climate models at the Geological Sciences Department at the University of Texas at Austin

CHAPTER 4

Intermediate Complexity Models

Everything that can be counted does not necessarily count; everything that counts cannot necessarily be counted.

Albert Einstein

4.1 WHY LOWER COMPLEXITY?

There has always been, and hopefully always will be, a diversity of climate models. At one end of the modelling spectrum lie the fully integrated and 'comprehensive' coupled climate system models while at the other is the set of highly idealized and simplified 'conceptual' models. In the 1980s, when the first edition of this book appeared, there was a clear progression of models, which we embodied in the climate modelling pyramid (Figure 2.1). This constructed hierarchy is useful for didactic purposes, but does not reflect all the uses to which models are put, nor the value that can be derived from them. The goal of developers of comprehensive models is to improve performance by including every relevant process, as compared to the aim of conceptual modellers who try to capture and understand processes in a restricted parameter space. Between these two extremes there is a large territory populated, in part, by leakage from both ends. This intermediate area is lively and fertile ground for modelling innovations. The spectrum of models we describe in this chapter should not be viewed as poor cousins to the coupled models in Chapter 5. This intermediate ground is well frequented by coupled modelling groups as they test parameterizations and attempt to understand more fully their complex model. It has also generated, over the last five or six years, a community of models and modellers so distinct that they are worthy of separate consideration. This community of modellers has constructed Earth Models of Intermediate Complexity (EMICs).

Although the idea of EMICs has existed for decades, the first international workshop designed to define and discuss them was held only in 1999 at the Potsdam Institute for Climate Impact Research. This meeting, while recognizing a variety of goals of EMIC developers, sought to define their model group. They determined that EMICs share with comprehensive models the characteristic that the number of their

A Climate Modelling Primer, Third Edition. K. McGuffie and A. Henderson-Sellers.
 ISBN: 0-470-85750-1 (HB); 0-470-85751-X (PB)

adjustable parameters is significantly less (by several orders of magnitude) than the modelled degrees of freedom.

EMICs are like comprehensive models in aspiration, but their developers make specific decisions to parameterize interactions so that these models can simulate tens to hundreds of thousands of years. The relative positioning of conceptual, comprehensive and EMIC model types in process, detail and integration space is shown in Figure 4.1, which complements the depiction in Figure 2.1.

The Potsdam workshop identified ten of the EMICs tabulated in Table 4.1 and there are certainly others that can claim this name. These can be seen to have a model dimensionality of approximately 2, placing them rather higher in the climate pyramid (Figure 2.1) than simple one-dimensional radiative–convective models but still significantly lower than fully comprehensive models.

We also explore this middle ground by looking at models with only one or two dimensions. Although these can trace their origin to the early days of climate modelling and the need to perform calculations with limited computing resources, they remain a vital tool for climate modellers today. Modellers now look to these models as a means of examining a particular aspect or aspects of the climate system in as efficient a manner as possible, or as a means of developing and testing new parameterizations. In this chapter, we will examine how these one- and two-dimensional models are constructed and how they are put to use, sometimes in the construction of EMICs. We also look in detail at the nature of some of these EMICs and consider how, as the spectrum of models has become populated, the distinction between model types has become less clear.

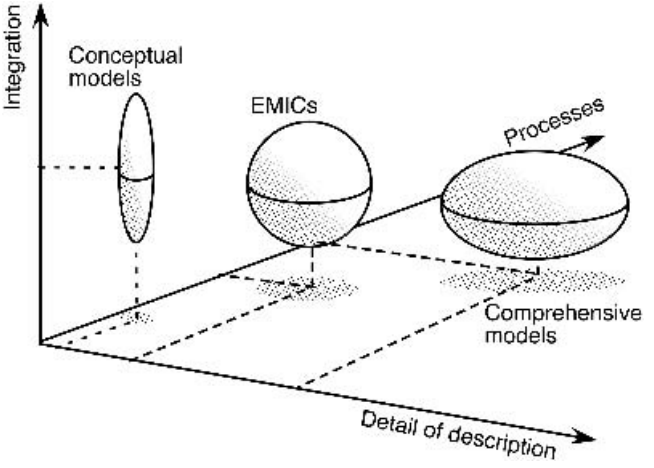

Figure 4.1 Schematic illustration of the domain of EMICs in the three-dimensional space of processes, integration and detail of description. Reproduced with permission from Claussen *et al.*, 2002, *Climate Dynamics*, **18**, 579–586. Copyright (2003) Springer

Table 4.1 Earth models of intermediate complexity (EMICs)

		Model Components (dimension)			
Name	*Example Applications*	*Atmosphere*	*Ocean*	*Cryosphere*	*Biosphere and Carbon*
Bern 2.5D	Thermohaline circulation. Ocean carbon cycle. Sea-level projections. Probability density functions of future climates	EBM (1.5), 17 meridional zones	Zonal (2), multi-basin, 14 vertical layers	Thermodynamic sea ice (2)	4 box terrestrial biosphere. Prognostic ocean carbon cycle including isotopes
CLIMBER-2	Last glacial maximum, especially the role of the ocean. Holocene carbon cycle. Land use/vegetation sensitivities	Statistical dynamical (2.5)	Zonal (2) Multi-basin	Thermodynamic and advected sea ice (2), Thermomechanical ice sheet (3)	Dynamic vegetation with 4 carbon pools. Marine biota and vertical profiles of carbon
ECBILT	Decadal variability in oceans. Holocene orbital variability in insolation. Multi-decadal variability *cf.* proxy data	GCM with 3 levels (<~3)	3-D (3)	Thermodynamic (2) and dynamic sea ice	(?none?)
ECBILT-CLIO-VECODE	Decadal to centennial polar variability. Transient Holocene climate. 8200 yr BP cold event	GCM with 3 levels (<~3)	3-D with 20 vertical layers (3)	Dynamic sea ice (2.5)	Dynamic vegetation
IAPRAS	Diurnal cycle changes in greenhouse. Intraseasonal climate variability. Interdecadal variability of the N. Atlantic oscillation	Statistical dynamical (2)	Statistical dynamical (2)	Energy balance sea ice (1)	Land surface with fixed vegetation

Table 4.1 *Continued*

Name	*Example Applications*	*Model Components (dimension)*			
		Atmosphere	*Ocean*	*Cryosphere*	*Biosphere and Carbon*
McGill Palaeo	Mechanisms of glaciation. Thermohaline circulation interactions with ice sheets. Non-linearities of cold climates	EMBM (1.5) resolving major continents and oceans	Zonally averaged (2.5) multi-basin	Thermodynamic sea ice (1). Dynamic ice sheets (2)	Land surface with active vegetation
MIT IGSM	Analysis of Kyoto Protocol. Uncertainties in model characterizations. Ecosystems and thermohaline circulation changes in greenhouse	Statistical dynamical (2). Chemistry includes 43 species	3-D with 15 vertical layers (3)	Thermodynamic sea ice (2). Mass balance of continental glaciers	Dynamic terrestrial ecosystems
MoBidiC	Milankovitch forcings. Holocene volcanic and solar variability. Freshwater inputs to oceans	Sectoral model with 2 levels (2)	3 basins with 15 layers (2)	Thermodynamic sea ice with prescribed advection (1)	Dynamic vegetation. Ocean carbon cycling
PUMA	Last glacial cycle. Greenhouse warming effects. Processes of glaciation and deglaciation	GCM (3)	3-D (3)	Thermodynamic sea ice (1)	Dynamic vegetation
UVicESCM	Last glacial maximum. North Atlantic variability. Dansgaard–Oeschger oscillations. Glacial inception/deglaciation	Dynamic energy-moisture balance model (1.5)	3-D with 19 vertical layers (3)	Thermodynamic and dynamic sea ice (2). Thermomechanical ice sheets	Dynamic vegetation. Ocean and terrestrial carbon cycle

See web resources for further information.
More details of some of these EMICs are on the Primer CD (see Appendix C).

4.2 ONE-DIMENSIONAL RADIATIVE–CONVECTIVE MODELS

In earlier chapters, the importance of the greenhouse effect was noted. This effect is due to the absorption of the upwelling thermal infrared radiation that has been emitted by the surface of the Earth. If none of the gases in the Earth's atmosphere possessed absorption features in the wavelength region in which the Earth emits radiation, there would be no greenhouse addition and the surface temperature would be equal to the planetary effective radiative temperature (see Figure 3.1). The greenhouse absorbers not only affect the surface temperature, they also modify the atmospheric temperature by their absorption and emission of radiation. Radiative–convective models were developed primarily to allow examination of these radiative effects in the Earth's atmosphere.

Radiative–convective (RC) climate models are one-dimensional models like the EBMs described in Chapter 3. In this case, however, the dimension is the vertical. These models resolve many layers in the atmosphere and seek to compute atmospheric and surface temperatures. They can be used for sensitivity tests and, importantly, offer the opportunity to incorporate more complex radiation treatments than can be afforded in GCMs.

RC models derive a temperature profile for the atmosphere by dividing it into a number of layers. Suppose we divide the Earth's atmosphere into two layers so that each layer just absorbs the infrared radiation incident on it and, for this very simple example, let each layer be described as having an infrared optical thickness of $\tau = 1$. The principal absorber in the Earth's atmosphere is water vapour, which is contained almost entirely within the lowest few kilometres. Thus our two layers can be taken to be centred at heights of 3 km (layer 1) and 0.5 km (layer 2). The infrared energy fluxes are shown in Figure 4.2. Both layers radiate as black bodies upwards and downwards and the ground radiates upwards. Since the planet is emitting at its effective temperature, T_e, and because all radiation from below is absorbed by the top layer, σT_e^4 must equal σT_1^4 and thus $T_1 = T_e$. The energy balance of the lower atmospheric layer is (emitted = absorbed) or $\sigma T_2^4 = 2\sigma T_1^4 = 2\sigma T_e^4$. In general, the temperature of layer n can be shown to be related to the effective temperature by

$$T^4(n) = \tau_{TOTAL}(n) T_e^4 \tag{4.1}$$

where $\tau_{TOTAL}(n)$ is the total infrared optical thickness from the top of the atmosphere to layer n. In our simple case, because each layer has $\tau = 1$, then $\tau_{TOTAL}(n) = n$. From Equation (4.1), we can now calculate that the temperature of the top layer is equal to the effective temperature (255 K) and that the lower-layer temperature is 303 K. The surface temperature can be obtained by considering the radiative budget of the second atmospheric layer. Here $2\sigma T_2^4 = \sigma T_g^4 + \sigma T_1^4$ so that $T_g = (3T_e^4)^{1/4}$, which is 335 K.

These approximations are drastic but the resultant temperature/height profile (Figure 4.2) is quite close to the radiative equilibrium profiles which were first produced by RC models. Note that the surface air temperature is lower than the ground temperature and the upper layer temperature lower than the lower one. Compared

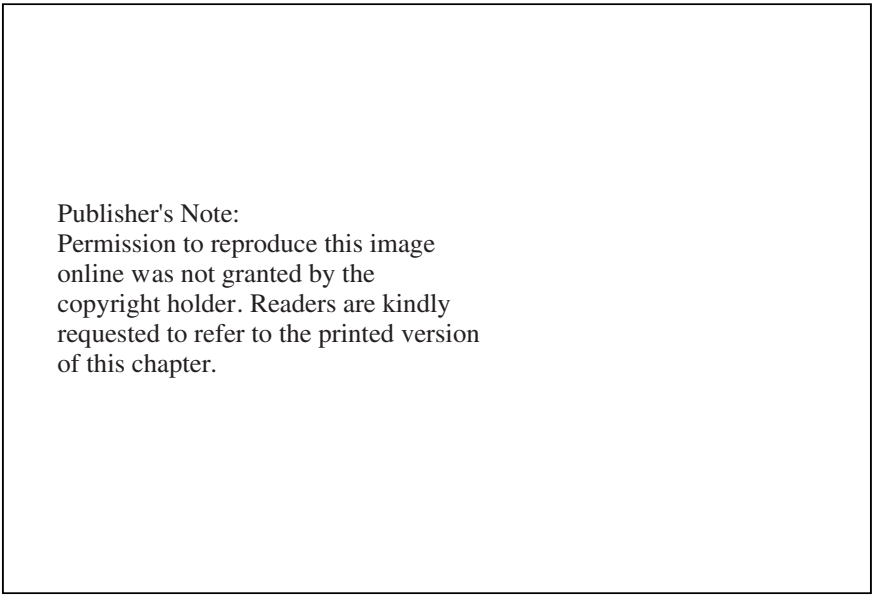

Figure 4.2 The radiative equilibrium temperature profile calculated using the very simple model described in the text compared with the lapse rate of $6.5\,\mathrm{K\,km^{-1}}$. This lapse rate is achieved by convection since the radiative temperature profile is unstable. On the right-hand side, the infrared radiative energy fluxes in the simple two-layer model

with the standard (i.e. observed) lapse rate (the decrease of temperature with height), which is about $6.5\,\mathrm{K\,km^{-1}}$, our calculated radiative temperature profile is unstable. Thus, if a small parcel of air were disturbed from a location close to the surface, it would tend to rise because it would be warmer than the surrounding air. Its temperature would decrease at (roughly) the observed lapse rate so that at some arbitrary height (H) its temperature would be greater than that of the atmosphere. It would therefore continue to rise. Such a rising parcel of air would carry energy upwards and the resulting convection currents would mix the atmosphere, in this example, throughout the whole depth of the troposphere. The convective mixing would alter the temperature profile until the atmosphere was dynamically stable.

This convective adjustment of a radiatively produced temperature profile is the essence of RC models. In the above, highly simplified, discussion, we have made several gross assumptions but the basic concept of a radiatively computed temperature profile being adjusted to stability by parameterized convection is sound.

The structure of global radiative–convective models

The RC model is a single column containing the atmosphere and bounded beneath by the surface. This bounded column usually represents the globally averaged con-

ditions in the Earth–atmosphere system. As the name of the model type indicates, radiation and convection are treated explicitly. The radiation scheme is detailed and occupies the vast majority of the total computation time while the 'convection' is accomplished by a numerical adjustment of the temperature profile at the end of each timestep. In addition, some RC models also include cloud prediction schemes. The atmosphere is divided into a number of layers not necessarily of equal thickness. The layering can be defined with respect to height or pressure but it is more common to introduce the non-dimensional vertical co-ordinate, σ (sigma – not to be confused with the Stefan–Boltzmann constant), which is a function of pressure

$$\sigma = \frac{p - p_T}{p_s - p_T} \tag{4.2}$$

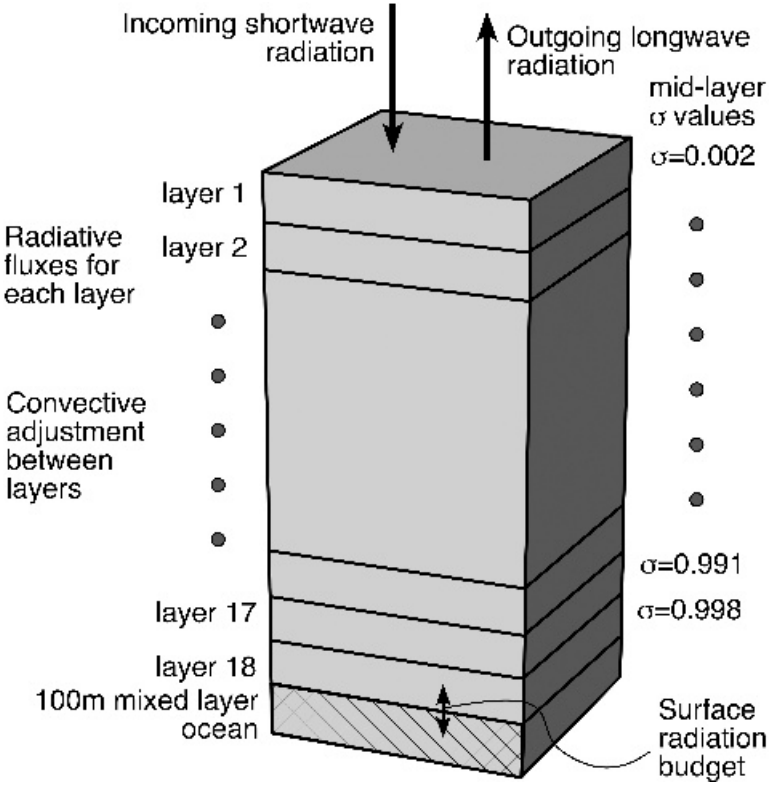

Figure 4.3 The vertical structure of an RC model. This particular model (which is included on the Primer CD) has 18 vertical layers and includes a 100 m ocean slab to represent the thermal inertia of the ocean mixed layer

where p is the pressure, p_T the (constant) 'top-of-the-atmosphere' (usually a low stratosphere location) pressure and p_s the (variable) pressure at the Earth's surface. The top of the atmosphere has $\sigma = 0$ and the surface always has $\sigma = 1$. The σ values at selected layer boundaries in an eighteen-layer atmosphere are given in Figure 4.3. In this example model, which is included on the Primer CD, the layers extend from the surface to around 42 km, where the pressure is assumed to be zero. The sigma co-ordinate system, when used in GCMs, avoids the complications associated with model levels intersecting mountain ranges. The choice of sigma level values is arbitrary. In the RC model on the Primer CD, the levels are evenly spaced in the sigma co-ordinate system, with the resulting advantage that the layer masses are equal.

4.3 RADIATION: THE DRIVER OF CLIMATE

Radiation is fundamental to the climate. Solar radiation is absorbed and infrared radiation emitted, with these two terms balancing over the globe when averaged over a few years. This simple energy balance was the basis of the EBMs described in Chapter 3, but in EBMs the way in which radiation is absorbed, transferred and re-emitted by the atmosphere was ignored. Here we stress the radiative transfer processes: the heating of the surface by absorption of shortwave energy and the heating and cooling of the atmosphere by absorption and emission of infrared radiation. The absorption and emission of radiation by the atmosphere is based on fundamental and well-established physics. We can make detailed measurements in laboratories and test our modelling by observation of stars and planets. Although the examples presented here are simple cases, the basic idea remains the same in more complex models and it is useful to spend some time on this topic.

The principles involved in radiative computations in climate models are most readily illustrated by considering a very simple global model in which a single cloud or aerosol layer is spread homogeneously over the surface (Figure 4.4). The incident solar radiation of S W m^{-2} can be traced as it interacts with the cloud. A part is reflected, a part absorbed and a part transmitted; the cloud albedo, α_c, and shortwave absorptivity, a_c, control these interactions. The remaining solar flux interacts with the surface. Here, only reflection and absorption occur and the reflected ray can be followed through the cloud and out to space. The infrared radiation emitted from the surface is partially absorbed by the cloud. Here, it is assumed that the infrared absorption of the cloud is equal to the infrared emissivity of the cloud, ε. The downwelling radiation from the cloud adds to the surface heating, thus contributing to the greenhouse effect.

Three main assumptions have been made in this simple model: (i) there is no reflection of the upward-travelling shortwave radiation by the cloud; (ii) the surface emissivity has been set equal to unity; and (iii) the cloud/dust absorption in the infrared wavelength region is equal to ε. With all these assumptions, three energy balance equations can be written if it is also assumed that the model has reached equilibrium. Absorbed and emitted or reflected radiation at each level are equated so that

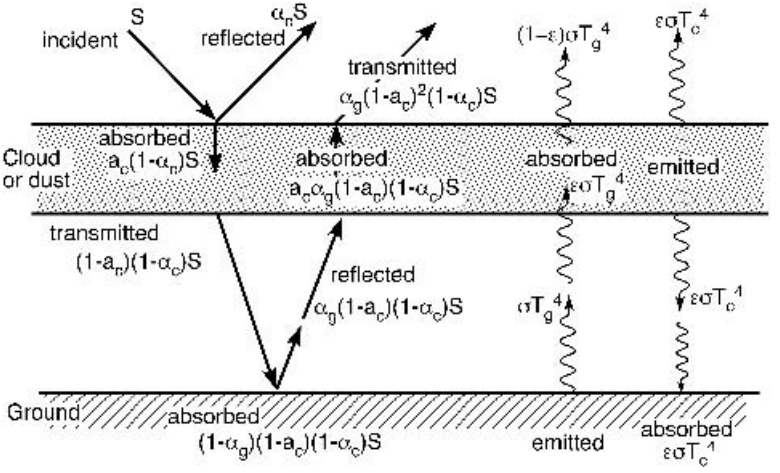

Figure 4.4 Idealized radiative interaction between a cloud or dust layer and the surface. There is assumed to be no reflection from the cloud base. The solar radiation suffers absorption on each passage through the layer. The infrared absorption is equal to the emissivity

$$S = \alpha_c S + \alpha_g (1-a_c)^2 (1-\alpha_c) S + \varepsilon\sigma T_c^4 + (1-\varepsilon)\sigma T_g^4 \tag{4.3}$$

$$a_c(1-\alpha_c)S + a_c\alpha_g(1-a_c)(1-\alpha_c)S + \varepsilon\sigma T_g^4 = 2\varepsilon\sigma T_c^4 \tag{4.4}$$

$$(1-\alpha_g)(1-a_c)(1-\alpha_c)S + \varepsilon\sigma T_c^4 = \sigma T_g^4 \tag{4.5}$$

Equations (4.3)–(4.5) represent the energy balances at the top of the atmosphere, the cloud level and the surface respectively. These equations can be solved directly by giving values for the dust/cloud shortwave absorption, a_c, albedo, α_c, its infrared emissivity, ε, and the surface albedo, α_g. Alternatively, the surface albedo term and the cloud temperature term can be eliminated from the equations leaving an expression for T_g:

$$\sigma T_g^4 = \frac{S(1-\alpha_c)}{(2-\varepsilon)}(2-a_c) \tag{4.6}$$

Taking the value of S as a quarter of the solar flux at the planet, i.e. $S = 343\,\mathrm{W\,m^{-2}}$, and considering first the cloudless atmosphere case, if $\alpha_c = 0.08$, appropriate to scattering by atmospheric molecules alone, $a_c = 0.15$, representing absorption by the atmosphere, and $\varepsilon = 0.4$, then the surface temperature is 283 K. This is quite close to the global average surface temperature of ~288 K.

We can now consider the addition of 'clouds' to this simple model; first a volcanic aerosol cloud and second a water droplet cloud. Inserting a volcanic aerosol into an otherwise cloudless atmosphere will increase the albedo slightly, say $\alpha_c = 0.12$, and will increase the solar absorption and the infrared emissivity, say to $a_c = 0.18$ and $\varepsilon = 0.43$. Thus this volcanic aerosol 'cloud' gives rise to a cooling with the

global mean temperature dropping to 280 K. (Note that Figure 1.16 shows a similar cooling caused by the introduction of a volcanic aerosol cloud into a more complex model.)

Alternatively, we could consider the introduction of a water droplet cloud into the original cloudless atmosphere. If we assume that the cloud cover is approximately the same as that of the present day then α_c increases, say to 0.30, a_c increases slightly to 0.20 and ε increases to 0.90. With these values for partly cloudy skies, the globally averaged surface temperature is 288 K. The introduction of this water droplet cloud has increased the calculated surface temperature because, with the radiative characteristics we have chosen, the greenhouse effect of the cloud is greater than the albedo effect. If, however, we alter the selected value of α_c so that $\alpha_c = 0.40$ and allow the other values to remain the same then the surface temperature becomes 277 K. The cloud albedo effect has 'beaten' the greenhouse effect this time. The sensitivity of this simple model's climate (as represented by the computed surface temperature) illustrates the interconnected role of various parameters in radiative transfer calculations and, in particular, the importance of the relative impact of the absorption of incoming solar radiation and the emission of infrared radiation.

The following treatment of atmospheric radiation is more complex than this stylized model but still somewhat simplified. The principles are the same in most models, the major complicating features being detailed consideration of the dependence of scattering and absorption on wavelength and other atmospheric variables.

The temperature profile of the atmospheric column is computed by calculating the net radiative heating in each layer. Calculations are made in terms of the layer potential temperature θ_i given by

$$\theta_i = T_i(p_o/p)^{\kappa} \tag{4.7}$$

where $p_o = 1000$ hPa is a reference pressure and $\kappa = R/c_p = 0.286$, R is the gas constant for air and c_p is its specific heat at constant pressure.

The simplified atmosphere we will consider is shown in Figure 4.5. The radiation is assumed to be absorbed by layers A_1 (between model levels 0 and 2) and A_3 (between model levels 2 and 4). The shortwave and longwave radiation are treated separately. The shortwave radiation includes all the solar radiation, the attenuation of this radiation by Rayleigh scattering, its reflection from the Earth's surface and from clouds, and its absorption in the atmosphere and in clouds. The longwave radiation includes all emissions by the atmosphere, clouds and the Earth's surface. The ground temperature, T_g, needed in order to evaluate the evaporation, the sensible heat flux from the surface and the net longwave surface radiation, is determined from the heat balance at the Earth's surface.

4.3.1 Shortwave radiation

In the simple case, we divide the incoming solar radiation into two parts by wavelength, the division being somewhere between 0.7 and 0.9 μm. The two wavelength regions can then either be treated identically or the absorption and scattering can be

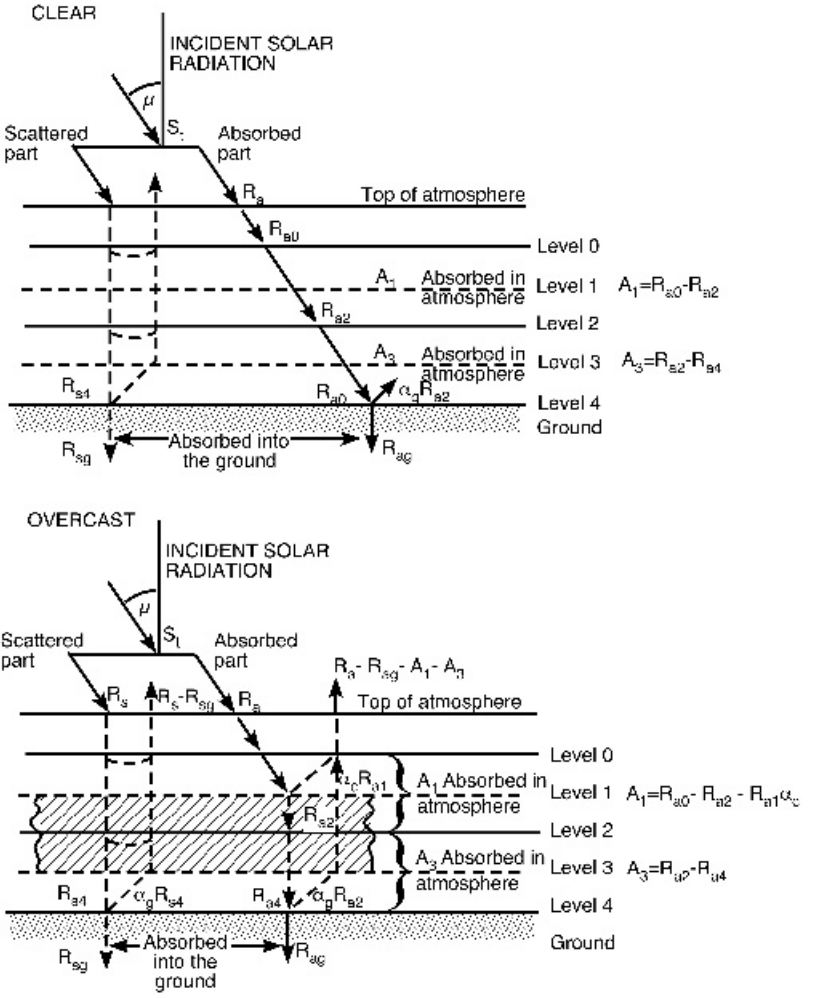

Figure 4.5 Schematic illustration of the principles of radiative transfer calculations. In this example there are only two atmospheric layers. More complex techniques involve many more layers and many spectral intervals. Although many schemes consider only clear and cloudy cases and deal with intermediate cloud amounts by weighting these results, advanced cloud-resolving models are being developed to compute explicitly the role of fractional cloud amount and these are likely to form the basis of future radiative schemes in climate models

partitioned by wavelength so that the two parts of the radiation are designated R_s (the shortwave part which is roughly 65 per cent of the total and is subject to Rayleigh scattering) and R_a (the near infrared wavelength part which is roughly 35 per cent of the total and is subject to atmospheric absorption). These can be approximated as

$$R_s = 0.65 S \cos\mu \tag{4.8}$$

$$R_a = 0.35 S \cos\mu \tag{4.9}$$

where S is the solar constant (adjusted for the Earth–Sun distance, which varies throughout the year) and μ is the zenith angle of the Sun. Some models calculate a mean value of μ, which is used during the hours of daylight. A summary of the disposition of these components of the shortwave radiation for both clear and cloudy skies is given in Figure 4.5 and is described in detail in the following paragraphs.

Albedo

The albedo of the clear atmosphere for the portion of the radiation subject to Rayleigh scattering is given by

$$\alpha_0 = \min[1,\ 0.085 - 0.247 \log_{10}\{(p_o / p_s)\cos\mu\}] \tag{4.10}$$

For an overcast atmosphere, the albedo for the scattered part of the radiation, α_{ac}, is composed of the contributions of Rayleigh scattering (by atmospheric molecules) and of Mie scattering (by cloud droplets). The simplest useful formulation is

$$\alpha_{ac} = 1 - (1 - \alpha_0)(1 - \alpha_c) \tag{4.11}$$

where α_c is the cloud albedo for both R_a and R_s.

Albedos are a function of the surface or cloud type. A reasonable global average surface albedo for the entire solar spectrum is $\alpha_g = 0.10$. For specific surfaces it is often considered advantageous to introduce a spectral dependence since vegetation albedos increase rather sharply at around 0.7 μm while snow and ice albedos begin to decrease at about the same wavelength (Figure 4.6).

Shortwave radiation subject to scattering (R_s)

The part of the solar radiation that is assumed to be scattered does not interact with the atmosphere, except to be partly scattered back to space. Thus the only part with which we are concerned is that amount that reaches, and is absorbed by, the Earth's surface. This is given by the expressions

$$\begin{aligned} R'_{sg} &= R_s \frac{(1-\alpha_g)(1-\alpha_0)}{(1-\alpha_0\alpha_g)} \quad \text{for clear sky} \\ R''_{sg} &= R_s \frac{(1-\alpha_g)(1-\alpha_{ac})}{(1-\alpha_{ac}\alpha_g)} \quad \text{for overcast sky} \end{aligned} \tag{4.12}$$

Multiple reflections between sky and ground or between cloud base and ground are accounted for by the terms in the denominators. For partly cloudy conditions (neither clear nor overcast) the scattered radiation absorbed at the Earth's surface is

$$R_{sg} = N R''_{sg} + (1 - N) R'_{sg} \tag{4.13}$$

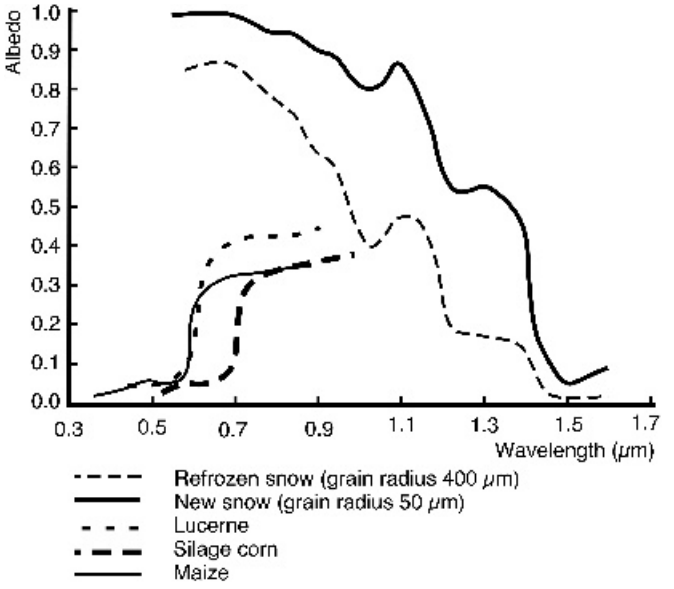

Figure 4.6 The spectral reflectance of different surface types. Note the markedly different spectral characteristics of snow surfaces and vegetated surfaces (reproduced by permission from Henderson-Sellers and Wilson (1983) *Rev. Geophys. Space Phys.*, **21**, 1743–1778, American Geophysical Union)

where N is the fractional cloudiness of the sky. Cloud albedo is a function of both the character and thickness of the cloud as is illustrated by the model and experimental results shown in Figure 4.7. The absorption of this radiation by the ground affects the ground temperature and subsequently affects the longwave emission from the ground and the ground-level heat balance.

Shortwave radiation subject to absorption (R_a*)*

The solar radiation subject to absorption is distributed as heat to the various layers in the atmosphere and to the Earth's surface. The absorption depends upon the effective water vapour content as well as the ozone and carbon dioxide amounts. Usually these absorptivities are computed semi-empirically using formulae appropriate to wide spectral intervals. For a cloudy sky the absorption in a cloud is generally prescribed as a function of cloud type only (e.g. Table 4.2).

The incoming beam becomes diffuse within any cloud, and its path is assumed to be 1.66 times the vertical thickness of the cloud. The factor 1.66 is often termed the Elsasser factor and is derived by assuming that the diffuse radiation is isotropic. Below the cloud, the beam is still diffuse and the factor 1.66 for path length is retained.

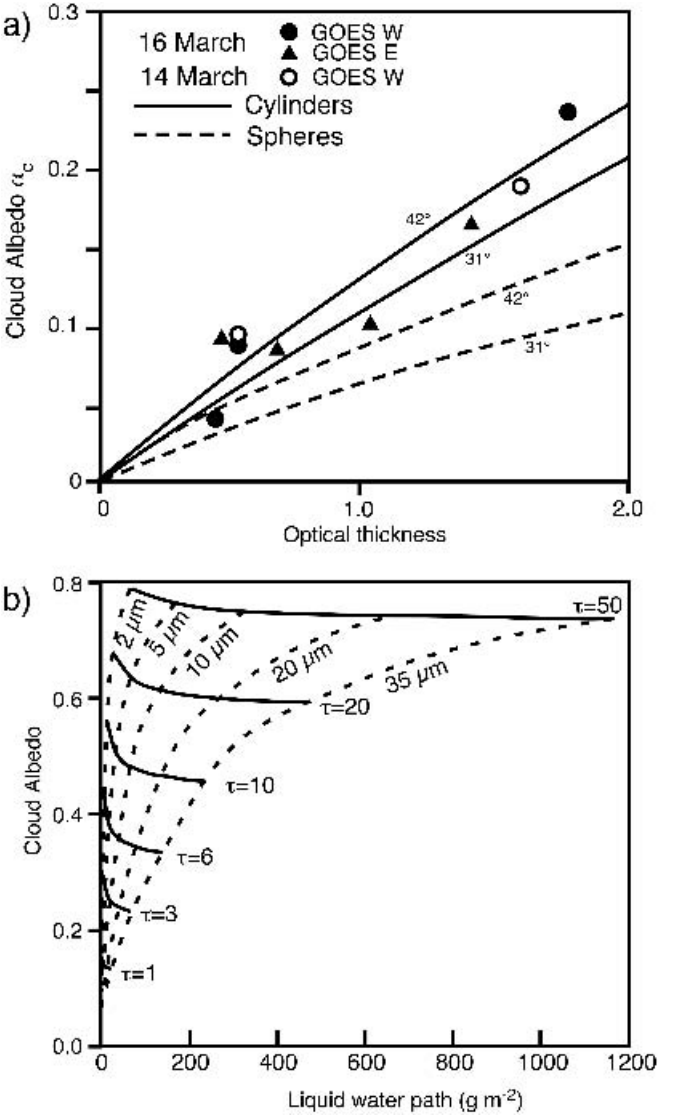

Figure 4.7 (a) Cloud albedo α_c, derived from the GOES satellite plotted as a function of lidar-derived cloud optical depths, δ_c. Also shown are theoretically predicted albedos, for two solar zenith angles, computed using ice spheres and ice cylinders (the latter being much more like the real cloud crystals) as the scattering objects (reproduced with permission from Platt *et al*. (1980) *Monthly Weather Review*, **108**, 195–204). (b) Cloud albedos, calculated as a function of effective droplet radius, r_e, and cloud liquid water path (reproduced by permission from Han *et al.* (1998), *J. Climate* **11**, 1516–1528, © Copyright American Meterorological Society, Boston)

Table 4.2 Typical albedos and absorptivities of clouds

Cloud level	*Albedo*	*Transmissivity*	*Absorptivity*
High	0.25	0.75	0.005
Middle	0.60	0.38	0.02
Low	0.70	0.36	0.035

When the sky is partly cloudy, the total flux at level i is given by a weighted average of the clear and overcast fluxes:

$$R_{ai} = NR''_{ai} + (1-N)R'_{ai} \tag{4.14}$$

That part of the flux subject to absorption which is actually absorbed by the ground is given (from Figure 4.5) by

$$R'_{ag} = (1-\alpha_g)R'_{a4} \tag{4.15}$$

for a clear sky, and by

$$R''_{ag} = \frac{(1-\alpha_g)R''_{a4}}{(1-\alpha_c\alpha_g)} \tag{4.16}$$

for a completely cloudy (overcast) sky, where the factor $1/(1-\alpha_c\alpha_g)$ again accounts for multiple reflections between the ground and cloud base. For partly cloudy skies, the radiation absorbed by the ground is therefore given by

$$R_{ag} = NR''_{ag} + (1-N)R'_{ag} \tag{4.17}$$

The total solar radiation absorbed by the ground will be the sum of that part of the solar radiation spectrum that is subject to (atmospheric) absorption and that part of the spectrum subject to atmospheric scattering; thus giving

$$R_g = R_{ag} + R_{sg} \tag{4.18}$$

4.3.2 Longwave radiation

The calculation of the longwave radiation, like that of the shortwave radiation, is based on an empirical transmission function depending primarily upon the amount of water vapour. The net longwave radiation at any level can be expressed as the sum of two terms (Figure 4.8):

$$F_{(net)} = F\downarrow - F\uparrow \tag{4.19}$$

The upward flux at $z = h$ for radiation at some wavelength, λ, consists of the sum of two terms:

$$F_\lambda\uparrow(h) = B_\lambda[T(0)]\tau_\lambda(h,0) + \int_0^h B_\lambda[T(z)](d/dz)\tau_\lambda(h,z)dz \tag{4.20}$$

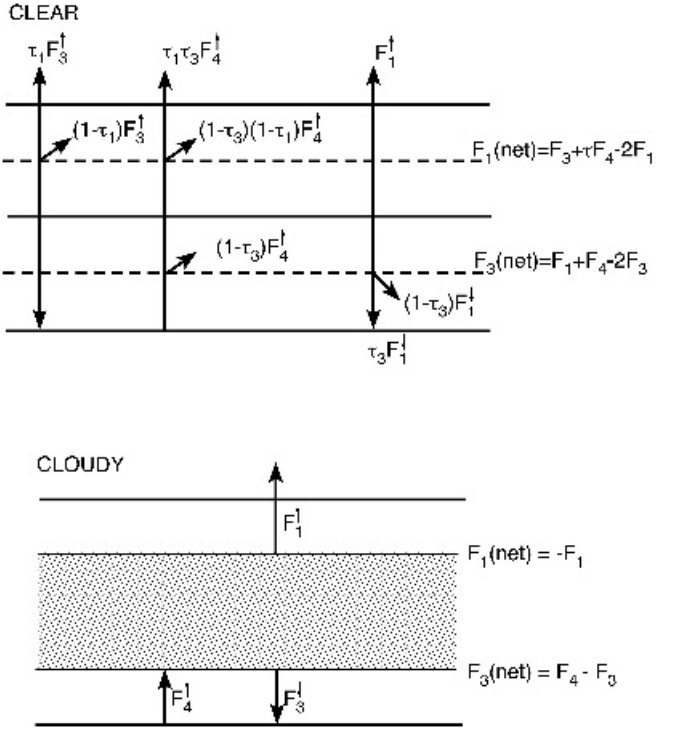

Figure 4.8 Schematic illustration of the transfer of terrestrial (longwave) radiation. There are fewer processes involved than for the case of shortwave radiation, but greater uncertainties in physical mechanisms make this portion just as difficult to deal with. (N.B. Both the shortwave transfer (Figure 4.5) and the longwave interactions shown here are considerably simplified by the assumption of horizontally infinite clouds.) New cloud-resolving models are beginning to allow the explicit computation of finite clouds and cloud edge effects

The first term in Equation (4.20) is the infrared flux arriving at $z = h$ from the surface, where $z = 0$. It is given by the surface flux $B_\lambda[T(0)]$ multiplied by the infrared transmittance of the atmosphere, τ_λ. The second term in Equation (4.20) is the contribution to the total upward flux from the emission of infrared radiation by atmospheric gases below the level $z = h$. Unlike the surface emission, which is nearly ideal black-body radiation, the atmospheric emission as incorporated into the z derivative of τ_λ is highly wavelength-dependent. This is a result of the selective absorption by CO_2 or H_2O in certain spectral regions. The downward infrared flux is composed solely of atmospheric emission, since the incoming infrared radiation from space is essentially zero. The downwelling radiation at a layer at $z = h$ is given by

$$F_\lambda\downarrow(h) = \int_h^\infty B_\lambda[T(z)](d/dz)\tau_\lambda(h, z)dz \tag{4.21}$$

The transmittance, τ_λ, of the atmosphere for infrared radiation in the wavelength interval (λ, $\lambda + \Delta\lambda$), and between atmospheric altitudes $z = h_1$ and $z = h_2$, can be expressed in terms of the optical thickness of the atmosphere in that wavelength region. The degree of detail used in the wavelength integration depends upon the computational power available and also on the type of application. The availability of fast computer routines for performing certain mathematical calculations often makes it desirable to rewrite a problem such as this in an alternative form. Two alternative methods of computing τ_λ use either a representation formulated in terms of exponential integrals or one involving proportionality to exponentials. Although the latter form is simpler to interpret, there are fast numerical routines available to calculate the exponential integrals as rapidly as exponentials, and the former are more accurate. Such techniques are common in climate modelling and the development of fast, efficient algorithms is an important contribution to this subject.

For some sensitivity experiments where overlap between absorption spectra of different atmospheric constituents can affect the sensitivity of the model, detailed integration through at least some wavelength regions will be required. In other types of experiments, such as those concerned with cloud–radiation interactions, for example, where the radiative fluxes are not strongly affected by the perturbed variable, band-averaging can be satisfactory. Band-averaging uses a wavelength (or more usually, frequency) averaged value of the Planck function, $B_\lambda(T)$, in Equation (4.20) together with an averaged value of transmissivity. In this case the layer-averaged transmissivity, τ_i, can be calculated from the layer temperature and pressure and the amount of gaseous absorber.

Generally, other uncertainties in a model, especially those generated by the somewhat arbitrary nature of the convective adjustment, will be greater than those associated with the difference between band-averaging or wavelength integration in the infrared calculations.

The spectrum is one of the dimensions along which model complexity can vary (Figure 2.1). Band-averaged models are cruder versions of ‘narrow band’ models, which in turn are simplified versions of ‘line-by-line’ models. The latter are never used as parts of climate models.

4.3.3 Heat balance at the ground

The ground temperature, T_g, is obtained from the heat balance at the ground. The treatment of the heating of the ground usually depends upon the assumed character of the ground or underlying surface. The albedo is wavelength-dependent and can also be dependent upon the surface moisture and vegetation. The ground can either be considered to be a perfect insulator with zero heat capacity or a heat capacity can be specified. The total flux of heat across the air/ground interface is given by

$$R_g + F - \varepsilon\sigma T^4 - H_L - H_S = \text{stored energy} \tag{4.22}$$

where H_S is the sensible heat flux from the surface, H_L is the flux of latent heat due to evaporation from the surface, R_g is the solar radiation absorbed by the ground and F is the downwelling longwave radiation at the surface.

4.4 CONVECTIVE ADJUSTMENT

The computational scheme described so far defines a radiative temperature profile, $T(z)$, determined solely from the vertical divergence of the net radiative fluxes. Computation of globally averaged vertical radiative temperature profiles for clear sky conditions and with either a fixed distribution of relative humidity or a fixed distribution of absolute humidity yields very high surface temperatures, and a temperature profile that decreases extremely rapidly with altitude. (In other words, despite the assumption made about the humidity distribution, the computed radiative temperature profiles $T(z)$ have large lapse rates in the lower troposphere, considerably in excess of the mean value given by a widely used standard atmosphere,

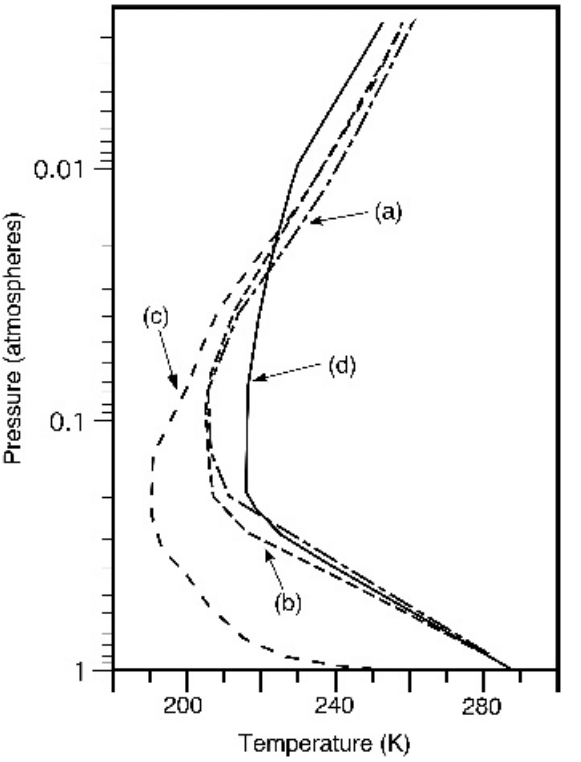

Figure 4.9 A comparison of vertical temperature profiles obtained using different values for the critical lapse rate in an RC model. Profiles obtained using (a) 6.5 K km^{-1}, (b) the moist adiabatic lapse rate, (c) no convective adjustment (radiative effects only) are compared with (d) the 1976 US standard atmosphere (after MacKay and Khalil, 1991)

which has a lapse rate $\gamma = 6.5\,\mathrm{K\,km^{-1}}$, e.g. Figure 4.2.) This observed (critical) lapse rate, γ_c, is less than the computed $-\partial T/\partial z$ in the lower troposphere because the radiative equilibrium profiles are modified by free and forced vertical (moist and dry) convection and the vertical heat transport due to large-scale eddies. Radiative equilibrium profiles are unstable to vertical (moist and dry) convection. Thus the tendency of radiative heating alone to produce large lapse rates adjacent to the Earth's surface, as shown in Figure 4.9, is offset by a rapid vertical transfer of heat.

By the mid-1960s, it was realized that, if column models were to produce meaningful values of surface and vertical temperatures, it was necessary for the computed unstable profiles to be modified. This modification was termed the 'convective adjustment'. It must be noted that it is not a computation of convection but rather a numerical re-evaluation that is applied whenever the critical lapse rate γ_c is exceeded in the time evolution of the numerical calculation. The temperature difference between vertical layers is adjusted to the critical lapse rate, γ_c, by changing the temperature with time according to the integrated rate of heat addition. It can be shown that, if continuity of temperature across the radiation/convection interface is satisfied at one time in the course of a time-dependent calculation, it will be satisfied for all later times. Although the term 'convective adjustment' is still used, modern parameterizations of convection are more physically based.

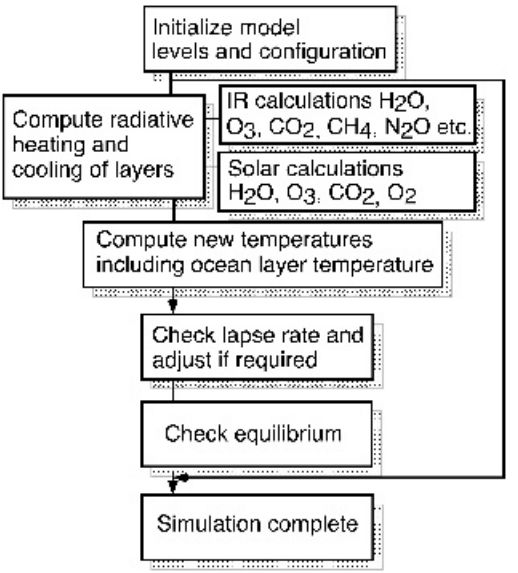

Figure 4.10 Schematic structure and flow through the code for a typical radiative–convective model

The complete structure of a basic RC model is shown in Figure 4.10. The flow continues until the atmospheric temperature profile converges to some final, equilibrium state. This convergence was well illustrated in one of the earliest works describing one-dimensional vertically resolved models (Figure 4.11). In this case, two versions of the model are shown: convergence to purely radiative equilibrium and convergence to 'thermal' equilibrium. The latter is similar to the now more usual RC model except that in this early (1964) model the absolute humidity, rather than the relative humidity, was prescribed. The latter condition has since been shown to be more appropriate as it varies little with atmospheric temperature. Thus, the flow diagram in Figure 4.10 shows the calculation of the water vapour mixing ratio in atmospheric layers using the assumed, constant vertical profile of relative humidity.

4.5 SENSITIVITY EXPERIMENTS WITH RADIATIVE–CONVECTIVE MODELS

Radiative–convective models are particularly useful for studying the probable effects of perturbations to the radiative characteristics of the atmosphere. Their disadvantage is that they are usually formulated in terms of global averages. On the other hand, this makes them computationally very efficient and more time can therefore be taken in making spectrally detailed calculations.

The RC model can be summarized by saying that the vertical temperature profile of the atmosphere plus surface system, expressed as a vertical temperature set, T_i, is calculated in a timestepping procedure, such that

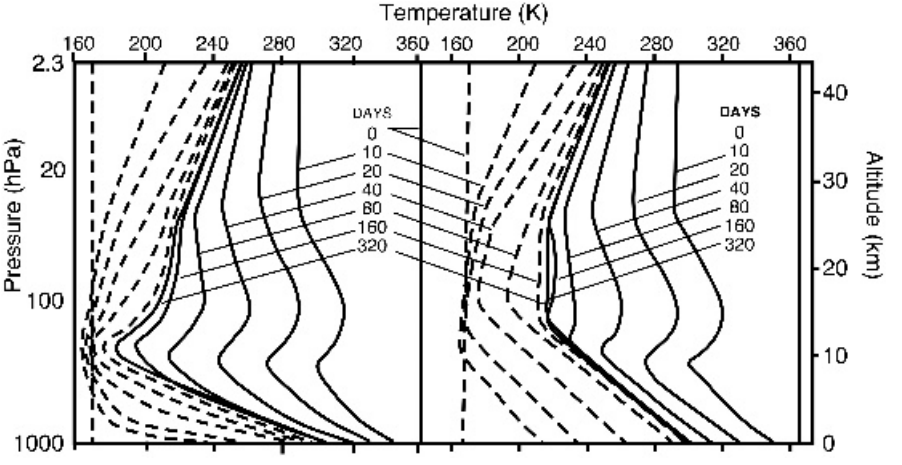

Figure 4.11 The left- and right-hand sides of the figure, respectively, show the approach to states of pure radiative and RC equilibrium. The solid and dashed lines show the approach from a warm and cold isothermal atmosphere respectively (reproduced by permission of the American Meteorological Society; Manabe and Strickler (1964) *Journal of the Atmospheric Sciences* **21**, 361–385)

$$T_i(z, t+\Delta t) = T_i(z, t) + \frac{\Delta t}{\rho c_p}\left[\frac{dF_r}{dz} + \frac{dF_c}{dz}\right] \tag{4.23}$$

Here the temperature, T_i, of a given layer, i, with height z and at time $t + \Delta t$ is a function of the temperature of that layer at the previous time t and the combined effects of the net radiative and 'convective' energy fluxes deposited at height z. In Equation (4.23), c_p is the heat capacity at constant pressure, ρ is the atmospheric density and dF_r/dz and dF_c/dz are the net radiative and convective flux divergences.

There are two common methods of using RC models: either to gain an equilibrium solution after a perturbation or to follow the time evolution of the radiative fluxes immediately following a perturbation. In the first case, the timestepping continues until there is a balance between the top-of-the-atmosphere shortwave and longwave fluxes. The radiative–convective model on the Primer CD includes a simple mixed layer ocean model (e.g. Figure 4.3). This introduces some thermal inertia into the system so that time-dependent simulations can be undertaken. The latter method was used to compute the impact of the eruption of Mount Agung on surface temperatures. Simulations similar to this can be conducted using the 1D RC model included on the Primer CD.

Sensitivity to humidity

Table 4.3 compares the predictions of ΔT (the increase in surface temperature) for differently formulated one-dimensional RC models for a perturbation in the form of

Table 4.3 Equilibrium surface temperature increase due to doubled CO_2 (300–600 ppmv): results from a suite of one-dimensional model sensitivity experiments (modified by permission from Hansen *et al*., 1981)

			Feedback Factors	
Model	*Description*	ΔT (K)	f	λ_{TOTAL}
1	Fixed absolute humidity, 6.5 K km^{-1}, fixed cloud altitude	1.22	1	3.75
2	Fixed relative humidity, 6.5 K km^{-1}, fixed cloud altitude	1.94	1.6	2.34
3	Same as 2, except moist adiabatic lapse rate replaces 6.5 K km^{-1}	1.37	0.7	5.36
4	Same as 2, except fixed cloud temperature replaces fixed cloud altitude	2.78	1.4	2.68

1. Model 1 has no feedbacks affecting the atmosphere's radiative properties.
2. The feedback factors f (dimensionless) and λ_{TOTAL} (W m^{-2} K^{-1}) are those defined in Section 1.4.4 and are two commonly used methods of representing the effect of each added process on model sensitivity to doubled CO_2.

a doubling of the atmospheric carbon dioxide from 300 to 600 ppmv. Model 1 has fixed absolute humidity. Hence, the amount of water vapour in the atmosphere does not change and, in response to the external perturbation of CO_2, temperatures increase and relative humidity decreases. The resulting temperature increase of ~1.2 K can be thought of as a basic RC result since this model does not incorporate any feedback effects (i.e. neither atmospheric water vapour nor clouds have changed in response to the temperature change and λ_{TOTAL}, as defined in Section 1.4.4, is equal to λ_B). Model 2 has, by contrast, fixed relative humidity. This means that, as the temperature increases, the saturation vapour pressure increases and thus, because the relative humidity is the ratio of actual vapour pressure to saturated vapour pressure, the actual vapour pressure must also increase. This extra water vapour must be the result of surface evaporation. It introduces a positive feedback of $\lambda = -1.41\,\mathrm{W\,m^{-2}\,K^{-1}}$ so that λ_{TOTAL} decreases and the surface temperature increase predicted is 1.94 K. The difference between the results from models 1 and 2 illustrates the effect of evaporation on radiative exchanges and its importance for any climate prediction model. Model 3 uses a convective adjustment to the moist adiabatic lapse rate rather than the value of $6.5\,\mathrm{K\,km^{-1}}$ that is used in models 1 and 2. It produces a slightly lower predicted temperature increase since the lapse rate decreases as additional water vapour is added to the atmosphere, i.e. two feedbacks of opposite sign combine. The difficulty of selecting an 'appropriate' global lapse rate to which convective adjustment should be made is considerable.

Comparison of models 4 and 2 illustrates the importance of cloud temperature and height effects. In model 4, the clouds, which are set at a constant, empirically determined amount, are at fixed temperatures rather than at the fixed heights used previously. The clouds therefore move to higher altitudes as the CO_2 perturbation increases temperature. Hence the computed surface temperature must be raised further so that the planetary (top-of-the-atmosphere) energy balance is maintained, resulting in a predicted surface temperature increase, $\Delta T = 2.8\,\mathrm{K}$, which is considerably larger than the ~1.9 K for fixed cloud altitude.

Sensitivity to clouds

Absorption of solar energy by the entire Earth–atmosphere system is most simply specified in terms of the albedo of that system, usually using separate albedos for the cloudless part of the Earth–atmosphere system and the cloud-covered part. Using an RC model, it was shown in 1972 (Figure 4.12) that increasing the cloud amount by about 8 per cent (retaining fixed cloud top height and albedo) would lower the global mean surface temperature by 2 K, whereas raising the level of the cloud top height by about 0.5 km (at constant cloud amount and albedo) would produce exactly the opposite effect on surface temperature. It is not possible to generalize globally averaged results to yield information on the local (in latitude and time) effect of variations in cloudiness, since the effect of changes in cloudiness on surface net heating depends upon the local values of the cloud amounts, heights and albedos, the albedo of the surface, the average solar zenith angle and the local vertical distribution of

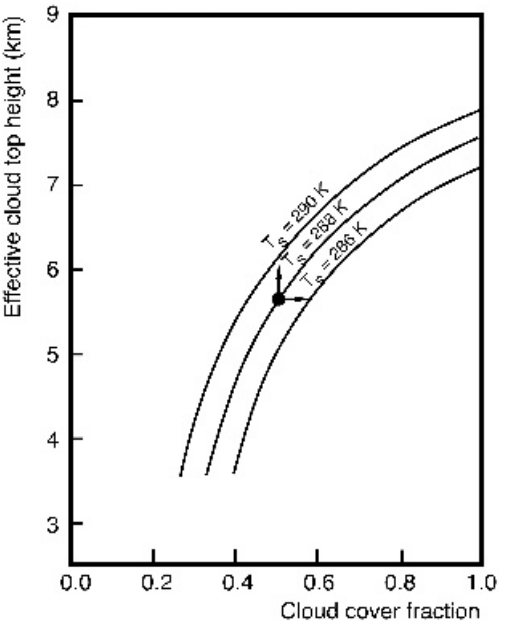

Figure 4.12 Effective cloud-top height and cloud cover fraction giving the indicated equilibrium surface temperatures. From a present-day value of 0.5 for cloud cover and an effective cloud height of 5.5 km, increasing the cloud amount for constant cloud height decreases the surface temperature, whereas retaining the fractional cloud cover at 0.5 and increasing the cloud height causes a surface temperature increase (reproduced with permission from Schneider (1972), *J. Atmos. Sci.*, **29**, 1413–1422)

temperature and radiatively active constituents. The radiative calculations do suggest that even the direction of possible cloud feedback on surface temperature is far from obvious.

Sensitivity to lapse rate selected for convective adjustment

The generally accepted value of the critical lapse rate of 6.5 K km^{-1}, the lapse rate to which 'convective' adjustment is made, may not be appropriate for many experiments. Observational data give a globally averaged value for the tropospheric lapse rate closer to 5.5 K km^{-1}. Experiments have also been undertaken in which the moist adiabatic lapse rate, rather than a fixed value, was used. In one such model for a doubled CO_2 experiment the resulting change in surface temperature was 0.79 K as opposed to 1.94 K when the 6.5 K km^{-1} value was used. These differences are similar to those found in another, different, model in which a 2.36 K increase in surface temperature from a doubling of atmospheric CO_2 concentration was computed using a band-averaged calculation. A temperature increase of only 1.9 K was found when using a model which was identical except for the subdivision into many limited spec-

tral intervals and where the CO_2–water vapour overlap region around 15 μm was divided into four sub-intervals. This lapse rate dependent difference is larger than that indicated in Table 4.3, where the temperature increase computed for doubled CO_2 using the saturated adiabatic lapse rate was 1.37 K.

This suite of sensitivity experiments illustrates the power of simple models. If these RC simulations were to be interpreted as zonal climate sensitivities, it would first be essential to show that the parameters being varied are reasonable, say in the context of a past or future climate change. Today, it is equally likely that an RC model is, in fact, a column from a three-dimensional global model (see Section 4.7). In this case, the sensitivity tests would be to evaluate the impact of a proposed parameterization modification.

4.6 DEVELOPMENT OF RADIATIVE–CONVECTIVE MODELS

4.6.1 Cloud prediction applied to the early Earth

Inclusion of an interactive cloud prediction scheme into a one-dimensional RC model would imply the incorporation of another facet of the climate pyramid (Figure 2.1), *viz*. dynamics. In this example, the model used is a one-dimensional, globally averaged RC model in which the atmosphere is divided into seventeen layers. The tropospheric lapse rate is set at the standard atmospheric lapse rate of 6.5 K km^{-1} and a fixed relative humidity is maintained.

Cloud prediction

The cloud cover is predicted by being calculated as proportional to the water mixing ratio, W, in each layer. This mixing ratio will be affected in turn by the latent heating, an indication of the amount of water added, and by precipitation, the water removed. The latent heat flux, H_L, will be determined from the model's convective adjustment and a calculated effective 'atmospheric Bowen ratio', B. It is necessary to make an assumption about the variation of B with altitude. The simplest assumption is that B is constant, i.e. independent of altitude. There are data that seem to substantiate this assumption but it remains a somewhat dubious claim as the data do not take into account small-scale turbulence.

The net latent heat flux into each layer is found from the net convective flux into the layer, H_C, which the model calculates at each timestep. The net convective flux into a layer, H_C, is then derived. This net total convective flux can be divided by $(1 + B)$ to give the net latent heat flux

$$\frac{H_C}{1+B} = \frac{H_L + H_S}{1 + H_S/H_L} = \frac{H_L(H_L + H_S)}{H_L + H_S} = H_L \tag{4.24}$$

since H_C, the total convective flux, equals the sum of the latent flux and the sensible flux. These latent fluxes in each layer are then multiplied by the gravitational

acceleration divided by the pressure change across the layer to give the flux per unit mass for unit area.

The cloud cover of the previous timestep multiplied by a constant gives the old water mixing ratio, W_o. This constant (here 5.5×10^{-4}) represents a typical mixing ratio for precipitating cloud systems. Thus, greater cloud is linearly equated with higher mixing ratios and thus greater precipitation. The precipitation rate is calculated by multiplying the old mixing ratio, W_o, by another empirical constant ($1.25 \times 10^{-4}\,s^{-1}$), representing the inverse of the conversion time from cloud droplets into rain. Thus the new water mixing ratio is the sum of three terms

$$W = W_o + \frac{H_C}{(1+B)L} - 1.25 \times 10^{-4} W_o \tag{4.25}$$

the first term being the old ratio, the second the amount of water released through condensation and the third that precipitated out, where L is the latent heat of vaporization. Equation (4.25) says that the new ratio is the old ratio updated by the addition of condensation and the subtraction of rainout. The new fractional cloud cover, C_i, for each of i layers is then determined from

$$C_i = W/(5.5 \times 10^{-4}) \tag{4.26}$$

Finally, an adjustment is made if the total cloud coverage is greater than unity, i.e. if $\Sigma C_i > 1$. In this case, a proportional amount of cloud is removed from each layer by converting it to rain.

Model sensitivity

This 1D RC model has been used to investigate the role that changing cloud cover and height may have played in the evolution of the Earth's atmosphere. Figure 4.13 shows three possible evolutionary states of the climate system. Case 1 has a lowered solar luminosity appropriate to the early Pre-Cambrian ($\sim 4.0 \times 10^9$ years ago) of 80 per cent of present-day solar flux, higher atmospheric CO_2 (1650 ppmv) and a surface albedo appropriate to a near global ocean (0.05). Despite the low value of incident solar flux, the computed surface temperature, 277 K, is well above freezing. Other situations can also be examined. If a greater emergence of land is postulated (case 2) then the surface albedo would be expected to be higher (say 0.10) and the computed surface temperature lower, 274 K. If, additionally, considerable silicate weathering is believed to have occurred reducing the atmospheric CO_2 to below present-day values (say 330 ppmv), then the mean global surface temperature drops still further to 270 K.

The inclusion of a cloud prediction scheme has caused this RC model to predict surface temperatures for these postulated early Earth situations that are significantly higher than would have been the case if clouds had been prescribed. In particular, the decreasing cloud amount as temperatures fall and the relative increase in cirrus cloud, with its associated greenhouse effect, gives rise to surface temperatures at

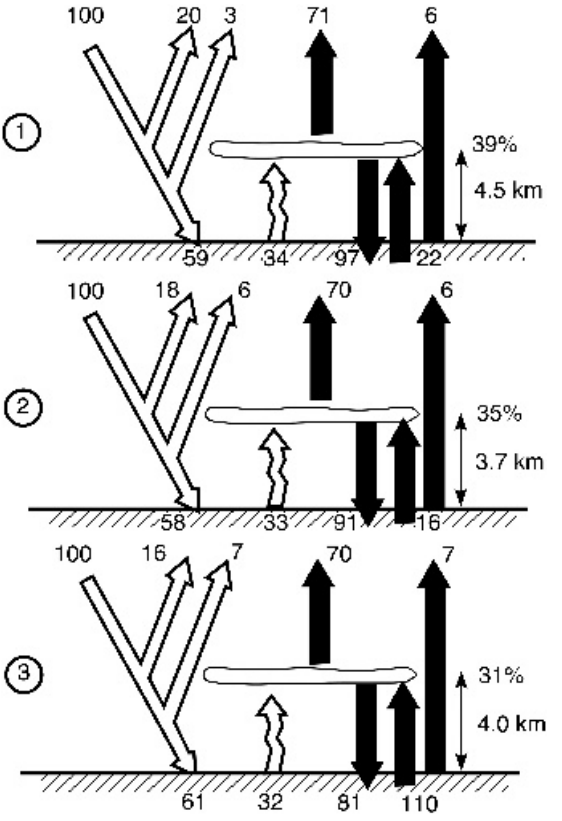

Figure 4.13 Three possible configurations of the atmosphere–hydrosphere of the early Earth. The calculated fluxes have been normalized to the incident solar radiation of the standard case 1 (i.e. 100 units = $0.25 \times 1100\,\mathrm{W\,m^{-2}}$). Solar fluxes (open arrows) are on the left of each sketch, upward arrows represent atmospheric (left) and surface (right) reflection. The wavy arrow represents convective heat flux from the surface, and infrared fluxes are on the right (solid arrows). Note the variations in mean cloud cover (as a percentage) and cloud height (in kilometres) on the right (reproduced by permission from Cogley and Henderson-Sellers (1984) *Rev. Geophys. Space Phys.* **22**, 131–175. © Copyright American Geophysical Union)

which sea ice just melts in the present-day ocean. Thus, results from this RC model, which includes prediction of cloud amounts, heights and types (derived from the height), offer a possible solution to the 'reduced solar luminosity–enhanced early surface temperature' paradox described in Section 3.3.

Regional and local applications

The convective adjustment that occurs in the atmosphere means that we introduce vertical motion into our climate model and can use this to parameterize movement of atmospheric water and the formation of clouds. The approximations we have

made are acceptable for global averages but, once we become interested in a specific region, we must consider horizontal transfer as well as vertical motion and radiation. In the next section, we look at more complex column models, appropriate for a particular location, and then move on to introduce the concept of large-scale horizontal motion.

4.6.2 Single column models

Single column models are often encountered in the literature and have mostly been introduced for sensitivity testing of the processes represented in the 'columns' of GCMs. As the name suggests, these models are derived from three-dimensional models. These column models apply, therefore, to the area of a single grid point in a GCM. The horizontal (advective) fluxes are specified, usually from full GCM runs. These column models are further examples of the increased fuzziness between types of climate models.

4.7 TWO-DIMENSIONAL STATISTICAL DYNAMICAL CLIMATE MODELS

Secondary school geography classes would appeal to the Flatlanders mentioned in Chapter 3 because at this level the general circulation of the atmosphere is often introduced as being composed of cellular circulations. These Hadley, Ferrel and polar cells are meridional features, i.e. they consist solely of latitudinally averaged movement between zones. Of course this is a gross simplification that ignores the major circulation features in mid-latitudes: the Rossby waves (see Figure 2.2).

4.7.1 Parameterizations for two-dimensional modelling

Most two-dimensional SD climate models are constructed to simulate the meridional motions only. The two dimensions they represent explicitly are height in the atmosphere and latitude. Variations around latitude zones (i.e. longitudinal variations) are neither resolved nor described. These models solve numerically the basic equations listed in Table 2.1. In general these models are able to produce realistic simulations of the large-scale two-dimensional flow (Figure 4.14). The fundamental difference between these models and full atmospheric GCMs is that all the variables of interest are zonally averaged values. This zonal averaging is identified below by angle brackets. The equations to be solved are as follows.

Zonal momentum

$$\frac{\partial \langle u \rangle}{\partial t} - f\langle v \rangle + \frac{\partial \langle u'v' \rangle}{\partial y} = \Phi \tag{4.27}$$

Meridional momentum (*geostrophic balance*)

$$f\langle u \rangle + R\langle T \rangle \frac{\partial}{\partial y}(\ln \langle p \rangle) = 0 \tag{4.28}$$

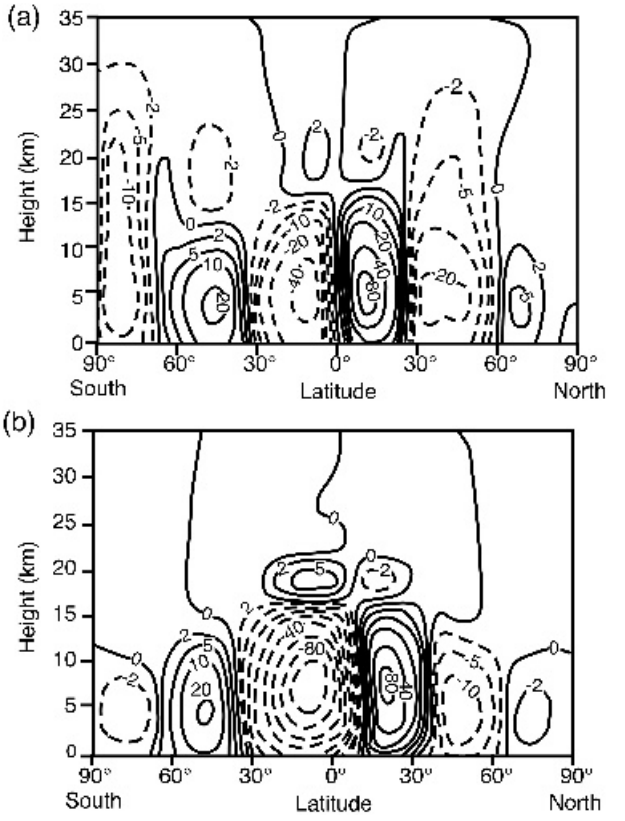

Figure 4.14 Annual and zonal mean meridional mass flux stream function (10^9 kg s^{-1}): (a) as observed (Oort and Peixóto, 1983); (b) as simulated by the Lawrence Livermore two-dimensional SD model (reproduced by permission from MacCracken and Ghan, 1987)

Hydrostatic balance (*vertical component*)

$$\frac{\partial(\ln\langle p\rangle)}{\partial z} = \frac{-g}{R\langle T\rangle} \tag{4.29}$$

Thermodynamic balance

$$\frac{\partial\langle T\rangle}{\partial t} + \frac{\partial\langle v'T'\rangle}{\partial y} + \frac{\partial\langle w'T'\rangle}{\partial z} + \langle w\rangle\left\{\frac{g}{\langle\rho\rangle c_p} + \frac{\partial\langle T\rangle}{\partial z}\right\} = \frac{Q}{\langle\rho\rangle c_p} \tag{4.30}$$

Continuity

$$\frac{\partial\langle\rho\rangle\langle v\rangle}{\partial y} + \frac{\partial\langle\rho\rangle\langle w\rangle}{\partial z} = 0 \tag{4.31}$$

where u, v and w are the velocities in the eastward (x), northward (y) and vertical (z) directions, T is the temperature, Q the zonal diabatic heating, Φ a friction term, R the gas constant for dry air, c_p the specific heat at constant pressure, g the acceleration due to gravity, f the Coriolis parameter and $\langle\rho\rangle = \langle p\rangle/(R\ \langle T\rangle)$. The primed notation denotes a deviation from the zonal average of these variables; for example $u' = u - \langle u\rangle$.

As these equations are essentially those solved in AGCMs, although here they are written in a simpler form, they are worth considering in some detail. The momentum equations are themselves expressed for unit mass, so that the density terms cancel and the momentum (mass times velocity) is represented simply by the velocity component in the direction of interest. Changes in zonal momentum with time (in other words, zonal accelerations) are thus represented by the first term on the left-hand side of Equation (4.27). These temporal changes are balanced by the Coriolis term, $f\langle v\rangle$, and the rate of change in the poleward direction of the correlation term, $\langle u'v'\rangle$, i.e. the eddy transport of momentum in the poleward direction. Finally, there is an additional frictional dissipation term, Φ, to be taken into consideration.

The meridional momentum equation is similarly constructed but the small temporal changes are neglected; if they were not, the model might accumulate errors and predict non-zero momentum fluxes at the poles. Consequently, the balance equation is simply between the Coriolis force and the pressure gradient force in the poleward direction, friction being neglected.

The hydrostatic equation is the third component of the conservation of momentum in the atmosphere (Table 2.1). In this case, resolution in the vertical direction yields no Coriolis component, but changes occur in the pressure field (with height). This balance (Equation (4.29)) between the vertical pressure gradient and gravity can be rewritten as

$$\frac{1}{\langle p\rangle}\frac{\partial\langle p\rangle}{\partial z} = -\frac{g}{R\langle T\rangle} \tag{4.32}$$

whence, from the ideal gas law, is derived the more common expression

$$\frac{\partial\langle p\rangle}{\partial z} = -\frac{g\langle\rho\rangle R\langle T\rangle}{R\langle T\rangle} = -g\langle\rho\rangle \tag{4.33}$$

Thermodynamic balance exists between the temporal rate of change of zonally averaged temperature and the rate at which temperature is transported both into and out of each latitude zone. This is accomplished by eddies in the lateral (northward) and vertical directions and represented by the two eddy correlation terms (second and third terms on the left-hand side of Equation (4.30)). A further term represents vertical transport, taking into account adiabatic heating and cooling due to the compressibility of the atmosphere. The balance is completed by the inclusion of the diabatic heating term on the right-hand side.

The continuity equation says simply that mass can neither be created nor destroyed, i.e. the rate of change of mass in all three dimensions overall is zero. However, since zonal averages are under discussion, the change in the x direction has been averaged out, as expressed by the use of angle brackets, and only two components remain. The sum of these two is zero. Thus, in regions where there is net divergence or convergence, there must of necessity also be a vertical motion.

In writing and discussing these 'prototype' equations, we have neglected the need for a spherical geometry, which arises because zones equally spaced in latitude (y) have unequal areas. Despite this, the representation is useful. The horizontal component of the eddy momentum flux $\langle u'v' \rangle$ is not only responsible for transferring zonal momentum but also drives the meridional circulations. Figure 4.15 shows mean meridional cross-sections of (a) zonal wind, (b) meridional wind, (c) vertical wind and (d) temperature. These can be calculated by specifying a vertically and latitudinally varying distribution of eddy momentum fluxes similar to those observed. Note that the magnitude of the three induced velocities differs considerably: the zonal wind can be as high as $30\,\mathrm{m\,s^{-1}}$ while the meridional wind is typically $0.25\,\mathrm{m\,s^{-1}}$ and the induced vertical motion is $0.005\,\mathrm{m\,s^{-1}}$.

For two-dimensional climate models, it is necessary to find representations for the eddy fluxes in Equations (4.27)–(4.29) so that this system of equations can be solved numerically. In these models, the atmosphere is represented on a latitude versus pressure (height) grid with approximately ten layers and ten to twenty grid points between the poles. Often, considerable effort goes into representing atmospheric

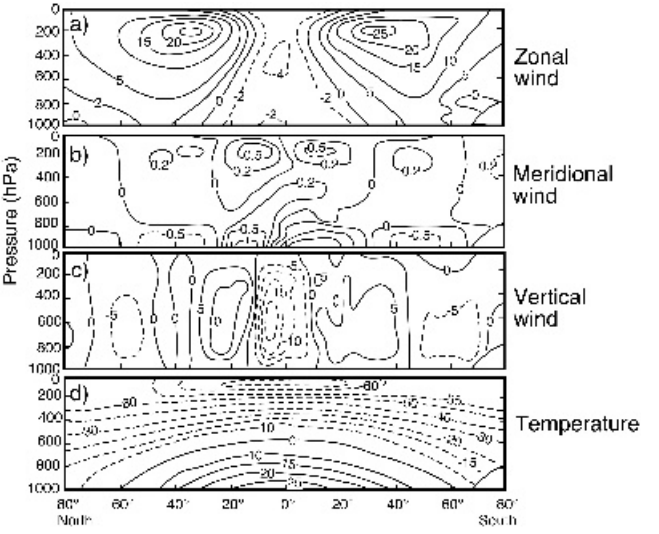

Figure 4.15 Observed zonal statistics for four atmospheric variables: (a) zonal wind ($\mathrm{m\,s^{-1}}$); (b) meridional wind ($\mathrm{m\,s^{-1}}$); (c) vertical wind ($\times 10^3\,\mathrm{m\,s^{-1}}$); (d) temperature (°C) (reproduced by permission of Academic Press from Oort and Peixóto, 1983)

radiative processes and surface features, although the main problem remains the characterization of eddy transports.

Eddy transport is of critical importance for determining the equator-to-pole temperature gradient and the vertically distributed zonal wind field, especially the strength of the jet-stream winds. Early parameterizations of eddy flux simply related eddy transports to gradients of zonal mean variables using empirically determined diffusion coefficients. This representation is similar to the parameterization used in some EBMs for the meridional energy transport (e.g. Equation (3.12) in Section 3.2). This parameterization was based on the argument that, since baroclinic waves are driven by the meridional temperature gradient, their eddy transports might also be simply parameterized as being proportional to this gradient. Thus the eddy heat flux is given by

$$\langle v'T' \rangle = -K_T \frac{\partial \langle T \rangle}{\partial y} \tag{4.34}$$

and the eddy momentum flux by

$$\langle u'v' \rangle = -K_M \frac{\partial \langle u \rangle}{\partial y} \tag{4.35}$$

where K_T and K_M are empirically derived coefficients for temperature and momentum. More detailed study has shown that, while the diffusive representation is fairly reasonable for eddy heat transport, it is a completely inadequate representation of eddy momentum flow, since momentum can be transported up as well as down the meridional gradient of momentum. Consequently, later parameterizations reformulated the transport equations in terms of the potential vorticity gradient.

Originally, the parameterizations described for two-dimensional models were empirically based. However, subsequent theoretical analysis by a number of authors in the early and mid-1970s demonstrated that the diffusion coefficients, as well as the eddy transport itself, may be proportional to the meridional temperature gradient. It was found that the equator-to-pole temperature gradient was considerably different when computed with EBMs that used a value for the diffusion coefficient dependent on the temperature gradient as opposed to a constant eddy diffusion coefficient (Figure 4.16). This finding suggests that one of the reasons why the energy balance climate models (EBMs) showed considerable sensitivity to a small decrease in solar constant was that the diffusion coefficient in these models was constant, rather than being a function of the temperature gradient. A much greater decrease in the solar constant is necessary to initiate an ice age in a model that includes a temperature gradient dependency of the diffusion coefficient. This is because the temperature gradient remains high at low values of solar input. This recognition may offer another partial solution to the cool Sun–enhanced early surface temperature paradox described earlier (see especially Sections 3.3 and 4.6).

The basis of the parameterization problem is the simplification that is generally made in the solution of the zonal flow equation in baroclinic wave theory. The usual

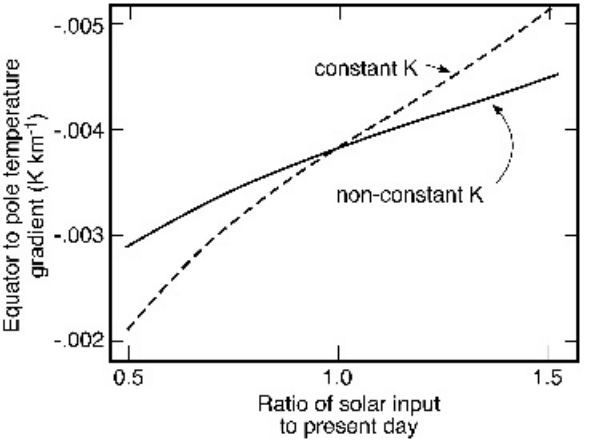

Figure 4.16 The effect of the inclusion of a variable diffusion coefficient, K (itself a function of the temperature gradient) and the equator-to-pole temperature gradient in an EBM (reproduced by permission of the American Meteorological Society from Stone (1973) *J. Atmos. Sci.* **30**, 521–529)

simplifications are to assume that the zonal wind, $\langle u(y, z)\rangle$, is a function of y only (the barotropic solution) or z only (the baroclinic solution). Instability to small disturbances of a zonal wind, which varies only in the vertical (z) direction (a baroclinic instability), converts to eddy energy the energy that is stored in the current latitudinal variation of zonal temperature, $\langle T\rangle$. This energy is released by the eddy flux of heat $\langle v'T'\rangle$. On the other hand, instability of a zonal wind to horizontal (y component) perturbations (a barotropic instability) converts kinetic energy of the zonal wind to eddy energy through the flux of horizontal eddy momentum $\langle u'v'\rangle$.

The parameterization of momentum fluxes is considerably more complex when theoretically based than the parameterization of heat fluxes. It has been shown that potential vorticity is more suitable for the treatment of $\langle u'v'\rangle$ as the eddy momentum flux can be obtained once eddy potential vorticity and eddy heat fluxes have been derived. A further problem with eddy flux parameterizations is the existence in the atmosphere of large stationary eddies forced both by topography and by land/ocean temperature contrasts. Since the parameterization schemes described above represent only transient baroclinic eddies, it is possible that there will be an underestimation of the total eddy transport produced due to the neglect of these stationary eddies. However, observational data suggest that a compensatory mechanism may exist since total eddy flux seems to be correlated better with observed temperature gradients than is the transient eddy flux alone.

Full formulations of two-dimensional SD models often also include vertical and horizontal eddy transports of water vapour as well as those of heat and momentum described above. Since two-dimensional models attempt to parameterize only the eddy transport, while the mean meridional transport terms are computed explicitly,

it is hoped that inadequacies in the eddy transport parameterizations are compensated for in the explicit calculation of meridional transport.

4.7.2 'Column' processes in two-dimensional statistical dynamical (SD) models

Vertical motion must be parameterized rather carefully in zonally averaged models. Around any one latitudinal band, there would normally be a range of different surface types and atmospheric states possessing different degrees of instability. The extent of these areas and of the instability would be expected to vary with season and time of day. Unfortunately, zonally averaged conditions can be quite stable even though there might be many locations within a latitude zone where convection would occur.

A more complex, and usually empirically derived, formulation is required in 2D SDs to determine the onset and extent of convection and often of cloud formation processes instead of the simple convective adjustment used in one-dimensional RC models (Section 4.2). Generally less than 100 per cent cloud cover is predicted within individual layers in an attempt, once again, to avoid 'on-off switching'. Similar sub-gridscale descriptions of vertical convection and cloud formation processes have been derived to limit the extent of precipitation and/or cloud within a grid cell of a GCM (see Chapter 5). Convective precipitation is likely to be the major contributor to rainfall in zonally averaged models. However, large-scale precipitation (from stratiform clouds) can also occur if the mixing ratio of an air parcel exceeds the saturation mixing ratio. Since it is most unlikely that zonally averaged relative humidities would ever reach saturation in anything other than the near surface layer, thresholds are often set somewhat lower, say for instance a zonally averaged relative humidity of 80 per cent.

Surface-to-atmosphere fluxes of momentum, sensible heat and latent heat are computed using standard bulk aerodynamical formulae:

$$H_D = \rho c_D u^2 \tag{4.36}$$

$$H_S = \rho c_p c_S u(T_s - T_a) \tag{4.37}$$

$$H_L = \rho L c_L u(q_s - q_a) \tag{4.38}$$

where c_D, c_s and c_L are the aerodynamic drag coefficients, u the wind speed evaluated at the same standard height as the drag coefficient, T the temperature, q the water vapour mixing ratio and L the latent heat of vaporization. This type of parameterization of surface to atmosphere fluxes is the same as is used in GCMs (see Chapter 5).

It is possible to incorporate some characteristics of ocean surfaces in two-dimensional models. If oceanic heat fluxes are specified, part of the meridional transport of energy can be subsumed into this oceanic transport term. These models can also be used to perform more detailed studies of ice-albedo feedback since sea ice and land snow-cover can be computed independently within a latitude zone, and

surface temperatures associated with the different surface types can be computed and stored independently of one another.

The most useful area of application of two-dimensional SD models is probably predicting the effects of small perturbations that are fairly zonally homogeneous, in atmospheric chemistry and palaeoclimate studies. Good examples include the increase in Arctic aerosol loading, transient increases in stratospheric and tropospheric aerosol and stratospheric ozone depletion. Two-dimensional SD models are especially useful in such studies for two reasons: (i) because detecting the signal produced by such small changes in a full three-dimensional model with eddy-related inherent variability would take very many years of climate simulation, and (ii) because the slight disturbances in the climatic state do not negate the assumption inherent in the formulation of two-dimensional models: that the eddy fluxes can be satisfactorily parameterized. A full two-dimensional SD model should be approximately 100–1000 times faster in execution than a GCM of roughly equivalent resolution and physical detail. These 2D models are a popular component of some EMICs (Table 4.1) and we will now look in more detail at what have become known as Earth System Models of Intermediate Complexity.

4.8 THE EMIC SPECTRUM

It is not possible to describe a typical EMIC. The middle ground between the complex, high maintenance, three-dimensional coupled climate models and the simple desktop computer models such as EBMs, is populated by a spectrum of models that have been termed EMICs (Figure 4.1). In these models, one or more aspects of the full climate system is neglected or parameterized with the goal of including a process or time-frame that could not otherwise be resolved with the available resources. As there is no specific rulebook for the construction of an EMIC, the spectrum is best illustrated by example. The idea is not new, so it is worth considering some historical EMICs as well as some of the newer models.

4.8.1 An upgraded energy balance model

Perhaps the earliest EMIC was developed by William Sellers in the 1970s. He worked with the thermodynamical energy equation for the Earth–atmosphere system applied separately to the land- and water-covered portions of each 10° latitude belt of an Earth with a single large continent extending from pole to pole. In other words, this two-dimensional model is a cleverly partitioned EBM. The model was formulated in terms of an idealized continent/ocean system. Except for latitudes between 40° and 70° S, the fraction of each 10° latitude belt occupied by land was set equal to the present-day value and the land masses were offset in relation to one another in order to give a meridional transport across each 10° latitude circle from water to land, water to water, land to land and land to water similar to that currently observed. The energy equation in each area is a function of the surface, e.g. the equation for

the vertical temperature profile, $T(p)$ (p is pressure), is written in terms of the surface temperature, T_s, and the vertical temperature gradient, $\partial T/\partial p$:

$$T(p) = T_s - (p_s - p)\partial T/\partial p \tag{4.39}$$

where $\partial T/\partial p$ is specified as $0.12\,\mathrm{K\,hPa^{-1}}$. This two-dimensional model also differs from the basic EBM of Sellers described in Chapter 3 in that eddy diffusivities are used to parameterize the poleward transport of heat by ocean currents and by atmospheric standing waves and transient eddies. The values of the atmospheric eddy coefficients for sensible heat, K_H, and water vapour, K_v (assumed to be equal) are proportional to the first power of the north–south temperature gradient:

$$K_H = K_v = 0.25\,|\Delta T| \times 10^6 \tag{4.40}$$

where ΔT is the temperature gradient between successive 10° latitude belts. In addition, an eddy diffusivity, K_w, for heat transfer by ocean currents was specified as

$$K_w = 1.7 \times 10^5 \times (1 - A_I)A_L \tag{4.41}$$

where A_I is the fractional area of the oceans covered by ice. The factor A_L, being the fraction of a given latitude belt occupied by land, allows for the effect of the continents in channelling the north–south ocean currents. The average value of K_w is about $5 \times 10^4\,\mathrm{m^2\,s^{-1}}$, which agrees well with values found in the vicinity of the Gulf Stream and is about one order of magnitude larger than values considered typical for the more quiescent parts of the oceans. This discrepancy was intentional and was an attempt to account partially for the neglected heat transport by vertical circulations (*cf.* Section 3.6).

The albedo–temperature feedback is still an important feature of this model, but now cloudiness is treated explicitly by computing surface net radiation for the separate cases of clear and cloudy skies. This model is very much more comprehensive than an EBM, but is still highly tuned as compared with the general circulation climate models that will be described in Chapter 5. Despite some discrepancies between modelled and observed climate, especially in high latitudes, this relatively simple model is able to reproduce seasonal signals in various climatic variables fairly successfully. Although this result might have been anticipated, since much of the climatic response is controlled by thermal inertia, it is still worthy of note because the seasonal range in most, if not all, variables is considerably greater than many anticipated climatic perturbations.

4.8.2 Multi-column RC models

It is possible to set up one-dimensional RC models for a number of latitude zones as characterized by an EBM. Such a combination would constitute a two-dimensional model. An example of such a two-dimensional model is shown in Figure 4.17. This particular example is based partly on the 1D RC discussed earlier in this chapter and included on the Primer CD. In addition, the surface heat balance equation for land is given by

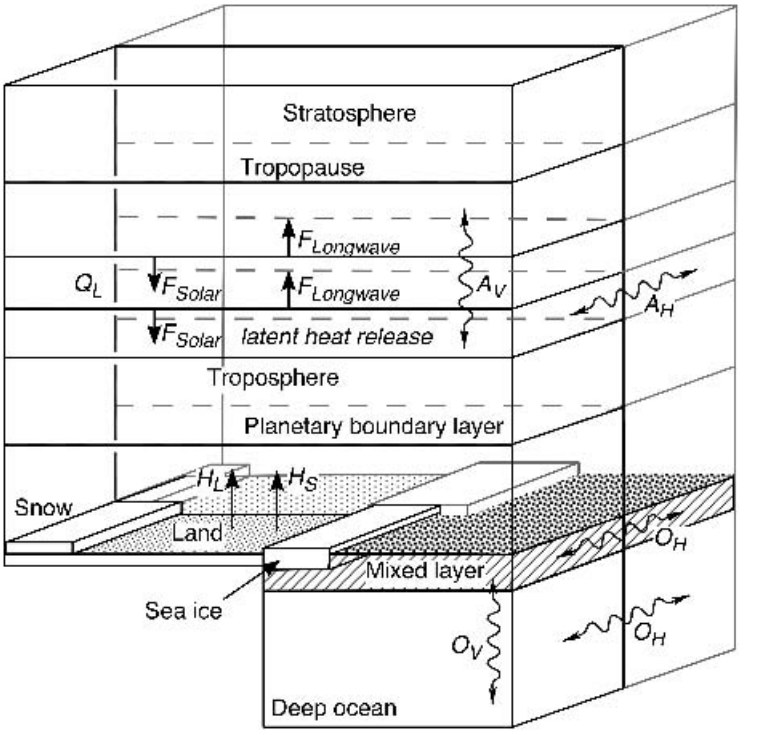

Figure 4.17 Schematic illustration of one latitude belt of a 2D zonal model. F_{Solar} and $F_{Longwave}$ denote shortwave and longwave radiation, respectively. A_V and A_H denote vertical and horizontal heat transport in the atmosphere, respectively; Q_L is latent heat release; H_L and H_S are latent and sensible heat fluxes, respectively, for land (with and without snow), sea ice and ocean; O_V and O_H denote vertical and horizontal heat transport, respectively, in the ocean (after De Haan *et al*., 1994)

$$C_L D \frac{\partial T_L}{\partial t} = R_g - I - H_S - H_L \tag{4.42}$$

where C_L, D and T_L are the heat capacity, effective depth and temperature of the land-surface layer, R_g is the solar radiation absorbed and I, H_S and H_L are the infrared, sensible and latent heat fluxes respectively. The atmospheric balance can be written as

$$\frac{\partial T}{\partial t} = Q_S + Q_I + Q_L + A \tag{4.43}$$

where T is the atmospheric temperature and Q_S, Q_I and Q_L are the heating rates due to solar, longwave and latent heating. A is the heating rate due to dynamical redis-

tribution of heat, which is formulated empirically. The model includes four different surface types, as illustrated in Figure 4.17.

The ocean model is composed of two components: an ocean climate model and an ocean biosphere and chemistry model. The ocean climate model includes heat exchanges with the atmosphere (but not with sea ice) and prescribed advective flows derived from observational data, as shown in Figure 4.18. The surface heat fluxes are simulated separately for the Atlantic and Indo-Pacific basins and the heat thereby transported from the equator to the poles. The ocean parameterization also includes the role of the ocean biomass in climate, through its uptake of carbon (thus reducing atmospheric CO_2 concentrations). The model includes downward transport of substances by phytoplankton and the subsequent settling of marine grazer faeces, each parameterized in terms of fluctuating environmental conditions. The simplified food web includes only phytoplankton and detritus. The phytoplankton are governed by

$$\frac{dB}{dt} = B\left(P_{max} f(I) \frac{N}{N+k} - r - m \right) \tag{4.44}$$

where B is the phytoplankton biomass, N the organic nitrogen, P_{max} the maximum production rate, $f(I)$ a light limitation function, k the half saturation fraction for N, m the mortality rate, and r the respiration rate. The detritus is governed by

$$\frac{dD}{dt} = mB - sD \tag{4.45}$$

where D is the detritus concentration and s is the settling rate for detritus.

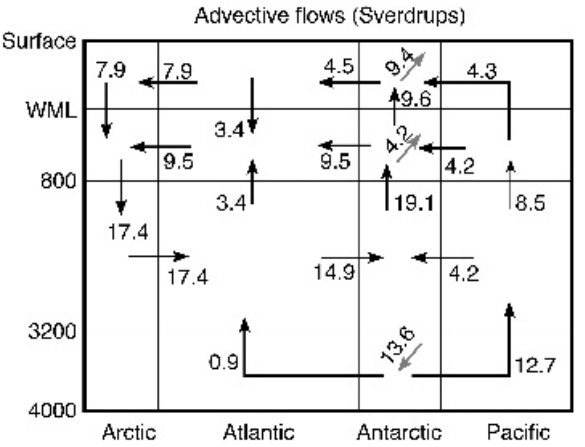

Figure 4.18 Schematic illustration of the ocean circulation as used in the 2D zonal model shown in Figure 4.17. Transports, expressed in Sverdrups (1 Sv = 10^6 m^3 s^{-1}), are derived from observational data (after De Haan *et al.*, 1994; with kind permission of Kluwer Academic Publishers)

This model provides for simulation of the main features of the ocean–atmosphere system on a latitudinally averaged basis. The climate sensitivity of the model was found to be within the IPCC range and the carbon uptake by the ocean biomass within the current range of state-of-the-art carbon cycle models (see Chapter 6). The model is designed as one component of a large integrated assessment model; hence the need for the inclusion of the ocean biomass, which is a major sink for atmospheric carbon (CO_2) and therefore an important factor in long-term climate simulation. Such integrated assessment models are discussed more fully in Chapter 6.

4.8.3 A severely truncated spectral general circulation climate model

As an alternative to embellishing a zonal model, an intermediate position on the climate-modelling pyramid (Figure 2.1) can be achieved by restricting a more complex model. One example is to severely truncate a global spectral model, retaining only its lowest waves. Figure 4.19, which complements Figure 1.5, illustrates the relative performance (estimated qualitatively as a percentage of the dynamical completeness of a GCM) against the computational effort expended. As the difference between the computational domains of spectral and Cartesian grid AGCMs will

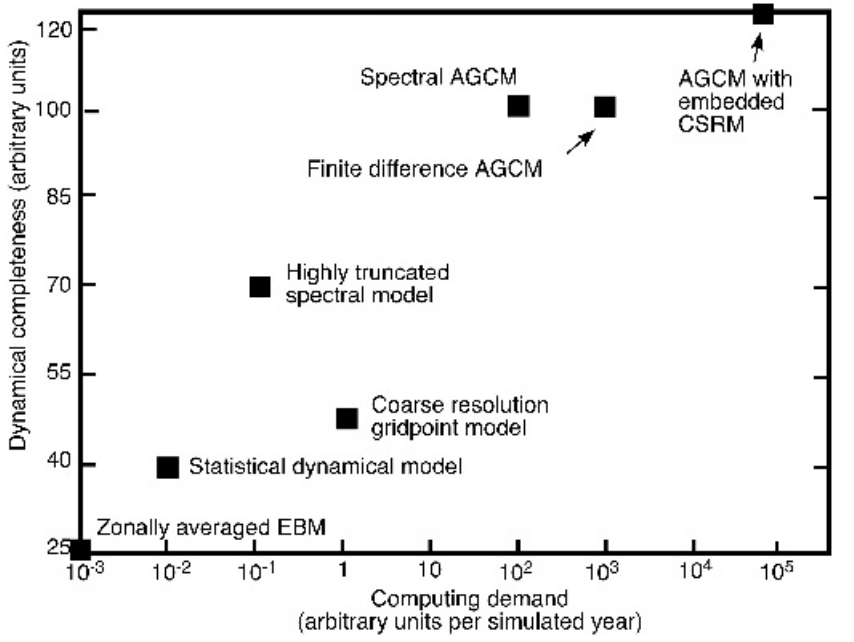

Figure 4.19 Variation of the 'dynamical soundness' of atmospheric models versus their computational effort. The scale of dynamical soundness is subjective and the computational effort scale has been updated to reflect relative effort. (Modified from Semtner (1984b) by permission of the American Meteorological Society, *Journal of Applied Meteorology* **23**, 353–374)

not be explained until Chapter 5, here it is sufficient to say that severe truncation of a spectral model is roughly equivalent to greatly coarsening the spatial grid of a Cartesian grid model. In many senses, however, the spectral truncation is less detrimental than the equivalent grid coarsening since, when the resolution is decreased in a Cartesian grid model, baroclinically unstable waves are more and more poorly resolved, reducing the dynamical soundness of the model simulation. On the other hand, spectral truncation can be very severe before the fundamental dynamics are badly misrepresented. This type of highly truncated GCM can be 'better' than a two-dimensional SD model since the large-scale eddy fluxes of momentum, heat and moisture are calculated explicitly rather than being parameterized. Despite this explicit computation, the computational effort is approximately two orders of magnitude smaller than that for a fully resolved GCM. The loss of spectral resolution means that many features are either poorly predicted or must be improved by better sub-gridscale parameterization. However, in order to improve climate representation, the distortions to the energy cascade, which are severe, must be compensated for by parameterization of energy conversion and dissipation. While physical modellers have deemed that a very detailed effort here would be inappropriate since the results would be unlikely to compensate for lost spectral resolution, those developing integrated assessment models (Chapter 6) are exploring and developing this type of truncated model.

4.8.4 Repeating sectors in a global 'grid' model

Another technique for reducing the complexity of three-dimensional models is the 'Wonderland' approach which has been used by modellers at the Goddard Institute for Space Studies in New York. The layout of the model is shown in Figure 4.20. Here the model domain is made up of continents which mimic the distribution of land on Earth but occupy only 120°. The remainder of the globe is made up by repeating the same geography. The model therefore allows simulations which are hundreds or thousands of years long with only modest computer resources. This approach is similar to that used by some of the early global models at GFDL. It is possible to argue that severely truncated models such as these are similar to two-dimensional models in that they approximate the complete climate system by highly parameterized representation of one or more aspects. On the other hand, as they retain three dimensions they are, perhaps, more appropriately termed two-and-a-half-dimensional models.

Some atmospheric dynamicists have chosen to solve a set of equations similar to Equations (4.27)–(4.31) but in three directions (i.e. including longitudinal variations). However, they exclude much of the detail of the treatment of the radiative fluxes that is usual in one-dimensional RC and two-dimensional SD models. Thus, although they are strictly three-dimensional modellers, in choosing to neglect the complexities of radiative processes, these modellers have slipped a part-dimension and once again the result might be more correctly termed a two-and-a-half-dimensional model.

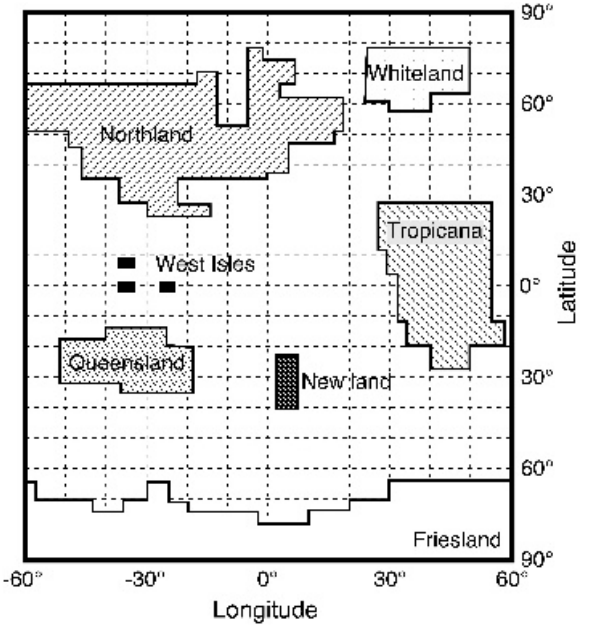

Figure 4.20 Distribution of 'Wonderland' continents in a global model with simplified geography (after Hansen *et al*., 1992). The model's surface and atmosphere occupy only 120° of longitude, this sector being repeated around the globe

4.8.5 A two-and-a-half-dimensional model: CLIMBER-2

CLIMBER-2 is another two-and-a-half-dimensional model, comprising modules that describe ocean, atmosphere, sea ice, land-surface processes, terrestrial vegetation cover and the global carbon cycle. Interaction between the modules is by way of moisture, energy, momentum and carbon fluxes. The model has a coarse but realistic geography (Figure 4.21a) that resolves to the scale of continents and ocean basins and can be used to perform climate simulations on multi-millennia scales.

The atmospheric component of CLIMBER-2 is based on a 2D SD model (similar to that described in Section 4.7). These 2D models were popular in the 1970s and, while they fell into disuse as 3D models came within the computational grasp of many, there has been a resurgence of interest in them from EMIC developers keen to exploit their computational efficiency. The simple 2.5D atmosphere is linked via an atmosphere–surface interface to the ocean (a set of one-dimensional primitive-equation basin models), the land surface (a simplified version of the BATS land-surface scheme developed in the 1980s for three-dimensional models) and a simple, one layer sea ice model (developed for GCMs in the 1970s). Comparisons with observations show realistic precipitation patterns, although the simulations lack detail because of the resolution of the model.

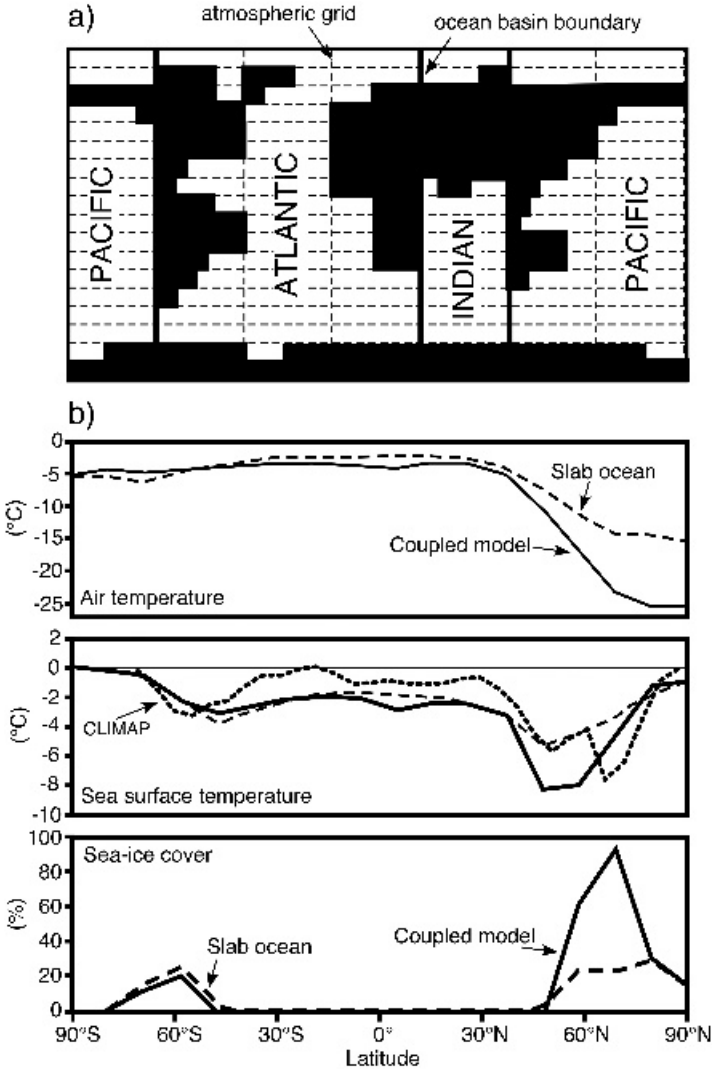

Figure 4.21 (a) The lower-resolution geography of the CLIMBER-2 model (from Petoukhov *et al*., 2000. © Springer-Verlag). (b) Glacial changes at 21 000 years BP in air temperature, sea surface temperature (SST) and sea ice cover as simulated by the CLIMBER-2 model (reproduced with permission from Ganapolski *et al*. (1998), *Nature* **391**, 351–356. Copyright 1998, Nature Publishing Group)

A model as simple as this must inevitably involve some tuning. The CLIMBER-2 developers formulated a set of simple tuning rules: (i) parameters that are known from empirical studies or from theory (such as the radiative properties of the atmosphere) must not be used for tuning; (ii) parameters are best tuned against observations, rather than against model performance as a whole; and (iii) parameters should

be physically based, rather than geographically based as might be the case for ocean flux adjustments. CLIMBER-2 has been used successfully for simulation of the climate at the last glacial maximum (21 000 years BP) and during the mid-Holocene (6000 years BP).

4.8.6 McGill palaeoclimate model

This model is based on a form of Energy Balance Model (as discussed in Chapter 3). The idea of energy balance can be extended to moisture balance, resulting in an Energy and Moisture Balance Model (EMBM). The model includes ocean, sea ice and land surface and has been used to simulate the onset of glaciations. The simulation found that in a cold climate, induced by reducing the solar flux, moisture transport to high latitudes is reduced, intensifying the thermohaline circulation and creating conditions that encourage snow accumulation at high latitudes. A dynamic ice-sheet model is also included in the model, allowing the role of iceberg calving from ice sheets in producing millennial-scale climate variability. Interactions between the ice sheets and the thermohaline circulation as a mechanism for rapid climate change can be examined and the model can be applied to distant periods such as the late Carboniferous–early Permian period (300 Ma BP), to provide clues about the ocean–atmosphere climate at that time.

4.8.7 An all-aspects, severely truncated EMIC: MoBidiC

MoBidiC (Modèle Bidimensionnel du Climat) is a model linking the atmosphere, hydrosphere, cryosphere and terrestrial biosphere (illustrated schematically in Figure 4.22). The atmosphere is a two-level model based on a formulation first proposed in 1971. The geography is not realistic, as for CLIMBER-2, but rather idealistic, hoping to capture the essential character of the Earth's climate with two continents. The ocean is composed of three 19-layer zonal (5° grid) models attached to the Indian, Pacific and Atlantic basins. In each continent, the relative cover of trees, grass and potential desert is computed as a function of precipitation and growing degree days. The model computes surface temperature for each surface type. The nature of the model means that it is suited to palaeoclimate studies, although some limitations exist because the model explicitly uses modern-day observational data in its computations. The model has been used to simulate the volcanic and solar impacts on climate since 1700 (Figure 4.23) and can explain at least part of the observed warming in the twentieth century as being due to solar and volcanic forcing changes, although the study concludes that the rise since 1930 cannot be explained by natural forcings.

4.8.8 EMICs predict future release of radiocarbons from the oceans

Radiocarbon is created when neutrons replace protons in nitrogen atoms. This process occurs naturally in the Earth's stratosphere where cosmic ray bombardment

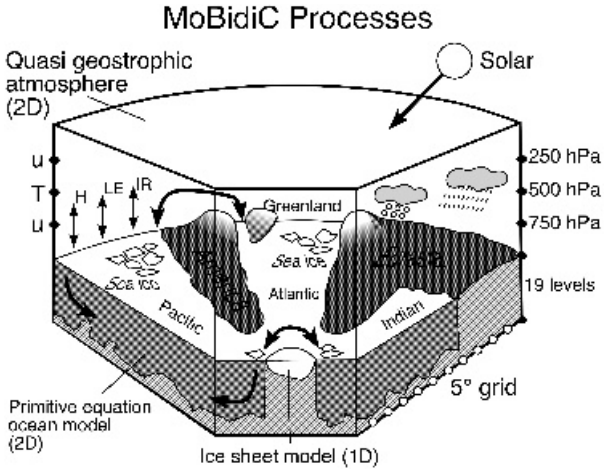

Figure 4.22 Schematic illustration of the makeup of MoBidiC, showing a severely truncated Earth Model of Intermediate Complexity (EMIC) (from http://www.climate.be/tools/mobidic.html)

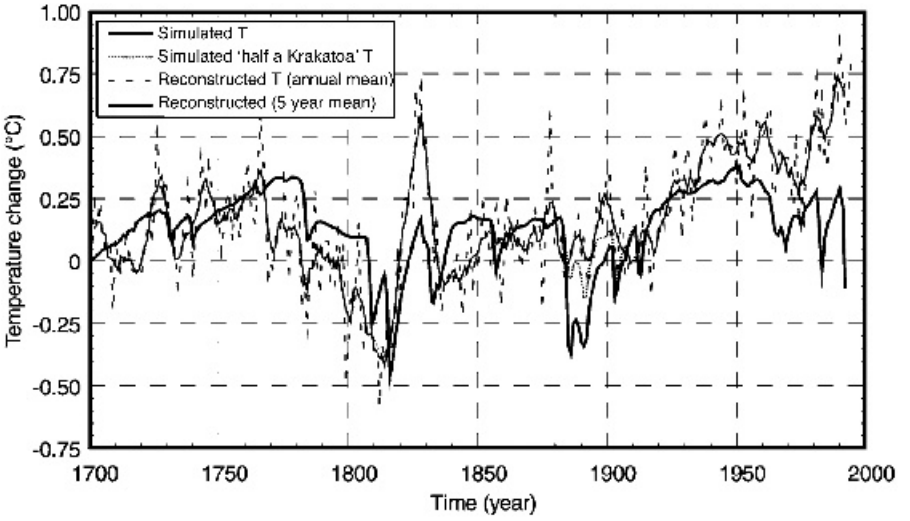

Figure 4.23 Comparison between reconstructed annual mean Northern Hemisphere temperature variations (1700 to 1992) and simulated temperatures from the MoBidiC 2D global climate model in response to the combined solar and volcanic forcings. The dotted line shows the model response to half a Krakatoa forcing (reproduced with permission from Bertrand *et al*., 1999, *Climate Dynamics*, **15**, 355–367. Copyright (1999) Springer)

generates ^{14}C from ^{14}N. Anthropogenerated atmospheric injections of ^{14}C occurred between 1945 and 1975 as a result of nuclear weapons tests, peaking in 1961–62. ^{14}C decays with a half-life of 5730 years and, prior to the industrial era, was in equilibrium with the net radiocarbon flux into the biosphere and ocean, roughly balancing radioactive decay losses. Carbon isotopic fluxes into and out of our atmosphere appear to behave oddly. This was first noted in the Suess effect: a 2 to 3 per cent reduction in atmospheric $^{14}C/^{12}C$ from pre-industrial times to 1950. Although in the expected direction (because fossil fuel CO_2 is biogenic and therefore strongly enriched in $^{12}CO_2$) this reduction in the relative proportion of ^{14}C was much smaller than predicted, recognizing the 10 per cent increase in atmospheric CO_2 over that period. Most of the difference is now explained by $^{14}CO_2$ fluxes from the land biosphere and the oceans which are caused by increasing atmospheric $^{12}CO_2$. Thus, even though fossil fuels are virtually devoid of ^{14}C (because it has decayed away) the fossil-fuelled increase in $^{12}CO_2$ prompts an indirect increase in ^{14}C in the atmosphere.

This peculiar result can be illustrated using an EMIC which combines a three-box terrestrial biosphere model with a box-diffusion ocean model. One such model has also been employed to project future ^{14}C fluxes among the major compartments of the Earth system (Figure 4.24). This simulation suggests that atmospheric ^{14}C reached a minimum around the beginning of the twenty-first century and will increase in the future as natural, cosmic ray, production in the stratosphere exceeds bomb pulse plus natural ^{14}C uptake by the land biosphere and ocean. This EMIC prediction of both the atmospheric ^{14}C minimum (around 2000) and the ocean becoming a source of atmospheric ^{14}C (around 2030) provides a valuable test for more comprehensive climate models' simulation of the global carbon cycle.

4.9 WHY ARE SOME CLIMATE MODELLERS FLATLANDERS?

In the introduction to Chapter 3, we noted that two-dimensional beings cannot understand three dimensions and must describe what they see in terms of the only dimensions they recognize. Since most climate modellers of our experience are three-dimensional, why is it that some of them choose to represent the climate system in terms of highly parameterized formulations that are essentially a reduction of the dimensionality of the real system?

One answer is, of course, that by simplifying they aim to represent important mechanisms without overburdening their computational resources. In this way, many of them can watch their simplified systems develop for longer time periods and/or in many more variants than would be possible if they were to use fully coupled OAGCMs operating on even the best available computers of today. This method can be carried further. For example, EBMs have been used to investigate Milankovitch variations. However, as we illustrated in Section 4.8, the demarcation between two- and three-dimensional models is often rather arbitrary. The use of two-dimensional models and especially EMICs to represent the climate is now widespread including in the response to predicted increases in CO_2 and other trace gases. By stripping

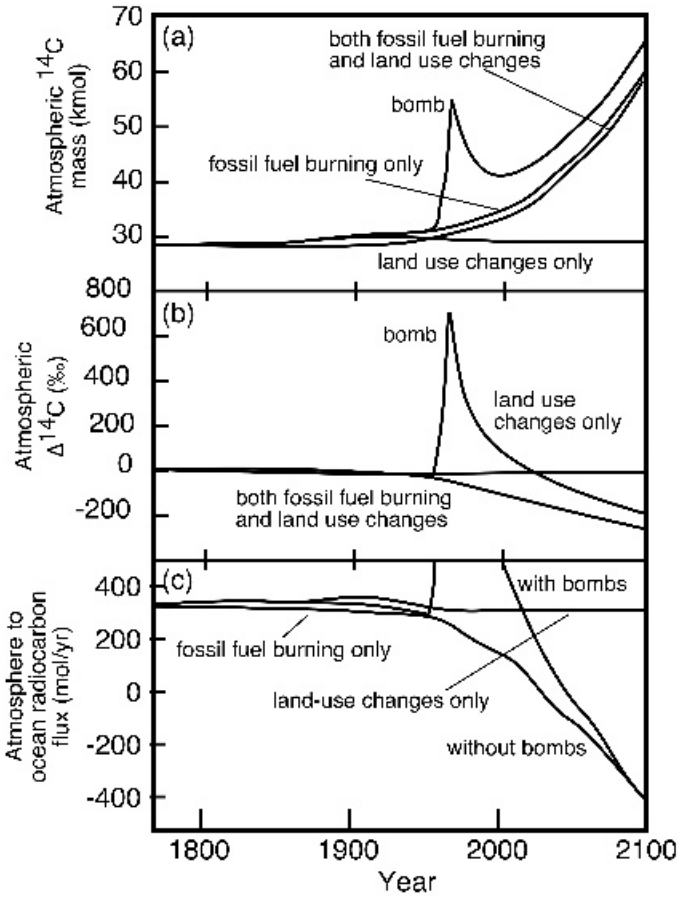

Figure 4.24 (a) Atmospheric ^{14}C mass, (b) atmospheric $\Delta^{14}C$, and (c) net fluxes of ^{14}C from the atmosphere to the ocean predicted by a model for the period 1765 to 2100 for simulations 'fossil fuel only', 'land use only', 'both' and 'data/bomb'. The large increase in atmospheric ^{14}C mass is primarily the result of ^{14}C fluxes induced by fossil fuel burning. Note that after the late 1990s, atmospheric $^{14}CO_2$ is predicted to increase, even though atmospheric $\Delta^{14}C$ is predicted to decrease. The model predicts that the ocean should start losing ^{14}C to the atmosphere some time in the next century (reproduced by permission of the American Geophysical Union from Caldeira *et al*. (1998), *Geophys. Res. Lett.,* **25**, 3811–3814)

away unnecessary complexities, the workings of any system are more readily viewed and, hence, more easily understood. Consequently, some questions, especially those pertaining to basic mechanisms and to long time periods, are better tackled with simpler (i.e. more highly parameterized) models.

An important message that we hope you have gained from this chapter and which will be underlined in Chapter 5 is that it is not scientifically short-sighted to choose

to parameterize some aspects of the climate system and thereby reduce the number of dimensions; it is valuable and probably inevitable. The skill of a good modeller lies in the ability to identify results which are characteristic of features of the real system, as opposed to those which are facets of the constrained framework of the model. Thus, climate modellers can choose to dwell happily in Flatland but they must not begin to think like the natives.

RECOMMENDED READING

Chylek, P. and Kiehl, J.T. (1981) Sensitivities of radiative–convective models. *J. Atmos. Sci.* **38**, 1105–1110.

Claussen, M., Mysak, L.A., Weaver, A.J., Crucifix, M., Fichefet, T., Loutre, M-F., Weber, S.L., Alcamo, J., Alexeev, V.A., Berger, A., Calov, R., Ganopolski, A., Goosse, H., Lohman, G., Lunkeit, F, Mokhov, I.I., Petoukhov, V., Stone, P. and Wang, Z. (2002) Earth system models of intermediate complexity: Closing the gap in the spectrum of climate system models. *Clim. Dyn.* **18**, 579–586.

de Haan, B.J., Jonas, M., Klepper, O., Krabec, J., Krol, M.S. and Olendrzynski, K. (1994) An atmosphere–ocean model for integrated assessment of global change. *Water, Air and Soil Pollution* **76**, 283–318.

Garcia, R.R., Stordal, F., Solomon, S. and Kiehl, J.T. (1992) A new numerical model of the middle atmosphere, 1, dynamics and transport of tropospheric source gases. *J. Geophys. Res.* **97**, 12 967–12 991.

Hansen, J.E., Johnson, D., Lacis, A.A., Lebedeff, S., Lee, P., Rind, D. and Russell, G. (1981) Climate impact of increasing atmospheric CO_2. *Science* **213**, 957–966.

MacKay, R.M. and Khalil, M.A.K. (1991) Theory and development of a one-dimensional time-dependent radiative–convective model. *Chemosphere* **22**, 383–417.

Manabe, S. and Wetherald, R.T. (1967) Thermal equilibrium of the atmosphere with a given distribution of relative humidity. *J. Atmos. Sci.* **24**, 241–259.

Potter, G.L. and Cess, R.D. (1984) Background tropospheric aerosols: incorporation within a statistical–dynamical climate model. *J. Geophys. Res.* **89**, 9521–9526.

Potter, G.L., Ellsaesser, H.W., MacCracken, M.C. and Mitchell, C.S. (1981) Climate change and cloud feedback: the possible radiative effects of latitudinal redistribution. *J. Atmos. Sci.* **38**, 489–493.

Ramanathan, V. and Coakley, J.A. (1979) Climate modelling through radiative–convective models. *Rev. Geophys. Space Phys.* **16**, 465–489.

Rossow, W.B., Henderson-Sellers, A. and Weinreich, S.K. (1982) Cloud-feedback – a stabilizing effect for the early Earth. *Science* **217**, 1245–1247.

Saltzman, B. (1978) A survey of statistical–dynamical models of terrestrial climate. *Advances in Geophysics* **20**, 183–304.

Schneider, S.H. (1972) Cloudiness as a global climatic feedback mechanism: the effects on the radiation balance and surface temperature of variations in cloudiness. *J. Atmos. Sci.* **29**, 1413–1422.

Sellers, W.D. (1973) A new global climate model. *J. Appl. Meteor.* **12**, 241–254.

Sellers, W.D. (1976) A two-dimensional global climate model. *Mon. Wea. Rev.* **104**, 233–248.

Taylor, K.E. (1980) The roles of mean meridional motions and large-scale eddies in zonally averaged circulations. *J. Atmos. Sci.* **37**, 1–19.

Thompson, S.L. and Schneider, S.H. (1979) A seasonal zonal Energy Balance Climate Model with an interactive lower layer. *J. Geophys. Res.* **84**, 2401–2414.

Wang, W-C. and Stone, P.H. (1980) Effects of ice–albedo feedback on global sensitivity in a one-dimensional radiative–convective model. *J. Atmos. Sci.* **37**, 545–552.

Web resources

http://www.pik-potsdam.de/	The Potsdam Institute for Climate Impacts Research (CLIMBER-2)
http://www.mcgill.ca/meteo/	McGill University Palaeo Model
http://www.knmi.nl/onderzk/CKO/ecbilt.html	Netherlands Centre for Climate Research
http://web.mit.edu/globalchange/www/	MIT Integrated Global System Model
http://www.climate.be/tools/mobidic.html	MoBidiC
http://puma.dkrz.de/puma/	PUMA
http://climate.uvic.ca/	UVicESCM
http://www.climate.unibe.ch/	BERN 2.5D
http://www.giss.nasa.gov/	NASA Goddard Institute for Space Studies

CHAPTER 5

Coupled Climate System Models

The most powerful tools available with which to assess future climate are coupled climate models, which include three-dimensional representations of the atmosphere, ocean, cryosphere and land surface.

W.L. Gates (1996)

5.1 THREE-DIMENSIONAL MODELS OF THE CLIMATE SYSTEM

The most 'complete' models of the climate system are constructed by discretizing and then solving equations which represent the basic laws that govern the behaviour of the atmosphere, ocean and land surface. These three-dimensional models of the general circulation of the atmosphere and ocean have come to be known generically as GCMs. The term 'GCM' is often used loosely and can be thought of as referring to a Global Climate Model or to a General Circulation Model. In the latter case, the acronym is often qualified by the addition of an 'A' when speaking of strictly atmospheric models or an 'O' when talking of ocean-only models. Sometimes the term 'coupled' and the acronym 'CGCM' are also used. The history of GCMs, outlined in Chapter 2, is such that these models have been thought of as atmospheric models with 'add-ons'. However, as the models have developed, the amount of computational effort for the 'add-on' components has come to rival and even exceed the effort required to simulate the atmosphere alone. CGCMs and some AGCMs can include complex representations of the land surface. Today's full, three-dimensional models are typically termed 'coupled climate system models', with an organization similar to that shown in Figure 5.1. The 'model' is really (or at least strives to be) a coherent collection of models connected by a specialized coupler module. Some of the technical issues associated with such a philosophy are explored in Chapter 6.

The differences in geometry and composition of the atmosphere and ocean mean that there are a number of significant differences in the modelling approaches taken and the coupler must deal with these. The atmosphere is a spherical shell of compressible gas which covers the whole Earth. It is, oddly, heated mostly from the

A Climate Modelling Primer, Third Edition. K. McGuffie and A. Henderson-Sellers.
 ISBN: 0-470-85750-1 (HB); 0-470-85751-X (PB)

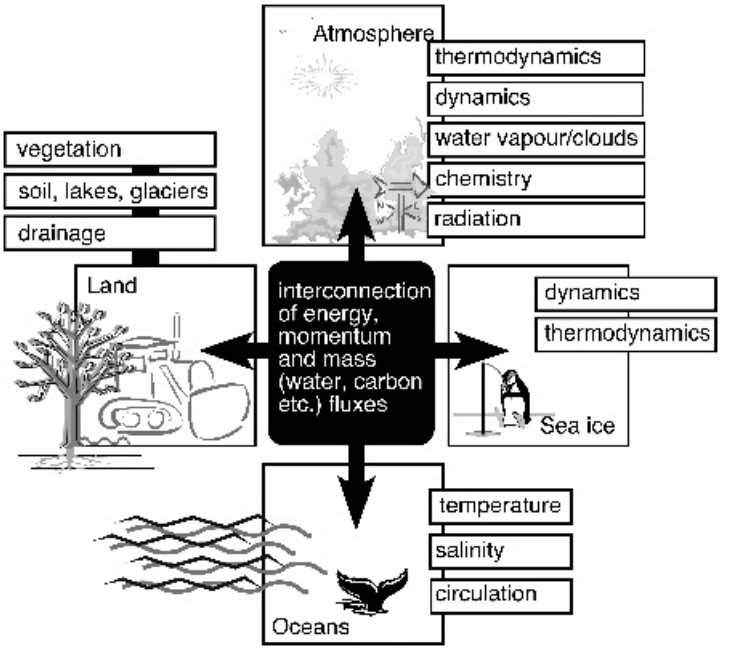

Figure 5.1 Modern coupled ocean–atmosphere models are constructed as modular components connected by a coupler (black), a program that transfers fluxes between the model components. In recent years, significant effort has been devoted to formal software design and the development of portable 'plug compatible' climate sub-models, meaning that development can focus on model physics rather than on operational and computational aspects of the model

Earth's surface below. The ocean, on the other hand, is relatively incompressible, is heated only at its top surface and is confined to particular parts of the Earth's surface: the ocean basins. The land surface is a complex system and the role of forests, grasslands, lakes, marshes, agricultural areas and seasonal and perennial snow cover must be included. Sea ice is a flexible, reflective material moved by both ocean currents and winds that acts as an effective barrier for heat transfer between atmosphere and ocean.

In this chapter, we will use Figure 5.1 as a framework for discussion. Some of the ways in which the climate system is modelled in three dimensions are described. The ways in which these atmospheric, oceanic, cryospheric and biospheric models are constructed and the ways in which they are used are also considered in this chapter.

5.2 MODELLING THE ATMOSPHERE

In this section, the basic formulation of three-dimensional models of the atmosphere (AGCMs) is considered with particular reference to the differences between so-

called 'spectral' and 'finite grid' models. The dynamics comprises the numerical schemes by which large-scale atmospheric transports are accomplished. The part of the model that accomplishes this is now commonly termed the dynamical core. Several families of dynamical core have been developed, but all use a similar set of governing equations. These dynamics are mostly computed in either physical space or spectral space, as described below. The equations that are solved in these models are similar to those first formulated for numerical weather forecast models, although in the early stages of climate modelling there was a requirement for increased emphasis on conservation (of energy and matter), which was less important for short-term weather forecasts. Any AGCM must be formulated with some fundamental considerations for:

1. Conservation of momentum

$$\frac{D\mathbf{v}}{Dt} = -2\boldsymbol{\Omega} \times \mathbf{v} - \rho^{-1}\nabla p + \mathbf{g} + \mathbf{F} \tag{5.1}$$

2. Conservation of mass

$$\frac{D\rho}{Dt} = -\rho\nabla \cdot \mathbf{v} + C - E \tag{5.2}$$

3. Conservation of energy

$$\frac{DI}{Dt} = -p\frac{D\rho^{-1}}{Dt} + Q \tag{5.3}$$

4. Ideal gas law

$$p = \rho RT \tag{5.4}$$

where $\mathbf{v}$ = velocity relative to the rotating Earth,
t = time,
$\frac{D}{Dt}$ = total time derivative $\left[= \frac{\partial}{\partial t} + \mathbf{v} \cdot \nabla\right]$
$\boldsymbol{\Omega}$ = angular velocity vector of the Earth,
ρ = atmospheric density,
$\mathbf{g}$ = apparent gravitational acceleration,
p = atmospheric pressure,
$\mathbf{F}$ = force per unit mass,
C = rate of creation of atmospheric constituents,
E = rate of destruction of atmospheric constituents,
I = internal energy per unit mass [$= c_p T$],
Q = heating rate per unit mass,
R = gas constant,
T = temperature,
c_p = specific heat of air at constant pressure.

An atmospheric model needs also to conserve enstrophy (the root mean square of the vorticity). Failure to conserve enstrophy means that the energy of motion is transferred unrealistically to smaller and smaller space-scales. Very early model structures did not conserve enstrophy and, consequently, became unstable after short integration times.

5.2.1 Finite grid formulation of atmospheric models

In order to simulate the atmospheric processes, the equations describing the atmosphere's behaviour have to be discretized. Modelling the atmosphere by dividing it into a series of 'boxes' is probably the easiest method to visualize and was the basis of the earliest attempts to model the atmosphere. The atmosphere is reduced to a matrix of numbers, usually evenly spaced in latitude and longitude. Depending on the complexity of the model, values of a number of variables may be stored at each point. Care must be taken in the discretization process to preserve the properties of the original equations. Not all variables are stored at the same point on the grid. Generally, vector quantities (such as winds) and scalar quantities (such as temperature) are computed on staggered grids (e.g. Arakawa C-grid) to more readily match the physics of the situation. In Figure 5.2a, the structure of a Cartesian grid AGCM

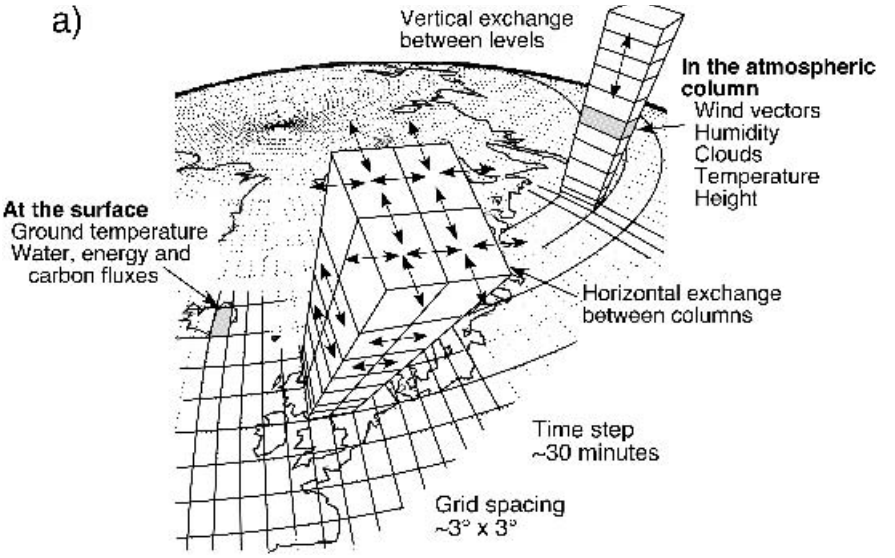

Figure 5.2 The construction of (a) a finite grid AGCM (a rectangular grid in this case); (b) a spectral AGCM. In a finite grid AGCM, the horizontal and vertical exchanges are handled in a straightforward manner between adjacent columns and layers. Recently, modellers have begun experimenting with icosahedral grids. In a spectral GCM, vertical exchanges are computed in grid point space (i.e. in the same manner as the finite grid model), while horizontal flow is computed in spectral space. The method of transfer between grid point space and spectral space can be followed with reference to the text and by reading around (b) from point 1 to point 4

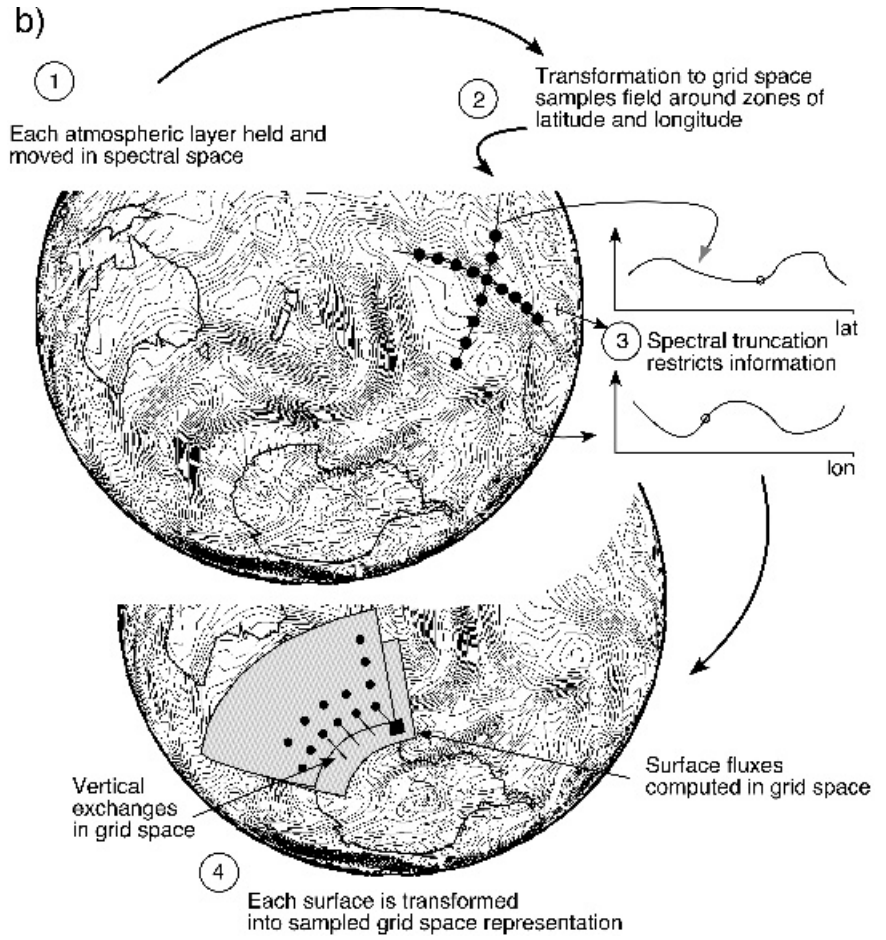

Figure 5.2 *Continued*

is illustrated. The grid boxes are usually regularly spaced horizontally. The atmospheric column above each surface point is divided into a prespecified number of layers. Typically these layers follow the terrain by what are termed sigma coordinates (Equation (4.2)). The pressure coordinate of the layer is determined as a fraction of the surface pressure, ensuring that there are no discontinuities over mountain ranges. Vertical resolution need not be uniform, and finer vertical resolution is often employed near the tropopause and the surface. Boundary layer processes influence the near-surface layers, and high resolution near the surface is required to determine temperature and humidity gradients and atmospheric stability, needed for modelling surface fluxes.

In a finite grid AGCM, the structure is as might be expected: variables for a particular location are moved into computer memory and all computations undertaken. Different grid structures involve the retaining of different variables at different points of the grid. Besides physical considerations, there are numerical influences on the grid spacing and timestep of an AGCM. The timestep must be short enough that the maximum speed of propagation of information does not permit any transfer from one grid point to another within one timestep. The timestep Δt is therefore governed by the restriction

$$\Delta t \leq \Delta x / c \tag{5.5}$$

where Δx is the grid spacing and c is the fastest propagation velocity, which in atmospheric GCMs is the speed of gravity waves. When the model grid is rectangular, the grid spacing becomes small at the poles, leading to the need for very short timesteps of the order of a few seconds. In this case, incorporating filtering procedures can overcome the numerical instability caused by not reducing the timestep to match this requirement. The semi-implicit timestepping scheme involves a special treatment of the motion of gravity waves (the main constraint on the timestep) with the result that longer timesteps are possible. In recent years, the use of a semi-Lagrangian timestepping approach in climate models has increased because of advantages in computational efficiency and stability.

The finite difference method computes variables at gridpoints and, although the first global models used this technique and the technique is widely used in ocean models, the bulk of modern atmospheric models are spectral models. However, developments in computer architecture mean that model architecture continues to change. Modellers are now moving from spectral models back to techniques reminiscent of grid models. Finite volume (as opposed to finite grid) methods compute the average value of variables over a cell and use an integrated form of the governing equations to track the flux of energy, mass and momentum at the cell boundaries. Hence finite volume methods are very good at conserving these quantities. Finite element models divide the domain into numerous elements, where the value of a variable is represented within each element by the summation of polynomial functions. Finite elements have been used successfully in engineering applications for decades, but were only introduced in GCMs in the late 1990s. These models use spectral elements, a subclass of finite elements which have high accuracy within each element. These techniques are also suited to use in adaptive mesh refinement, where the model resolution can be adjusted to suit the area of interest, with high resolution over land areas and lower resolution over the ocean.

5.2.2 Spectral models

The spectral method is particularly applicable to the atmosphere, because the atmosphere is a continuous spherical shell of air, suggesting that the use of a spherical coordinate system is appropriate. Spectral AGCMs are formulated in a fundamentally different way from finite grid AGCMs. Although the surface is retained as a grid,

the atmospheric fields are held and manipulated in the form of waves (Figure 5.2b). The advantage of this is that the computation of gradients is easier and computation times are consequently reduced. Many wave-like features of the atmosphere are best simulated with a wave formulation, so the method has been very popular over the years. Spectral models are, however, not usually formulated in all directions using waves: a rectangular grid is used for vertical transfers, and radiative transfer and surface processes are modelled in this grid space. The computational flow of a spectral AGCM is illustrated schematically in Figure 5.3. The data fields are transformed to grid space at every timestep via fast Fourier transforms and Gaussian quadrature (a form of numerical integration) and back to spectral space via Legendre transforms and Fourier transforms. The timestepping is performed with the waveform representation and grid-point physics is incorporated after the transformation into grid space. Roughly, 'physics' means everything that is not dynamics (Equations (5.1)–(5.4)).

Representing the atmosphere with waves

Fourier's theorem states that any ordered sequence of numbers can be represented as a summation of sine and cosine waves. The variation of any quantity around a latitude zone is necessarily periodic and can therefore be represented as a summa-

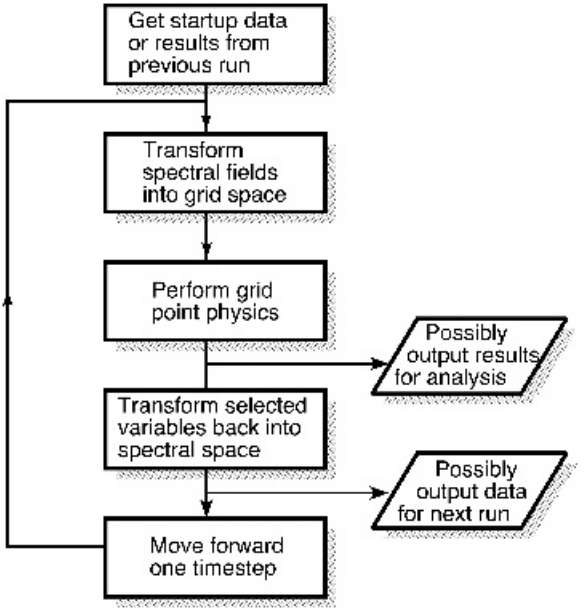

Figure 5.3 The flow through the computational scheme of a spectral AGCM. In this case, there is only one transformation loop, although models with two transformation loops have been developed

tion of a number of waves. These waves are the Fourier transform of the original data series. In the same way that the logarithm of a number contains the same information as the number, so the Fourier transform of a data series contains the same information as the original grid representation. Analogously to logarithms, Fourier transforms allow mathematical operations to be performed more easily than if the original form were worked upon.

The same principle of increased computational time being required for increased resolution applies to spectral representation as well as to Cartesian grid models. Resolution in a spectral AGCM is governed by the wavenumber of truncation. Early climate modelling applications used 15 waves to represent each variable in each latitude zone at each vertical level. If a model has 15 zonal waves then it is said to be truncated at wavenumber 15 (often referred to as R15 – the R standing for rhomboidal truncation, see below). Basic resolution for most climate models is now T42 ('triangular' truncation with 42 zonal waves) and, as computer capabilities and storage capacities have increased, it has become possible to compute and retain larger numbers of waves and some climate simulations have used T106. An example of the effect of truncation is the smoothing of the real orography of the Alps for two versions of the European Centre for Medium Range Weather Forecasting (ECMWF) model. Like a GCM, this model is also spectral but, as it is used for 10–20-day weather forecasts rather than climatic simulations, it is truncated at much higher wavenumbers. Figure 5.4 compares the orography for model versions truncated at wavenumbers 63 and 106. The 2004 version of the ECMWF forecast model uses T511 (~40 km grid) with 60 levels.

When considering the processes in grid space, an array of points, termed the Gaussian grid points, is defined, the number of these points being governed by the particular truncation level of the model. Over-specification of these grid points results in excessive computation times, whereas under-specification results in aliasing (the transferring of energy from high frequencies to low frequencies through poor sampling) of the high frequencies. Recent developments have allowed the use of different grids for the dynamics and the physics of a spectral model and the use of a reduced grid (fewer points in longitude) near the poles.

Structure of a spectral model

We have discussed how a spectral AGCM handles information both in wave form and in grid point form. In this section, the manner in which information is transferred between these two spaces, being the principal feature of such models, will be described. The full procedure for a single timestep of a spectral model is outlined below.

An arbitrary variable, X, which has values over the surface of a sphere (e.g. Figure 5.2b) can be expanded as

$$X = \sum_{m=-M}^{M} \sum_{n=K+1}^{N} X_n^m Y_n^m \tag{5.6}$$

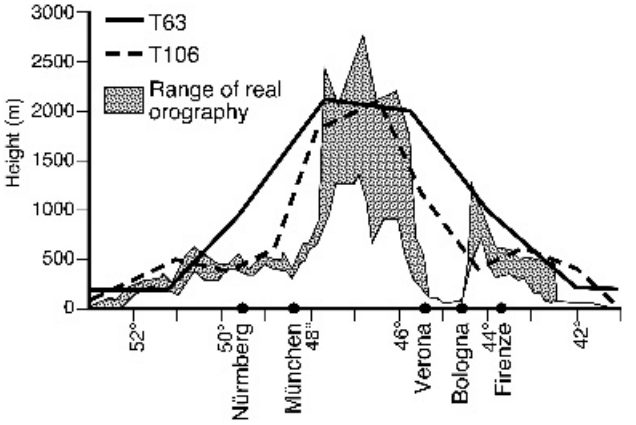

Figure 5.4 Comparison of the range in the real orography of the Alps (shown in cross-section) with the representation used in two versions of a spectral AGCM truncated at wavenumbers 63 and 106 (reproduced from Simmons and Bengtsson, 1988, with kind permission of Kluwer Academic Publishers)

with X_n^m, the spectral coefficients, being complex (i.e. containing an imaginary part premultiplied by $i = \sqrt{-1}$ as well as a real part) and a function of time. The spherical harmonic, Y_n^m, is a function of longitude, λ, and latitude, ϕ, such that

$$Y_n^m = P_n^m(\sin\phi)\exp(im\lambda) \tag{5.7}$$

where P_n^m is an associated Legendre polynomial of degree n and zonal wavenumber m and the meridional wavenumber has a value of $n - m$. This is the case at point 1 on Figure 5.2b. The shape of this functional representation of the atmospheric variables is governed by the spherical coefficients. In the next stage of the model cycle (point 2), the spectral coefficients of the dynamics variables (vorticity, divergence, wind components, water vapour mixing ratio and pressure) are transformed to a latitude–longitude grid (the Gaussian grid). First, a Legendre transform is evaluated for each spectral variable at each of the Gaussian latitudes, ϕ_j. These latitudes are related to the resolution of the model such that they are the roots of the associated Legendre polynomial of order zero. For a variable X,

$$X_n^m \rightarrow X_{(m)}(\phi_j; t) = \sum_{n=|m|}^{|m|+j} X_n^m P_n^m \tag{5.8}$$

The resulting Fourier harmonics, $X_{(m)}$, at each of the Gaussian latitudes ϕ_j and at time t are transformed via a fast Fourier transform (FFT) algorithm to longitudes $\lambda_l = 2\pi l/L$, $1 < l < L$

$$X_n^m \rightarrow Z(\lambda_l, \phi_j; t) = \sum_{m=-M}^{M} X_{(m)} \exp(im\lambda_l) \tag{5.9}$$

By these two steps we have achieved a spatial distribution of values at a series of grid points. Physical processes, such as radiative transfer, convection and the ground energy budget, can now be calculated in this rectangular grid (point 4 in Figure 5.2b). Subsequent to such calculations, variables are transformed back into wave space via fast Fourier transform, and then the inverse Legendre transformations are built up, one latitude at a time, using Gaussian quadrature (Figure 5.3) such that

$$Z_n^m = \sum_{j=1}^{k} w_{j,k}(\phi_j) Z_{(m)}(\phi_j) P_n^m(\sin \phi_j) \tag{5.10}$$

With the model reassembled in spectral form and appropriate expressions for the time rate of change of the variables incorporated, some form of timestep procedure is applied to find the values of the spectral fields at the advanced time point. This returns us to point 1 in Figure 5.2b. Timestepping can be accomplished in several different ways, but all rely on approximating the time differential in a finite difference form. This rate of change is applied for the appropriate time period and a value for each variable is derived at the next time point.

Truncation

The type of truncation of a spectral AGCM is often quoted in model descriptions. The simplest explanation is that the truncation number represents the number of waves which are resolved around a latitude zone (point 3 in Figure 5.2b). This is the governing factor in determining the resolution of a spectral AGCM. More completely, it is a description of the relationship between the largest Fourier wavenumber, the highest degree of the associated Legendre polynomial and the highest degree of the Legendre polynomial of order zero. These are termed M, K and N respectively. With reference to Figure 5.5, the truncation types are defined as

Triangular:	$M = N = K$	(Figure 5.5b)
Rhomboidal:	$K = N + M$	(Figure 5.5c)
Trapezoidal:	$N = K > M$	(Figure 5.5d)

These are all subsets of the pentagonal case illustrated in Figure 5.5a. These truncation types carry with them requirements for the resolution of the Gaussian grid of the model. For example, for triangular truncation

$$N_{long} \geq 3M + 1; \quad N_{lat} \geq (3M + 1)/2 \tag{5.11}$$

Obeying constraints of Equation (5.11) is sufficient to remove most of the aliasing in the model.

The two most common truncations used in atmospheric GCMs are the triangular (T) and rhomboidal (R) methods. The choice of truncation is somewhat arbitrary. Although rhomboidal truncation gives higher resolution in high latitudes, has some advantages for vectorization on some supercomputers and can be considered a more

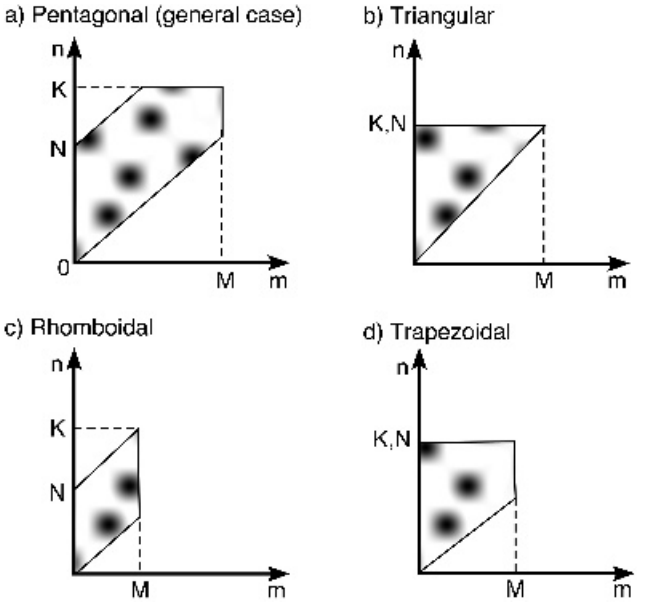

Figure 5.5 The relationship of spectral variables from different truncation types used in spectral AGCMs. The most common truncation types are triangular and rhomboidal

'exact' representation, triangular truncation is generally considered satisfactory and has special properties which result in a more uniform representation.

Owing to the divergence of solutions at alternate timesteps, a time filter may need to be employed, with certain timestepping schemes, to prevent computational instability. Additionally, in rectangular grid schemes, a multipoint filter is applied in the east–west direction in the polarmost rows.

5.2.3 Geodesic grids

The advantages and disadvantages of spectral and finite-grid formulations of the dynamical core of a GCM have spawned research into new formulations of model dynamics that combine the advantages of both finite difference methods and spectral methods, while moderating the deficiencies of each. If the model is formulated on a geodesic grid, then the surface of the Earth can be covered with the grid and the advantages of the finite grid models can be enjoyed, together with some of the techniques associated with spectral models without the annoying singularities at the poles and associated numerical fixes. The geodesic grid was first trialled in simple models in the 1960s, but technical difficulties with model formulation remained unsolved until the late 1980s. Even then, the computational overhead limited progress with the geodesic formulation.

The geodesic grid is familiar to most through the popularization of the structure by architect Buckminster Fuller (1895–1983), soccer balls and the C_{60} molecules associated with the 1996 Nobel Prize for chemistry. A geodesic grid can be viewed as an arrangement of triangular tiles covering the sphere. Each vertex on this shape is a model grid point. Figure 5.6 shows a geodesic representation of the sphere and its associated grid. The movement away from the familiar Cartesian co-ordinate system has a significant impact on the formulation of the model equations and the complete revision of the model structure means that the other components of the climate system model (Figure 5.1) need to be revised and reformulated to operate on a geodesic grid. The geodesic grid has particular advantages when it comes to the decomposition of the computational tasks for modern, highly parallel computer systems. Figure 5.7 shows a geodesic grid assembled into quasi-rectangular groups. Each group consists of two of the triangles illustrated in Figure 5.6a and interacts with four other groups. At the computation stage, these groups can be assigned to different processors in a relatively straightforward and scaleable manner. These new developments are ongoing, but the next ten years should see the full emergence of a new family of climate models.

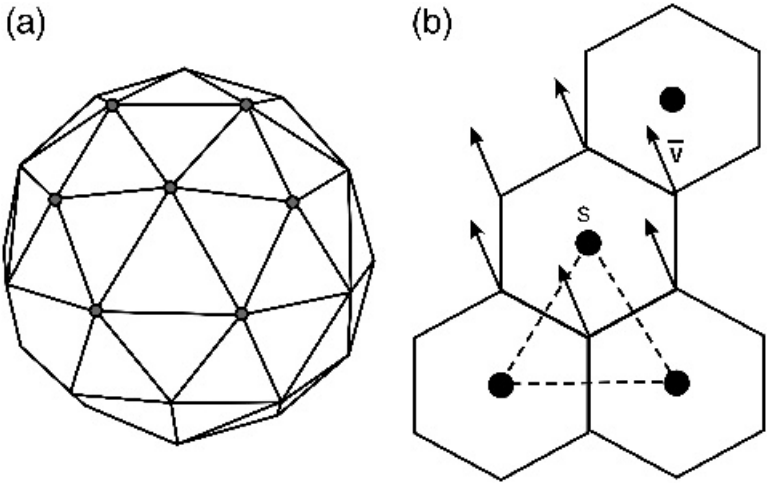

Figure 5.6 (a) The geodesic formulation covers the sphere with a virtually even grid. Starting from an initial icosahedron, each triangular face is divided into four and the vertices projected onto an enclosing sphere. The grid points are the vertices of the polyhedron. The number of grid points, N, is related to the level of recursion from the initial icosahedron by $N = 5 \times 2^{2R+3} + 2$. $R = 4$ gives a grid spacing on the Earth of around 240 km. Six edges meet at each vertex so that each vertex can be regarded as the centre of a hexagonal grid box. (b) A two-dimensional projection of part of the hexagonal grid implied by panel (a). The arrangement of model variables on the grid has an important influence on the performance of the model (as with other dynamical core types). Here, the Z–M grid stores scalar quantities (s) such as temperature at the centres of the grid boxes and vector quantities ($\bar{v}$) such as wind velocities at the vertices

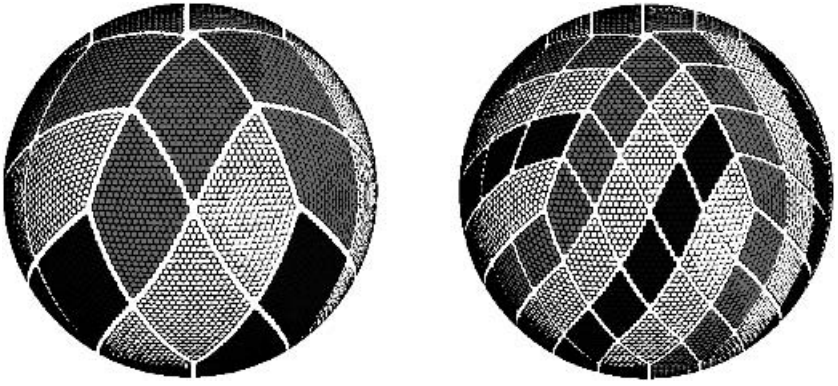

Figure 5.7 The formation of a grid using a geodesic pattern has a number of advantages despite the increased computational requirements. The grid can be broken up into a series of blocks, each having four neighbouring blocks, to suit the architecture of massively parallel computer systems (reproduced with permission of the IEEE from Randall *et al.* (2002), *Comp. Sci. Eng.*, **4**, 32–41)

5.2.4 The influence of computer architecture on numerical methods

Computers that are large enough to run three-dimensional climate models use hundreds or thousands of individual processors, which operate simultaneously to perform the many calculations required. In a shared memory machine, all the processors have access to the same memory space. In contrast, the processors of a distributed memory machine can only see their own memory and must send messages over a network to exchange data with the other processors. Shared memory supercomputers of the 1970s, 1980s and early 1990s, like those developed by Cray and Silicon Graphics, have given way to distributed, massively parallel machines such as Beowulf clusters. These clusters use off-the-shelf components and are much cheaper than earlier custom-designed machines. The disadvantages of distributed memory machines is that they require special algorithms and programming languages for message passing between processors, and that communication between processors is much slower than computation within each processor.

Spectral models were the dominant numerical method for GCMs from the 1960s to the 1990s. They have high accuracy, compute gradients extremely efficiently, and do not concentrate grid points at the poles. The trade-off is that the variables must be transformed between spectral and physical space at every timestep. These transforms require most of the computation time in a spectral model. For low- and mid-resolution GCMs on shared memory machines, spectral methods were the algorithm of choice because of their speed.

Spectral models are not well suited for distributed memory machines. (Note the transforms at points 1 and 4 in Figure 5.2b.) In physical space, each processor in a distributed memory machine stores the variables for a block of grid boxes in its own memory. In spectral space, each processor stores a subset of the wave coefficients.

In order to transform from spectral space to physical space, all the wave coefficients must be summed, as shown in Equation (5.6). This requires each processor to receive wave coefficient data from every other processor in order to compute its own grid box values, a process dubbed 'all to all communication'. As inter-processor communication is the slowest part of distributed memory computations, spectral methods are not competitive with finite grid methods on distributed memory machines. Finite grid methods are well suited for distributed memory machines because each processor must only communicate with the processors which own neighbouring blocks of grid boxes in physical space.

In order to increase the accuracy with which a numerical model simulates the governing equations, one must increase the resolution of the model. This results in a higher density of grid boxes everywhere, even though this density is most beneficial where the 'action' is, like steep pressure gradients in fronts and hurricanes. An alternative strategy is adaptive mesh refinement (AMR), which concentrates grid boxes at steep gradients and leaves a low density over large homogeneous areas. Finite grid methods have incorporated AMR successfully on distributed memory machines. Spectral models, which use waves to represent functions with uniform accuracy across the sphere, cannot use AMR.

Computer technology will continue to evolve, and models will evolve with it. The direction that future models are taking is either finite volume or spectral element. Whether the grid is geodesic, a cubed sphere, adaptive or otherwise is less important.

5.2.5 Atmospheric GCM components

In AGCMs, three-dimensional, time-dependent equations govern the rate of change of the six basic model variables: surface pressure, two horizontal wind components, temperature, moisture and geopotential height. The six basic equations solved to derive these variables are, as described in Sections 2.2.4 and 5.2.1, the hydrostatic equation, two equations for horizontal motion (Equation (5.1)), and the thermodynamic (Equation (5.3)), water vapour and mass continuity (Equation (5.2)) equations. The use of σ co-ordinates combined with the assumption that the atmosphere can be considered to be in hydrostatic equilibrium permits the vertical wind component, w, to be obtained diagnostically from the convergence of horizontal wind components, u and v. The equations for the dynamics are solved in either wave (spectral) space or grid space, as explained above. The horizontal grid used in model integrations varies but a typical resolution (T42) has grid boxes roughly $2.5° \times 2.5°$. Modelling groups often use a range of model resolutions so that, for example, a coarser version may be developed for the coupled ocean–atmosphere experiments. A typical timestep length is 10–30 minutes.

For the purpose of computation of the physics (as opposed to the dynamics), all GCMs can be visualized as consisting of an array of columns, which extend into both the atmosphere and the subsurface, distributed over the globe on a grid (Figure 5.2a).

The physical processes typically include the radiation scheme, the boundary layer scheme, the surface parameterization scheme, the convection scheme (including convective precipitation and clouds) and the large-scale precipitation scheme. All of these schemes, with the possible exception of the radiation scheme, are used at each location and each timestep.

Radiative transfer

The radiation scheme of an AGCM is likely to incorporate both daily and annual solar cycles. The radiation schemes are, in general, less complex than those incorporated in one-dimensional RC models (see Section 4.3) but are broadly similar. The shortwave and longwave fluxes are, of course, treated separately. For computational economy the radiation scheme is not called at every timestep, but rather only once every 1–3 hours. The radiation fluxes are usually held fixed over the intervening timesteps. Solar radiation is absorbed and scattered by atmospheric gases, clouds and the Earth's surface. Most AGCMs have shortwave radiation schemes which explicitly consider scattering and absorption by clouds as a function of zenith angle (e.g. the Delta–Eddington scheme used in the NCAR Community Atmospheric Model). Scattering properties are usually based on physical characteristics of the cloud, such as liquid water content and droplet size distributions, now sometimes specified differently over land and ocean, although the very early models used specified albedos for clouds (e.g. Table 4.2). The scattering and absorption of solar radiation is typically considered in fewer than 20 or so spectral regions (depending on the GCM). Usually the only gaseous absorbers considered at solar wavelengths are ozone and water vapour, although some models also consider CO_2 and O_2. Models may also include the scattering effects of aerosols in these wavelength regions.

Clouds are diagnosed from the state of the atmosphere, from the values for vertical motion and humidity. Special cases are sometimes constructed for difficult situations such as marine stratocumulus and cirrus anvils. Recently, climate models have begun to use prognostic cloud schemes in an attempt to represent more realistically cloud microphysics and cloud feedbacks in the climate system. The radiative scheme is likely to have to account for the overlap of various cloud layers, but the sides of convective clouds are not usually allowed to interact thermodynamically with the surrounding clouds or air, or to reflect radiation. The radiative fluxes are calculated explicitly from the temperature, humidity, cloud and ozone distributions. Mixing ratios for ozone are either derived from a diagnostic scheme, from prescribed and frequently updated climatological values, or from dynamical chemistry.

The solar constant used in models varies a little among models, with $1370\,\mathrm{W\,m^{-2}}$ being the typical value. If the model is to be used to simulate past climates, then orbital (Milankovitch) variations in the solar radiation are included. The radiation scheme will take into account the effect of reflection of radiation by different surface types (varying spectrally) and the effect of multiple reflections between surface and cloud (important for the energy balance of sea ice and snow).

The treatment of longwave radiation absorption is just as complex as that for shortwave. For example, in one such radiation scheme, seven spectral divisions are used. The first interval includes the 6.3 μm vibration–rotation water vapour band and the far-infrared rotation band of water vapour; a further two intervals include the overlap between water vapour and the 15.0 μm CO_2 absorption bands. The fourth and fifth bands include the effect of the 9.6 μm ozone band and the water vapour continuum.

The emissivities and transmissivities for each gas in each interval at some temperature, e.g. 263 K, are sometimes stored in the computer code as 'look-up tables'. Carbon dioxide is usually assumed to be uniformly mixed and to have a mean concentration of ~330 ppmv (the Atmospheric Model Intercomparison Project (AMIP) used 345 ppmv) and, in 'greenhouse' experiments, this amount is increased. There are many trace gases, such as N_2O, CFCs and CH_4, that may also need to be included in the calculations of infrared absorption. The surface and clouds are sometimes assumed to act as black bodies for longwave calculations, although in some schemes cloud properties are derived from the liquid water or ice content of the cloud and, recently, satellite-derived values of surface emissivity have been incorporated into some models.

Evaluation of the calculated radiative fluxes can be conducted by comparing the computed top-of-the-atmosphere fluxes with those observed by satellites. For example, data from the Earth Radiation Budget Experiment (ERBE; Feb. 1985–89) and the Moderate Resolution Imaging Spectrometer (MODIS) are widely used. Some aspects of model evaluation and intercomparison are considered in Chapter 6.

Boundary layer

The atmospheric boundary layer is the region in which surface friction has a large effect on the flow, typically the lowest kilometre or so. In particular, the near-surface wind is backed from the wind direction in the free atmosphere, creating the Ekman spiral (Figure 5.8a). This layer can also suffer large fluctuations in temperature and humidity (Figure 5.8b) and its depth changes over the diurnal cycle. These features cannot be fully represented in most GCMs, primarily because the vertical resolution is inadequate and the parameterization schemes are unable to produce adequate approximations to the processes involved.

An important characteristic of the boundary layer is its stability. This is calculated in terms of the potential temperature difference, $\Delta\theta(z)$, between the surface and the lowest model level, at height z, and the difference, $\Delta q(z)$, between the saturated specific humidity at the surface temperature and pressure and the specific humidity of the lowest layer. The bulk Richardson number, R_i, is calculated as a function of $\Delta\theta(z)$, $\Delta q(z)$, the temperature of the lowest layer, T, and the wind speed, $V(z)$, of the lowest layer, such that

$$R_i = \frac{gz[\Delta\theta(z) + 0.61T\Delta q(z)]}{TV^2(z)} \tag{5.12}$$

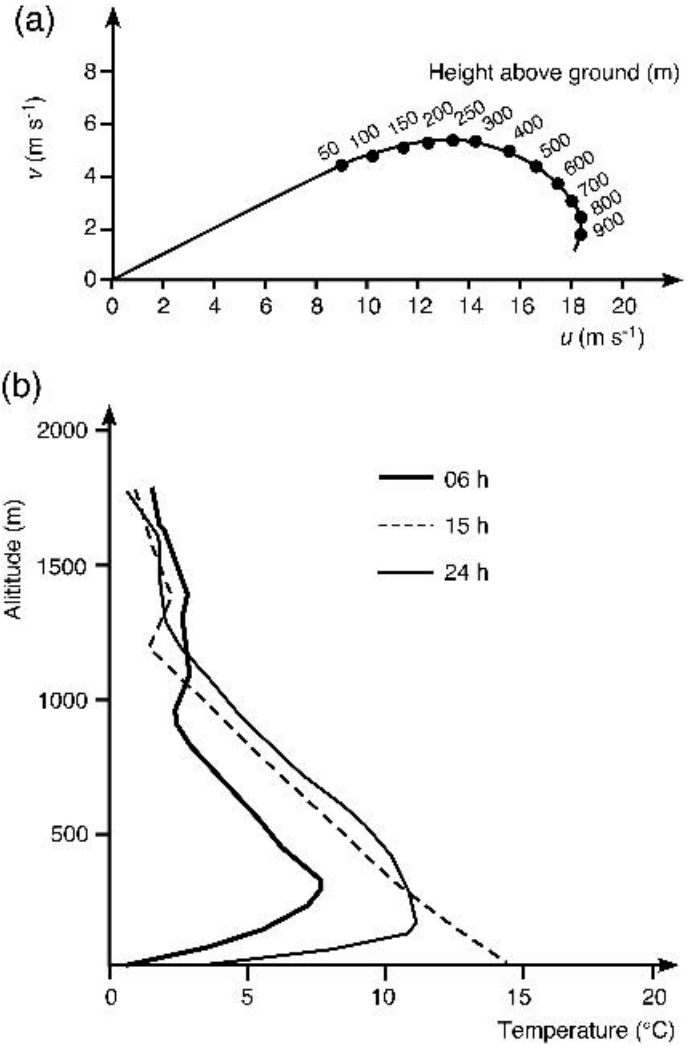

Figure 5.8 (a) The Ekman wind spiral plotted as a function of the two horizontal wind components; (b) a winter diurnal temperature variation in the planetary boundary layer. Typically, neither of these phenomena can be fully represented in GCMs because the vertical resolution in the models near the surface is too coarse

is used in conjunction with a specified surface roughness length to determine the bulk transfer coefficients for momentum, sensible heat and moisture. In AGCMs with a simple land-surface scheme, values of surface roughness are typically about 0.1 m over land and 10^{-4} m over ocean. The surface flux, F_x, of any variable x is given by

$$F_x = -C_x V(z)\Delta x(z) \tag{5.13}$$

where C_x is the bulk transfer coefficient (which could be different for different fluxes) and $\Delta x(z)$ the difference between the value of x at height z and at the surface. The surface fluxes are calculated. The temperature and moisture contents of the surface and lowest atmospheric layer are updated accordingly.

Although a wide range of boundary layer schemes are used in AGCMs, the interaction between the surface and the lowest model layer is similar in all these schemes. They differ in their treatment of the turbulent exchanges between model layers in the boundary layer. The turbulent exchanges between atmospheric layers in the boundary layer are usually modelled using the concept of eddy diffusivity, but higher-order closure schemes are becoming more common. In the eddy diffusivity approach, it is assumed that the turbulent flux F'_x between adjacent model levels is proportional to the vertical gradient of that quantity and is given by

$$F'_x = -K_x(dx/dz) \tag{5.14}$$

where K_x is the diffusion coefficient for property x. The diffusion coefficient above can be expressed as

$$K_x = l^2(dV/dz) \tag{5.15}$$

where V is the horizontal wind speed and l is the mixing length.

Cloud prediction

The cloud amount is important to the radiation scheme, but there is no single, simple law that governs the formation of clouds. The considerable sensitivity of the radiation calculations to the cloud distribution means that cloud–radiation interactions have been recognized as critical to further model development. The early GCMs specified cloud amounts either zonally or globally according to climatological values. Modern climate models diagnose the cloud amount and type from other model variables. Most models have schemes which differentiate between convective clouds and stratiform clouds, relating predictions of the former to the result of the convection scheme and the latter to large-scale condensation. Increasingly, models include prognostic schemes for cloud liquid water and ice and hence are able to calculate cloud optical properties.

Early cloud prediction schemes simply related the cloud amount to the large-scale relative humidity. Such a technique can be as simple as assuming that the cloud cover is 100 per cent for relative humidities above a certain threshold (usually between 80 and 100 per cent) and zero for humidities below this. There have also been schemes where the cloud amount, A_c, was some simple function of relative humidity, RH, such as the quadratic form

$$A_c = \left(\frac{RH - a}{b}\right)^2 \tag{5.16}$$

where a and b are empirical constants. Schemes have also been designed that are more general than this; for example, evaluating cloud on the basis of vertical velocity and atmospheric stability in addition to relative humidity.

The scheme used by the NCAR Community Atmospheric Model diagnoses three types of cloud: convective cloud, layer cloud and marine stratocumulus. Clouds are allowed to form in any layer except the lowest layer, and the minimum fraction for convective cloud is 20 per cent. Marine stratocumulus clouds are diagnosed based on an empirical relationship between cloud fraction and the properties of the atmosphere below 700 hPa. Cirrus anvils are formed when there is outflow above 500 hPa associated with convective activity. Other clouds form based on relative humidity, stability and vertical motion. The different cloud schemes used by different models and the differences in the underlying variables used for prediction results in a situation that is well illustrated by Figure 5.9. The very large differences in cloud distribution among these models (Figure 5.9a) are generally compensated for by assigning different cloud properties and heights. In this way, the top-of-the-atmosphere (Figure 5.9b) and surface radiation fluxes are often much closer in model intercomparisons than the cloud fields themselves.

Many of the difficulties in cloud prediction arise from the requirement for sub-gridscale parameterization: cumuliform clouds are significantly smaller than the grid size of AGCMs and stratiform condensation is likely to occur over smaller vertical distances than the vertical resolution of the AGCM. The difficulties of sub-gridscale parameterization are very hard to overcome, as improvements depend on gaining more detailed observational data and then developing and generalizing relationships. Increasingly, both shortwave and longwave radiative properties of clouds are being calculated as a function of a single variable such as cloud liquid (or frozen) water content. Although the quality of observational data that can be used for validation of models has improved immensely since the start of the International Satellite Cloud Climatology Project in 1985, we still do not have good models for cloud formation that can be incorporated in GCMs and that can couple the radiative and hydrological role of clouds. The role of clouds in climate prediction remains one of the dominant sources of uncertainty.

Convection processes

As discussed in Chapter 4 in relation to radiative–convective models, the thermal structure of the atmosphere that results from purely radiative processes is unstable and would result in convective motion. The major difficulty in modelling the result of this process is parameterizing the sub-gridscale nature of convection. Often convection would be occurring in the real atmosphere over part of a $5° \times 5°$ area but the average conditions would not satisfy the convection criterion. Similarly, the height of penetration of convection may often be less than the vertical distance between AGCM layers. There are very many interactions between, for example, the members of an array of cumulus clouds, and the effects of all these processes must be parameterized. Over the years, several schemes have been developed which

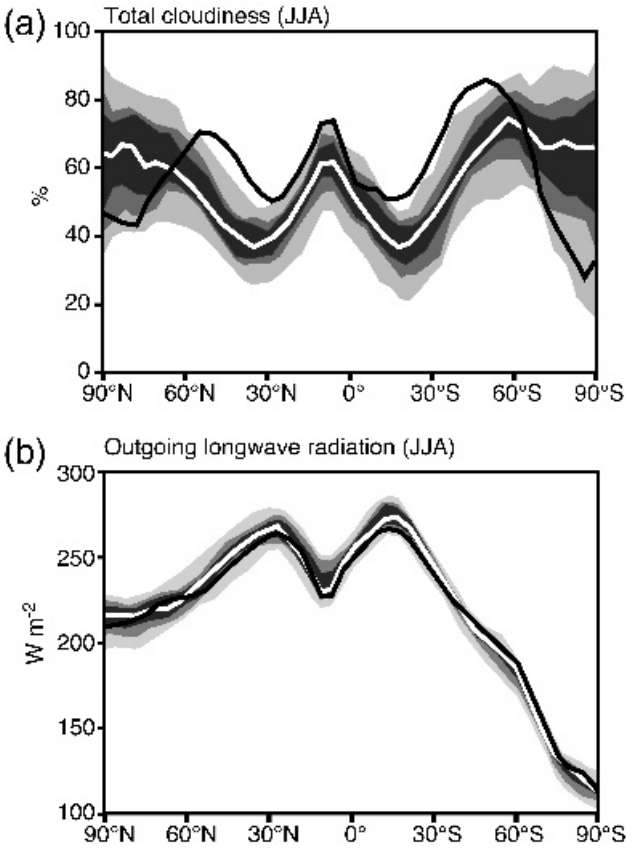

Figure 5.9 (a) Total cloud cover (%) for July from the models participating in the Atmospheric Model Intercomparison Project (AMIP), showing model mean and percentiles at 10, 20, 30, 70, 80 and 90, and observational data from the International Satellite Cloud Climatology Project (ISCCP). (b) As for (a), but for outgoing longwave radiation, with observations from NOAA polar orbiter satellite data. There is much greater agreement between model simulations of outgoing longwave radiation than there is for cloudiness. This is because models have been 'tuned' to match the observed radiation fluxes (reproduced by permission from Houghton *et al*., 1996)

accomplish this process. The earliest scheme, discussed in Chapter 4, is the simplest. This convective adjustment redistributes the energy within the column so that the lapse rate becomes some value assumed to be typical or average. Although the simplicity of this scheme is attractive, the instantaneous adjustment does not allow for the real lifecycle of cumulus clouds. A relatively simple scheme of moist convective adjustment developed at GFDL in the 1960s was the first to produce many of the important features of the global precipitation patterns. Today, more complex schemes are generally employed in three-dimensional atmospheric models.

The Kuo scheme was once popular in climate models because of its relative simplicity. It relates the effects of cumulus convection to the rate of moisture convergence in the whole column. The Kuo scheme assumes that a fraction of the moisture converging into the column is available to moisten the air and the remainder is condensed as rain. It has been largely superseded by various 'mass flux' schemes.

The mass flux approach is based on the notion that the grid box is populated by an array of cumulus clouds with a spectrum of sizes. The mass flux scheme assumes that a 'bulk' cloud can represent the behaviour of these many different clouds. It tries to represent explicitly the fluxes of mass, energy and moisture within the cloud and the downward fluxes outside the cloud. The scheme is attractive because it can be argued to be more physically based and more amenable to increasingly complex treatments. The addition of new treatments like this into climate models must be carefully considered. One modelling group found that including a penetrative convection scheme in their model increased the sensitivity of the model climate (right-hand side of Figure 5.10). It was discovered that the inclusion of the more complex convection treatment required a comparable upgrade in the cloud albedo scheme (left-hand side of Figure 5.10) to avoid a misrepresentation of the climate sensitivity.

One technique that offers potential for significant advance in coupled climate system modelling is termed superparameterization. In superparameterization, a two-

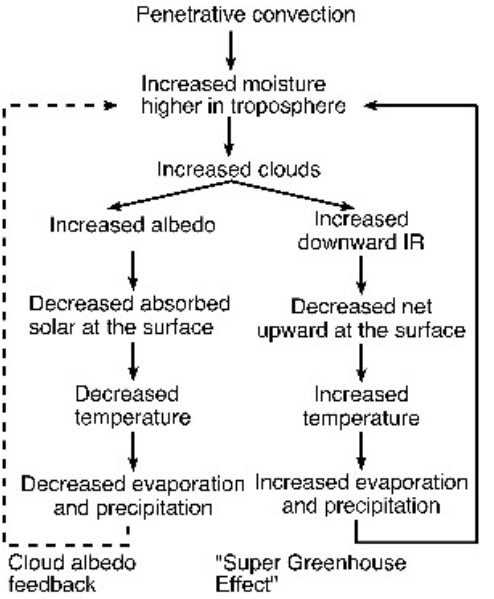

Figure 5.10 Feedback loops associated with enhanced penetrative convection in a global climate model. The right-hand loop results in increased sensitivity of the system through enhanced circulation of moisture, and the left-hand loop results in a decrease in sensitivity due to the enhanced cloud albedo (reproduced with permission from Meehl *et al.* 1995, *Climate Dynamics*, **11**, 399–412. Copyright (1995), Springer)

dimensional cloud-resolving model with a resolution small enough to simulate individual cloud elements is coupled to the GCM at each grid point. A schematic of this implementation is shown in Figure 5.11. Instead of simulating a single cloud covering the entire grid square, this technique allows explicit modelling of fractional cloudiness, cloud overlap and convective organization (such as squall lines). In the simplest case, each cloud system model uses cyclic boundary conditions (left-hand side is 'connected' to the right-hand side) and is independent of its neighbour. More advanced implementations could involve adding a second, perpendicular cloud system model and coupling to cloud system models in adjacent grid boxes in both latitude and longitude. In this latter case, the two-dimensional model almost becomes a three-dimensional cloud-resolving model. It avoids preferential treatment of particular orientations, and cloud features can propagate from one grid element to another. This technique has been shown to improve statistical representation of cloudiness (traditional GCM schemes tend to overestimate the frequency of complete cloud cover compared to observations) and to improve simulation of large-scale dynamical features in the atmosphere and the 30–60-day oscillations seen in the tropics. Breaking the problem into smaller explicit cloud elements means that other parameterization problems, such as cloud microphysics, become more tractable. However, models employing this technique are likely to stretch the capabilities of high-performance computers for years to come. Current implementations

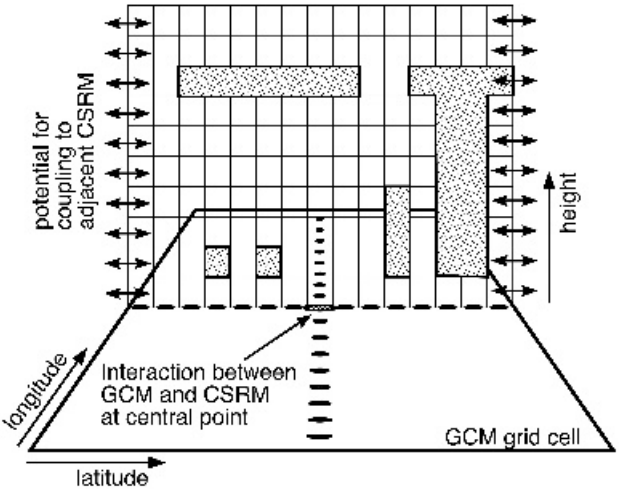

Figure 5.11 The technique of superparameterization involves the embedding of a cloud system resolving model (CSRM) within each grid cell of an atmospheric GCM. The cloud-resolving model can run in an isolated mode, or can be coupled in either or both horizontal dimensions of the larger model grid. The GCM and the cloud-resolving model interact through the mean at the centre of the grid, but many interactions take place in the cloud-resolving model itself, avoiding many of the scaling issues associated with large-scale grid models

are several hundred times slower than the current generation of models and are only practical on massively parallel architectures.

Precipitation

Precipitation (rain or snow) occurs as a function of the available moisture in the model atmosphere. Condensation occurs over a time (sometimes before the onset of saturation) and falls relatively quickly through the atmosphere. If the temperature is below 273 K in a layer into which the precipitation falls, then it is assumed to be snow; otherwise it is liquid. The model precipitation may also interact with the processes in the boundary layer (and be re-evaporated) and has the potential in some situations to interact with a coupled chemistry model to scavenge aerosols from the atmosphere. There are two parts to a precipitation parameterization: first, the gross condensation rate and the energy exchanges associated with the change of state of water from vapour to liquid, and second, the microphysical component, which controls the rate of transfer of vapour to the droplets. Much of the climate model parameterization of precipitation is based on careful observation and modelling of the microphysical behaviour of clouds. Factors such as the availability of condensation nuclei and the rate at which droplets coalesce must be parameterized or specified.

Gravity wave drag

Gravity wave drag is the drag of the mountains on the atmosphere which is manifested in the production of gravity waves. This is illustrated schematically in Figure 5.12. These gravity waves can break in a manner analogous to waves on a beach

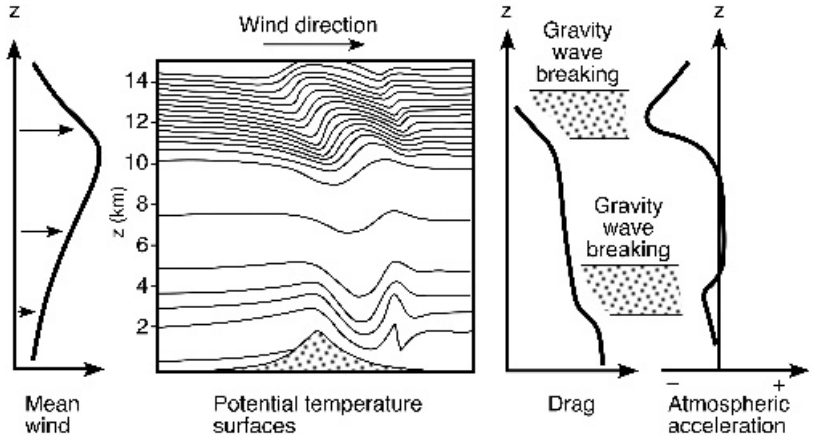

Figure 5.12 Schematic representation of the cause, impact and effect on drag and atmospheric motion of gravity waves induced by an orographic obstacle. Atmospheric gravity waves behave in a manner analogous to water waves in the ocean

and can transfer momentum from the large-scale flow at low levels to the flow at upper levels. Although neglected until the mid-1980s, gravity waves have come to be recognized as an important feature that requires inclusion in order to simulate the global and regional scale circulations. The richness of the gravity wave spectrum considerably complicates attempts to incorporate the effects into GCMs.

5.3 MODELLING THE OCEAN

5.3.1 Background

The ocean is driven mainly by the mechanical forcing of the winds and the net effect on the density and salinity of the water and surface exchanges of heat and moisture. It is confined to the ocean basins and governed by physical laws for the conservation of mass, momentum, energy and other properties. The ocean currents are, as a result of these forcings and the rotation of the Earth, particularly narrow and strong at the western sides of the ocean basins. Many of the properties of the ocean, such as temperature, salinity (salt content), dissolved oxygen and other tracers, have maximum values in the cores of these strong currents. As a consequence of this, the proper representation of transports in an ocean model requires some very detailed calculations and careful assessment of the sensitivities of these transports to modifications in forcing. The challenge for ocean modellers is that many problems, from palaeoclimatic reconstruction to future climate prediction, require the correct simulation of these ocean responses. The modelling of the ocean has, until recently, been in two separate streams. Ocean modellers have striven to model the full three-dimensional nature of the ocean and capture the nature of the currents and the deep circulation. Atmospheric modellers have, on the other hand, progressively constructed 'workable' oceans that act as a boundary condition to their atmospheric models but do not have the physical detail or response of the real ocean.

Thus, the modelling of ocean processes by climate modellers (who historically have mostly concerned themselves with the atmosphere) has been an hierarchical procedure and the coupling of ocean–atmosphere models can be thought of in terms of an hierarchy of oceanic components. The early, simple oceanic representations included the 'swamp' model (Figure 5.13a) with no heat storage capacity and the fixed depth ocean surface layer models (slab models, Figure 5.13b) where there is a heat capacity but no dynamics. The latter has proved useful in helping us to understand the processes acting at the air–sea interface and in providing a means for sensitivity testing of the results of coupled three-dimensional models. For example, utilizing a mixed layer of prescribed depth permits the inclusion of a full seasonal cycle in the atmospheric GCM that is not possible with the oceanic 'swamp'. Despite their limitations, the swamp and slab models were valuable, in times of limited computer capacity, in identifying feedback mechanisms.

The 'mixed layer' or 'slab' ocean model (Figure 5.13b) represents the ocean at each grid point as a slab of water with a prescribed depth, usually between 70 and 100 m. Occasionally the mixed-layer depth may be geographically variable, but it is

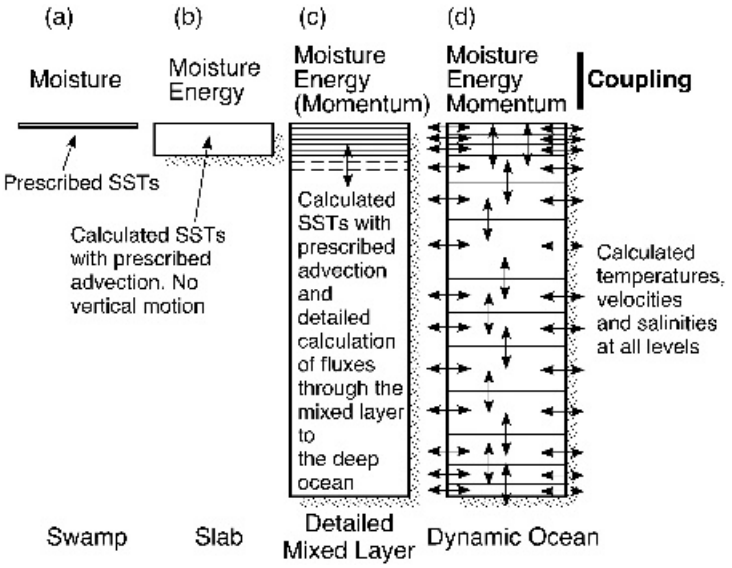

Figure 5.13 Schematic illustration of the level of complexity and coupling associated with various types of ocean model. (a) Swamp ocean with only moisture coupling; (b) a slab ocean with moisture and energy coupling; (c) a diffusive mixed layer model with energy and moisture and some momentum coupling; (d) a full three-dimensional ocean model with momentum, moisture and energy coupling and full three-dimensional interactions in the water column

usually globally homogeneous. The use of a prespecified mixed layer depth without any allowance for horizontal and vertical motion is inadequate for the simulation of the annual cycle of zonal heat storage, especially in the tropics, and most implementations of slab oceans do a very poor job at predicting the temperature and sea ice distributions. The problem is that oceans advect a great deal of energy from the tropics to the poles and sequester heat into the deep ocean. The parameterization of dynamic ocean processes is very limited in slab models but an adjustment of surface fluxes at every ocean point can be used as a surrogate for horizontal energy transfer. Some modellers have been successful in simulating reasonable temperature distributions and seasonality of temperatures and sea ice type using this means of parameterization. However, the nature of predictions that can be made and questions that can be answered with this type of model is limited. For example, their response to enhanced greenhouse gases is simplistic and they can offer no insight into phenomena such as El Niño since this requires coupling of the ocean model to the atmospheric wind field.

The modelling of the mixed layer has been enhanced by some modellers by the use of more complex treatments of the vertical diffusion of heat away from the surface (Figure 5.13c). It has been suggested that these more complex models are appropriate for middle latitudes since the sea-surface temperatures are governed

largely by the local exchanges of heat and mechanical energy in these latitudes, whereas in equatorial latitudes lateral advection of energy needs to be included. These more complex treatments of heat storage in one dimension have also found application in simplified global models such as those discussed in Chapter 3 and in some EMICs described in Chapter 4.

In parallel to the atmospheric modellers developing their hierarchy of 'ocean models' was the development of three-dimensional ocean circulation models using the same principles of fluid dynamics and thermodynamics that had been used for the atmosphere.

The best known type of three-dimensional ocean model was developed at GFDL in the late 1960s (see Chapter 2). The earliest GFDL model was very slow to run and so was reformulated at a lower resolution (5° latitude × 5° longitude). At this resolution, ocean currents were broad and sluggish, but the model became very popular, largely because it was the first, and it is now a standard tool for climate modellers and has been the basis for many other ocean models.

The scale over which ocean currents exist can be described by the internal radius of deformation, which varies from about 100 km in the tropics to less than 10 km in polar regions. The currents meander and produce cut-off features on scales similar to the radius of deformation. These mesoscale eddies, and the way in which they disperse the kinetic energy of the oceans, are difficult to describe theoretically. If currents and eddies are to be described in a numerical model of the ocean, then the grid size of the model must be suitably fine. Ocean models can be used on their own to answer climate questions. For example, Figure 5.14 shows the rate of poleward transport of heat in a model of the Atlantic basin in response to three different prescriptions of the flow of saline water from the Mediterranean through the Straits of Gibraltar. In the extreme case, representing the complete cessation of flow (characteristic of periods when the sea level was much lower, e.g. 18 000 BP), the rate of energy transport by the Atlantic Ocean is greatly reduced.

As computer capabilities have increased, the capacity to include three-dimensional ocean circulation models as components in climate simulation models has developed rapidly. Far from being an 'adjunct' to atmospheric models, ocean models are now becoming another critical component in coupled climate system models. In the next section, we explore the terminology of ocean climate modelling and in Section 5.7 consider how the two disparate systems of ocean and atmosphere can be coupled.

5.3.2 Formulation of three-dimensional ocean models

Like atmospheric models, three-dimensional ocean models have developed along different lines to tackle different problems. The different characteristics of the ocean mean that ocean models are quite different from atmospheric models, despite being based, fundamentally, on similar physics related to energy and mass balance and fluid movement. Ocean models can be characterized in a number of different ways: for example, in terms of spatial scale, whether the model covers the global ocean or a bay or sea. The model may be categorized by the way the surface is treated or by

Figure 5.14 Maximum poleward heat transport simulated by a model of the North Atlantic Ocean under three different conditions of Mediterranean salt input: relaxation to climatology; no input from the Mediterranean; input from the results of a high resolution model of the Mediterranean Sea (reproduced by permission of Thomson Publishing Services from Hecht *et al*., 1996)

the way the vertical co-ordinate is defined. In addition, the formulation of the model determines whether the model treats the dynamics of the ocean or how the model treats density variations.

Co-ordinate system

As with any model, important decisions are made early in the development stage regarding the co-ordinate system that determines how the model will be implemented and how it will perform. The vertical co-ordinate for an ocean model is in many ways a function of the focus of the model. The earliest models, such as the GFDL model, used a simple z co-ordinate system where $z = 0$ at the surface (easy to define when the surface is a rigid lid (Figure 5.15a)). However, the z co-ordinate does not deal well with rapid changes in depth at the ocean edges and various schemes must be implemented to deal with the motion of the ocean at the coasts. It is possible to improve on this by using a co-ordinate system that follows the bathymetry of the ocean basin in a manner similar to the way σ co-ordinates have been used in the atmosphere (Figure 5.15b). Away from the influence of the ocean bottom and from the surface and coasts, the motion of the water in the ocean is largely along constant density surfaces, as waters of different densities 'slide' over or under other layers. This concept leads to the development of isopycnal co-ordinates as in Figure

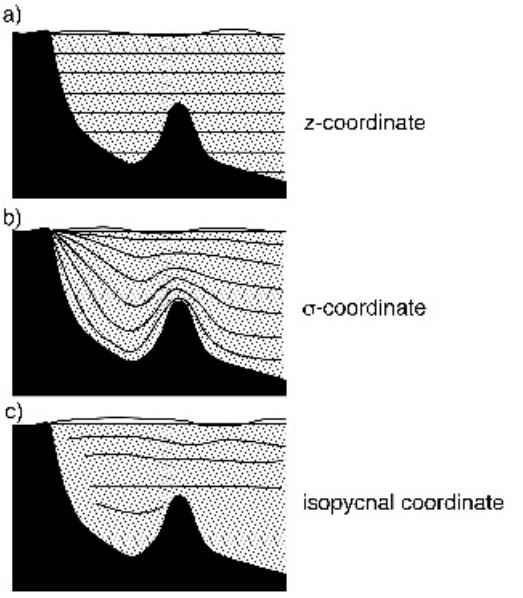

Figure 5.15 Illustration of co-ordinate systems in use in ocean models. No one co-ordinate system is good for all aspects of the ocean. Ocean modellers are working towards hybrid systems, such as are used by atmospheric modellers, to describe the ocean circulation in models better

5.15c. These co-ordinates work best in the open ocean, but face similar problems to the z co-ordinate system when the isopycnal surfaces intersect the ocean bottom.

In the real world, we know that the surface of the ocean moves up and down in response to the winds and tides. There are smaller variations in the height of the surface associated with the ocean currents. The earliest models invoked the idea of an ocean with a rigid lid in order to limit the problems associated with waves travelling on the surface of the ocean. Because large-scale motions such as ocean currents affect the surface profile only slightly, this approximation does not have a great effect on the performance of the model. Modern ocean models, having greater computational power available, as well as the benefit of years of experience with rigid lid models, now have a free surface, and energy can propagate through waves on the surface.

A z co-ordinate model splits the ocean into a 3D array of points like those shown in Figure 5.16. The resolution of the model grid is higher near the boundaries of the ocean basin and the levels are unevenly spaced in the vertical, to allow for more detail near the upper and lower boundaries. The z co-ordinate system is the simplest and best-established, primarily because it was adopted in the first model and valuable experience has been built up over the years with this model. However, there are problems with the isobaric or z co-ordinate system caused by spurious transports

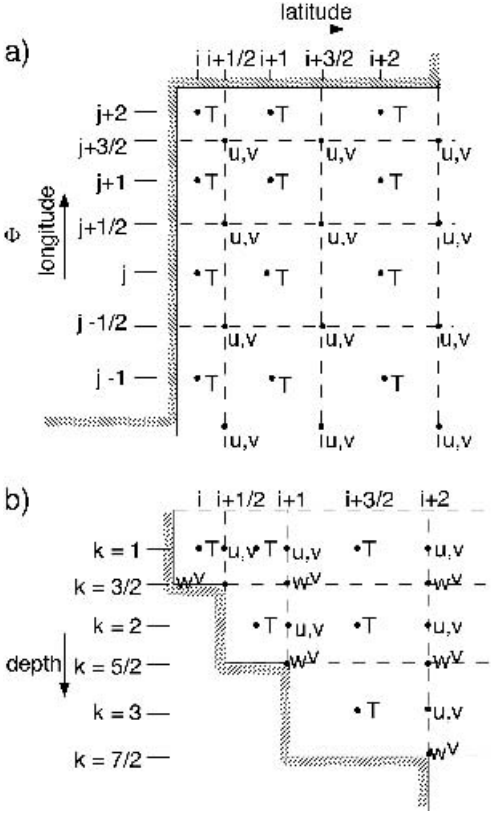

Figure 5.16 Schematic illustration of the calculation grid used in a typical z co-ordinate ocean model (reprinted from Bryan, K., **4**, *J. Comp. Phys.*, pp. 347–376, Copyright 1969, with permission from Elsevier)

across density surfaces. In response to this and other problems with the isobaric formulation, models using the isopycnal co-ordinate system have been developed. Models with isopycnal co-ordinates have the equations of motion formulated on constant density surfaces. In the real ocean, mixing processes are believed to be predominantly across constant density surfaces. The isopycnal co-ordinate system therefore mimics, as much as possible, real structures within the ocean. The isopycnal co-ordinate system has the advantage of formulating the model in a manner that rigorously preserves potential vorticity. On the other hand, problems arise when the thickness of isopycnal layers drops to near zero or when they intersect with the surface. Hybrid co-ordinate systems and model schemes have been developed to overcome some of these problems. Topography is as important for ocean modelling as for atmospheric modelling, with basin geography more important than bottom topography. Successful parameterization of mixing processes is also very important for the success of an OGCM.

The ocean is a turbulent fluid and this turbulence covers a huge range of space- and time-scales. Turbulent mixing on scales of metres and less occurs in waves and on scales of hundreds of kilometres in the case of the baroclinic eddies in Figure 5.17. Some of these processes can be resolved, but others cannot. When ocean models are used for climate studies, the grid size is usually at least $1^\circ \times 1^\circ$. Wave action and the associated interchange with the atmosphere clearly cannot be included explicitly in the models and must be parameterized although the baroclinic eddies associated with ocean currents are a borderline case. Some ocean models with grid spacing of less than 0.2° are able to resolve these (the so-called eddy-resolving or eddy-permitting models) whereas those commonly used as components in coupled climate system models do not. An ocean model must also have some means of distributing the absorbed solar radiation through the surface layers; it must be able to

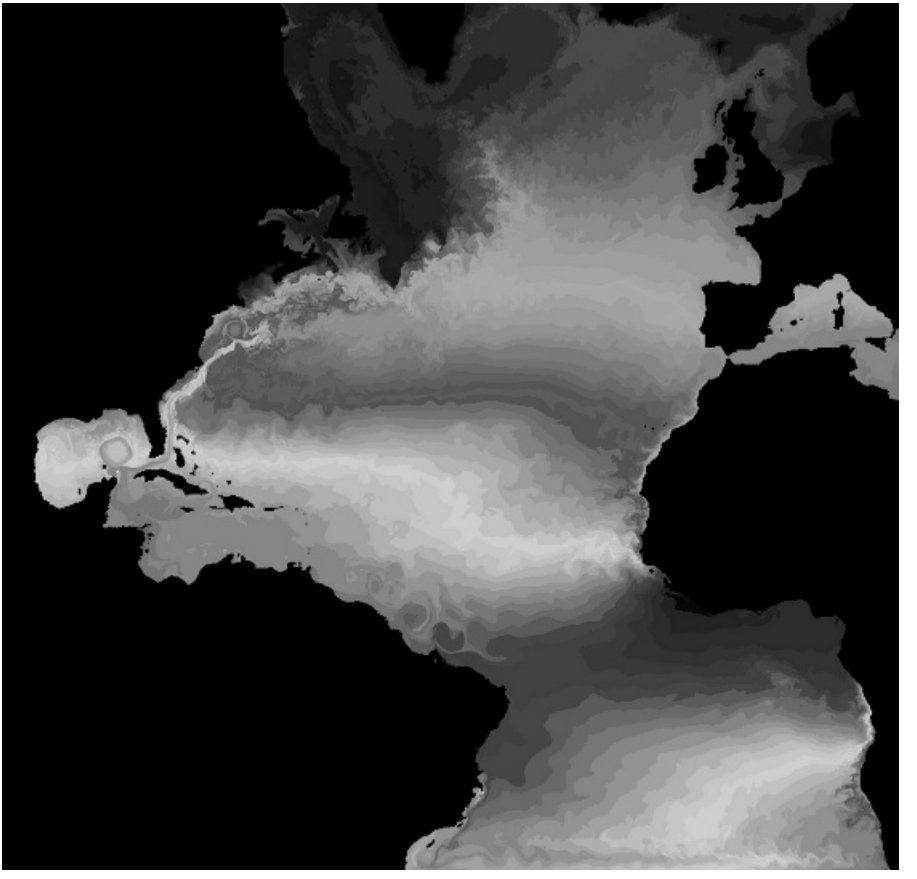

Figure 5.17 Instantaneous picture of surface temperature from a 0.08 degree simulation of the North Atlantic using the Miami isopycnal model (MICOM). This is one frame from an animation included on the Primer CD

Table 5.1 Impact of an ocean eddy mixing parameterization on ^{14}C uptake (reproduced by permission of the American Geophysical Union from Duffy *et al.* (1995), *Geophys. Rev. Lett.*, **90**, 2207–2222)

	Observed	*Original*	*With improved temperatures*
Ocean surface concentration ($\Delta^{14}C$)	154	173	181
Column inventory (10^9 atoms cm^{-3})	9.3	8.4	8.3
Penetration depth (m)	390	348	316

deal with the effect on density of freshwater input from rivers and rainfall, and it must interface with the sea ice model to accept the cold dense water that is created during sea ice formation. These are areas of active research.

Considerable effort in the development of ocean models has been in the adaptation of the model code to make effective use of available computer resources. The combination of small space-scales and long time-scales is a major constraint on ocean modellers; they have been among the first to utilize the latest high-performance architectures and have pushed supercomputer performance to very high levels.

5.3.3 Validating ocean parameterization with ^{14}C isotopic simulation

Modern ocean models need to be able to capture physical processes (e.g. temperature and salinity) and biogeochemistry (e.g. carbon uptake and release). As there is always a danger that modifying a parameterization to improve the physics might worsen the simulation of the biogeochemistry, modellers try to evaluate all aspects of each model improvement.

In the 1990s, ocean modellers were struggling to improve vertical temperature simulations, specifically the thermocline, without disturbing the adequacy of the representation of transient tracer uptake, usually bomb ^{14}C. Vertical diffusivities found to be too low for the ^{14}C uptake were, simultaneously, too high to capture the thermocline properly. This dilemma manifested itself in both 3D models (e.g. GFDL) and 1D box models.

A novel solution proposed by two groups in 1994 involved isopycnal mixing of tracers as part of a new parameterization of sub-gridscale turbulent eddies. This approach improved the vertical temperature predictions in all types of ocean models and was shown to reduce the total vertical penetration of ^{14}C by only about 11 per cent. This combined response can be fully explained since replacing horizontal mixing by isopycnal mixing both reduces convective transport and increases vertical diffusive transport. These two effects tend to balance out in the case of transient tracer transport while improving the temperature simulation. Table 5.1 compares the impact of the new parameterization on simulations of ^{14}C uptake.

5.4 MODELLING THE CRYOSPHERE

The third component of the coupled model in Figure 5.1 is the cryosphere. The most dynamic element of this component model is the polar sea ice. Any complete model

of the climate must of course include prediction of snow cover, sea ice, glaciers and frozen ground. Current climate models attempt to simulate all aspects of the climate system, although the accuracy with which they can do this is limited by several factors. The most important of these for the cryosphere is the very long time-scales associated with some elements (e.g. Table 1.2).

Permafrost is not widely modelled in GCMs, with only a few models having the capability to represent this feature of polar hydrology. The prediction of snowfall depends on the temperature of the layer of the atmosphere through which the precipitation falls. Temperatures below 0°C cause snow to fall. If the surface is above 0°C then the snow melts, cooling the surface and adding to groundwater or runoff. Snow prediction is therefore dependent on the ability of the model to simulate the hydrological cycle and the distribution of surface and air temperatures. The effect of snowfall depends on incorporation of the effect of vegetation and such processes are usually dealt with by the land-surface model. For example, snow falling on tundra can raise the albedo from 0.2 to 0.8, whereas the same snow cover on a dense coniferous forest may not raise the albedo at all in the long term because the forest canopy shades the surface snow. The modelling of snow surface albedos in GCMs differs and thus even similar predictions of snowfall and snow extent could lead to different radiative effects.

The major glaciers of Antarctica and Greenland are represented in GCMs as surface features that extend vertically. Snow falls on to them and is allowed to melt or sublime, but the major mode of ablation of these glaciers, the formation of icebergs, is not represented in GCMs (as discussed in Chapter 3). Temperate glaciers and all glacier dynamics are neglected in GCMs, although some modellers have forced glacier models or models of ice sheets with the output from GCMs.

Sea ice is the primary cryospheric focus for climate modellers when the coupled climate system is modelled. The sea ice cover interacts with both atmosphere and ocean, and must be treated carefully if realistic simulations of the climate system are to be achieved. Even though sea ice occurs in the polar regions, its effects are felt across the globe. Any sea ice model must consist of two components: thermodynamics and dynamics. The earliest model of sea ice formulated for climate studies dealt with only thermodynamic processes. Thermodynamic models use forcing information from the atmosphere and ocean, such as ocean temperature, snowfall rate and air temperature, to predict a growth rate for the ice. Almost the standard formulation for the thermodynamic behaviour of sea ice is known as the Semtner model (named for its author, Bert Semtner). This can be operated in a three-layer or one-layer mode and predicts the accumulation and ablation of the sea ice and overlying snowpack, and predicts temperature in the snowpack and at various levels within the ice. Since it was designed for incorporation in models with only mixed layer oceans, or for use in a standalone mode, the model was one-dimensional. The limited number of layers in the model (Figure 5.18) proved to be an adequate approximation to the more sophisticated multi-layer models of the time. The fractional areal extent of the sea ice can be made to be a function of ice thickness predicted by these models. This allows for the inclusion of the effect of leads and other open areas in

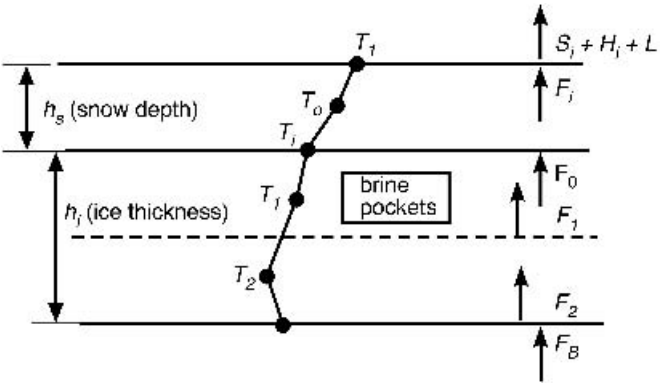

Figure 5.18 One of the simplest sea ice models is the three-layer thermodynamic model of Semtner (1976). The model predicts two ice temperatures and a snow temperature. Typically, the temperature of the underlying ocean is assumed to be constant

the modelled ice-pack. Such a model may also include some formulation of the rate of brine production in the ice. The rejection of brine as sea ice forms results in the sinking of dense water to the deep ocean, driving part of the ocean circulation. The ice feeds back to the atmosphere by cutting down the flow of heat from the ocean and by reducing the amount of energy absorbed at the surface. Even a very thin layer of ice is very effective at reducing heat fluxes from the ocean.

Where dynamic sea ice is included, it is usually based on the 'cavitating fluid' model developed by Greg Flato and Bill Hibler. This model allows ice to be advected across the grid by the wind fields of the AGCM. The dynamics of sea ice are influenced by the winds and ocean currents and by internal stresses in the ice cover, which is formulated as a thin deformable 'plastic' material. As the ice cover is 'stretched', open areas (leads and polynyas) form, which allow more energy transfer from the ocean. As the ice cover is compressed, ridges form, thickening the ice and changing the surface roughness and modifying heat transport. The scale at which these processes happen varies widely. Many processes are too small-scale to be modelled explicitly and need to be parameterized. As the dominant component of the summertime surface energy balance in cryospheric regions is solar radiation, it is essential that the large-scale surface albedo be parameterized correctly.

The albedo of sea ice is predicted variously in GCMs. For example, one parameterization is $\alpha = 0.5$ if latitude $<55°$, $\alpha = 0.7$ if latitude $>66.5°$, with linear interpolation for intermediate locations. If the ice is melting, the albedo is reduced to 0.45 and when the thickness is less than 0.5 m albedo decreases as a square root function of thickness until it equals the albedo of the underlying surface. However, capturing all aspects of a process in a parameterization is difficult to achieve: for example, the sudden decrease observed in Arctic sea ice albedo when melt puddles form does not occur on the Antarctic pack ice. This means that the summertime

decrease of albedo in the Southern Ocean is much less than near the North Pole and, thus, a globally applicable empirical albedo parameterization is hard to develop.

Many of the difficulties associated with the successful incorporation of cryospheric elements into GCMs result from the fact that parameterization depends upon successful prediction of other features such as oceanic heat transports and atmospheric wind fields. The strong influence of oceanic and atmospheric dynamics on sea ice growth and decay in the Antarctic region inhibits successful modelling of these features of the cryosphere. The behaviour of Arctic sea ice is very sensitive to the polar wind field. An example is in the representation of sea ice processes.

The sea ice fraction and thickness around Antarctica, as predicted by the GENESIS model implementation of the Flato and Hibler sea ice model, is shown in Figure 5.19. The vertical growth and decay of the ice in such models is still modelled using the thermodynamic approach developed in the 1970s.

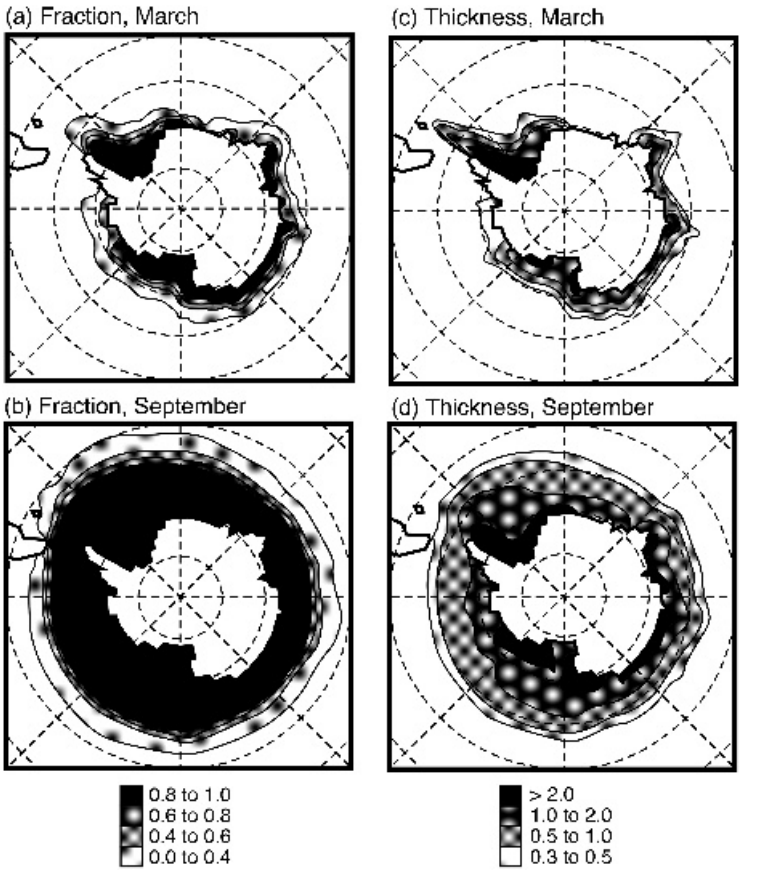

Figure 5.19 Seasonal range of sea ice fraction and thickness for the Antarctic, predicted using the GENESIS global climate model with a dynamic sea ice model

Two further aspects of the climate system are of considerable interest to most GCM modelling groups. The continental vegetation and atmospheric chemistry had been neglected until very recently, but both areas have undergone significant developments in recent years. Both have received increased attention because model simulations of, for example, the effects of increasing atmospheric CO_2 focused interest upon the impacts of water stress, altered growing season length and the addition of greenhouse gas and aerosol emissions from land-use and changed vegetation. In Sections 5.5 and 5.6, some of the recent developments in vegetation parameterization and in coupling ocean and atmospheric models are described.

5.5 MODELLING THE LAND SURFACE

Over 70 per cent of the energy absorbed into the climate system is absorbed by the surface, and experiments with climate models have underlined the sensitivity of the climate to the continental surface hydrology and to the vegetation cover. The treatment of the land surface has changed markedly over the history of climate modelling (Chapter 2). The Budyko or 'bucket' model dates back to 1969. This 'bucket' (Figure 5.20a) has some maximum depth, usually termed by the modellers 'field capacity' (which is not what hydrologists understand by the term). The bucket fills when precipitation exceeds evaporation and, when it is full, excess water runs off. Although a remarkably good approximation in its time, the bucket model has been demonstrated to be inadequate, particularly when the host model includes a diurnal cycle. It is also important to note that runoff in most models does not play any further role in the hydrological cycle of the model, although recently parameterizations of river routing have permitted the computation of fresh water inflow into the ocean basins.

Various modelling studies have identified the importance of the surface hydrology for climatic simulations. For example, Figure 5.21, from a classic paper, shows the considerable impact on rainfall of modifying surface evaporation. In this experiment, evaporation from the land surface was forced to be equal to the potential evaporation (evaporation from a fully moist surface) or set equal to zero at all land-surface points. As can be seen, for the month of July the resulting precipitation is vastly reduced (Figure 5.21b cf. Figure 5.21a). As well as the considerable reduction, there is also a shift in the position of the remaining maxima of rainfall over the continental areas. This experiment, although extreme, suggests that the modelling of evapotranspiration from the land surface may be crucial to the accurate modelling of the global hydrological regime. As schemes for energy and moisture exchanges have become more realistic (Figure 5.20b) a major problem in land-surface modelling is the reconciliation of basin hydrological studies with the resolution typical of general circulation climate models: $3° \times 5°$ grid elements. These difficulties are linked to the problems of 'downscaling' GCM results to smaller areas, a topic discussed in Chapter 6. The second, and equally acute, problem is the dearth of hydrological data with which to initialize and validate global models. Current observational and modelling programmes are making some headway on these

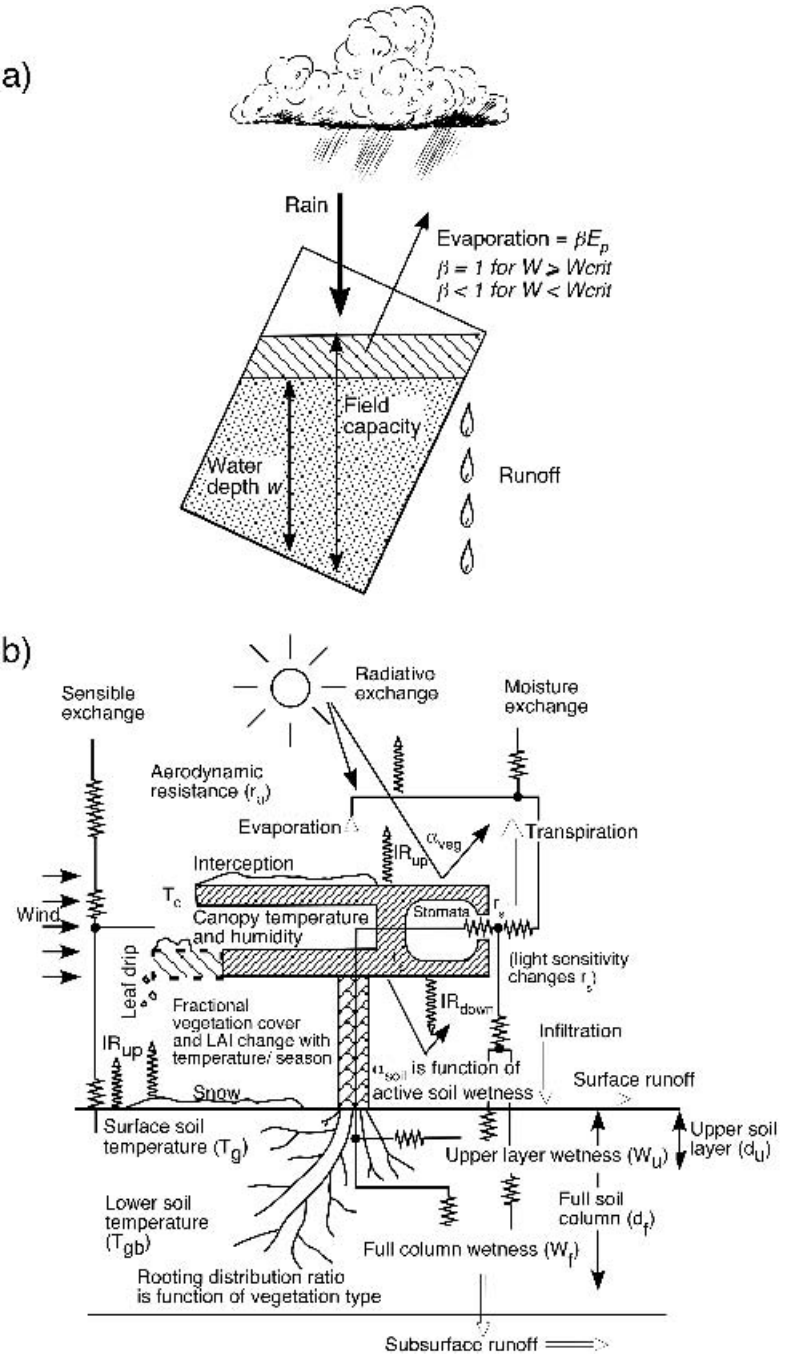

Figure 5.20 (a) Illustration of the simple 'bucket' land surface scheme; (b) an illustration of the processes included in more complex SVATS. This example scheme controls the radiative, latent and sensible heat fluxes occurring at the surface, and models the movement of soil moisture below ground and through the plants

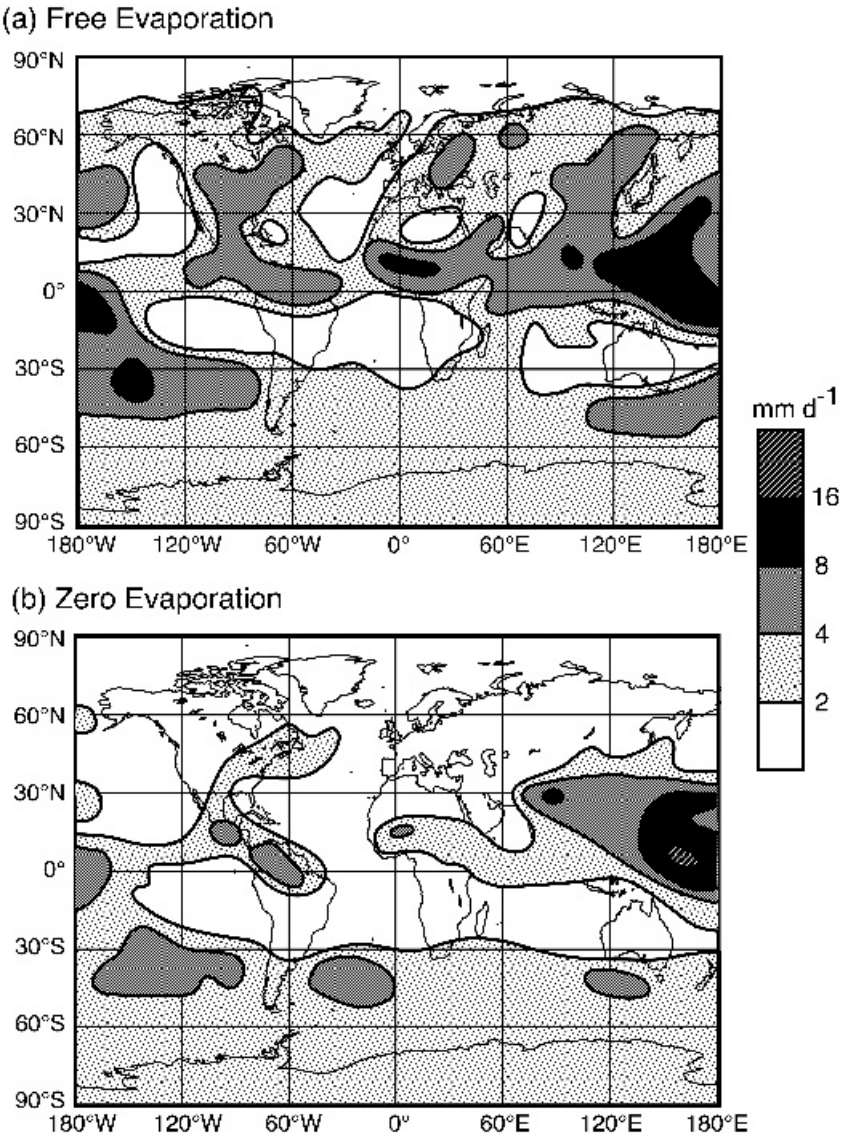

Figure 5.21 The effect on precipitation of reducing to zero the evaporation from the continental land surface as compared with permitting evaporation at the potential rate, as simulated by a general circulation climate model. Results are averaged from the last 30 days of two 60-day 'perpetual July' simulations (after Shukla and Mintz, 1982)

problems. The Project for Intercomparison of Land-surface Parameterization Schemes (PILPS), which is discussed in Chapter 6, has been successful in bringing together land-surface modellers and in fostering the use of datasets for intercomparison and validation.

From being a surface of uniform roughness with very limited hydrological capabilities (e.g. Figure 5.20a), the land surface as represented in GCMs has evolved into a complex subcomponent of the fully coupled Atmosphere–Ocean–Biosphere GCM (AOBGCM). Plants, the dominant component of the land-surface climate, have been modelled using three main strategies: (i) the physically-based approach, which has resulted in the development of complex Soil–Vegetation–Atmosphere Transfer Schemes (known generically as SVATS (e.g. Figure 5.20b)); (ii) biogeochemical models of vegetation and soil processes which emphasize exchanges of carbon, nitrogen, phosphorus and sulphur, and (iii) equilibrium biospheric prediction models, which either define the nature of an 'equilibrium' vegetation based on a simple classification scheme or use succession models to simulate the nature of a biome as a combination of species, all of which have different growth functions. These different scheme types therefore emphasize (i) energy and moisture exchanges over time periods of minutes to months, (ii) chemical storage and exchange over time periods of months to decades, and (iii) ecosystem dynamics over very long time periods of decades to millennia. Current models of the land surface are beginning to include the effects of 'sub-gridscale' patches of different land type, while river routing models are now being used to 'drain' runoff into oceans. These strategies, developed from very different positions, are only recently beginning to converge to meaningful models of the biosphere and its response to, and role in, the climate system.

5.6 ATMOSPHERIC CHEMISTRY

In the same way as climate modellers once thought of the vegetation and ocean as fixed boundary conditions for the atmosphere, we also used to consider the chemical composition of the atmosphere as fixed. Greenhouse warming is the most dramatic proof of the folly of this assumption, but stratospheric ozone depletion and the chemistry of radiatively active aerosols also underline the risks for modelling of holding global atmospheric composition fixed. Furthermore, when subtle feedbacks and anthropogenic effects are to be considered, the range of chemical reactions in the atmosphere of importance to climate simulations expands greatly. These days, the important chemical links between CFCs, O_3 (ozone) and ultraviolet radiation in the stratosphere are well known, but there are many other species of importance. Emissions of sulphur from biomass and burning of fossil fuel are the starting points for the formation of aerosols, a factor so 'unknown' as to be neglected in our analysis of forcings in Chapter 1. Plants photosynthesize and respire, as well as emitting various hydrocarbons to the atmosphere, while the decay of dead organic matter produces methane. Each of these chemical species has a characteristic lifetime in the atmosphere, determined by the various reactions involved in production and destruction of the species.

The OH radical, a single oxygen ion combined with a hydrogen ion, is an interesting example of a chemical subsystem of importance in climate modelling. The OH radical reacts quickly with the species in Table 5.2 to begin the complex process of cleansing the atmosphere. The simplest reaction is the oxidation of carbon monoxide (CO) such that:

$$CO + OH \rightarrow CO_2 + H$$

$$H + O_2 + (\text{inert molecule}) \rightarrow HO_2 + (\text{inert molecule})$$

$$HO_2 + HO_2 \rightarrow H_2O_2 + O_2$$

or

$$HO_2 + NO \rightarrow OH + NO_2$$

$$HO_2 + O_3 \rightarrow 2O_2 + OH$$

Additionally, the hydrogen peroxide produced may be removed by deposition or photolysed, generating more OH:

$$H_2O_2 + \text{light} \rightarrow 2OH$$

or

$$H_2O_2 + OH \rightarrow H_2O + HO_2$$

Table 5.2 Atmospheric lifetimes of selected species important in climate models (after Jacob, 2003)

Species	*Lifetime*	*Relevance*
CH_3CCl_3	4.8 y	Halogenated hydrocarbon. Important for the infrared absorption and for stratospheric chemistry associated with the 'ozone hole'
CH_4	8.4 y	Methane: a greenhouse gas produced by decay of organic material (e.g. rice paddies and ruminants)
CHF_2Cl	11.8 y	Halogenated hydrocarbon
CH_3Br	0.7 y	Halogenated hydrocarbon
Isoprene	~1 h	A complex hydrocarbon emitted by vegetation
CO	2 mo	Carbon monoxide, a product of incomplete combustion of fossil fuels or biomass
$NO_y(NO + NO_2)$	~1 d	Nitrogen oxides, a product of incomplete combustion of fossil fuels or biomass
SO_2	~1 d	Sulphur dioxide, a product of incomplete combustion of fossil fuels or biomass
$(CH_3)_2S$	~1 d	Dimethyl sulphide, produced naturally by marine phytoplankton

Each species tracked by an atmospheric chemistry model must have a set of possible pathways mapped out as reactions, as shown above. Reactions take place at rates determined by the concentrations of the species in question, so each chemical species and intermediate product must be tracked at all stages in the model. As well as including additional variables, the timestep of the chemical model must be appropriate to the reactions. Chemical models have been applied to the sulphur cycle, to track the production of aerosols, to the O_3 cycle and to the production and dissipation of CO in the atmosphere.

Some GCMs now include a limited number of chemically reactive species (typically five to ten) but the computationally efficient EMICs (see Chapter 4) can invest time in much more detailed reactive chemistry. One of the EMICs listed in Table 4.1 includes 43 different species.

5.7 COUPLING MODELS: TOWARDS THE PREDICTIVE EARTH SYSTEM MODEL

The notion of coupling models in the manner of Figure 5.1 is not new. The nature of climate model construction has been that of a *de facto* modular approach. Modellers constructed routines to deal with clouds, land-surface processes, ocean thermal response and sea ice. The complexity of the schemes is now rivalled by the complexity of the coupling.

Land-surface models, for example, have grown from very simple schemes to the exceedingly complex SVATS discussed in Section 5.5. These are coupled closely with the atmospheric model and exchange fluxes every timestep. On longer timescales, modellers are beginning to use schemes to predict the characteristics of the vegetation and soils and the exchanges of chemical elements. The time-scales of coupling range from minutes to millennia.

A very important coupling is that between atmosphere and ocean models. In early climate models, the atmosphere was driven by prescribed climatological sea-surface temperatures and sea ice distributions. Most climate predictions of the early 1980s were based on atmospheric models with prescribed (seasonally varying but present-day) sea-surface temperatures and sea ice. By the late 1980s, mixed layer ocean models were used in which the meridional energy transport of the oceans was prescribed at present-day values. This latter approach allows the temperature of the ocean to change in response to changed forcings (such as enhanced CO_2) but clearly constrains the simulation by prescribing present-day transports. The full ocean system with deep ocean processes as well as those in the upper mixed layer is now included in three-dimensional climate models.

The difficulties inherent in ocean–atmosphere coupling are identified in Figure 5.22. This diagram underlines the different response times associated with the atmosphere and the ocean subsystems, and emphasizes that the ocean subsystem spans a greater range in both time and space than the atmospheric subsystem.

The considerable discrepancy in response (or equilibration times) of the atmosphere and the ocean including the deep ocean have already been described (see

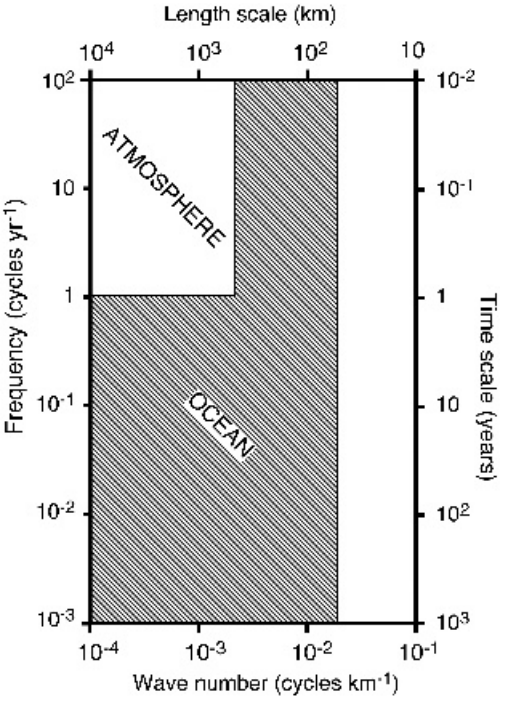

Figure 5.22 The range of significant horizontal wavenumbers and frequencies in climate models of the atmosphere and ocean. The lowest frequency is determined by the thermal relaxation times of the subsystem and the highest by gravity waves. The lowest wavenumber is determined by the planetary scale and the highest by the radius of deformation of the subsystem medium. The inverse of the scales gives the more familiar time and length scales. Note that the ocean spans a greater range of both fundamental scales than the atmosphere

Section 1.3, especially Table 1.2). Since the time to reach equilibrium is much longer for the ocean than for the atmosphere, linking of an ocean model with an atmospheric model is challenging. Ideally the linkages should be between the thermodynamic systems, among the variables represented in the equations of motion and in terms of the parameters and variables of the water cycle (Figure 5.23).

The difference in response time between atmosphere and ocean means that for effective use of computer resources, the models are not always run in a continuously coupled mode; rather, they are coupled asynchronously. An example coupling scheme is shown in Figure 5.24a. Each component of the coupled model can only communicate with the coupler, and sends or receives a bundle of model fields in each communication. The coupler controls the flow of data and separate models are kept 'informed' of the other models at regular intervals. Models can also be configured to interact directly with each other. In Figure 5.24b, an ocean model and an atmospheric model are coupled asynchronously. Initially, atmosphere and ocean are

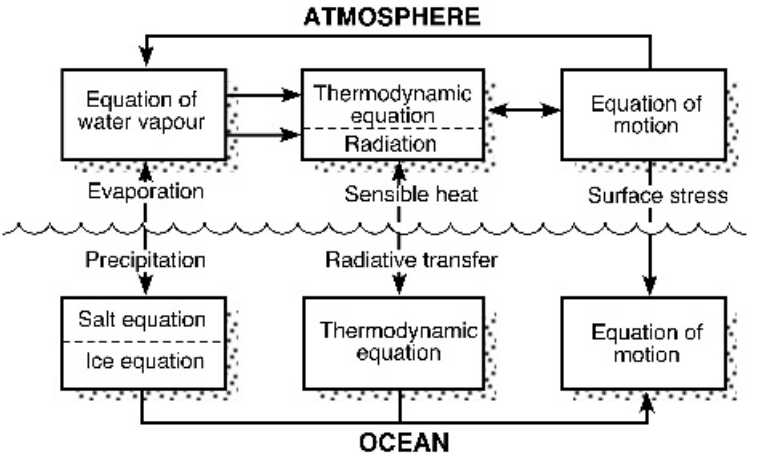

Figure 5.23 Box diagram showing the major components of a joint ocean–atmosphere model and the interaction among the components (reprinted from *Dynamics of Atmosphere and Ocean*, **3**, Manabe *et al.*, pp. 103–133. Copyright 1979, with permission from Elsevier)

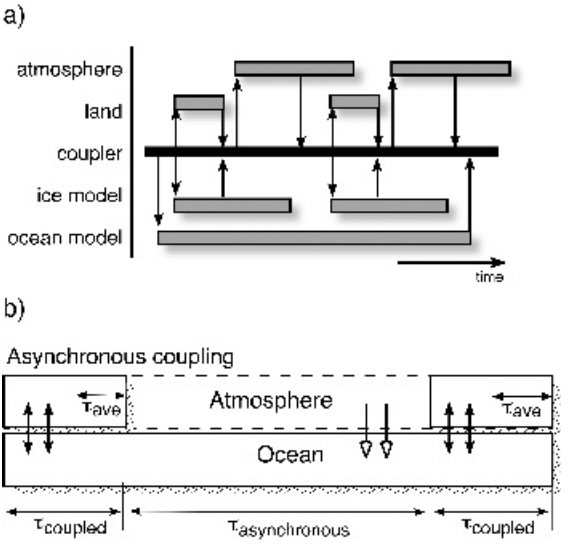

Figure 5.24 (a) A flux coupler acts to control the flow of information between components of a coupled climate system model. The vertical arrows indicate messages passing between component and coupler, with each component only communicating with the coupler and not with the other modules. (b) An illustration of a more direct and less flexible asynchronous coupling between an atmospheric GCM and an oceanic GCM. The models are run together for only a short fraction of the total integration time. Most of the integration involves running the ocean model with only mean forcing information from the atmosphere

run together, fully coupled for a period given by $\tau_{coupled}$. The latter part of this period, τ_{ave}, is used to derive an average atmospheric climate with which to force the ocean model during the $\tau_{asynchronous}$ period. During this second period, the atmospheric model is not operated. The cycle is then repeated. This saves considerable amounts of computer time since the cost of computing the atmospheric model is typically many times that of the ocean model per year. In the GENESIS asynchronous coupling, $\tau_{coupled}$ is around 15 years, τ_{ave} is around 10 years and $\tau_{asynchronous}$ is around 85 years.

Another problem associated with modelling the ocean is that the response time of the deep ocean to climate changes is several thousand years. To avoid running the entire model for thousands of years to 'spin up' the deep ocean, a technique called 'distorted physics' is used. The specific heat capacity of the deep ocean water is reduced by a factor of up to 10 so that the deep ocean temperatures respond more rapidly than the surface layers (an analogous distortion is applied to salinity). These alterations distort the dynamical behaviour of the ocean to some extent, so that at the end of a long 'distorted physics' run, a period of several decades without distorted physics is needed. Typical results from such a coupled model are shown in Figure 5.25 – in this case the model is Version 0 of the NCAR Community Climate Model. In this June–July–August cross-section of the atmosphere and ocean, the

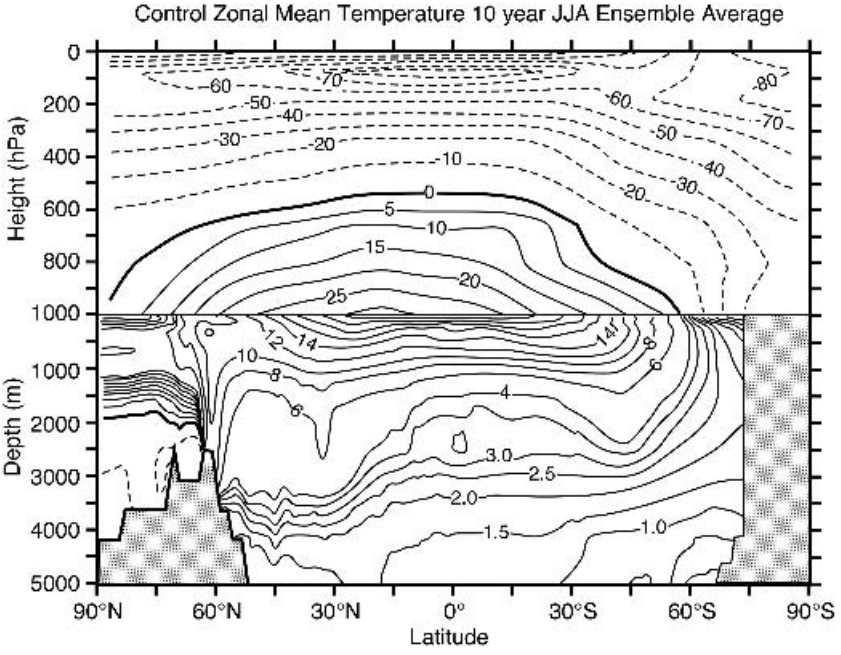

Figure 5.25 Zonal mean cross-sections of vertical temperatures in the atmosphere and ocean from an ensemble average over June–July–August (JJA) from a coupled ocean–atmosphere model (CCM0)

cold deep waters in the Arctic are clearly shown, as is the variation in mixing depths with latitude.

Climate drift and flux correction

On a local scale, the fluxes between the atmosphere and ocean are such that the ocean is warmed in the summer and cooled in the winter. The coupling of ocean and atmospheric models can highlight discrepancies in the fluxes calculated by the two models. A good estimate of the difference between two large and similar numbers is not easily obtained. Because the relative errors in this resultant forcing are large, they can cause problems in the ocean circulation. Some modellers have chosen to apply flux adjustments to their coupled model in order to prevent the climate drifting from present conditions. Other modellers prefer to run long climate simulations without the aid of such adjustments, but have had to accept a drift in climate. As coupled models have developed, the problem of flux correction is becoming less. The model in Figure 5.25, which has no flux corrections, exhibits little, if any, drift, but is consequently left with some significant systematic errors in the simulation compared with observations. Although the process of flux adjustment has been viewed sceptically in some quarters, it, and the alternative of climate drift, should be thought of as a necessary stage in the process of model development and improvement. The need for flux adjustment will continue to lessen as model components are improved.

The 'cold start' phenomenon

The use of fully coupled climate models, because of the complications associated with 'cold start' and 'climate drift', necessitates careful attention to the impact of the coupling process itself. Normally, model simulations of the effect of changing carbon dioxide concentrations are thought of as changes with respect to the 'present day'. If we start a coupled model from present-day (say 1990) conditions and apply forcing to the model as shown in Figure 5.26a, then, because of the thermal inertia of the oceans, the warming rate is low at first (Figure 5.26b). As the forcing in the real world has been applied since before 1900, that period of slow warming has passed. If model simulations do not account for this prior warming, then the projected warming path will be different. This slow initial warming is known as the 'cold start' phenomenon. Models must therefore simulate this earlier period if they are to provide realistic responses to perturbations.

Model complexity comes full circle: using 'MAGICC'

Throughout this book, we have stressed that there is no one 'best' climate model type and have tried to underline the continuing benefits from exploiting a variety of models. This truth has been demonstrated in the assessments of the IPCC's Working Group 1. Its reports employed a methodology in which a large number of results

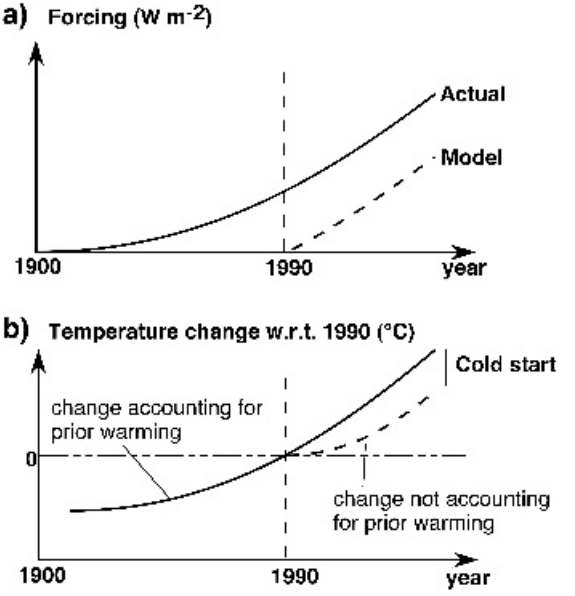

Figure 5.26 (a) The forcing applied to a model which starts running in 1990 matches the slope of the actual forcing which began before 1900. (b) The sequestration of heat by the oceans results in a slow start ('cold start') to the model warming (w.r.t., with regard to)

were generated with the characteristics of fully comprehensive models but using a simple model to undertake the simulations.

The 'MAGICC' model is a box model comprising an upwelling–diffusion ocean component and an EBM atmosphere which, for IPCC use, is tuned to a number of fully comprehensive (AOGCM) climate models (Table 5.3). Once tuned, this box model is used to compute the temperature changes that would be predicted by the fully coupled models for a large number of forcing scenarios. The range in MAGICC

Table 5.3 Some of the MAGICC climate model parameters used in the IPCC Third Assessment tuning (after Houghton *et al.*, 2001)

AOGCM	*Radiative forcing for 2 × CO_2* (W m^{-2})	*Climate sensitivity* (°C)	*Warming causing collapse of THC* (°C)	*Vertical ocean diffusivity* (cm^2 s^{-1})
GFDL	3.71	4.2	8	2.3
CSIRO	3.45	3.7	5	1.6
Had CM3	3.74	3.0	25	1.9
Had CM2	3.47	2.5	12	1.7
ECHAM4/OPYC	3.80	2.6	20	9.0
CSM	3.60	1.9	–	2.3
DOE PCM	3.60	1.7	14	2.3

parameters also illustrates one measure of diversity in fully comprehensive models.

This means of reducing the total computation effort required while maintaining as wide a range of predicted outcomes as possible is especially important for exercises like the IPCC for which many different future scenarios of forcing and mitigation need to be investigated.

5.8 EARTH SYSTEM AND CLIMATE MODELS

As suggested in Figure 1.5, the next generation of models may include subsystems never before considered in climate models but required in Earth System Modelling. It seems likely that the same principles will apply to the design, testing and use of these models as have been used to develop today's climate models. The concepts of different time-scales and subsystem equilibration times introduced in Chapter 1 are critical to the effective use and appropriate interpretation of results. Three-dimensional climate models have developed over the years to form vital tools in studies of the climate and Earth system.

In Chapter 6 we will look briefly at some of the technical support systems that have been developed for coupled climate models, and we will examine some examples of how such models can be used to evaluate possible regional-scale impacts associated with tropical deforestation, predict the impact of changes in greenhouse gases, and analyse palaeoclimates. This range of applications of climate models and the diversity and complexity of the models have led to a set of projects aimed at the coordination, validation and interpretation of model results. These are also discussed in Chapter 6.

RECOMMENDED READING

Boer, G.J., McFarlane, N.A., Laprise, R., Henderson, J.D. and Blanchet, J-P. (1984) The Canadian Climate Centre spectral atmospheric general circulation model. *Atmos.-Ocean* **22**, 397–429.

Briegleb, B.P. (1992) Delta–Eddington approximation for solar radiation in the NCAR Community Climate Model. *J. Geophys. Res*. **97**, 7603–7612.

Bryan, K. (1969) A numerical method for the study of the world ocean. *J. Comput. Phys*. **4**, 347–376.

Cess, R.D., Zhang, M.H., Minnis, P., Corsetti, L., Dutton, E.G., Forgan, B.W., Garber, D.P., Gates, W.L., Hack, J.J., Harrison, E.F., Jing, X., Kiehl, J.T., Long, C.N., Morcrette, J-J., Potter, G.L., Ramanathan, V., Subasilar, B., Whitlock, C.H., Young, D.F. and Zhou, Y. (1995) Absorption of solar radiation by clouds: observations versus models. *Science* **267**, 496–499.

Collins, W.D., Hack, J.J., Boville, B.A., Rasch P.J., Williamson, D.L., Kiehl, J.T., Briegleb, B., McCaa, J.R., Bitz, C., Lin, S-J., Rood, R.B., Zhang, M. and Dai, Y. (2003) Description of the NCAR Community Atmosphere Model (CAM2). Available from www.ccsm.ucar.edu.

Deardorff, J. (1978) Efficient prediction of ground temperature and moisture with inclusion of a layer of vegetation. *J. Geophys. Res*. **83**, 1889–1903.

Dickinson, R.E. (1984) Modelling evapotranspiration for three-dimensional global climate models. In J.E. Hansen and T. Takahashi (eds) *Climate Processes and Climate Sensitivity*, Geophysical Monograph 29, Maurice Ewing Vol. 5, Amer. Geophys. Union, Washington DC, pp. 58–72.

Dickinson, R.E. (1995) Land processes in climate models. *Rem. Sens. Env*. **57**, 27–38.

Dickinson, R.E., Henderson-Sellers, A. and Kennedy, P.J. (1993) Biosphere/atmosphere transfer scheme Version 1e (BATS1e) as coupled to the NCAR community climate model, NCAR Technical Note TN–387+STR.

Eagleson, P.S. (ed.) (1982) *Land Surface Processes in Atmospheric General Circulation Models*. Cambridge University Press, Cambridge, 560 pp.

Gordon, C.T. and Stern, W.F. (1982) A description of the GFDL global spectral model. *Mon. Wea. Rev*. **110**, 625–644.

Griffies, S. (2004) *Fundamentals of Ocean Climate Models*. Princeton University Press, Princeton, 503 pp.

Griffies, S.M., Böning, C., Bryan, F.O., Chassignet, E.P., Gerdes, R., Hasumi, H., Hirst, A., Treguier, A-M. and Webb, D. (2000) Developments in ocean climate modelling. *Ocean Modelling* **2**, 123–192.

Flato, G.M. and Hibler, W.D. III (1992) Modelling sea ice as a cavitating fluid. *J. Phys. Oceanogr*. **22**, 626–651.

Hack, J.J. (1993) Parameterization of moist convection in the NCAR Community Climate Model (CCM2). *J. Geophys. Res*. **99**, 5551–5568.

Hansen, J., Russell, G., Rind, D., Stone, P., Lacis, A., Lebedeff, S., Ruedy, R. and Travis, L. (1983) Efficient three-dimensional global models for climate studies: Models I and II. *Mon. Wea. Rev*. **111**, 609–622.

Jacob, D.J. (2003) The oxidizing power of the atmosphere In T. Potter, B. Colman and J. Fishman (eds) *Handbook of Weather Climate and Water*. John Wiley & Sons, Chichester, 974 pp.

Manabe, S. and Bryan, K. (1985) CO_2 induced changes in a coupled ocean–atmosphere model and its palaeoclimatic implications. *J. Geophys. Res*. **90**, 1689–1707.

Manabe, S., Bryan, K. and Spelman, M.J. (1979) A global ocean–atmosphere climate model with seasonal variation for future studies of climate sensitivity. *Dyn. Atmos. Oceans* **3**, 393–426.

Matthews, E. (1983) Global vegetation and land use: New high-resolution databases for climate studies. *J. Clim. Appl. Meteor*. **22**, 474–487.

Meehl, G.A. (1990) Development of global coupled ocean–atmosphere general circulation models. *Clim. Dynam*. **5**, 19–33.

Mintz, Y. (1984) The sensitivity of numerically simulated climates to land-surface boundary conditions. In J.T. Houghton (ed.) *The Global Climate*, Cambridge University Press, Cambridge, pp. 79–106.

Mitchell, J.F.B., Davis, R.A., Ingram, W.J. and Senior, C.A. (1995) On surface temperature, greenhouse gases and aerosols: models and observations. *J. Climate* **10**, 2364–2386.

Ramanathan, V. (1981) The role of ocean–atmosphere interactions in the CO_2 climate problem. *J. Atmos. Sci*. **38**, 918–930.

Randall, D.A., Ringler, T.D., Heikes, R.P., Jones, P. and Baumgardner, J. (2002) Climate modeling with spherical geodesic grids. *Computing in Science and Engineering* **4**(5), 32–41.

Rasch, P.J. and Williamson, D.L. (1990) Computational aspects of moisture transport in global models of the atmosphere. *Quart. J. Roy. Met. Soc*. **116**, 1071–1090.

Sellers, P.J., Mintz, Y., Sud, Y.C. and Dalcher, A. (1986) A Simple Biosphere model (SiB) for use with general circulation models. *J. Atmos. Sci*. **43**, 505–531.

Semtner, A.J. (1995) Modelling ocean circulation. *Science* **269**, 1379–1385.

Shukla, J. and Mintz, Y. (1982) Influence of land-surface evapotranspiration on the Earth's climate. *Science* **215**, 1498–1501.

Siedler, G., Church, J. and Gould, J. (eds) (2001) *Ocean Circulation and Climate: Observing and Modelling the Global Ocean.* Academic Press, New York, 640 pp.

Simmons, A.J. and Bengtsson, L. (1988) Atmospheric general circulation models: their design and use for climate studies. In M.E. Schlesinger (ed.) *Physically Based Climate Models and Climate Modelling*. Proceedings of a NATO ASI, Reidel, Dordrecht, pp. 23–76.

Slingo, A. (1989) A GCM parameterization for the shortwave radiative properties of water clouds. *J. Atmos. Sci*. **46**, 1419–1427.

Taylor, M., Tribbia, J. and Iskandarani, M. (1997) The spectral element method for the shallow water equations of the sphere. *J. Comp. Phys*. **130**, 92–108.

Washington, W.M. and Parkinson, C.L. (2004) *An Introduction to Three-Dimensional Climate Modelling*. University Science Books, Mill Valley, California.

Washington, W.M., Semtner, A.J. Jr., Meehl, G.A., Knight D.J. and Mayer, T.A. (1980) A general circulation model experiment with a coupled atmosphere, ocean and sea ice model. *J. Phys. Oceanog*. **10**, 1887–1908.

Wells, N.C. (1979) A coupled ocean–atmosphere experiment: the ocean response. *Quart. J. Roy. Meteor. Soc*. **105**, 355–370.

Wilson, M.F. and Henderson-Sellers, A. (1985) Land cover and soils data sets for use in general circulation climate models. *J. Climatol*. **5**, 119–143.

Web resources

http://www.metoffice.com/research/hadleycentre/index.html	The Hadley Centre
http://www.gfdl.noaa.gov/oceanic.html	GFDL Geophysical Fluid Dynamics Laboratory
http://www.ccsm.ucar.edu/	National Center for Atmospheric Research, CCSM Project
http://aom.giss.nasa.gov/code.html	GISS Atmosphere–Ocean model
http://www.mpimet.mpg.de/	Max Planck Institute for Meteorology
http://mitgcm.org/	The MIT GCM
http://www.meteo.fr	Météo France
http://www.ecmwf.int	European Centre for Medium-Range Weather Forecasts
http://www.dkrz.de	German Climate Research Centre
http://www.bom.gov.au/bmrc/	Australian Bureau of Meteorology Research Centre
http://www.dar.csiro.au/	CSIRO Australia, Atmospheric Research

CHAPTER 6

Practical Climate Modelling

Scenario . . . 'a sketch, outline, or description of an imagined situation or sequence of events; esp. (a) a synopsis of the development of a hypothetical future war, and hence an outline of any possible sequence of future events; (b) an outline of an intended course of action; (c) a scientific model or description intended to account for observable facts. The over-use of this word in various loose senses has attracted frequent hostile comment'.

Oxford English Dictionary,
Compact Edition (OED, 1992, p. 1669).

6.1 WORKING WITH CLIMATE MODELS

It is clear from the preceding chapters that there is a wide variety of climate models with different characteristics and different applications. Even within one particular climate model type (e.g. three-dimensional models) there are many different features and stages of development. Moreover, because climate models share a commonality of purpose, it is possible, and often useful, to apply different climate model types to the same prediction task. The result of this profusion of model types and model characteristics is a bewildering array of models and model predictions. This array of predictions and predictive capability, combined with the continuing role of computer technology in model development, has prompted the climate modelling community to undertake a number of different initiatives that formalize some previously *ad hoc* practices. The community has developed a range of data interchange standards, has begun to generate a framework for the development of climate system models, and has initiated a series of model intercomparisons and evaluations of performance. As well as understanding the make-up of model types, as introduced in Chapters 1 to 5, it is vital that anyone planning the use of climate model results, or embarking on a climate modelling project, is familiar with the development framework in which these models are produced. This chapter will provide an introduction to such aspects of climate modelling, review some example model experiments that illustrate some of the applications of climate models, and examine the important interface between climate models and policy.

A Climate Modelling Primer, Third Edition. K. McGuffie and A. Henderson-Sellers.
 ISBN: 0-470-85750-1 (HB); 0-470-85751-X (PB)

6.2 DATA INTERCHANGE

Much of the early development of climate models was undertaken in well-resourced government laboratories such as the United Kingdom Meteorological Office and GFDL. These establishments developed monolithic frameworks for their models. Models were focused on the computer architecture available and tailored to the local data storage system. Data formats were invariably unique to the model, often with compression or other techniques used to manage the use of the limited non-volatile storage space (what we now know as 'disk space'). For example, to save space, a modeller might combine two different variables in a single two-dimensional field, with special 'decoding' instructions required to understand the significance of the 'odd' numbers in regions of (say) sea ice. The digital archives so created necessarily had an accompanying paper archive that explained the intricacies of the stored files. With limited interoperability of computer systems and the lack of direct network connections, data interchange between computer systems was a cumbersome and technically involved process. As computer systems developed, the infrastructure for data interchange and interoperability also developed. The development of the Unix™ operating system and its near siblings and their near universal implementation on modern computers and the rapid development of high-speed data communications have been the key enabling factors in the growth of model intercomparisons.

New technologies for data interchange amplified the problems associated with monolithic development. For intercomparisons to be successful, some standard for data interchange and documentation must be developed. One such standard is the NetCDF (Network Common Data Format) file standard developed by Unidata as a means for data transfer between Unidata applications. The concept is implemented as a library of computer 'functions' that can be assembled by a user to access or create NetCDF files. The files are self-describing, machine-independent datasets that can be readily interchanged between users without the need for supplementary materials. The files can contain data of different types, multiple variables as well as ancillary data or descriptive text. This philosophy is intended to reduce errors arising from misinterpreting data and reduces the costly effort associated with conversion between data formats.

Table 6.1 shows an example output from a simple NetCDF utility. The 'ncdump' utility provides a basic summary of the data within the file. The programmer need only reference the required variable by the name of the NetCDF structure to retrieve the values into the application. This avoids problems associated with locating and identifying individual records in simple binary files after consulting a printed format description – a very time-consuming task. In addition to the technical specifications of the file format, modellers have also developed conventions for utilizing these formats in order to promote the interchange and sharing of files. For example, the ALMA (Assistance for Land-surface Modelling Activities) format describes conventions for storage of data related to land-surface variables, defining sign conventions for fluxes, etc. The close connection between data and metadata that flows from

Table 6.1 A sample printout from the NetCDF utility 'ncdump' shows the properties of a NetCDF file. In this example there is a significant amount of supplementary data (metadata) that indicates the date of creation of the file and appropriate software versions along with grid size, units and summary details of the data values (this example has been edited for illustrative purposes)

```
%% ncdump('prate.sfc.gauss.1979.nc')
%% Generated 10-Nov-2003 14:30:58
%% Global attributes:
nc.Conventions = ncchar('CF-1.0');
nc.title = ncchar('4x Daily NCEP/DOE Reanalysis 2');
nc.history = ncchar('created 2002/03 by J.Doe (netCDF2.3)');
nc.comments = ncchar('Data is from ... ');
nc.platform = ncchar('Model');
nc.source = ncchar('NCEP/DOE AMIP-II Reanalysis (Reanalysis-2)
  Model');
nc.institution = ncchar('National Centers for Environmental
  Prediction');
nc.references = ncchar('http://wesley.wwb.noaa.gov/reanalysis2/');
%% Dimensions:
nc('lon') = 192;
nc('lat') = 94;
nc('nbnds') = 2;
nc('time') = 1460; %% (record dimension)
%% Variables and attributes:
nc{'lat'} = ncfloat('lat'); %% 94 elements.
nc{'lat'}.units = ncchar('degrees_north');
nc{'lat'}.actual_range = ncfloat([88.5419998168945
  -88.5419998168945]);
nc{'lat'}.long_name = ncchar('Latitude');
nc{'lat'}.standard_name = ncchar('latitude_north');
nc{'lat'}.axis = ncchar('y');
nc{'lat'}.co-ordinate_defines = ncchar('point');
...
...
nc{'prate'} = ncshort('time', 'lat', 'lon'); %% 26350080
  elements.
nc{'prate'}.long_name = ncchar('6-Hourly Precipitation Rate ');
nc{'prate'}.valid_range = ncshort([-32765 19735]);
nc{'prate'}.unpacked_valid_range = ncfloat([0
  0.00524999992921948]);
nc{'prate'}.actual_range = ncfloat([0 0.00524999992921948]);
nc{'prate'}.units = ncchar('Kg/m^2/s');
nc{'prate'}.missing_value = ncshort(32766);
nc{'prate'}.GRIB_name = ncchar('PRATE');
nc{'prate'}.var_desc = ncchar('Precipitation Rate');
nc{'prate'}.dataset = ncchar('NCEP/DOE AMIP-II Reanalysis
  (Reanalysis-2)');
nc{'prate'}.level_desc = ncchar('Surface');
nc{'prate'}.statistic = ncchar('Mean');
nc{'prate'}.parent_stat = ncchar('Individual Obs');
nc{'prate'}.standard_name = ncchar('precipitation_rate');
nc{'prate'}.cell_methods = ncchar('time: mean');
```

such formats and conventions means that effort can be directed to interpretation of results and away from data management tasks.

Data management is, however, a growing part of the climate modeller's skill set. Modellers must manage datasets produced by their model (perhaps several Gb per simulated year) and also manage observational datasets used for validation and forcing. The exponential growth of this data volume, as model resolutions and integration times have increased, has led to the development of various distributed data technologies. Instead of modellers transferring data from one machine to another, the NetCDF libraries have been recently extended to function in a distributed manner. Originally designed for oceanographic data, the OPeNDAP/DODS data access protocol simplifies data distribution and is a protocol for requesting and transporting data across the Internet, based on the client–server model. Data are distributed without regard to local storage format. Anyone with a digital data archive can configure their archive as an OPeNDAP/DODS server and make it available to clients in the science community. OPeNDAP/DODS is a community-driven project and is based on the idea that datasets are often best distributed by their creators. This allows for appropriate updating and documentation of changes and saves the need for multiple copies of data (potentially differently described) being stored at multiple locations. Data can be accessed at remote locations and these remote data analysis and visualization systems can be modified to be OPeNDAP/DODS clients, retrieving data at the application level, instead of requiring the user to collect and store copies of a dataset.

6.3 EARTH SYSTEM MODELLING FRAMEWORKS

The history of the climate modelling community, which grew up around, and in support of, models developed at large institutions, has also affected the level to which modelling developments have propagated through the community. A modeller at one institution, developing a new cloud parameterization scheme for example, cannot easily transfer this scheme to another model. If a modelling group decides to implement such a scheme in their model, it is likely that significant code development will need to be undertaken. Even if the module can be compiled on the adopter's computer, there are likely to be problems integrating the new scheme with a different model grid or timestepping scheme. There may also be aspects of the new module that implicitly require a specific environment to be available at the developer's institution (e.g. particular disk and tape storage technologies).

The desire to improve collaboration and reduce development time, together with the development of climate model intercomparisons, has meant an increased demand for interchangeability of model components. Modellers are keen to test the performance of their atmospheric models with different ocean model schemes and different land-surface schemes. To this end, the development of an Earth System Modelling Framework (ESMF) has been proposed, to enhance interoperability and performance of large modelling ventures. The motivation for ESMF is three-fold: (i) climate models are increasingly composed of highly specialized modules con-

tributing to a modelling 'system'; (ii) computer hardware and software are becoming increasingly complex as high-performance computing relies more heavily on massively parallel systems and scalable computing architectures such as the 'Earth Simulator'; and (iii) a number of modelling frameworks have been developed that encourage interoperability and reuse of software. ESMF is likely to make significant headway in promoting exchange of model components. Not only does such a scheme make interchange between large organizations possible, but modelling innovations by smaller groups (typically university groups) can be readily implemented into large coupled modelling projects without expensive recoding, making model development a truly distributed process.

At its most basic, ESMF provides a means for assembling geophysical component models into applications. This is best illustrated by means of an example. If a modelling group wishes to create an ESMF component model from (say) their land-surface scheme, a number of steps are involved. The ESMF architecture is characterized by a 'sandwich' design (Figure 6.1). The three components are illustrated in Figure 6.1a for the ESMF application. The superstructure provides a shell to encompass the user's code and an infrastructure layer provides foundation components that

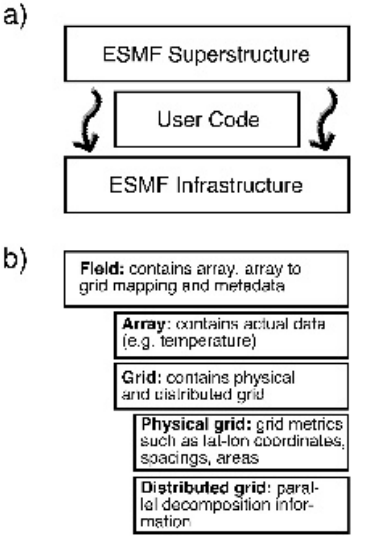

Figure 6.1 (a) Schematic structure of the Earth System Modelling Framework. The 'user code', for example a model of the processes occurring at the land surface, is sandwiched between two standard layers. The creator of the land-surface model uses standard library routines to access data and store results (infrastructure) and must interface to the ESMF superstructure in standard ways, so that other models or other components of the same model can access the required parameters in a consistent and physically correct way without being rewritten. (b) An example of the hierarchical structure of the ESMF infrastructure. Information can be addressed at the Field level, with intricacies of units, grid size and computational strategies hidden (reproduced by permission of the IEEE from Hill *et al.* (2004), *Comp. Sci. Eng.*, **6**, 18–28)

users can use to speed construction and ensure consistent behaviour. For example, the ESMF clock 'objects' provide a consistent notion of time between components. This is an important aspect of model coupling, since different model components may operate on different timesteps. The encapsulation of legacy code within ESMF means that modern object-oriented techniques can be applied where traditional programming techniques would normally prohibit such an approach. ESMF could be used to link three models with very different grid structures. Because each developer would have created an ESMF application from her or his code, coupling becomes relatively straightforward. A spectral atmospheric model could be connected to a finite grid ocean model and a land-surface scheme configured as a 'mosaic' grid. Figure 6.1b illustrates how the infrastructure layer organizes grid information in an hierarchical manner. A 'field' contains much more than the data; it also contains metadata about the variable (e.g. humidity). The 'grid' class contains information about the physical grid and information about how computations can be made.

Although the addition of extra code inevitably results in reduced model performance, the ESMF project has a goal of showing less than 10 per cent degradation in performance of the model. The first version of ESMF was released in 2003 and development is set to continue into 2005.

6.4 MODEL EVALUATION

All models of the climate system must face evaluation as part of their development. Computer systems in the 1960s and 1970s had very limited interoperability and networking capability and, because of these limitations on the exchange of model output, early modellers had to be satisfied with comparisons to observed data where available. Intermodel comparisons were frequently restricted to 'eyeball' evaluations of differences. The advent of interoperable computer networks since those early comparisons has led to increased data interchange between modelling groups, to the development of protocols for evaluation of models and to organized model intercomparison projects (MIPs).

Evaluation of climate models can produce a range of outcomes that have been grouped as (i) predictions that are unreasonable; (ii) predictions that are so reasonable as to be already known; (iii) unexpected predictions, which can be readily understood and accepted; or (iv) predictions that, while being reasonable, identify novel outcomes that challenge current theories. Normal practice in model development would screen out all developments producing unreasonable results, and there is little benefit in intercomparison of results that are totally reasonable and well known. Thus, the intercomparisons and group evaluations tend to try to focus on results in categories (iii) and (iv): new predictions that are consistent with theory and those that challenge existing ideas.

The process of comparison of model predictions and group evaluation is complex as it has to encompass models and modelling groups from around the world and has to be organized so that comparable results are being compared. To facilitate the

process of model evaluation and intercomparison, the WCRP's Working Group on Numerical Experimentation (WGNE) categorized intercomparisons into three levels (Figure 6.2). Level 1, the simplest, uses any available model results and a common diagnostic set. The IPCC assessments are Level 1 intercomparisons. Level 2 requires that the simulations are made according to pre-specified, identical conditions, that common diagnostics are employed and that there is a common diagnostic set against which all the predictions are evaluated. Level 3, the 'best' intercomparison process, requires, in addition to the requirements of the lower two levels, that all the models employ the same resolution and that the intercomparison includes the use of some common routines or code modules.

Until the 1990s, intercomparisons were conducted at Level 1. The Atmospheric Model Intercomparison Project initiative (begun in the early 1990s) has spawned around 30 different MIPs which are intercomparisons at Level 2 – some of these are described in the following sections. At the time of writing, there are no Level 3 intercomparisons, although some of the Level 2 intercomparisons are planned later to develop common code modules. The Earth System Modelling Framework (ESMF), discussed in Section 6.3, will provide a robust methodology for Level 3 intercomparisons, with interchangeable code modules.

6.4.1 Intercomparisons facilitated by technology

Most of the recent climate model intercomparisons have only been possible because of the advent of global telecommunications and the accompanying data interchange standards. The Internet is an essential part of a Level 2 or higher intercomparison. Typically, a coordinating group is identified and this group takes responsibility for the provision of the agreed model simulation instructions, including the

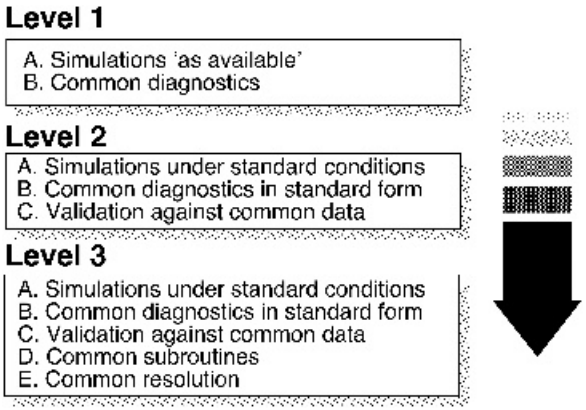

Figure 6.2 Levels of model intercomparison as defined by the Working Group on Numerical Experimentation (WGNE) in support of the World Climate Research Programme (WCRP) (modified from Gates, 1992)

experimental design and the forcing data based on either email discussions or a face-to-face workshop. The coordinating group typically also provides independent data against which to compare the model results, and facilitates model intercomparisons by providing quality control procedures and a central electronic results and data 'library', which can be accessed by all the participating modelling groups.

The demands associated with providing these facilities are quite considerable. This is one of the reasons why Level 2 intercomparisons have so far been restricted to specific aspects of the whole climate system. The following sections review, as examples, intercomparisons of atmospheric and coupled models, radiation schemes, land-surface schemes and ocean carbon models.

6.4.2 AMIP and CMIP

AMIP, the Atmospheric Model Intercomparison Project, was established in 1989 and moved into its second stage (AMIP II) in 1996. It focuses on structured (Level 2) intercomparisons of the atmospheric component of global climate models. Participating models use prescribed ocean surface temperatures and sea ice extents as well as agreed values of the solar constant (1365 $W m^{-2}$) and the atmospheric concentration of CO_2 (345 ppmv) as input to a fixed length simulation. The simulation period for AMIP I was from 1 January 1979 to 31 December 1988 and that for AMIP II from 1 January 1978 to 1 March 1996. The prescribed forcings did not extend to the use of common surface elevation information nor, in AMIP I, to an agreed spin-up procedure, although for AMIP II there was such a recommended procedure.

All participating model groups (around 30–40) were required to submit output in an agreed format, but there was no requirement for a particular resolution. The results from these global atmospheric simulations have been reported in various of the IPCC Assessments as a partial demonstration of the validity of GCMs.

Table 6.2 illustrates the differences found between observed values and the mean of participating AMIP I models. Some of these differences are fairly small (e.g. sea-

Table 6.2 Hemispheric mean seasonal root mean square differences between observations and the mean of the AMIP models (after Gates, 1996)

	DJF		*JJA*	
Variable	*NH*	*SH*	*NH*	*SH*
Mean sea-level pressure (hPa)	1.4	1.4	1.3	2.4
Surface air temperature (°C) (over land)	2.4	1.6	1.3	2.0
Precipitation ($mm\,d^{-1}$)	0.80	0.71	0.62	0.77
Cloudiness (%)	10	21	14	16
Outgoing longwave radiation ($W m^{-2}$)	2.8	3.2	2.9	5.5
Cloud radiative forcing ($W m^{-2}$)	9.1	20.5	16.2	6.5
Surface heat flux ($W m^{-2}$) (over ocean)	22.5	27.3	30.5	17.2
Zonal wind ($m s^{-1}$) (200 hPa)	2.4	1.8	1.8	2.4

level pressure and surface air temperature) but others, especially those associated with clouds and radiative forcing, can be seen to be rather large.

The Coupled Model Intercomparison Project (CMIP) aims to extend the analysis of AMIP to coupled models. The project is ongoing and involves collecting both 'control run' simulations from available coupled models (18 at the time of writing) and from enhanced CO_2 experiments, with a specified increase in CO_2 of 1 per cent per annum. The models in CMIP are models of the atmosphere and ocean that include interactive sea ice and simulate the physical climate system, given only a small number of external boundary conditions such as the solar 'constant' and atmospheric concentrations of radiatively active gases and aerosols.

6.4.3 Radiation and cloud intercomparisons

Interactions between clouds and radiation are known to be the source of many of the differences among climate model predictions. This recognition, and developments in GCM analysis including those at GFDL, prompted two complementary intercomparisons: the Intercomparison of Radiation Codes in Climate Models (ICRCCM) and the Feedback Analysis of GCMs and Intercomparison with Observations (FANGIO). Both studies predate AMIP, ICRCCM being initiated in 1984 and FANGIO in 1988. They focus on different aspects of cloud–radiation interactions.

ICRCCM has a straightforward mandate: to intercompare results from participating radiation codes in the long and short wavelength regions of the spectrum for the cases of clear and cloudy skies. Around 30–40 modelling groups participated in the first phase, representing both climate models and also radiative transfer algorithms employed in retrieval of fluxes from satellite measurements. The calculations of these schemes were compared with the most detailed radiative transfer calculations available, termed 'line-by-line' calculations. In the second phase, these line-by-line calculations are being augmented by observational data from satellite and surface-based field programmes including ERBE, the International Satellite Cloud Climatology Project (ISCCP) and the Surface Radiation Budget Climatology Programme.

The ICRCCM intercomparisons revealed very large differences among the predictions of radiation models. In the longwave region, ranges of 30–70 $W m^{-2}$ were discovered while, in the shortwave region, ranges varied from 3 per cent for the (simplest) pure water vapour cases to 46 per cent for the cases with thick cloud and as high as 60 per cent for situations with high aerosol loadings. An ICRCCM report summarized these findings as showing that many algorithms have inherent, unknown but large errors which may significantly affect the conclusions of the studies in which they are used. However, the same summary noted that it is difficult to draw conclusions regarding the accuracy, or otherwise, of climate model simulations overall because of their dependence on other compensating processes and adjustments of model parameters.

ICRCCM is now in Phase 3, which aims to assess the performance of modern one-dimensional radiative transfer algorithms and to compare their performance

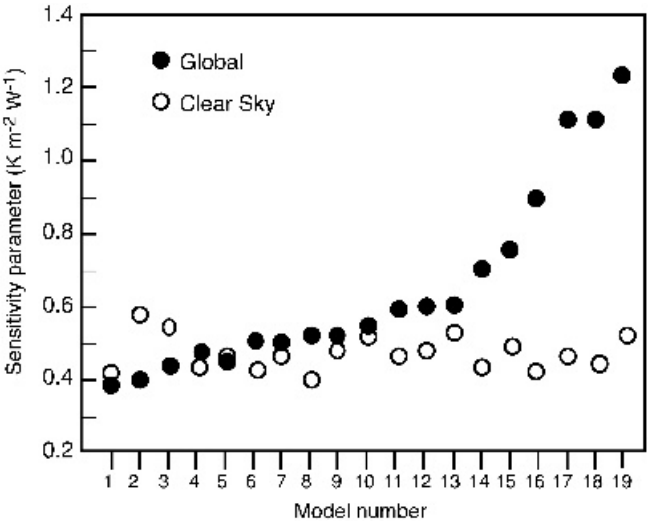

Figure 6.3 Clear sky and global sensitivity parameters for 19 GCMs participating in FANGIO (reproduced by permission of the American Geophysical Union from Cess *et al*., 1990, *J. Geophys. Rev.*, **95**, 16 601–16 615)

with the earlier results for models developed in the 1980s. The development of new applications, such as cloud-resolving models, means that Phase 3 will also assess the performance of these new radiative transfer codes in situations such as partially cloudy skies.

The FANGIO project sought to improve understanding of the feedback processes in climate models involving cloud and radiation calculations. Defining a climate model sensitivity parameter, λ', as

$$\lambda' = \frac{1}{(\Delta F/\Delta T_s - \Delta Q/\Delta T_s)} \tag{6.1}$$

where ΔQ is the change in shortwave flux, ΔF is the change in infrared flux and noting that for conditions typical of the present day Earth (F = 240 W m^{-2}, T_s = 288 K) the value of λ' in the absence of any feedbacks is 0.3 K m^2 W^{-1}, the FANGIO investigators have calculated the value of λ' for their models in the cases of clear skies, cloudy skies and for the global response overall (Figure 6.3 and *cf*. Chapter 1). The range in the clear-sky values is very small, underlining the main conclusion of this intercomparison: the three-fold variation among AGCMs' sensitivity to a prescribed climate change is due almost entirely to cloud feedback processes.

6.4.4 Project for Intercomparison of Land-surface Parameterization Schemes (PILPS)

The World Climate Research Programme (WCRP) launched the Project for the Intercomparison of Land-surface Parameterization Schemes (PILPS) in 1992 with the

goal of understanding and improving the parameterization of fluxes of heat, moisture and mass (including carbon and momentum) between the atmosphere and the continental surface in climate and weather forecast models. PILPS diagnoses the behaviours of participating land-surface schemes (LSSs) in controlled experiments implemented in four phases. The first two phases included studies of scheme behav-

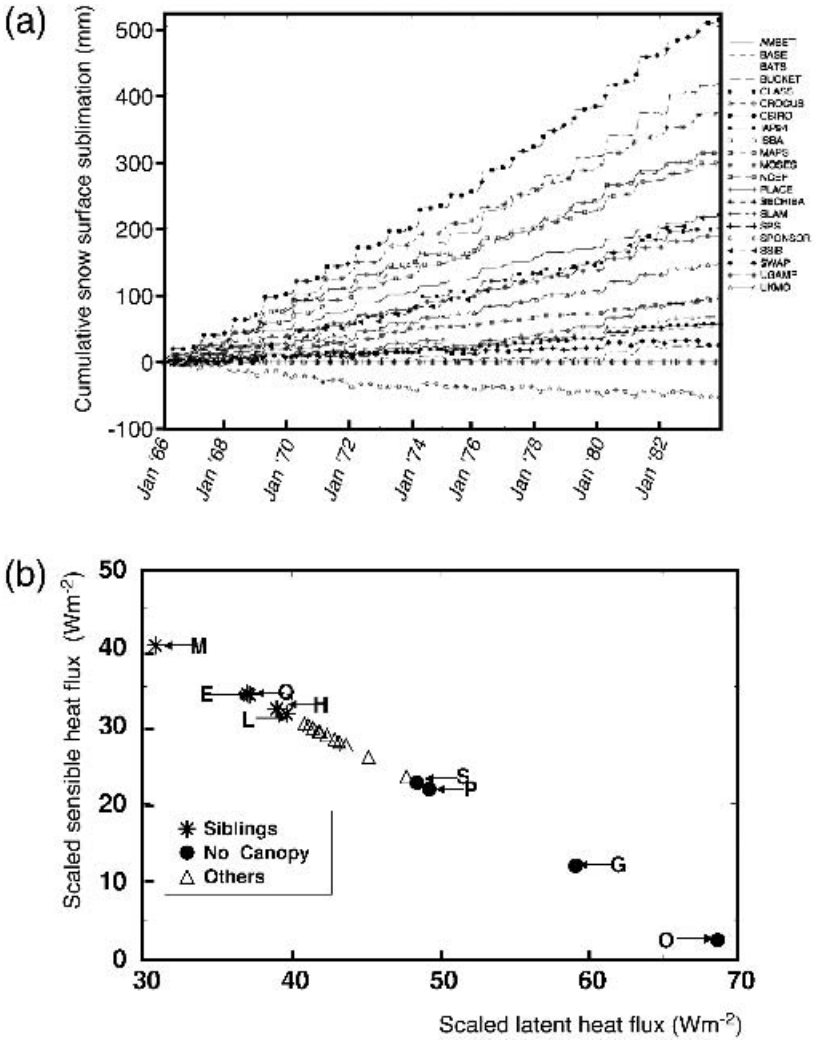

Figure 6.4 (a) The cumulative evaporation (mm) from snow over the 18 years of the control simulation for PILPS 2(d) (reproduced with permission from Slater *et al*. (2001), *J. Hydromet.,* **2**, 7–25). (b) The relative partitioning of surface net radiation into sensible and latent heat is plotted here for AMIP II land-surface schemes. Buckets (No Canopy) and 'SiBlings' occupy characteristic portions of the plot

iour when driven in 'off-line' (one-way feedback) mode by atmospheric forcings prescribed from GCM output (Phase 1) or from varied observational data sets (Phase 2). In Phase 1, participating land-surface schemes were integrated for many years using synthetic meteorological forcing from a global climate model. The same descriptions of surface vegetation and soil were used by all land-surface schemes. A single year's meteorology was used for as many annual cycles as were required for a particular LSS to come into equilibrium with the prescribed atmospheric conditions, i.e. until mean changes in the surface heat and moisture storage were negligible. Phase 2 used observational datasets to force the models for particular locations and vegetation types. Both of these revealed a great variety in the performance of atmospheric models, including problems with water and energy conservation in some land-surface schemes (Figure 6.4).

Phase 3 entails the diagnosis of land-surface schemes coupled to their 'home' atmospheric host models, while Phase 4 concerns the analysis of results from coupling different land-surface schemes to a common host. In practice, Phase 3 has involved the analysis of land-surface schemes in the Atmospheric Model Intercomparison Project (AMIP) models. From the perspective of land-surface specialists, AMIP affords a unique opportunity to study the interactions of a wide range of land-surface schemes with their atmospheric host models, and PILPS' studies of this type aim to address an overarching question: 'To what extent does GCM performance in simulating continental climates depend on the parameterizations of the coupled land-surface scheme?' The suite of results available from AMIP has permitted researchers to confirm the importance of the land-surface scheme to the climate of the atmospheric model (Figure 6.4b).

Validation of GCM continental climates does not verify the workings of the land-surface schemes *per se* since, in addition to the intrinsic properties of the land-surface scheme, the continental simulation is also affected by atmospheric forcings and by mediating land-surface characteristics. Despite these complications, there are preliminary indications that characteristic 'signatures' of different land-surface schemes can be detected in coupled climate and weather simulations, provided that suitable diagnostics are chosen (Figure 6.4b). Simple bucket models (Figure 5.20a) cluster together at one extreme, while a group of models developed in the 1980s (e.g. Figure 5.20b) cluster at the other. An intermediate group of modern land-surface schemes is also apparent.

6.4.5 Comparing carbon-cycle subcomponents of climate models

The uptake and release of carbon dioxide at the land and ocean surfaces controls its atmospheric concentration. The magnitude and extent of terrestrial and oceanic sources and sinks of CO_2 must be fully understood if predictions are to be made of the ultimate levels of atmospheric CO_2 and hence of the future climate. Two intercomparison projects have been designed to evaluate the performance of ocean carbon simulation and of terrestrial vegetation exchanges of CO_2 with the atmosphere.

The Vegetation/Ecotype Modelling and Analysis Project (VEMAP) has the goal of intercomparing the performance of vegetation model simulations. These models simulate the influence of the physical environment on: (i) the availability of plant functional types (i.e. which plants can grow and reproduce); (ii) competition for resources; and (iii) the emergent equilibrium vegetation cover. Associated models, termed terrestrial biogeochemistry models, have been used to simulate the flow of carbon and mineral nutrients within vegetation, surface litter and soil organic matter pools. These models have also been used to examine the global patterns of net primary production, carbon storage and mineral uptake and their sensitivity to climate change.

The emergence of divergent types of biosphere models makes it difficult to address complex issues of global change and terrestrial ecosystems. In particular, examining the response of ecosystems to multiple, and potentially interacting, factors and appraising how the resulting changes in the terrestrial biosphere may influence the Earth system as a whole require an integrated perspective. The VEMAP intercomparisons (Table 6.3) include the synergistic effects of different vegetation models, different biochemistry models and the different climates simulated by different GCMs. This intercomparison shows a very large range in the projected impact on the total terrestrially-stored carbon: estimates range from a predicted reduction of −39% when BBGC is run with the MAPSS vegetation and the UKMO climate to an increase in stored carbon of +32% when TEM is run with MAPSS for both the OSU and GFDL climate projections (Table 6.3).

Oceanic uptake and release of CO_2 completes the global carbon system. Ocean–atmosphere carbon exchanges occur both as a result of the degree of

Table 6.3 Annual total carbon storage (10^{15} g C) and percentage change for the linkage of the three biogeochemistry models (BGC) (BIOME-BGC [BBGC], CENTURY [CEN], and the terrestrial ecosystem model [TEM]) with the vegetation distributions of the three biogeography models (VEG) (BIOME2, DOLY and MAPSS) for contemporary climate (CON) at 335 ppmv CO_2 and three GCM climates (OSU, GFDL and UKMO) at 710 ppmv CO_2 (after VEMAP, 1995)

		Models			
BGC	*VEG*	*CON*	*OSU*	*GFDL*	*UKMO*
BBGC	BIOME2	122	−13.2%	−9.5%	−34.7%
	DOLY	122	−18.1%	−13.6%	−36.4%
	MAPSS	120	−8.3%	−13.8%	−39.4%
CEN	BIOME2	125	−0.8%	+12.6%	−1.8%
	DOLY	124	+9.8%	+17.7%	+7.8%
	MAPSS	120	+17.0%	+20.4%	−1.5%
TEM	BIOME2	114	+11.9%	+25.7%	0.0%
	DOLY	114	+19.7%	+25.3%	+12.5%
	MAPSS	109	+32.3%	+32.2%	+1.7%

solubility and as a function of the ocean biology. The Ocean Carbon Model Intercomparison Project (OCMIP) is evaluating the capability of models to predict both anthropogenic and natural CO_2 exchange by comparison with observations of radiocarbon data, with determinations of the extent and type of ocean biology derived from satellite observations of ocean colour. It is anticipated that results from OCMIP will be a valuable resource for the further development of the 3D ocean components of coupled models and will, ultimately, permit improved simulations of the global carbon system in coupled climate system models.

Isotopes quantify the global carbon budget

To understand, and hence predict, greenhouse warming, we must be able to identify components of the global carbon budget precisely. The IPCC Third Assessment Report lists these with uncertainties represented by ±1 standard error (Table 6.4). The land–atmosphere flux is the sum of CO_2 sources derived from land clearance and the CO_2 sinks caused by net biospheric uptake. These two components cannot be separated using CO_2 flux measurements alone.

Stable isotope measurements provide a means of partitioning the absorption of CO_2 into oceanic and photosynthetic uptake. Photosynthesis of terrestrial plants has a unique isotopic signature: photosynthetic discrimination of carbon by C_3 plants varies from 22 to 35‰ while for C_4 plants typical values are 12 to 15‰. As a consequence, the CO_2 respired from ecosystems differs from that of the atmospheric baseline depletion of ^{13}C, which is −8‰. Since there is little discrimination during dissolution of CO_2 into the ocean (−1‰), gradients of $^{13}C/^{12}C$ in the atmosphere may be used to distinguish between terrestrial and oceanic sinks and even among predominantly C_3 as compared to mostly C_4 terrestrial communities.

Atmospheric measurements of $^{18}O/^{16}O$ also contain information about the role of the terrestrial biosphere in the carbon cycle. This occurs because CO_2 leaving an ecosystem carries the ^{18}O signature of water in leaves and soil, as oxygen in CO_2 exchanges with oxygen in water. This signature is very different from $^{18}O/^{16}O$ of ocean water, so that measurements of oxygen isotopes in atmospheric CO_2 provide an additional, independent method for partitioning oceanic and terrestrial sinks of carbon.

Table 6.4 Global CO_2 budget (in Pg C yr^{-1} with ±1 standard error). Positive values are fluxes into the atmosphere

	1980–1989	*1990–1999*
Atmospheric increase	3.3 ± 0.1	3.2 ± 0.1
Emissions (fossil fuel etc.)	5.4 ± 0.3	6.3 ± 0.4
Ocean–atmosphere flux	−1.9 ± 0.6	−1.7 ± 0.5
Land–atmosphere flux	−0.2 ± 0.7	−1.4 ± 0.7

Modellers have tried to exploit these isotopic signatures in their efforts to refine and verify descriptions of the global carbon budget. C_3 and C_4 plants have different photosynthetic processes and the uptake of ^{12}C relative to ^{13}C is different. Figure 6.5 depicts two graphical solutions to the global ^{13}C budget. The upper graph considers

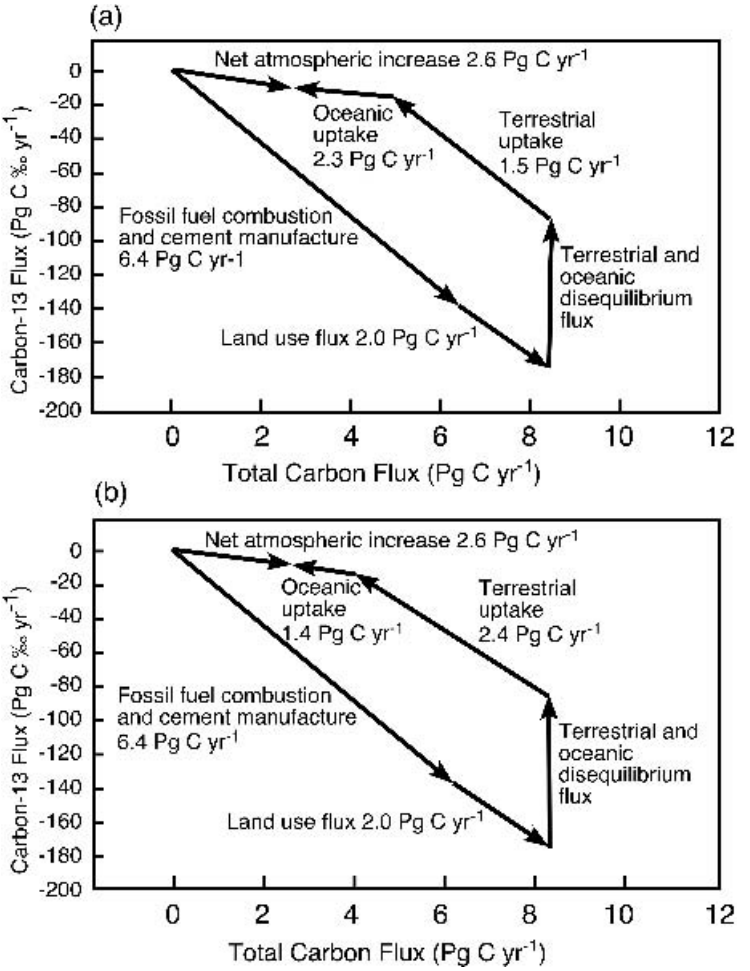

Figure 6.5 The carbon cycle can be visualized as a two-dimensional graph. Vectors in the plane of the graph show the various carbon fluxes in terms of their effect on the total carbon and in terms of ^{13}C. Differentiation between ^{13}C and ^{12}C in different processes means that the arrows have different slopes. (a) Graphical solution to the ^{13}C budget, assuming that the net land uptake is entirely due to C_3 vegetation (95 per cent of plant species). (b) Graphical solution to the ^{13}C budget approach, assuming that the plant population is around 25 per cent C_4 plants. The change in land discrimination alters both the magnitude and slope of the terrestrial uptake and thus the relative land : ocean partition. (Reproduced from Still *et al*., 2003, *Global Biogeochemical Cycles* **17**, 1002, doi:10.1029/2001GB001807. Copyright © American Geophysical Union)

a regime with only C_3 plants while the lower graph employs an estimated global proportion of C_4 vegetation of 25 per cent. The terrestrial uptake increases from 1.5 Pg C yr^{-1} for C_3 plants to 2.4 Pg C yr^{-1} with 25 per cent C_4 plants. There is a resultant change in the computed oceanic uptake although both values lie within the IPCC error ranges.

With C_3 plants alone, the graphical model (Figure 6.5a) computes a net terrestrial source of CO_2 of 0.5 (−1.5 + 2.0) Pg C yr^{-1} whereas, with a mix of C_3 plus C_4 plants (Figure 6.5b), the terrestrial biosphere becomes a net sink of CO_2 of −0.4 (−2.4 + 2.0) Pg C yr^{-1}. Such model simulations play a role in quantifying interannual variations in terrestrial carbon fluxes.

6.4.6 More and more MIPs

Since the groundbreaking AMIP efforts, the number of model intercomparison projects (MIPs) has grown steadily. Projects like AMIP and PILPS have been shown to have an excellent 'return on investment' for model developers. These projects have forced developers to focus on the fundamentals of their model through basic 'qualification' tests while systematic comparisons have produced improved understanding of model behaviour.

Table 6.5 lists close to 40 model intercomparison projects that are ongoing or planned. The list is dynamic, and new projects are being proposed all the time. Recent additions include the Ocean Model Intercomparison Project (OMIP), which aims to address the general performance of ocean models, along with other aspects of ocean models such as the identification of critical issues associated with air–sea interaction, and to improve understanding of model sensitivities.

The Sea Ice Model Intercomparison Project (SIMIP) aims to develop improved methods for representation of sea ice in climate models. SIMIP is part of a larger programme of observation (the Arctic Climate System Study (ACSYS)). In dynamic sea ice models, it is generally assumed that sea ice can be treated as a two-dimensional continuum, which is characterized by fields of five variables: snow and ice thickness, snow compactness and two components of horizontal velocity. More sophisticated models include additional prognostic variables such as ice roughness or age or a more complete treatment of the ice thickness distribution. The interaction between the atmosphere and ocean is a major weak spot in current climate models. SIMIP focuses on the comparison of four different techniques for modelling a dynamic sea ice cover on the ocean. In its second phase (SIMIP2), the focus is on the one-dimensional thermodynamics of sea ice, using data collected during the SHEBA (Surface Heat Budget of the Arctic Ocean) experiment between 1 October 1999 and 1 October 2000, in order to improve understanding of the coupling between atmosphere and ocean in this region.

SNOWMIP brings together several types of snow models: parameterizations from climate models, snow melt models (used by hydrologists) and detailed snow models (used for avalanche forecasts or research in snow physics). As discussed in Chapters 3 and 5, snow cover acts as an effective barrier to heat transfer from the land

Table 6.5 Model intercomparison projects

Name	*Acronym*
Arctic Ocean Model Intercomparison Project	AOMIP
Arctic Regional Climate Model Intercomparison Project	ARMIP
Asian-Australian Monsoon Atmospheric GCM Intercomparison Project	–
Atmospheric Model Intercomparison Project	AMIP
Atmospheric Tracer Transport Model Intercomparison Project	TransCom
Carbon-Cycle Model Linkage Project	CCMLP
Climate of the Twentieth Century Project	C20C
Coupled Model Intercomparison Project	CMIP
Coupled Carbon Cycle Climate Model Intercomparison Project	C4MIP
Dynamics of North Atlantic Models	DYNAMO
Ecosystem Model-Data Intercomparison	EMDI
Earth system Models of Intermediate Complexity	EMICs
ENSO Intercomparison Project	ENSIP
GEWEX Atmospheric Boundary Layer Study	GABLS
GEWEX Cloud System Study	GCSS
GCM-Reality Intercomparison Project for SPARC	GRIPS
Global Land–Atmosphere Coupling Experiment	GLACE
Global Soil Wetness Project	GSWP
Models and Measurements II: Stratospheric Transport	MMII
Ocean Carbon-Cycle Model Intercomparison Project	OCMIP
Ocean Model Intercomparison Project	OMIP
Paleo Model Intercomparison Project	PMIP
Project for Intercomparison of Landsurface Parameterization Schemes	PILPS
Potsdam DGVM Intercomparison Project	–
Potsdam NPP Model Intercomparison Project	–
Project to Intercompare Regional Climate Simulations	PIRCS
Regional Climate Model Intercomparison Project for Asia	RMIP
Seasonal Prediction Model Intercomparison Project-2	SMIP-2/
Seasonal Prediction Model Intercomparison Project-2/Historical Forecast	SMIP-2/HFP
Sea Ice Model Intercomparison Project	SIMIP
Snow Models Intercomparison Project	SnowMIP
Stable Water Isotopes Intercomparison Group	SWING
Stretched Grid Model Intercomparison Project	SGMIP
Study of Tropical Oceans In Coupled models	STOIC
WCRP F11 Intercomparison	–
WCRP Radon Intercomparison	–
WCRP Scavenging Tracer Intercomparison	–

surface to the atmosphere. The thermal properties of the snow are affected by many factors, notably the age and thermal history of the snowpack. Other factors such as the albedo and the effect of pollution on the snowpack are also relevant. The aim of SNOWMIP, a common feature of many MIPs, is not to select the 'best' model, but to identify processes important for each application. The comparison of detailed and simple models is likely to be of particular interest to the designers of future GCM

snow parameterizations and simple snow melt models, but the strength of such projects lies in the unexpected synergies with efficient schemes developed by climate modellers often finding their way back to more detailed schemes after evaluation.

6.4.7 Benefits gained from climate model intercomparisons

The most important outcomes of the international intercomparisons of climate model performance described here are: (i) the estimation of the range of confidence (or uncertainty) inherent in predictions of any one of the 'reasonable' models; (ii) the identification of group outliers; and (iii) the development and dissemination of datasets for continuing model evaluation. MIPs have generally found that:

- no one model performs well in all the evaluations employed;
- no one test evaluates all aspects of the participating models; and
- the model group mean (after excluding unreasonable results/outliers) outperforms any one model, where performance is measured against observational data.

There are dangers as well as benefits associated with large intercomparisons. The most omnipresent is the tendency to favour group medians as best estimates. However, if the intercomparisons are of Level 2 or 3 (Figure 6.2), the existence of observational data, especially if released only after the simulations, should counterbalance this central tendency. To date, considerable benefits have been derived from well-structured climate model intercomparisons.

The intercomparison of models also leads to the investigation of sets of statistics that can be used to characterize climate behaviour. For example, the spectrum of variability of the global daily mean near-surface temperature derived from coupled models (Figure 6.6) illustrates the differences (and agreements) between observational data and ten different coupled models. Since the observational data are of a relatively short period (140 years), estimation of long time-scale variability is not possible. Unfortunately, it is in this part of the spectrum where the models are in greatest disagreement.

6.5 EXPLOITATION OF CLIMATE MODEL PREDICTIONS

Climate models have the potential to develop information about future and past climates that has applicability to a wide range of human activities. For example, the search for 'safe' disposal sites for nuclear waste materials has involved not only geological evaluation of possible sites, but also climatological assessment using climate model predictions. Some mineral exploration companies have examined the results of past climate predictions in order to try to infer the likely locations of mineral deposits. The model predicted 'threat' of a 'nuclear winter' following a nuclear war is believed by some commentators to have contributed to the de-escalation in weapons development and holdings in the late 1980s. However, the most widespread application of climate model predictions currently is the evaluation of the impacts of greenhouse warming.

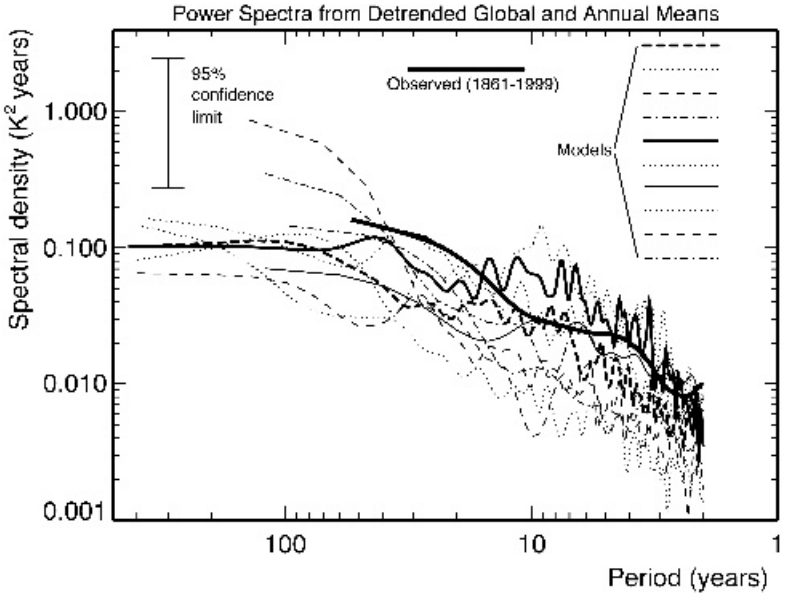

Figure 6.6 Power spectra of detrended globally and annually averaged surface air temperature simulated by the ten longest-running CMIP control runs and as observed by Jones *et al*. (2001). (Reproduced with permission of Elsevier from Covey *et al*., 2003, *Global and Planetary Change*, **37**, 103–133)

6.5.1 Expert assessment

During the 1980s, a growing body of evidence on the likely impacts of global climate change led to increased public concern. As discussed in Chapter 1, this growing body of evidence from both models and observations led to the establishment of the Intergovernmental Panel on Climate Change (IPCC) by the World Meteorological Organization and the United Nations Environment Programme (UNEP). Since it was set up in 1988, the IPCC has acted to focus efforts of hundreds of climate scientists of all descriptions (e.g. modellers, observational meteorologists, data analysis experts, impacts assessors and economists) on the problem of climate change associated with the enhanced levels of greenhouse gases produced by human activities (particularly fossil fuel combustion). So far, the IPCC has operated with three working groups, focusing on (i) the assessment of scientific information on climate change; (ii) the assessment of environmental and socio-economic impacts of climate change; and (iii) the formulation of response strategies. In addition, the IPCC has established a special panel on the participation of developing countries and has produced reports on specific topics including emissions scenarios, effects of aviation and issues in technology transfer. The Assessment Reports were published in 1990 (First), 1996 (Second), 2001 (Third) and the Fourth is planned to appear in 2007.

Since 1990, the structure of IPCC working groups has evolved. Working Group I still focuses on the assessment of available scientific information on climate change, especially as related to human activities. Working Group II is now charged with the assessment of environmental and socio-economic impacts and possible response options, while Working Group III is examining cross-cutting issues related to climate change, particularly socio-economic and technological issues. Although not itself a scientific research programme, the IPCC has acted as a focus for climate researchers. It has drawn heavily on the established research and intercomparison projects discussed earlier in this chapter and has also encouraged them.

The IPCC process has required modellers, and those who have examined records of recent and past climates, to make an assessment of their confidence in the different aspects of their results and this in turn has generated impetus in the research community towards model improvements. These assessments of confidence have been subject to change since 1990. In some cases, an enhanced understanding and implementation of processes in models has not led to an increase in confidence in the results. For example, the confidence in soil moisture predictions from GCMs was reduced between 1990 and 1996 because we learned more about soil moisture processes: specifically, by 1996 modellers knew that they are more complex than early GCMs allowed. The information presented in the First IPCC Assessment Report was used as a foundation for a global agreement to formulate policy on climate change: the United Nations Framework Convention on Climate Change. The ongoing process of scientific evaluation and assessment continues to feed into a political framework of commitments and targets such as the Kyoto Protocol.

6.5.2 GCM experiments for specific applications

Land use change

Land use change has become a focus for many researchers in recent times as it has become clear that forests and other natural biomes are coming under sustained pressure from development. At the same time, in some parts of the world, farmed areas are being abandoned, reverting to unmanaged vegetation. The impacts of these widespread changes on the climate and their role in the carbon budget of the planet are coming under increased scrutiny as greenhouse 'targets' start to become a critical political topic.

The possible impacts of tropical deforestation on the local, regional and global climate have received considerable attention from climate analysts and modellers in recent years, since forests provide the habitats of about half of the world's species and are an important natural sink of CO_2 and a source of tropical aerosols and trace gases. In the context of global atmospheric circulation, since strong ascending branches of the Walker and Hadley circulation are located over tropical forest regions, it has been suggested that changing the land-surface characteristics in regions of tropical forest may affect the atmospheric circulation.

GCMs are one tool that can be used in an attempt to answer the many questions raised with regard to the impacts of tropical deforestation. In experiments designed

to examine the effects of such processes, modellers change the characteristics of the vegetation and soil surface at a number of points. These changes depend on the nature of the land-surface scheme employed in the model. The choice of parameters is difficult, since relatively little information is available on the characteristics of deforested regions. Modellers must choose values of roughness length, leaf area index, soil colour and vegetation type (trees, grass, shrub etc.). Models do not yet attempt to simulate the gradual change that really occurs as tropical forest is removed and replaced. The best that can be done currently is to compare long-term means before and after an imposed deforestation.

Among the significant properties of tropical rainforests are that they have a very low surface albedo throughout the year, their leaf area and stem area are larger than those of any other vegetation and the trees are tall. Replacing the tropical rainforest with grassland leads to three main changes in the land-surface properties: (i) the surface albedo is increased, which directly causes a reduction in the surface net radiation; (ii) the reductions in the leaf area and stem area lead to a decrease in the water holding capacity of the vegetation – thus the evaporation of the intercepted precipitation and, probably, the vegetation transpiration are decreased following deforestation; and (iii) the grassland replacing the tropical forest is much shorter and smoother than the forest so that the surface roughness is dramatically reduced and the surface friction is reduced. The decreased surface roughness length has two competing effects on the evapotranspiration. Strengthened surface wind speed acts to enhance evaporation, whereas the effect of decreased surface roughness is to reduce evaporation. Most model simulations indicate that the surface evapotranspiration is decreased overall.

The changes in surface evapotranspiration, acting as the connection between the changes in the hydrological processes (determining the regional water recycling) and the changes in the land-surface and atmospheric energy budget (the sink of the surface energy budget and the source of the atmospheric energy budget) have a crucial role in determining the local impact of tropical deforestation. Moreover, the reduction in the vertical motion caused by less solar radiation being absorbed by the land surface and decreased latent heat from the land surface result in a reduction in the cloud cover amount over the deforested regions and may affect the regional atmospheric dynamics, especially the atmospheric moisture flow.

Rather small changes in surface temperature have been simulated with many models. This was concluded to be the result of the compensating effects of the reduction in the surface net radiation (due to the increased albedo) and the reduction in the surface evapotranspiration. However, the diurnal variation of surface temperature is enhanced following deforestation due to cooling during the night and warming during the day (Figure 6.7). These changes are due to a reduction in cloud cover and a reduction in evaporation. The changes in incoming solar radiation and outgoing longwave radiation from the surface are consistent with this interpretation.

The disturbance of the atmosphere induced by tropical deforestation may also interact with large-scale circulation features and thereby have impacts in extra-tropical locations. A major topic of current study is whether tropical deforestation will have mid-latitude impacts similar to those of ENSO events. Future challenges

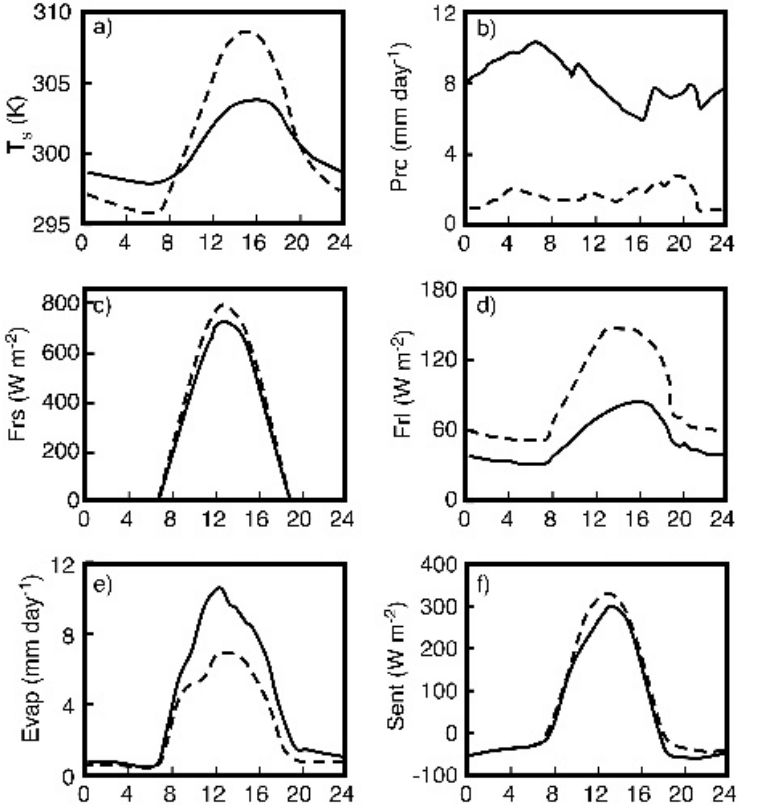

Figure 6.7 The diurnal cycle (average January) of (a) canopy air temperature (K), (b) precipitation (mm d^{-1}), (c) net absorbed solar flux (W m^{-2}), (d) net infrared flux (W m^{-2}), (e) evaporation (mm d^{-1}), and (f) sensible heat flux (W m^{-2}) before (solid) and after (dashed) deforestation of the Amazon Basin (after Zhang *et al*., 1996a)

for modellers include the simulation of the dynamic processes associated with vegetation destruction and (potential) regeneration. For example, after tropical deforestation, the climate of the regions may be so modified by the removal of the forest that the forest will be unable to regenerate, even if the land-use disturbance were to be removed.

Palaeoclimate and mineral deposits

Palaeoclimate simulations with GCMs offer modellers the chance to test their models with parameters beyond the normal 'present-day' range (for which the model was probably constructed) and thereby increase confidence in their models. GCMs have been used in simulations of the last glacial maximum ~18 000 BP, and condi-

tions ~6000 BP have been suggested as a useful complement to future climate simulations. Palaeoclimate modelling not only helps us understand the details of past climates, but it also encourages modelling based on physical and biogeochemical processes rather than tuning to match present-day distributions. Palaeoclimatic data, which sometimes only offer classifications such as 'hot–dry' or 'humid' as descriptions of past climates, can be augmented by quantitative determinations of, for example, temperature and precipitation from model simulations. The model simulations can also offer indications of the past climate in areas where no proxy data are available. One such GCM experiment is described below as an example.

Evaporites (such as rock salt and gypsum) form near the boundaries of oceans and in shallow basins that are subject to frequent flooding and desiccation. The levels of salinity that are reached in the basins determine the nature of the evaporite deposits. Regions that are amenable to evaporite formation would be indicated in a GCM by regions where the total precipitation minus total evaporation ($P - E$) is strongly negative. In one study, an evaporite basin model, consisting of a saline 'slab' of water with fixed depth and salinity, was run off-line (that is, the model was run using output from the GCM as forcing data, rather than being coupled to the GCM). This offers no feedback to the GCM climate and, if the feedback is assumed to be small, then this is acceptable. The evaporite basin model was used to determine whether evaporite potentially *could* form rather than to model the process of deposition. The evaporite model (which computed evaporation based on GCM forcing) was forced with a GCM-simulated climate at all model grid points. Figure 6.8a shows the $P - E$ values derived from such a simulation of the Triassic (~225 Ma) when the basin salinity was 35‰. Areas with negative $P - E$ are potential locations where lakes could dry out. The dots show the locations of major known evaporite deposits in North America, South America (around 120°W), Arabia (10°S, 20°W) and the Western Tethys, Central Atlantic region (10°N, 50–80°W). The basin model was run with two different levels of salinity: 35‰ and 300‰. The simulation with salinity at 300‰ (Figure 6.8b, characteristic of the salinity required for the later stages of gypsum formation) therefore shows areas where sustained deposition might occur. Discrepancies between modelled and observed evaporite distribution can be attributed at least in part to small-scale topography that is not resolved by the GCM but are also an indication that the model-simulated climate is not adequate.

By using models such as those described above with different continental configurations and forcings, modellers can make suggestions about the relative strength of other aspects of the climate (such as the salinity-driven deep ocean circulation) in different geological periods. Such assessments have been suggested as a useful component in determining the possible locations of oil-bearing rocks. The formation of such rocks is thought to be linked to sluggish thermohaline circulation, which results in reduced oxygen content of the deep ocean water and hence a reduction in the decay of organic matter. This matter can then accumulate as oil shale in the floors of ocean basins. The GCM is therefore able to provide tentative indications of oil-bearing strata where no direct palaeo-evidence exists.

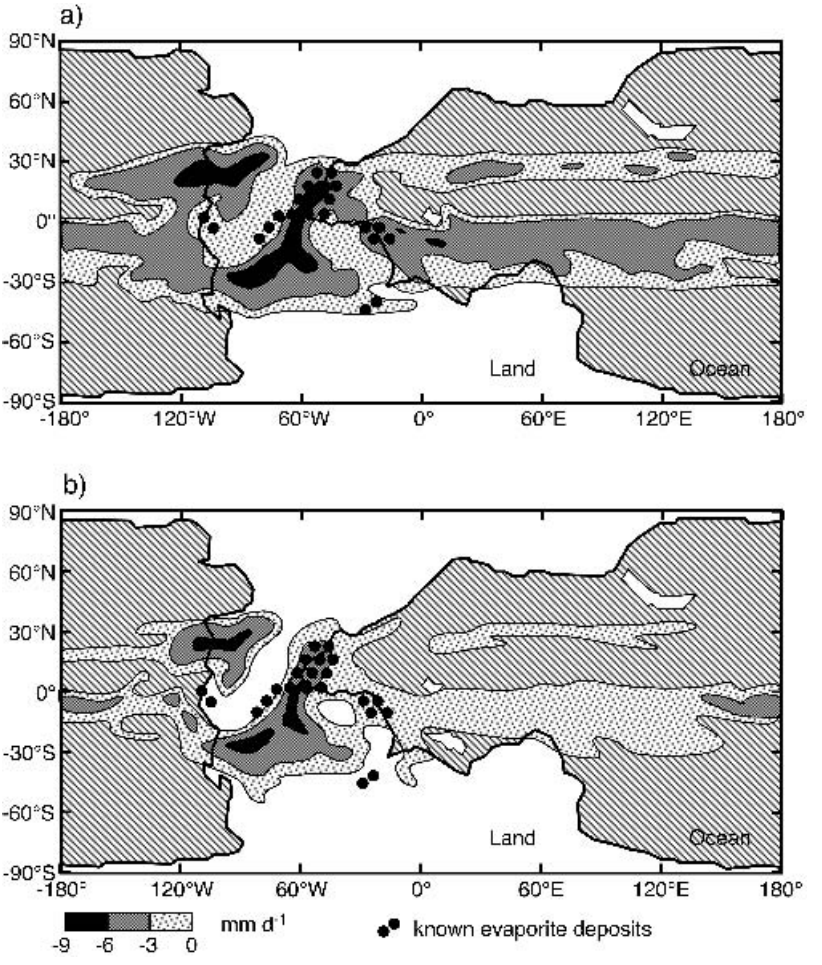

Figure 6.8 Basin model net $P - E$ for the Triassic (225 Ma). Only negative $P - E$ values are shown for clarity. (a) Basin salinity is 35‰. (b) Basin salinity is 300‰. At higher salinities, evaporation is reduced, so the areas where high salinities are required for the evaporite deposition are reduced. Dots show the locations of major known evaporite deposits (from Schutz and Pollard, 1995)

6.5.3 Regional climate prediction

It is clear from the two specific applications described in the previous section (tropical deforestation and mineral deposits) that climate model predictions need to be generated at finer scales than current models if their results are to be of use. The *need* is for regional climate scenarios but, arguably, the most complete models are the coupled GCMs run at coarse resolutions as explained in Chapter 5. This is one of the major problems faced in trying to apply GCM projections to regional impact

assessments. One solution is to employ EMICs developed to emphasize particular aspects of the climate system (see Chapter 4). Another is to 'downscale' GCM predictions.

'Downscaling', as the production of increased temporal and/or spatial resolution climates from GCM results has come to be termed, has three current forms: statistical, regional modelling and time slice simulations (Figure 6.9). In model-based downscaling, a high-resolution, limited-area model is run using boundary forcing from the GCM, or a global atmospheric model is run for limited time 'slices' at high spatial resolution using sea-surface temperatures and sea ice distributions predicted by a lower resolution coupled OAGCM.

Statistical downscaling can take many forms including the assignment of the nearest grid box estimate, statistical analysis of local climatic fields and the merging of several scenarios based on expert judgement. Although GCMs typically have high temporal resolutions, 'downscaling' has also been applied in the time domain because GCM results are found to have rather poor temporal characteristics when examined at time-scales less than about a month.

As modelling techniques continue to develop, the use of global models with enhanced resolution in regions of interest will become more common. Stretched or distorted grids allow a model to be used at high resolution in one part of the domain and at lower resolution in regions of lesser interest. Problems associated with model coupling are eliminated and these models are ideally suited to the massively parallel computer systems of today. In semi-Lagrangian models, grid boxes move with the flow of the atmosphere instead of remaining fixed in space. This transfers the computational work from calculating fluxes in and out of the box to tracking the movement and deformation of each grid box. After several timesteps the original

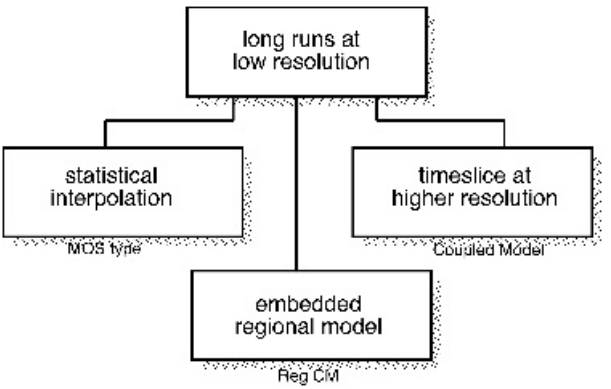

Figure 6.9 Three different techniques: statistical analysis – modelled output statistics (MOS); embedded high-resolution 'regional climate models' (RegCM); and timeslicing (high-resolution global atmospheric model forced by the SST results from a lower-resolution coupled model for a specific time period) are all employed to derive higher-resolution results from low-resolution model simulations for application to regional climate simulation

grid must be reimposed so that grid boxes do not become too severely deformed. The semi-Lagrangian technique improves conservation properties and may reduce computational requirements. It can be used in any type of finite grid method, and in combination with adaptive mesh refinement.

Unfortunately, all the currently available means of downscaling, and hence of producing climate change scenarios at a useful regional spatial resolution, have some limitations. This was demonstrated most clearly in the 1990s by a European Union-sponsored comparison of regional model simulations from the Hadley Centre (RegCM), the Max Planck Institute (HIRHAM) and Météo-France's variable resolution GCM with high resolution over Europe, which concluded that, where there were poor regional climates (in the coarse-resolution OAGCM), the dynamic embedding made things worse and that neither downscaling nor embedding can solve problems inherent in the GCM simulation.

6.5.4 Policy development

The Framework Convention on Climate Change (FCCC), signed by 153 countries and the European Community at the United Nations Conference on Environment and Development (UNCED) in Rio de Janeiro in June 1992 and now ratified by 185 states, has as its central goal the stabilization of atmospheric greenhouse gas concentrations at a level that would prevent dangerous anthropogenic interference with the climate system. It also states that this goal should be realized soon enough that ecosystems could adapt naturally to climate change, that food production would not be threatened and that sustainable economic development could proceed. The Convention does not specify, however, the meaning of 'dangerous anthropogenic interference', how its occurrence or the risk of its occurrence should be detected or what measures, applied at what level of stringency, would be justified in avoiding it. The other central concepts in the objective, natural adaptation of ecosystems, threats to food production and sustainable economic development, are also not articulated precisely. These issues clearly transcend the capabilities of climate models which incorporate 'only' physics and biogeochemistry. The demands of the deliberations relating to the Framework Convention on Climate Change, together with other pressures, have prompted the application of climate predictions and, sometimes, the entire incorporation of climate models into a new class of numerical models called integrated assessment models.

Evaluating future climate in this context takes into account the ramifications of human health; food supply; population policies; national economies; international trade and relations; policy formulation and attendant political processes; national sovereignties; human rights; and international, inter-ethnic and inter-generational equity. In considering the estimated damages due to current emissions of greenhouse gases, the arguments for action are now extending beyond 'no regrets' measures – those policies whose benefits, such as reduced energy costs and reduced emissions of conventional pollutants, equal or exceed their cost. Decisions to be taken in the near future will necessarily have to be taken under great uncertainty. However, these

decisions may be very sensitive to the level at which atmospheric concentrations are ultimately stabilized and to the environmental effects on ecosystems – the net productivity of the oceans, the response of trees and forests to carbon dioxide fertilization and climate change, and methane production by thawing tundra. It is clear that evaluation of this large suite of possible responses to the threats implied by projections of future climate must incorporate a myriad of issues outside the scope of conventional climate models but, perhaps, encompassed by integrated assessment models.

It may be valuable to make a distinction between 'integrated assessment' and 'integrated assessment modelling' analogous to the distinction between 'climate assessment' and 'climate modelling'. Most human activities that are affected by weather and climate (e.g. building or reservoir design, swimwear and umbrella sales) are developed or designed in the context of a 'climate assessment'. However, few of these (at least as yet) draw on the results of climate model simulations. Similarly, all nations which are party to the Framework Convention on Climate Change are developing national assessments of the effects of, and possible responses to, climate change. These assessments are 'integrated' in the sense that they include societal, economic and ecological characteristics. Although most nations use results from climate models, relatively few, as yet, draw on the results of integrated assessment models. The developers of these models believe that this situation is changing and that integrated assessments will, in the future, draw much more fully on the results of integrated assessment models. Figure 6.10 depicts one uneasy representation of a future in which an inverted pyramid of integrated assessment is 'balanced' on the existing pyramid of climate modelling.

The criteria that governments are likely to consider when selecting future policies include distributional (including inter-generational) equity, flexibility in the face of technological change and new information, efficiency or cost-effectiveness, compatibility with the institutional structure and existing policies, and understandability to the general public. A mix of political instruments is likely to be needed in order to achieve the best results. Governments may apply different criteria with different weights to the selection of international and domestic policy instruments. Cost-effectiveness should always be a criterion for selecting policy instruments, but it becomes more important at both the international and domestic levels as the abatement effort becomes more stringent. The immense challenges for integrated assessment include identifying the political processes that will lead and guide change, recognizing the information needs of that process, conducting the physical and social-science research needed to fill those information needs, and presenting that information in a candid and understandable manner.

6.6 INTEGRATED ASSESSMENT MODELS

In some ways, the development of integrated assessment models is similar to the history of climate models, including different disciplinary perspectives and different views on the need for capturing all processes as compared with parameterizing

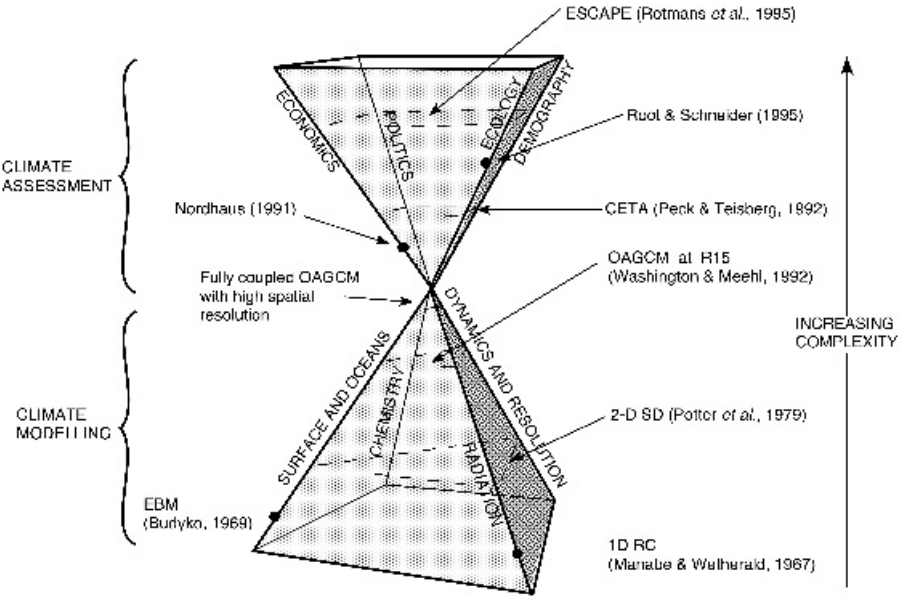

Figure 6.10 The assessment pyramid is delicately balanced on top of the hierarchy of climate models

behaviour in terms of a few better understood variables. There are also many differences between climate modelling and integrated assessment modelling, particularly the lack of 'laws' or guidelines describing social, political, technological and economic changes and the need, or preference, for multiple scenarios of the future as compared with the goal of predicting the climate.

The history of integrated assessment modelling is much shorter than that of climate modelling (around 10 years as compared with over 40 years) but, despite the relative youth of the subject, there are a substantial number of integrated assessment models (Table 6.6) and many of the EMICs described in Chapter 4 have been developed for, or are being applied to, climate assessment. There is, as yet, little documentation of the relative strengths and weaknesses of the available integrated assessment models but some general characteristics can be recognized: (i) integrated assessment models should offer added value compared to single disciplinary (e.g. climate) oriented assessment; and (ii) integrated assessment models should provide useful information to decision makers.

All integrated assessment models attempt to represent and predict the relationships between human society and the environment with a primary focus on climatic change, its causes and effects (Figure 6.11). They have been roughly grouped in terms of top-down versus bottom-up schemes. 'Top-down' models are aggregate models, often based on macroeconomic models, that analyse how changes in one sector of the economy affect other sectors and regions. Early top-down models

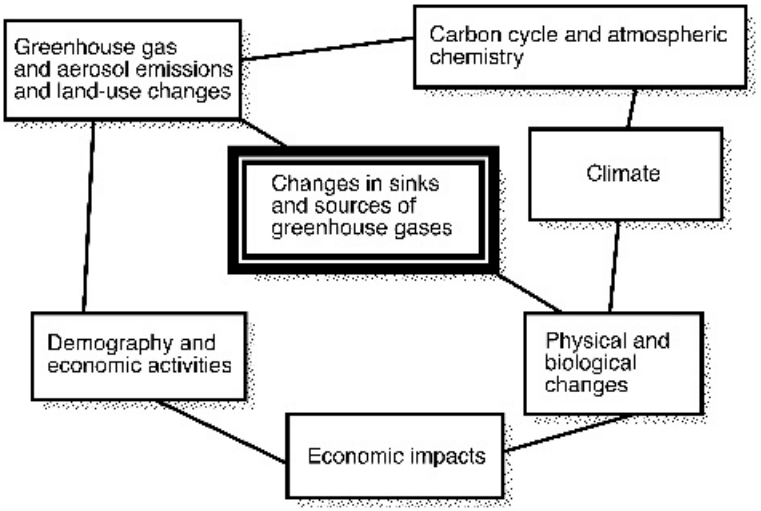

Figure 6.11 Some elements of, and interactions in, the integrated assessment (IA) process. In this example, the focus is on greenhouse impacts and possible responses

tended to contain little detail on energy consumption, especially at the technology-specific level, but included explicit treatment of behaviour and economic interactions. In contrast, 'bottom-up' models tended to describe energy consumption in detail, while consumer behaviour and interactions with other sectors of the economy originally tended to be dealt with much less thoroughly. Recent integrated assessment models have tended to provide greater detail in areas that were previously less developed so that differences in model results are increasingly driven by differences in input assumptions rather than in model structure. Nevertheless, differences in integrated assessment model structure remain important because, as is the case with climate models, different model types are better suited to answer different types of questions.

The similarities between climate models and integrated assessment models also extend to the underlying philosophy of the model developers. These different philosophies can be characterized, in their extreme forms, as either (i) a small and highly generalized group of equations or (ii) a very large number of equations. In climate modelling, these paradigms are represented by (i) EBMs or simple box models (Chapter 3) and (ii) coupled ocean–atmosphere global climate models (Chapter 5). In integrated assessment, they are represented by (i) simple economic forms (termed response surfaces or reduced form models) and (ii) very complex systems of equations designed to capture all the processes under consideration. Examples of these two extreme forms of models are DICE and TARGETS, which can be seen in Table 6.6 to capture very different numbers of processes explicitly.

Table 6.6 Summary characterization of integrated assessment models (after Dowlatabadi and Rotmans, 1997)

Model	***Forcings***	***Geographic specificity***	***Socio-economic dynamics***	***Geophysical simulation***	***Impact assessment***	***Treatment of uncertainty***	***Treatment of decision making***
	0. CO_2 *1. other GHG* *2. aerosols* *3. land use* *4. other*	*0. global* *1. continental* *2. countries* *3. grids/ basins*	*0. exogenous* *1. economics* *2. tech choice* *3. land use* *4. demographic* *5. cultural perspectives*	*0. ΔF* *1. Global ΔT* *2. 1-D ΔT, ΔP* *3. 2-D ΔT, ΔP*	*0. ΔT indexed* *1. sea-level rise* *2. agriculture* *3. ecosystems* *4. health*	*0. none* *1. basic* *2. advanced*	*0. optimization* *1. simulation* *2. simulation with adaptive decisions*
AIM	0,1,2,3,4	2,3	1,2,3,4	2,3	0,1,2,3	0	1
CETA	0	0,1	1,2	1	0	1	0
Connecticut	0	0	1	1	0	1	0
CSERGE	0	0	1	1	0	1	0
DICE	0	0	1	1	0	1	0
CFUND	0,1	1	1	0	0,1,2,3,4	2	0
Grubb	0	0	1	1	0	1	0
ICAM-2	0,1,2,3	1,2	1,3,4	2,3	0,1,3	2	1,2
IMAGE 2.0	0,1,2,3	3	0,2,3	3	1,2,3	1	1
MERGE 2.0	0,1	1	1,2	1	0	1	0
MiniCAM	0,1,2,3	2,3	1,2,3	3	0	1	1
MIT	0,1,2,3	2,3	1	3	0,2,3	1	0,1
PAGE (EEC)	0,1	1,2	1	1	0,1,2,3,4	2	1
PEF	0,1	1	0	1	0	2	1
ProCAM	0,1,2,3	2,3	1,2,3,4	3	0,2	1	1
TARGETS	0,1,2,3,4	0	1,2,3,4,5	2	1,2,3,4	2	1,2

There is a second characteristic of integrated assessment models which is shared with climate models: the issue keenly felt in the integrated assessment community of whether to focus on precision or accuracy. Examples of the two extreme forms are IMAGE-2 which projects location-specific changes in 1/2° by 1/2° grid cells across the Earth, and ICAM-2 which is designed to deliver probability estimates of likely futures but intentionally avoids location-specific projections, generating instead aggregated outcomes for the world. Both modelling paradigms have strengths and weaknesses as is the case with climate modelling where the analogy might be with the 'accuracy' of the global responses predicted by a 1D RC (Chapter 4) as compared to the apparent precision of a high resolution OAGCM (Chapter 5). However, the contrast between model types appears, and probably is, very much more stark for integrated assessment models than for climate models because of the inherently 'unknowable' nature of the fully integrated human and environmental system (*cf.* the EMICs in Chapter 4).

Recently, simple integrated assessment models have been used to devise new stabilization profiles that explicitly (albeit qualitatively) incorporate economic considerations, estimate the corresponding anthropogenic emissions requirements and assess the significance of the profiles in terms of the global mean temperature and sea-level changes. These calculations are a response to Article 3 of the Framework Convention which states that 'policies and measures to deal with climate change should be cost-effective so as to ensure global benefits at the lowest possible cost' since they assume that if two greenhouse gas emission futures were indistinguishable in terms of their environmental implications, then the emission future with the lower mitigation (i.e. emissions reduction) costs would be preferred. Thus this integrated assessment model adds an additional constraint to the usual three: (i) prescribed initial (1990) greenhouse gas concentrations and rate of change of concentrations; (ii) a range of prescribed stabilization levels and attainment dates; and (iii) the requirement that the implied emissions should not change too abruptly. To these is added (iv) that the resulting emissions trajectories initially track a 'business as usual' path: an idealization of the assumption that the initial departure from the business as usual path would be slow, for economic and developmental reasons which include (a) the further into the future the economic burden lies, the smaller the present resource base required to undertake it; (b) time is therefore needed to re-optimize the capital stock; and (c) the availability of substitutes is likely to improve and their costs to reduce over time.

The results of these global-mean calculations are pathway-related differentials up to about 0.2°C in global mean temperature and 4 cm in global mean sea-level change. In benefit–cost analyses of climate change policy options, the implications for market (e.g. agriculture, timber, fisheries) and non-market (e.g. biodiversity, environmental quality, human health) impacts of these climatic differentials are unclear. The cost of a more economical transition away from fossil fuels depends on the regional details associated with the projected climate changes in these and other key climate variables. Great uncertainty surrounds these evaluations.

6.7 THE FUTURE OF CLIMATE MODELLING

This book has been written with the basic aim of building up a framework within which all types of climate models can be considered. The need to recruit scientists, social and economic researchers, and political and demographic planners and policy-makers into climate modelling and assessment has never been greater. We have also drawn readers' attention to unexpected results of climate modelling and to the continuing need for a spectrum of models, from the simplest EBM to the most complex coupled climate model, as a way of aiding understanding of the climate system.

Climate change imposes a variety of impacts on society. Future climate changes are likely to include effects on agriculture, forests, water resources, the costs of heating and cooling, the impact of a rising sea level on small island states and low-lying coastal areas, and this generation's choice of nuclear waste disposal and perhaps carbon sequestration sites.

Any climate change presents society as a whole with a set of formidable difficulties: large uncertainties, the potential for irreversible damages or costs, a very long planning horizon, long time lags between causes and effects, the potential for there to be 'losers' as well as 'winners', and an irreducibly global problem with very wide, but as yet unknowable, regional variations. Beyond these tangible impacts are a variety of intangible effects, including damage to existing ecosystems and the threat of species loss. Climate scientists agree that greenhouse gas emissions are rising and that both industrial and biomass-derived aerosols will continue to be emitted. They agree on the mechanisms linking these changes to climate, but do not yet agree on the speed of change, or the ultimate amount of change. In addition, social scientists do not agree on the size of the behavioural responses or economic effects that would follow, or on the effect of these changes on well-being. Climate change, by its nature, is a global challenge.

Despite the very considerable importance of, for example, human-induced warming and stratospheric ozone depletion and the relevance of climate model predictions to their understanding and ultimate solution, it needs to be recognized that a warmer planet and higher surface UV radiation are not the only possible benefits or future hazards. Climate models also predict a 'nuclear' winter and very similar climate catastrophes resulting from a meteorite impact on Earth. The Earth's climate has been shown to be susceptible to long-term changes in solar radiation and its distribution by models which also predict that human-induced land-use change can cause regional shifts in climate of similar magnitude to those likely to be caused by greenhouse warming and industrial aerosols.

These challenges continue to be the concern of climate modellers around the world. The range of application of climate models is great. Modellers cannot answer all the questions about the climate system, but the continuing search for a more complete understanding of the climate system is a most laudable and fascinating endeavour.

The developments that we see now in coupled models are the result of a long history of simpler studies that provided the basis for the components that are now

included in EMICs and in GCMs. As our understanding of the climate system improves through observation and analysis, the use of these models and the computational resources devoted to climate modelling continue to increase. Thus, continuing sophistication and improved validation can be anticipated. One aspect of future climate models will be continuing synergy and tension between simpler (e.g. EMIC) and more complex (e.g. GCM) model types and their respective capabilities to deliver predictions of value for policy development.

Climate modellers have yet to tackle some aspects of their science. For example, the climate system is currently modelled by systems of coupled, non-linear differential equations. Chaotic behaviour is the prime characteristic of all such systems. This results in unpredictable fluctuations at many time-scales and a tendency for the system to jump between highly disparate states. It is not yet known if chaos is the primary characteristic of the climate system but the Earth's climate has been documented as undergoing very rapid transitions on time-scales of decades to centuries. There is no reason to believe that this characteristic will disappear in the future. Similarly, it is now well-established that the Earth's climatic history has included catastrophic events induced by the impacts of comets and asteroids. A body 2 km in diameter impacting on the Earth is estimated as having a 1 in 10 000 chance of occurrence in the next 100 years. Catastrophic climatic shifts including very rapid cooling and a massive reduction in incident solar radiation at the surface will follow such an impact and will persist for, at the least, hundreds of years.

Numerical models of long-period climatic evolution indicate that, in the absence of human-induced climate warming, the Earth would tend to move into cooler climatic conditions culminating in a full glacial epoch. Quasi-oscillatory cooling would be expected with progressively colder episodes occurring around 5000, 23 000 and 60 000 years into the future. The culminating glaciation occurring 60 000 years in the future is predicted as having a similar intensity to the last glacial maximum. Based on astronomical forcing alone, the Earth would not be expected to return to conditions similar to the current Holocene thermal optimum any earlier than 120 000 years from now. One possible result of anthropogenerated global warming is that enhanced greenhouse warming will so greatly weaken the positive feedback mechanisms which are believed to transform the relatively weak orbital forcing signal into global interglacial–glacial cycles that the initiation of any future glaciations will be prevented indefinitely. The possibility of chaotic characteristics and the proposal that anthropogenic effects might shift the Earth's climate into a new state are topics that could benefit from probing by future climate models.

Human beings are curious: we seek to understand and hence to predict. Although we cannot, yet, predict future climates, we often behave as if we can. Policy, development, business, financial and even personal decisions are made every day around the world as if we knew what climates people will face in the future. While local-scale climatic dependencies may remain weak in many places, technology and engineering, international trade and aid, food and water resources are likely to become increasingly dependent upon, and even an integral part of, the climate system (Figure 1.2). Human infrastructure and well-being are dependent upon the climate and so

the desire to predict future climates is not driven solely by curiosity but by a need to plan for the possible future system states. So far our predictive skills are rather poor.

Improved understanding by politicians and policy-makers, and by those who vote governments into power, of all aspects of the climate system is one way of increasing the chances of sustaining Earth's climate in an hospitable state. Although technology and the harnessing of natural resources appear to have decreased the need to predict weather and climate, industrial, architectural, agricultural and water resource developments, such as oil and gas pipelines laid across melting permafrost, aircraft icing incidents, floods, droughts, air pollution and extreme heatwaves, cost lives and revenue every year. International policies regarding the global climate have been successfully negotiated and some (for example, the Montreal Protocol) implemented, while others, such as the Kyoto Protocol of the Framework Convention on Climate Change, which calls for a reduction in emission of greenhouse gases, have yet to be ratified by many nations.

Now you have read about the wide range of models available, it must be clear that models have not developed in clear-cut ways in direct response to needs or in some ordained hierarchy. Rather, they have advanced, and sometimes retreated, when new observations, new ideas, increased computational power and failures and successes in evaluation and intercomparison exercises have become known. There is no one 'right' climate model or even one 'best' climate model type. All have the potential to add value if they are honestly evaluated and appropriately applied.

RECOMMENDED READING

Alcamo, J. (ed.) (1994) *Image 2.0: Integrated Modelling of Global Climate Change*. Kluwer Academic Publishers, Dordrecht, The Netherlands, 328 pp.

Cess, R.D., Potter, G.L., Blanchet, J.P., Boer, G.J., Del Genio, A.D., Déqué, M., Dymnikov, V., Galin, V., Gates, W.L., Ghan, S., Kiehl, J.T., Lacis, A.A., Le Treut, H., Li, Z-X., Liang, X-Z., McAvaney, B.J., Meleshko, V.P., Mitchell, J.F.B., Morcrette, J-J., Randall, D.A., Rikus, L., Roeckner, E., Royer, J.F., Schlese, U., Sheinin, D.A., Slingo, A., Sokolov, A.P., Taylor, K.E., Washington, W.M., Wetherald, R.T., Yagai, I. and Zhang, M-H. (1990) Intercomparison and interpretation of climate feedback processes in 19 atmospheric general circulation models. *J. Geophys. Res.* **95**, 16 601–16 615.

Chao, H.P. and Peck, S.C. (2000) Greenhouse gas abatement: How much? Who pays? *Resource & Energy Economics* **22**, 1–20.

Covey, C., AchutaRao, K., Cubasch, U., Jones, P., Lambert, S.J., Mann, M.E., Phillips, T.J. and Taylor, K.E. (2001) An overview of results from the Coupled Model Intercomparison Project (CMIP). *Global Planet. Change* **37**, 103–133.

Dowladabati, H. and Morgan, M.G. (1993) A model framework for integrated assessment of the climate problem. *Energy Policy* **21**, 209–221.

Gates, W.L. (1992) AMIP: The atmospheric model intercomparison project. *Bull. Amer. Meteor. Soc.* **73**, 1962–1970.

Gates, W.L. (1996) *Proceedings of the first AMIP scientific conference* (*15–19 May 1995, Monterey, CA*), WMO Technical Document No. 732, World Meteorological Organization, Geneva, 552 pp.

Henderson-Sellers, A. (1987) Effects of change in land-use on climate in the humid tropics. In R.E. Dickinson (ed.) *The Geophysiology of Amazonia*. John Wiley & Sons, New York, pp. 463–93.

Henderson-Sellers, B. (1997) *A BOOK of Object-Oriented Knowledge*, 2nd edition. Prentice Hall, Upper Saddle River, NJ, 253 pp.

Henderson-Sellers, A., Pitman, A.J., Love, P.K., Irannejad, P. and Chen, T.H. (1995) The project for intercomparison of land-surface parameterization schemes (PILPS): Phases 2 & 3. *Bull. Amer. Meteor. Soc*. **76**, 489–503.

Houghton, J.T., Meira Filho, L.G., Callander, B.A., Harris, N., Kattenberg, A. and Maskell, K. (eds) (1996) *The Science of Climate Change; The Second Assessment Report of the Intergovernmental Panel on Climate Change: Contribution of Working Group I*. Cambridge University Press, Cambridge, 572 pp.

Howe, W. and Henderson-Sellers, A. (1997) Evolution of the MECCA project. In W. Howe and A. Henderson-Sellers (eds) *Assessing Climate Change: The Story of the Model Evaluation Consortium for Climate Assessment*. Gordon and Breach, London, pp. 29–51.

Luther, F.M., Ellingson, R.G., Fouqart, Y., Fels, S., Scott, N.A. and Wiscombe, W. (1988) Intercomparison of radiation codes in climate models (ICRCCM): longwave clear-sky results – a workshop summary. *Bull. Amer. Meteor. Soc*. **69**, 40–48.

McCarthy, J.J., Canziani, O.F., Leary, N.A., Dokken, D.J. and White, K.S. (eds) (2001) *Climate Change 2001: Impacts, Adaptation & Vulnerability, Contribution of Working Group II to the Third Assessment Report of the Intergovernmental Panel on Climate Change* (*IPCC*), Cambridge University Press, Cambridge, UK, 1000 pp.

Metz, B., Davidson, O., Swart, R. and Pan, J. (eds) (2001) *Climate Change 2001: Mitigation, Contribution of Working Group III to the Third Assessment Report of the Intergovernmental Panel on Climate Change* (*IPCC*). Cambridge University Press, Cambridge, UK, 700 pp.

Nordhaus, W.D. (1991) To slow or not to slow: the economics of the greenhouse effect. *The Economic Journal* **101**, 920–937.

Peck, S. and Teisberg, T.J. (1992) CETA: A model for carbon emissions trajectory assessment. *The Energy Journal* **13**, 55–77.

Pollard, D. and Schulz, M. (1994) A model for the potential locations of Triassic evaporite basins driven by palaeoclimatic GCM simulations. *Glob. Plan. Change* **9**, 233–249.

Root, T.L. and Schneider, S.H. (1995) Ecology and climate: research strategies and implications. *Science* **269**, 334–341.

Rotmans, J., Hulme, M. and Downing, T. (1995) Climate change implications for Europe. *Glob. Env. Change* **4**, 97–124.

Schlosser, C.A., Slater, A.G., Robock, A., Pitman, A., Vinnikov, K.Ya., Henderson-Sellers, A., Speranskaya, N.A., Mitchell, K. and PILPS 2(d) Contributors (2000) Simulations of a boreal grassland hydrology at Valdai, Russia: PILPS Phase 2(d). *Mon. Wea. Rev.* **128**, 301–321.

Skiles, J.W. (1995) Modelling climate change in the absence of climate change data. *Climatic Change* **30**, 1–6.

Taplin, R. (1996) Climate science and politics: the road to Rio and beyond. In T. Giambelluca and A. Henderson-Sellers (eds) *Coupled Climate System Modelling: A Southern Hemisphere Perspective*. John Wiley & Sons, Chichester, 377–395.

VEMAP (1995) Vegetation/ecosystem modelling and analysis project (VEMAP): Comparing biogeography and biogeochemistry models in a continental scale study of terrestrial ecosystem responses to climate change and CO_2 doubling. *Glob. Biogeo. Cyc*. **9**, 407–437.

Wetherald, R.T. and Manabe, S. (1988) Cloud feedback processes in a general circulation model. *J. Atmos. Sci*. **45**, 1397–1415.

Wigley, T.M.L. and Santer, B.D. (1990) Statistical comparison of spatial fields in model validation, perturbation and predictability experiments. *J. Geophys. Res*. **95**, 857–865.

Wigley, T.M.L., Richels, R. and Edmonds, J.A. (1996) Stabilizing CO_2 concentrations: the choice of emissions pathway. *Nature* **379**, 240–243.

Web resources

http://unidata.ucar.edu/	Unidata Home: Tools and data for climate research
http://www-pcmdi.llnl.gov/	Program for Climate Model Diagnosis and Intercomparison
http://www.gewex.org/	Global Energy and Water Cycle Experiment
http://www.wmo.ch	World Meteorological Organization
http://www.clivar.org/science/mips.htm	CLIVAR Catalogue of Model Intercomparison Projects
http://www.esmf.ucar.edu/	The Earth System Modelling Framework
http://www.ipcc.ch	The Intergovernmental Panel on Climate Change
http://www.lmd.jussieu.fr/ALMA/	The ALMA data exchange convention
http://www.es.jamstec.go.jp/esc/eng/ES/	The Earth Simulator

Appendix A Twentieth-century Classics

This book was first conceived as an introduction to climate modelling in late 1985. In the intervening 20 years, the volume of climate modelling literature has expanded enormously, particularly in response to the IPCC assessments. Recognizing that any climate modelling neophyte may feel overwhelmed by the volume of books and research papers that exist on the topic, we have taken this opportunity to present a distillation of some of the classics of the climate literature from its inception to 2000.

We have tried to pick out not only consolidating material, such as review papers and textbooks, but also other significant papers that have highlighted the development of climate modelling. This is by no means an objective process: there can be no definitive list of 'best' climate modelling references. However, in addition to our own prejudices, we also present the enthusiasms of a few, select colleagues. We hope that you will get a flavour for the thrill of discovery that accompanies climate modelling and, through this 'original source' material, come to understand milestones that have made this exciting discipline what it is today.

EBMs and other 'simple' models

Budyko, M.I. (1969) The effect of solar radiation variations on the climate of the Earth. *Tellus* **21**, 611–619.

Sellers, W.D. (1969) A global climatic model based on the energy balance of the Earth–atmosphere system. *J. Appl. Met.* **8**, 392–400.

Schneider, S.H. and Gal-Chen, T. (1973) Numerical experiments in climate stability. *J. Geophys. Res.* **78**, 6182–6194.

North, G.R. (1975) Theory of energy balance climate models. *J. Atmos. Sci.* **32**, 3–15.

Ramanathan, V. (1976) Radiative transfer within the Earth's troposphere and stratosphere: A simplified radiative–convective model. *J. Atmos. Sci.* **33**, 1330–1346.

Wigley, T.M.L., Raper, S.C.B., Hulme, M. and Smith, S. (2000) The MAGICC/SCENGEN Climate Scenario Generator: Version 2.4, Technical Manual, Climatic Research Unit, UEA, Norwich, UK, 48 pp. [Available online at http://www.cru.uea.ac.uk/~mikeh/software/manual.pdf].

A Climate Modelling Primer, Third Edition. K. McGuffie and A. Henderson-Sellers.

ISBN: 0-470-85750-1 (HB); 0-470-85751-X (PB)

Classic model experiments

Phillips, N.A. (1956) The general circulation of the atmosphere: A numerical experiment. *Quart. J. Roy. Meteor. Soc*. **82**, 123–164.

Revelle, R. and Suess, H.E. (1957). Carbon dioxide exchange between atmosphere and ocean and the question of an increase of atmospheric CO_2 during the past decades. *Tellus* **9**, 18–27.

Lorenz, E.N. (1963) Deterministic, non periodic flow. *J. Atmos. Sci.* **20**, 130–141.

Manabe, S. and Strickler, R.F. (1964) Thermal equilibrium of the atmosphere with a convective adjustment. *J. Atmos. Sci.* **21**, 361–385.

Leith, C.E. (1965) Numerical simulation of the Earth's atmosphere. In B. Adler *et al.* (eds) *Methods in Computational Physics*. Academic Press, NY, **4**, 1–28.

Manabe, S., Smagorinsky, J. and Strickler, R.F. (1965). Simulated climatology of a general circulation model with a hydrologic cycle. *Mon. Wea. Rev.* **93**, 763–798.

Manabe, S. and Wetherald, R.T. (1967) Thermal equilibrium of the atmosphere with a given distribution of relative humidity. *J. Atmos. Sci.* **24**, 241–259.

Schneider, S.H. and Dickinson, R.E. (1974) Climate modeling. *Rev. Geophys. Space Phys.* **12**, 447–493.

Manabe, S. and Wetherald, R.T. (1975) The effect of doubling the CO_2 concentration on the climate of a general circulation model. *J. Atmos. Sci.* **32**, 3–15.

Wetherald, R.T. and Manabe, S. (1975) The effects of changing the solar constant on the climate of a general circulation model. *J. Atmos. Sci.* **32**, 2044–2059.

Chervin, R.M. and Schneider, S.H. (1976) On determining the statistical significance of climate experiments with General Circulation Models. *J. Atmos. Sci.* **33**, 405–412.

Lyne, W.H., Rowntree, P.R., Temperton, C. and Walker, J.M. (1976) Numerical modelling using GATE data. *Meteorol. Mag*. **105**, 261–271.

Chervin, R.M., Washington, W.M. and Schneider, S.H. (1976) Testing the statistical significance of the response of the NCAR general circulation model to North Pacific Ocean Surface Temperature Anomalies. *J. Atmos. Sci.* **33**, 413–423.

Ramanathan, V. and Dickinson, R.E. (1979) The role of stratospheric ozone in the zonal and seasonal radiative energy balance of the Earth–troposphere system. *J. Atmos. Sci.* **36**, 1084–1104.

Manabe, S. and Stouffer, R.J. (1980) Sensitivity of a global climate model to an increase of CO_2 concentration in the atmosphere. *J. Geophys. Res.* **85**, 5529–5554.

Schneider, S.H. and Thompson, S.L. (1981) Atmospheric CO_2 and climate: importance of the transient response. *J. Geophys. Res.* **86**, 3135–3147.

Hansen, J., Johnson, D., Lacis, A., Lebedeff, S., Lee, P., Rind, D. and Russell, G. (1981) Climate impact of increasing carbon dioxide. *Science* **213**, 957–966.

Shine, K.P. and Henderson-Sellers, A. (1983) Modelling climate and the nature of climate models: A review. *J. Climatol.* **3**, 81–94.

Joussaume, S., Sadourny, R. and Jouzel, J. (1984) A general circulation model of water isotope cycles in the atmosphere. *Nature* **311**, 24–29.

Washington, W.M. and Meehl, G.A. (1984) Seasonal cycle experiment on the climate sensitivity due to a doubling of CO_2 with an atmospheric general circulation model coupled to a simple mixed layer ocean model. *J. Geophys. Res.* **89**, 9475–9503.

Crowley, T.J., Short, D.A., Mengel, J.G. and North, G.R. (1986) Role of seasonality in the evolution of climate during the last 100 million years. *Science* **231**, 579–584.

Hansen, J., Fung, I., Lacis, A., Rind, D., Lebedeff, S., Ruedy, R., Russell, G. and Stone, P. (1988) Global climate changes as forecast by Goddard Institute for Space Studies three-dimensional model. *J. Geophys. Res.* **93**, 9341–9364.

Mitchell, J.F.B. (1989) The 'greenhouse' effect and climate change. *Rev. Geophys.* **27**, 115–139.

Stouffer, R.J., Manabe, S. and Bryan, K. (1989) Interhemispheric asymmetry in climate response to a gradual increase of atmospheric CO_2. *Nature* **342**, 660–662.

Gates, W.L. (1992) AMIP: The Atmospheric Model Intercomparison Project. *Bull. Amer. Meteor. Soc.* **73**, 1962–1970.

Penner, J.E., Dickinson, R.E.D. and O'Neil, C. (1992) Effects of aerosol from biomass burning on the global radiation budget. *Science* **256**, 1432–1434.

Cubasch, U., Santer, B.D., Hellbach, A., Hegerl, G.C., Höck, H., Maier-Reimer, E., Mikolajewicz, U., Stössel, A. and Voss, R. (1994) Monte Carlo climate change forecasts with a global coupled ocean–atmosphere model. *Clim. Dyn.* **10**, 1–19.

Houghton, J.T., Meira Filho, L.G., Callander, B.A., Harris, N., Kattenberg, A. and Maskell, K. (eds) (1996) *Climate Change 1995. The Science of Climate Change*. Cambridge University Press, Cambridge, 572 pp.

Cubasch, U., Hegerl, G.C., Voss, R., Waszkewitz, J. and Crowley, T.C. (1997) Simulation with an O–AGCM of the influence of variations of the solar constant on the global climate. *Clim. Dyn.* **13**, 757–767.

Dynamics

Smagorinsky, J. (1963) General circulation experiments with the primitive equations. I. The basic experiment. *Mon. Wea. Rev.* **91**, 99–164.

Bourke, W., McAvaney, B., Puri, K. and Thurling, R. (1977) Global modelling of atmospheric flow by spectral methods. In J. Chang (ed.), *Methods in Computational Physics*, Vol. 17. Academic Press, New York, pp. 267–324.

Hoskins, B. and Karoly, D.J. (1981) The steady linear response of a spherical atmosphere to thermal and orographic forcing. *J. Atmos. Sci.* **38**, 1179–1196.

Gordon, C.T. and Stern, W.F. (1982) A description of the GFDL global spectral model. *Mon. Wea. Rev.* **110**, 625–644.

Washington, W.M. and Parkinson, C. (1986) *An Introduction to Three-Dimensional Climate Modelling.* University Science Books, New York, 450 pp.

Schlesinger, M.E. (ed.) (1987) *Physically Based Climate Models and Climate Modelling.* Proceedings of a NATO ASI, Reidel, Dordrecht, 1062 pp.

Williamson, D.L. and Rasch, P.J. (1989) Two-dimensional semi-Lagrangian transport with shape-preserving interpolation. *Mon. Wea. Rev.* **117**, 102–129.

Meehl, G.A. (1990) Seasonal cycle forcing of El Niño in a global coupled ocean–atmosphere climate model. *J. Climate* **3**, 72–98.

Meehl, G.A. and Washington, W.M. (1993) South Asian summer monsoon variability in a model with doubled atmospheric carbon dioxide concentration. *Science* **260**, 1101–1104.

Held, I.M. and Suarez, M.J. (1994) A proposal for the intercomparison of the dynamical cores of atmospheric general circulation models. *Bull. Amer. Meteor. Soc.* **75**, 1825–1830.

Trenberth, K.E. and Hurrell, J.W. (1994) Decadal atmosphere–ocean variations in the Pacific. *Clim. Dyn.* **9**, 303–319.

Gregory, D., Shutts, G.J. and Mitchell, J.R. (1998) A new gravity wave drag scheme incorporating anisotopic orography and low level wave breaking: impact upon the climate of the UK Meteorological Office Unified Model. *Quart. J. Roy. Meteor. Soc.* **124**, 463–493.

Clouds and radiation

Schneider, S.H. (1972) Cloudiness as a global climatic feedback mechanism: The effects on the radiation balance and surface temperature of variations in cloudiness. *J. Atmos. Sci.* **29**, 1413–1422.

Lacis, A.A. and Hansen, J.E. (1974) A parameterization for the absorption of solar radiation in the Earth's atmosphere. *J. Atmos. Sci.* **31**, 118–133.

Arakawa, A. and Schubert, W.H. (1974) Interaction of a cumulus cloud ensemble with the large scale environment, Part 1. *J. Atmos. Sci.* **31**, 674–701.

Arakawa, A. (1975) Modeling clouds and cloud processes for use in climate models. In *The Physical Basis of Climate and Climate Modelling*. GARP Publications Series No. 16, 181–197, ICSU/WMO, Geneva.

Fels, B.S. and Schwarzkopf, M.D. (1975) The simplified exchange approximation – A new method for radiative transfer calculation. *J. Atmos. Sci.* **32**, 1475–1488.

Joseph, J.H., Wiscombe, W.J. and Weinman, J.A. (1976) The delta–Eddington approximation for radiative flux transfer. *J. Atmos. Sci.* **33**, 2452–2459.

Twomey, S. (1977) The influence of pollution on the shortwave albedo of clouds. *J. Atmos. Sci.* **34**, 1149–1152.

Twomey, S. and Seton, K.J. (1980) Inferences of gross microphysical properties of clouds from spectral reflectance measurements. *J. Atmos. Sci*. **37**, 1065–1069.

Cess, R.D., Briegleb, B.P. and Lian, M.S. (1982) Low-latitude cloudiness and climate feedback: Comparative estimates from satellite data. *J. Atmos. Sci.* **39**, 53–59.

Ramanathan, V. and Downey, P. (1986) A nonisothermal emissivity and absorptivity formulation for water vapour. *J. Geophys. Res.* **91**, 8649–8666.

Cess, R.D., Potter, G.L., Blanchet, J.P., Boer, G., Ghan, S.J., Kiehl, J.T., Liang, X-Z., Mitchell, J.F.B., Morcrette, J-J., Randall, D.A., Riches, M.R., Roeckner, E., Schlese, U., Slingo, A., Taylor, K.E., Washington, W.M., Wetherald, R.T. and Yagai, I. (1989) Intercomparison and interpretation of cloud-climate feedback as produced by fourteen atmospheric general circulation models. *Science* **245**, 513–516.

Randall, D.A. (1989) Cloud parameterization for climate models: Status and prospects. *Atmospheric Research* **23**, 345–362.

Ramanathan, V., Cess, R.D., Harrison, E.F., Minnis, P., Barkstrom, B.R., Ahmand, E. and Hartmann, D. (1989) Cloud radiative forcing and climate: results from the Earth Radiation Budget Experiment. *Science* **243**, 57–63.

Senior, C.A. and Mitchell, J.F.B. (1993) CO_2 and climate: the impact of cloud parameterizations. *J. Climate* **6**, 393–418.

Cess, R.D., Zhang, M.H., Minnis, P., Corsetti, L., Dutton, E.G., Forgan, B.W., Garber, D.P., Gates, W.L., Hack, J.J., Harrison, E.F., Jing, X., Kiehl, J.T., Long, C.N., Morcrette, J-J., Potter, G.L., Ramanathan, V., Subasilar, B., Whitlock, C.H., Young, D.F. and Zhou, Y. (1995) Absorption of solar radiation by clouds: observations versus models. *Science* **267**, 496–499.

Cusack, S., Slingo, A., Edwards, J.M. and Wild, M. (1998) The radiative impact of a simple aerosol climatology on the Hadley Centre GCM. *Quart. J. Roy. Meteor. Soc.* **124**, 2517–2526.

The ocean

Bryan, K. (1969) A numerical method for the study of the world ocean. *J. Comp. Phys.* **4**, 347–376.

Hoffert, M.I., Wey, Y.C., Callegari, A.J. and Broecker, W.S. (1978) Atmospheric response to deep sea injections of fossil fuel carbon dioxide. *Clim. Change* **2**, 53–68.

Hoffert, M.I., Callegari, A.J. and Hsieh, C-T. (1980) The role of deep sea heat storage in the secular response to climatic forcing. *J. Geophys. Res.* **85**, 6667–6679.

Bretherton, F.P. (1982) Ocean climate modeling. *Prog. Oceanog.* **11**, 93–129.

Hibler, W.D. and Bryan, K. (1984) Ocean circulation: Its effects on seasonal sea-ice simulations. *Science* **224**, 489–491.

Semtner, A.J. and Chervin, R.M. (1988) A simulation of the global ocean with resolved eddies. *J. Geophys. Res.* **93**, 15 502–15 522, 15 767–15 775.

Gent, P.R. and McWilliams, J.C. (1990) Isopycnal mixing in ocean circulation models. *J. Phys. Oceanogr.* **20**, 150–160.

Kantha, L.H. and Clayson, C.A. (2000) *Numerical Models of Oceans and Oceanic Processes*, Academic Press, San Diego, 940 pp.

The land surface

Manabe, S. (1969) Climate and ocean circulation: 1. The atmospheric circulation and the hydrology of the Earth's surface. *Mon. Wea. Rev*. **97**, 739–774.

Charney, J.G. (1975) Dynamics of deserts and drought in the Sahel. *Quart. J. Roy. Meteor. Soc*. **101**, 193–202.

Eagleson, P.S. (ed.) (1982) *Land Surface Processes in Atmospheric General Circulation Models.* Cambridge University Press, Cambridge, 560 pp.

Shukla, J. and Mintz, Y. (1982) Influence of land-surface evapotranspiration on the Earth's climate. *Science* **215**, 1498–1501.

Henderson-Sellers, A. and Wilson, M.F. (1983) Surface albedo for climate modelling. *Rev. Geophys. Space Phys.* **21**, 1743–1778.

Dickinson, R.E. (1983) Land surface processes and climate-surface albedos and energy balance. *Adv. Geophysics* **25**, 305–353.

Henderson-Sellers, A. and Gornitz, V. (1984) Possible climatic impacts of land cover transformations, with particular emphasis on tropical deforestation. *Clim. Change* **6**, 231–256.

Sellers, P.J., Mintz, Y., Sud, Y.C. and Dalcher, A. (1986) A simplified biosphere model (SiB) for use within general circulation models. *J. Atmos. Sci.* **43**, 505–531.

Rowell, D.P. and Blondin, C. (1990) The influence of soil wetness distribution on short range rainfall forecasting in the West African Sahel. *Quart. J. Roy. Meteor. Soc.* **116**, 1471–1485.

Koster, R. and Suarez, M. (1992) Modeling the land surface boundary in climate models as a composite of independent vegetation stands. *J. Geophys. Res*. **97**, 2697–2715.

Dickinson, R.E. (1996) Land surface processes and climate modeling. *Bull. Amer. Meteor. Soc*. **76**, 1445–1448.

Koster, R. and Milly, P.C.D. (1997) The interplay between transpiration and runoff formulations in land surface schemes used with atmospheric models. *J. Clim.* **10**, 1578–1591.

Sellers, P.J., Dickinson, R.E., Randall, D.A., Betts, A.K., Hall, F.G., Berry, J.A., Collatz, G.J., Denning, A.S., Mooney, H.A., Nobré, C.A., Sato, N., Field, C.B. and Henderson-Sellers, A. (1997) Modeling the exchanges of energy, water, and carbon between continents and the atmosphere. *Science* **275**, 502–509.

Cox, P., Betts, R., Bunton, C., Essery, R., Rowntree, P.R. and Smith, J. (1999) The impact of new land surface physics on the GCM simulation of climate and climate sensitivity. *Clim. Dyn.* **15**, 183–203.

Coupled models

Manabe, S. and Bryan, K. (1969) Climate calculations with a combined ocean atmosphere model. *J. Atmos. Sci.* **26**, 786–789.

Manabe, S., Bryan, K. and Spelman, M.J. (1979) A global ocean atmosphere climate model with seasonal variation for future studies of climate sensitivity. *Dyn. Atmos. Oceans* **3**, 393–426.

Washington, W.M., Semtner, A.J. Jr., Meehl, G.A., Knight, D.J. and Mayer, T.A. (1980) A general circulation experiment with a coupled atmosphere, ocean and sea ice model. *J. Phys. Oceanogr.* **10**, 1887–1908.

Manabe, S. (ed.) (1985) *Issues in Atmospheric and Oceanic Modelling. Part A. Climate Dynamics.* Advances in Geophysics, Vol. 28, Academic Press, New York, 591 pp.

Meehl, G.A. (1990) Development of global coupled ocean–atmosphere general circulation models. *Clim. Dyn.* **5**, 19–33.

Trenberth, K.E. (1992) *Climate System Modelling.* Cambridge University Press, Cambridge, 788 pp.

Randall, D.A. (ed.) (2000) *General Circulation Model Development: Past, Present, and Future*. Academic Press, San Diego, USA, 807 pp.

Sea ice and snow

Maykut, G.A. and Untersteiner, N. (1971) Some results from a time-dependent thermodynamic model of sea-ice. *J. Geophys. Res.* **76**, 1550–1575.

Semtner, A.J. (1976) A model for the thermodynamic growth of sea-ice in numerical investigations of climate. *J. Phys. Oceanogr.* **6**, 379–389.

Parkinson, C.L. and Washington, W.M. (1979) A large-scale numerical model of sea-ice. *J. Geophys. Res.* **84**, 311–337.

Cess, R.D., Potter, G.L., Zhang, M-H., Blanchet, J.-P., Chalita, S., Colman, R., Dazlich, D.A., Del Genio, A.D., Dymnikov, V., Galin, V., Jerrett, D., Keup, E., Lacis, A.A., Le Treut, H., Liang, X-Z., Mahfouf, J-F., McAvaney, B.J., Meleshko, V.P., Mitchell, J.F.B., Morcrette, J-J., Norris, P.M., Randall, D.A., Rikus, L., Roeckner, E., Royer, J-F., Schlese, U., Sheinin, D.A., Slingo, J.M., Sokolov, A.P., Taylor, K.E., Washington, W.M., Wetherald, R.T. and Yagai, I. (1991) Interpretation of snow-climate feedback as produced by 17 general circulation models. *Science* **253**, 888–892.

Gallimore, R.G. and Kutzbach, J.E. (1995) Snow cover and sea-ice sensitivity to generic changes in Earth orbital parameters. *J. Geophys. Res.* **100(D1)**, 1103–1120.

Cattle, H. and Crossley, J. (1995) Modelling Arctic climate change. *Phil. Trans. Roy. Soc. London* **A352**, 201–213.

Novel ideas and applications: outside the box

Paltridge, G.W. (1975) Global dynamics and climate – a system of minimum entropy exchange. *Quart. J. Roy. Meteor. Soc.* **101**, 475–484.

Lovelock, J.E. (1979) *Gaia. A New Look at Life on Earth.* Oxford University Press, Oxford, 157 pp.

Hoffert, M.I., Callegari, A.J., Hsieh, C.T. and Ziegler, W. (1981) Liquid water on Mars: an energy balance climate model for CO_2/H_2O atmospheres. *Icarus* **47**, 112–129.

Watson, A.J. and Lovelock, J.E. (1983) Biological homeostasis of the global environment: The parable of Daisyworld. *Tellus* **35**, 284–288.

Turco, R.P., Toon, O.B., Ackerman, T., Pollack, J.B and Sagan, C. (1983) Nuclear winter: Global consequences of multiple nuclear explosions. *Science* **222**, 1283–1292.

Thompson, S.L. and Schneider, S.H. (1986) Nuclear winter reappraised. *Foreign Affairs* **64**, 981–1005.

Charlson, R.J., Lovelock, J.E., Andreae, M.O. and Warren, S.G. (1987) Ocean phytoplankton, atmospheric sulphur, cloud albedo and climate. *Nature* **326**, 655–661.

Schneider, S.H. and Boston, P.J. (eds) (1991) *Scientists on Gaia.* MIT Press, Cambridge, 443 pp.

Morgan, M.G. and Keith, D.W. (1995) Subjective judgments by climate experts. *Environmental Science and Technology* **29**, 468A–476A.

Hansen, J., Ruedy, R., Lacis, A., Russell, G., Sato, M., Lerner, J., Rind, D. and Stone, P. (1997) Wonderland climate model. *J. Geophys. Res.* **102**, 6823–6830.

Climate system

GARP (1975) *The Physical Basis of Climate and Climate Modelling*, GARP Publication Series 16, 181–187, ICSU/WMO, Geneva.

Saltzman, B. (ed.) (1983) *Theory of Climate.* Advances in Geophysics, Vol. 25, Academic Press, New York, 505 pp.

Hansen, J.E. and Takahashi, T. (eds) (1984) *Climate Processes and Climate Sensitivity.* Maurice Ewing Series 5, American Geophysical Union, Washington, DC.

Ghil, M. (1985) Theoretical climate dynamics: an introduction. In *Turbulence and Predictability in Geophysical Fluid Dynamics and Climate Dynamics*, Soc. Italiana di Fisica – Bologna, Italy, pp. 347–401.
Peixoto, J.P. and Oort, A.H. (1991) *Physics of Climate.* American Institute of Physics, Washington DC, 520 pp.
Garratt, J.R. (1992) *The Atmospheric Boundary Layer*, CUP, Cambridge, UK, 316 pp.
Kiehl, J. and Briegleb, B. (1993) The relative roles of sulfate aerosols and greenhouse gases in climate forcing. *Science* **260**, 311–314.
Gibson, J.K., Kallberg, P., Uppala, S., Hernandez, A., Normura, A. and Serrano, E. (1997) ERA description, ECMWF Re-Analysis Project Report Series, 1, 72 pp. ECMWF, Reading, RG2 AX, UK.
Harvey, L.D.D. (1999) *Global Warming: The Hard Science.* Prentice Hall, Harlow, 408 pp.

Palaeoclimate models

Matthews, W.H., Kellogg, W.H. and Robinson, G.D. (eds) (1971) *Inadvertent Climate Modification: Report Of the Study of Man's Impact on Climate.* MIT Press, Cambridge, MA, USA, 594 pp.
Gates, W.L. (1976) The numerical simulation of ice-age climate with a general circulation model. *J. Atmos. Sci.* **33**, 1844–1873.
Walker, J.C.G. (1977) *Evolution of the Atmosphere*. Macmillan Publishing, New York, 318 pp.
Oerlemans, J. (1982) Glacial cycles and ice-sheet modeling. *Clim. Change* **4**, 353–374.
Rind, D. and Peteet, D. (1985). Terrestrial conditions at the last glacial maximum and CLIMAP sea-surface temperature estimates: are they consistent? *Quatern. Res.* **24**, 1–22.
Kutzbach, J.E. and Gallimore, R.G. (1989) Pangean climates: megamonsoons of the megacontinent. *J. Geophys. Res.* **94**, 3314–3358.
Mitchell, J.F.B. (1990) Is the Holocene a good analogue for greenhouse warming? *J. Clim.* **3**, 1177–1192.
Street-Perrot, F.A., Mitchell, J.F.B., Marchand, D.S. and Brunner, J.S. (1990) Milankovitch and albedo forcing of the tropical monsoons; a comparison of geological evidence and numerical simulations for 9000 y BP. *Trans. Roy. Soc. Edinburgh: Earth Sciences* **81**, 407–427.
Gallee, H., van Ypersele, J.P., Fichefet, Th., Tricot, Ch. and Berger, A. (1991) Simulation of the last glacial cycle by a coupled, sectorially averaged climate-ice-sheet model. I. The Climate Model. *J. Geophys. Res.* **96**, 13139–13161.
Kutzbach, J.E. and Ziegler, A.M. (1993) Simulation of the late Permian climate and biomes with an atmosphere/ocean model: comparison with observations, *Phil Trans. Roy. Soc. London, Series B*. **341**, 327–340.
Crowley, T.J. (2000) Causes of climate change over the past 1000 years. *Science* **289**, 270–277.

Feedbacks and forcings

Cess, R.D. (1976) Climatic change: An appraisal of atmospheric feedback mechanisms employing zonal climatology. *J. Atmos. Sci.* **33**, 1831–1843.
Charlson, R.J., Lovelock, J.E., Andreae, M.O. and Warren, S.G. (1987) Oceanic phytoplankton, atmospheric sulfur, cloud albedo and climate. *Nature* **326**, 655–661.
Mitchell, J.F.B., Senior, C.A. and Ingram, W.J. (1989) CO_2 and climate: A missing feedback? *Nature* **341**, 132–134.

Charlson, R.J., Langner, J., Rodhe, H., Leovy, C.B. and Warren, S.G. (1991) Perturbation of the northern hemisphere radiative balance by backscattering from anthropogenic sulfate aerosols. *Tellus* **43AB**, 152–163.

Santer, B.D., Brüggemann, W., Cubasch, U., Hasselmann, K., Maier-Reimer, E. and Mikolajewicz, U. (1994) Signal-to-noise analysis of time-dependent greenhouse warming experiments. Part 1: Pattern analysis. *Clim. Dyn.* **9**, 267–285.

Mitchell, J.F.B., Johns, T.C., Gregory, J.M. and Tett, S.F.B. (1995) Climate response to increasing levels of greenhouse gases and sulphate aerosols. *Nature* **376**, 501–504.

Santer, B.D., Taylor, K.E., Wigley, T.M.L., Johns, T.C., Jones, P.D., Karoly, D.J., Mitchell, J.F.B., Oort, A.H. *et al.* (1996) A search for human influences on the thermal structure of the atmosphere. *Nature* **382**, 39–46.

Wigley, T.M.L., Richels, R. and Edmonds, J.A. (1996) Economic and environmental choices in the stabilization of atmospheric CO_2 concentrations. *Nature* **379**, 240–243.

Hegerl, G.C., von Storch, H., Hasselmann, K., Santer, B.D., Cubasch, U. and Jones, P.D. (1996) Detecting anthropogenic climate change with an optimal fingerprint method. *J. Climate* **9**, 2281–2306.

Tett, S.F.B., Mitchell, J.F.B., Parker, D.E. and Allen, M.R. (1996) Human influence on the atmospheric vertical temperature structure: detection and observations. *Science* **274**, 1170–1173.

Hansen, J., Sato, M. and Ruedy, R. (1997) Radiative forcing and climate response. *J. Geophys. Res.* **102**, 6831–6864.

Hansen, J., Sato, M., Ruedy, R., Lacis, A., Asamoah, K., Beckford, K., Borenstein, S., Brown, E., Cairns, B., Carlson, B., Curran, B., de Castro, S., Druyan, L., Etwarrow, P., Ferede, T., Fox, M., Gaffen, D., Glascoe, J., Gordon, H., Hollandsworth, S., Jiang, X., Johnson, C., Lawrence, N., Lean, J., Lerner, J., Lo, K., Logan, J., Luckett, A., McCormick, M.P., McPeters, R., Miller, R., Minnis, P., Ramberran, I., Russell, G., Russell, P., Stone, P., Tegen, I., Thomas, S., Thomason, L., Thompson, A., Wilder, J., Willson, R. and Zawodny, J. (1997) Forcings and chaos in interannual to decadal climate change. *J. Geophys. Res.* **102**, 25 679–25 720.

Stott, P.A., Tett, S.F.B., Jones, G.S., Allen, M.R., Mitchell, J.F.B. and Jenkins, G.J. (2000) External control of 20th century temperature by natural and anthropogenic forcings. *Science* **290**, 2133–2137.

Cox, P.M., Betts, R.A., Jones, C.D., Spall, S.A. and Totterdell, I.J. (2000) Acceleration of global warming due to carbon-cycle feedbacks in a coupled climate model. *Nature* **408**, 184–187.

A full bibliography, including all sources cited in this book, appears on the Primer CD.

Appendix B Glossary

AABW. Antarctic bottom water. Bottom water (*q.v.*) formed in the Antarctic as a result of the cold dense water released during the formation of sea-ice. This bottom water is a major component of the thermohaline circulation. Figure B.1 shows a compilation of deepwater palaeotemperatures obtained from isotopic analysis of the remnants of deep sea foraminifera. Studies of the thermohaline circulation and the rate of formation of AABW are helping to explain why the bottom water temperatures in the Cretaceous were so much warmer than they are today.

Ablation. The collective description of the processes by which a cryosphere mass is diminished in size. The term is applied to the depletion of ice sheets, glaciers, sea ice and to a snowpack. Ablation occurs by melting, sublimation and by physical disruption (i.e. bits fall off, for example, icebergs breaking off from the Antarctic ice sheet).

Absorption bands. Molecules absorb radiation by being excited into vibration and rotation. In the case of water vapour, these absorption bands lie in the same region as the longwave radiation emitted by the Earth and are therefore of significance in climate studies. Carbon dioxide does not possess rotation bands but its main vibration band also lies in this region, as do the absorption bands of some trace gases such as methane and the chlorofluorocarbons.

Absorptivity. The fraction of the radiation incident upon a body which the body absorbs is called its absorptivity; also known as absorptance, although this usually refers to a particular wavelength.

Adiabatic. An adiabatic process is one where heat does not enter or leave the system. The term is common in meteorology since the vertical motion of air results in changes in the temperature of air that are not due to external energy sources. As pressure is reduced when air rises, the temperature decreases and as pressure increases as air descends, the temperature rises. The process gives rise to a characteristic 'adiabatic lapse rate' in the atmosphere.

Advection. Horizontal transport, usually of energy, mass etc., in the atmosphere or ocean.

Aerosol. A suspension of small solid particles or liquid droplets in the atmosphere. Aerosols can be both natural (e.g. volcanic) and of human origin (e.g. industrial), and may have significant radiative effects on climate.

A Climate Modelling Primer, Third Edition. K. McGuffie and A. Henderson-Sellers.
 ISBN: 0-470-85750-1 (HB); 0-470-85751-X (PB)

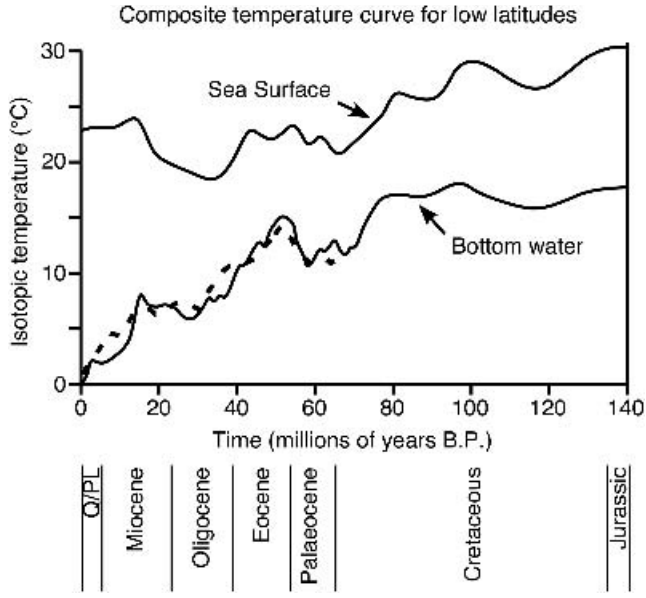

Figure B.1 Compilation of oxygen isotope palaeotemperature data obtained by analysis of benthic and planktonic foraminifera from Deep Sea Drilling Project cores. (Q/PL denotes the Pliocene epoch and the Quaternary period, the latter beginning about 2 million years before present (BP)). The upper curve is drawn through tropical sea-surface temperatures and the lower curve through bottom water temperatures (reproduced with permission from Douglas and Woodruff, 1981). The dashed line shows temperatures from a separate Mg/Ca analysis from Lear *et al.* (2000)

Albedo. From the Latin *albus*, meaning white. It is the reflected fraction of incident radiation. It is synonymous with hemispheric reflectance.

Aliasing. In the sampling of a continuous variable at discrete points, the sampling frequency must be high enough to resolve the highest frequency present in the continuous variable. If not, the high-frequency information will appear as a false enhancement of a related lower frequency. The high-frequency signal is then said to be aliased into a lower frequency.

AMIP. The Atmospheric Model Intercomparison Project is coordinated by the Program for Climate Model Diagnostics and Intercomparison (PCMDI) for the Working Group on Numerical Experimentation.

Attractor. The time evolution of a physical system can be characterized by system variables. If these variables converge to a single set of values, then this is the attractor of the system. Conservative dynamical systems never reach equilibrium and therefore do not exhibit attractors. The Poincaré section (or phase portrait) is commonly used to display attractors.

Attribution. The linking of cause and effect. For example, in terms of human-induced climate change it has to be determined, first, if change can be detected and then if the detected change can be unambiguously attributed to one or more causes.

Baroclinic. The atmosphere is baroclinic when isotherms are not parallel to isobars, i.e. there is a temperature gradient along the isobars.

Baroclinic waves. A disturbance in a smooth zonal flow which is equivalent barotropic will generate baroclinic waves. They are characteristic of the upper-level atmospheric flow in mid-latitudes.

Barotropic. The atmosphere is barotropic when there are horizontally uniform temperatures at all heights. Thus pressure gradients can exist but horizontal temperature gradients cannot. In an equivalent barotropic atmosphere, horizontal temperature gradients may exist but isotherms must be parallel to the isobars.

Beowulf cluster. A strategy for the creation of a high-performance computer from 'commercial-off-the-shelf' (COTS) components (typically computers that would be used as 'personal' computers). The development of these systems started in 1994 at the Center of Excellence in Space Data and Information Science at NASA Greenbelt.

Black body. A term for a perfect radiator of energy. The efficiency with which a body radiates energy is characterized by the factor ε (emissivity) in the Stefan–Boltzmann (*q.v.*) equation. A black body has an emissivity of 1.

Bottom water. The cold dense water which lies at the bottom of the oceans in contact with the ocean floor having distinctly different characteristics from the water immediately above it. It is formed in high latitudes as a result of the formation of sea ice. See also *Deep water*.

Boundary layer. The lowest 1 km or so of the atmosphere. It is the location of all interactions between the Earth's surface (land, ocean and ice) and the free atmosphere.

Bowen ratio. The ratio of sensible heat flux to latent heat flux from a surface.

BP. Before Present. A measure of time (usually years) before the present day.

Business as usual. A term coined by the IPCC (and others) to describe likely future human activities if steps are not taken to mitigate climate change. This prediction of social, technical and economic evolution is, of itself, open to considerable debate and dispute. In general terms, it always indicates increased emissions into the atmosphere.

Chaos, Chaotic. The term has come to be applied to a system which is deterministic (i.e. its future state is determined by its present state), but which is governed by a range of processes which have non-linear behaviour. Small changes in the initial state of the system are amplified over time, so that the final states of two instances of a system with similar initial conditions are likely to be very different. The inability to specify accurately the initial conditions of a weather forecast model and the highly non-linear processes involved result in the forecast diverging from the real weather over a period of 10–15 days. Climate model simulations, because they are a forecast of an ensemble climate (e.g. mean January precipitation), rather than a single instance of weather (e.g. rainfall on 26 January), are not affected by chaos.

Clausius–Clapeyron (equation). The dependence of the saturation vapour content of the atmosphere upon its temperature.

Climate system. Variously defined. The atmosphere, hydrosphere, cryosphere, land surface and biosphere, i.e. all the components of the Earth's environment, are, to a greater or lesser extent, components of the climate system.

Cloud resolving model. A high-resolution model (often only two-dimensional) that resolves the physics responsible for the formation of individual cloud systems, rather than dealing with them by parameterizing their effects over a larger area. Since the clouds are resolved explicitly, the radiative calculations deal explicitly with fractional cloud amounts and the interaction between convective and radiative processes is more realistic. These models have begun to be incorporated into global models with some success, although the computational expense is considerable.

Convection. When a parcel of air is warmer than its environment it will move upwards and carry energy with it. This is the process of convection.

Convergence. See *Divergence*.

Coriolis force. The apparent force experienced by an entity moving over a rotating body such as the Earth. On the surface of the Earth the direction of travel is deflected towards the right in the Northern Hemisphere and to the left in the Southern Hemisphere.

Correlation coefficient. This measures the degree of association between two variables. If two data series are in step, so that peaks, increases or decreases in one series are closely associated with peaks, increases or decreases in the other, then the variables are said to be positively correlated. The correlation coefficient varies from -1 to $+1$, with $+1$ indicating perfect positive correlation and -1 perfect negative correlation.

Coupled model. A generic term, referring to a model made up of two or more (usually) independently developed models that interact by exchange of information on a few key variables.

Coupler. The process of coupling models of the various climate subsystems has developed from early direct coupling systems to a method based on the more flexible concept of a coupler module. This module of the coupled model exists to pass information in a controlled way between atmosphere, ocean, sea ice, land-surface and chemistry modules.

Cryosphere. A collective term describing the frozen water masses of the Earth. These are ice sheets, snow cover, glaciers, permafrost and sea ice.

Deep water. A term used to describe water in the ocean which lies below the surface water layer and has different temperature and salinity characteristics. The formation and circulation of this dense, cold and saline deep water are important components in the global ocean circulation. It may be possible to distinguish distinct layers in this water. Also: water that is 'taller than Eccles'. See also *Bottom water.*

Degree day. Summer warmth can be expressed as the sum of degree days: the product of the excess of daily temperatures above a preset threshold, which is often the threshold for plant growth (about 5°C), and the number of days exceeding the threshold by that amount. Winter cold can also be summarized this way except that the temperature depression below a threshold is used.

Degrees of freedom. Each observation in a random sample of size n can be compared with $n - 1$ other observations and hence there are $n - 1$ degrees of freedom. In climatology, many samples are not random; they have fewer than $n - 1$ degrees of freedom; sometimes many fewer.

Dependent variables. If a quantity y is a function of a quantity x then y is the dependent variable. It is dependent upon x. It follows that x is the independent variable.

Depletion. The abundance of an isotope expressed relative to a standard value (rather than an absolute amount). The enrichment or depletion of an isotope, i, is expressed as

$$\delta_i = \left(\frac{R_i}{R_{iStd}} - 1 \right) \times 1000‰$$

where R_i is the abundance of the isotope and R_{iStd} is the abundance in the standard. When the enrichment, δ, is negative (fewer isotopes, i, than in the standard), the sample is said to be depleted. The unit ‰ is pronounced 'per mil'.

Detection. The determination of a climate change. Although this sounds straightforward it has proved to be an exceedingly fraught issue for IPCC. Detection of human-induced climate change is not a simple yes/no determination. It depends on a statistical evaluation of both model results and observations. Detection must occur before *attribution* (*q.v.*).

Diffuse radiation. When radiation passes through the atmosphere, it is scattered in interactions with molecules and particles in the air. This scattering alters the direction of travel of the radiation progressively and randomly. After a great deal of scattering the radiation becomes totally diffuse (i.e. the same quantity of radiation is travelling in all directions). Generally the radiation received at the Earth's surface is composed of a diffuse component (from the sky) and a direct (unscattered) component from the solar disc. The factor 1.66 is often introduced into calculations to allow for the larger distance (on average) travelled by diffuse radiation through an atmospheric layer. Thermal radiation is emitted in all directions within the atmosphere and therefore is totally diffuse to a good approximation.

Diffusion coefficient. This determines the rate of diffusion of a quantity along a gradient of that quantity.

Divergence. The 'spreading out' of a flow or the flux of a quantity away from a point. Convergence is its opposite.

Downscaling. The process by which coarse resolution GCM results are brought to a higher resolution. It generally implies a space-scale change but can also be used for temporal information. Different downscaling methods produce different results.

Earth Simulator. A computer system comprising 640 processors and 10 Terabytes of main memory with a theoretical peak performance of 40 Teraflops (10^{12} floating point operations per second). The maximum application performance is around 27 Teraflops for a global atmospheric model.

EBM. An Energy Balance Model. Probably the simplest model of the Earth system, based on the energy balance between the solar energy absorbed from the Sun and the thermal radiation emitted to space by the Earth.
Eddy. A characteristic feature of turbulent fluid flow consisting of a coherent swirling motion.
Eddy flux. The flux of a quantity by means of turbulent disturbances propagating in a fluid. Such a flux is made possible by the process called eddy diffusion.
Eddy resolving model. A model (usually used with reference to the ocean) which explicitly includes the motions associated with eddies rather than simply parameterizing their effects.
Effective temperature. The temperature of the Earth, derived by simple energy balance considerations assuming the Earth to be a black body emitter.
Elevation angle. The angular distance above the horizon of a point in the sky at any time. See also *Zenith angle.*
EMIC. Earth System Model of Intermediate Complexity. These models have come to occupy a middle ground of climate modelling. The physical detail and complexity of the model are reduced to allow the inclusion of more components on longer timescales.
Emissivity. The ratio of the emittance from a body to that of a black body (a perfect emitter) at the same temperature is the emissivity of that body.
Ensemble simulation. To test the role of initial conditions and to gain an estimate of uncertainty in climate predictions, climate models can be integrated repetitively from slightly different initial conditions, providing a number of 'different' simulations covering the same period in the future. Such a climate ensemble provides an estimate of the inherent unpredictability of the model and, perhaps, a measure of natural variability.
Enstrophy. The root mean square of the vorticity of a body (usually a fluid).
Entrainment. The process by which matter external to a parcel of matter (usually fluid) is incorporated into the parcel.
Equilibration time. The time taken for a component of the climate system to reach equilibrium with one or more of the other components.
Evaluation. The process of examining and judging carefully the worth of something.
FANGIO. Feedback Analysis of GCMs and Intercomparison with Observations. The acronym honours Juan Manuel Fangio, who was world driving champion in 1951, '54, '55, '56 and '57. He had 24 Formula One wins in 51 starts.
FCCC. The UN Framework Convention on Climate Change. Signed at the UN Conference on Environment and Development in 1992 and ratified in 1994. The FCCC has defined climate change to be only the human-induced effects (i.e. not natural variability) for its negotiations.
Feedback. The phenomenon whereby the output of a system is fed into the input and the output is subsequently affected.
Fingerprint. A set of tests which together allow for the detection (*q.v.*) of climate

change. The analogy is to a human fingerprint which has many characteristics which, together, permit unambiguous identification.

Flux. The flow of a quantity through a surface. The flux of, for example, energy is always *from* somewhere *to* somewhere else, i.e. its vector nature is important.

Forcing. A change in an internal or external factor which affects the climate.

Fourier transform. A continuous variable can be represented mathematically either by its value at many grid points or as the sum of many waves of differing frequency, amplitude and phase. The two representations are formally equivalent, i.e. they contain the same information. (A good analogy is a number and its logarithm to any base.) The Fourier transform of a variable is the frequency domain equivalent of its time or space domain representation. A fast Fourier transform (FFT) is a computer algorithm for moving between the frequency and spatial domains.

Gain. The gain of a system is a measure of the amplification of the input to the system. In its simplest form it equals output divided by input.

Gaussian quadrature. A particular type of numerical computation of a one-dimensional integral from the knowledge of individual values of the function.

GCM. A General Circulation Model or Global Climate Model. Initially used with reference to three-dimensional models of the atmosphere alone, the term has come to be loosely used to encompass three-dimensional models of the ocean (OGCMs) and coupled models.

General circulation of the atmosphere. Two factors control the general circulation of the atmosphere: the energy imbalance between the equator (net absorption of energy) and the poles (net emission of energy) and the rotation of the Earth. In low latitudes the direct Hadley cell circulations transfer energy polewards, but in the middle latitudes the rotation of the system causes a wave-like flow in the troposphere (Figure 2.2). These Rossby waves travel in a westerly direction and energy transfer is via horizontal eddies which form the familiar depression systems and anticyclones of mid-latitude weather. In polar regions there are weak direct cellular flows but the seasonal variation in insolation from polar day to night dominates the pattern.

Geodesic grid. A model grid constructed by progressively bisecting the triangles of an icosahedron (a 20-triangular-sided polyhedron) and projecting the vertices of the resulting set of new triangles onto the enclosing sphere. The resulting grid depends on the level of progressive subdivision. The geodesic grid was popularized as an architectural device by American architect Buckminster Fuller. The vertices of the triangles form the grid points for the model grid, representative of a hexagonal grid box. First developed for atmospheric modelling in the 1960s, the grid has the advantage of providing uniform coverage over the surface of a sphere, avoiding singularities at the pole. It has recently been reintroduced to the climate modelling community but is computationally expensive to implement.

Geopotential height. A measure of height in the atmosphere, standardized by the amount of energy required to ascend. This varies slightly from the geometrical height because the acceleration due to gravity varies between equator and pole.

Gravity waves. Analogous to waves on the surface of the ocean. Because the density of the atmosphere decreases with height, waves similar to ocean waves occur at a large scale in the atmosphere. They occur in the atmosphere due to forcing by orography and manifest themselves as undulations in potential temperature surfaces.

Greenhouse effect. The warming effect of the atmosphere caused by gases re-radiating longwave radiation back to the surface of the Earth. It has nothing to do with glasshouses, which trap warm air at the surface.

Hadley cell. The thermally driven circulation comprising upward motion at the ITCZ and downward motion in the subtropics. The air moves poleward at high altitude and equatorward near the surface.

Halocline. A region of the ocean where the vertical salinity gradient is high. See also *Pycnocline* and *Thermocline.*

Heat capacity. The energy required to increase the temperature of a body by 1 K.

Hybrid co-ordinates. It is unusual for a single co-ordinate system to be appropriate for all situations in climate modelling. Many models now use a co-ordinate system that is an amalgamation of different systems. A sigma co-ordinate system might be used near the surface (or ocean bottom) and a pure height/depth or pressure co-ordinate near the top of the atmosphere or at the surface of the ocean.

Hydrostatic equation. The relationship between pressure (p) and height (z) in the atmosphere (or depth in the ocean). $\Delta p = -\rho g \Delta z$. ρ is the fluid density and g is the acceleration due to gravity.

Ideal gas law. The statement that the ratio of the product of pressure and volume of a gas to its temperature is a constant.

Independent variable. See *Dependent variables***.**

Infinite. Quite a lot – really an awful lot.

Integrated assessment. The incorporation of all aspects of climate change into the decision-making process, for example, social, political, economic and technological as well as ecological, environmental and climatic.

Intertropical Convergence Zone (ITCZ). The zone of convergence between the northern and southern Hadley cells. Characterized by strong rising motion of air.

IPCC. The Intergovernmental Panel on Climate Change. Established in 1988 and jointly sponsored by UNEP and WMO. Note that the IPCC is an assessment, not a research, organization.

Isobar/Isobaric. Processes which occur at a constant pressure are isobaric. Isobars are lines that typically join points of the same surface pressure on a weather map. Isobaric surfaces in the atmosphere or ocean are surfaces where all points are at the same pressure.

Isopycnal. Having the same density everywhere. A vertical co-ordinate system for modelling the ocean based on density. Away from the surface and the bottom of the ocean, the flow is largely determined by the density of the water and the flow is along isopycnal surfaces.

Isothermal. Having the same temperature everywhere. Often used to describe the situation where no vertical temperature gradient exists in the atmosphere.

Isotope. Strictly describes atoms with the same atomic number but different atomic weight. It is commonly used to refer to what should more properly be called isotopologues (*q.v.*).

Isotopologue. The correct term for what are sometimes called isotopes, an isotopologue is a molecular entity where one of the atoms has been replaced by a 'special atom'. For water, there are a number of stable isotopologues (e.g. H_2O, HDO, D_2O, $H_2{}^{18}O$, $H_2{}^{17}O$).

Isotropic. Having the same properties in all directions.

ITCZ. See *Intertropical Convergence Zone*.

Kyoto Protocol. A United Nations Protocol of the Framework Convention for Climate Change that aims to reduce anthropogenic emissions of CO_2. It sets limits for anthropogenic CO_2 emissions with a view to reducing overall emissions to 5 per cent below 1990 levels by 2008 to 2012. See http://unfccc.int.

Lapse rate. The rate of decrease of temperature with height in the atmosphere.

Latent heat. The energy used in conversion between different phases of water. It is the energy used in evaporation of water (vaporization) or in the melting of ice (fusion).

Leaf area index (LAI). The area of foliage per unit area of ground. Usually only the upper side of the leaves is considered but an alternative definition includes both upper and lower leaf surfaces.

Little Ice Age. A period between the fifteenth and eighteenth centuries when temperatures were lower than today over many areas of the Northern Hemisphere. The timing differs from region to region and recently there has been some doubt cast upon whether a 'climatic epoch' really occurred.

Meridional circulation. The circulation of the atmosphere is dominated by meridional motions caused by the equator-to-pole temperature gradient.

Metadata. Meta, from the Greek, now meaning beyond, here signifies data of a higher order. For example, a dataset of temperature at a station might have metadata indicating the type of thermometer used and any corrections applied. Metadata associated with model output would typically include software versions, model resolution, units and variable names designed to aid the analysis of the numbers in the data file. Metadata can either be included in the file (such as the NetCDF file structure discussed in Chapter 6) or be in a separate electronic or paper file.

Milankovitch mechanism. The orbital parameters of the Earth are constantly changing due to the influence of other planets. These changes in the orbital geometry result in changes in the pattern of insolation at the Earth. This may provide a forcing agent for climate variations, the Milankovitch mechanism.

MIP. Model Intercomparison Project. Following the success of the Atmospheric Model Intercomparison Project, AMIP, and its planned and structured intercomparison of atmospheric models, a number of different model intercomparison projects has been developed (see Chapter 6). These projects have been a driving force behind the development of data interchange standards and performance metrics.

Mixed layer. Because of wind and wave action and convection at the surface, the top part of the ocean is well mixed (very small gradients of temperature and salin-

ity). This layer, the thickness of which varies geographically and seasonally, is called the mixed layer. Climate models have often assumed that the layer is 50–100 m thick globally.

Mixing ratio (of water vapour). The quantity of water vapour (in kg) per kilogram of air.

Model noise. In climate models, inaccuracies in calculations, rounding, and truncation errors introduce variability into model simulations which are classed as model noise.

Momentum. The product of mass and velocity. In a closed system, momentum is conserved.

Montreal Protocol. This is an international agreement designed to protect stratospheric ozone. The treaty was originally signed in 1988 and substantially amended in 1990 and 1992. It stipulates that the production and consumption of compounds that deplete ozone in the stratosphere are to be phased out by 2000 (2005 for methyl chloroform).

NADW. North Atlantic Deep Water. Cold dense water formed in the North Atlantic from the dense cold water released during the formation of sea ice. Deep water lies below the surface waters, but above the 'bottom water' (*q.v.*). See also *AABW*.

Non-linear. An equation with dependent variable y containing terms in y^n, where $n \neq 1$, is non-linear. Such equations exhibit a response to perturbations which is not related in a constant fashion to the forcing.

No regrets. If a community takes some course of action in response to a threat which will result in a benefit to the community even if the threat does not materialize, then that response can be considered a 'no regrets' measure.

Ocean circulation. The Earth's surface is 70 per cent covered by water. Differential heating of this ocean, combined with the frictional effect of winds and the effects of density gradients caused by rivers (input of less dense water) and sea ice formation (production of dense saline water) mean that the ocean is in continual motion with a timescale of hundreds to thousands of years. Motions at the surface include waves, tides and currents, but the circulation is importantly three-dimensional. Because of these long timescales, the ocean has been termed the flywheel of the climate system.

Optical thickness. Radiation passing through a body is attenuated by a factor $e^{-\tau}$, where τ is the optical thickness of the body. It is a strong function of wavelength. Alternatively, the length of time required by any student of climate modelling to 'see the light'.

Oxygen isotope data. Can relate to information about any of the three oxygen isotopes: ^{16}O, ^{17}O and ^{18}O. Usually, such data relate to the relative occurrence of the two most common, ^{16}O and ^{18}O. For example, the ratio of ^{18}O to ^{16}O can be used to indicate the nature of palaeoclimates since it is related to ocean temperatures. Because of their different masses, water molecules containing different oxygen isotopes are evaporated and precipitated at different rates.

Ozone hole. A description of the appearance at the end of winter, in the polar stratosphere (most pronounced over Antarctica), of an area of distinctly reduced ozone levels. These reduced levels are linked to the availability of free chlorine and rapid

reactions on solid particulates in the stratosphere. The Antarctic ozone hole was first described in 1985.

Parameterization. The method of incorporating a process by representation as a simplified function of some other fully resolved variables without explicitly considering the details of the process.

Physical, physically based (models). Models which are constructed on the basis of physical relationships (and laws) and known processes rather than being based on correlations where there is no clearly defined causal relationship. In climate models, this term has come to embrace aspects of chemistry and biology as well as physics.

PILPS. The Project for Intercomparison of Land-surface Parameterization Schemes.

Pinatubo. In June 1991, Mount Pinatubo in the Philippines erupted and injected large amounts of dust and sulphate into the upper atmosphere. The eruption was important because it occurred at a time when satellite observing systems were well configured to provide the climate community with information on the dynamics and chemistry of the processes following a major eruption.

Planck function. The description of the amount of radiation emitted by a black body (*q.v.*) at a given temperature as a function of the wavelength of the radiation.

Poincaré section. This term is used in chaotic (*q.v.*) dynamics. When a plot is made of two or more of the characterizing variables of a chaotic system, this is termed a Poincaré section. The two- or three-dimensional plot often has a distinct pattern, which cannot be seen if only one variable is examined. The term phase portrait is often used.

Potential evaporation. Potential evaporation can be defined as the evaporation which would occur given a free and plentiful supply of water. Clearly such a situation would occur only over ice or water bodies or wet vegetation and soil.

Potential temperature. In the atmosphere the potential temperature of a parcel of air is the temperature it would have if moved under adiabatic conditions (without gaining or losing energy) to a reference level (usually 1000 hPa). Potential temperature is more useful than actual temperature because the compressibility of gases means that temperature increases as pressure increases.

Primitive equation model. A model constructed from the basic (primitive) equations that describe the physics of a system, such as conservation of mass and conservation of momentum. This contrasts with an empirical model of some process, based on observations.

Prognostic variable. A variable in a model which is utilized in prediction of itself at a later time.

Pycnocline. A boundary in the ocean which is characterized by a large change in density. The density difference between two bodies of water may be due to differences in temperature or salinity or both.

Radius of deformation. A description of the characteristic size of eddies in the atmosphere or ocean. It is a function of the density of the fluid and the Coriolis parameter.

Resolution. Model resolution, in the context of climate models, is generally quoted as the size of the computational interval in the horizontal. It is typically quoted in

degrees of latitude, although the resolution can also be indicated by specifying a spectral truncation (e.g. T42, T63, T106). These spectral truncations have an implied underlying latitude–longitude grid.

Richardson number. A measure of the stability of a fluid layer: a ratio of buoyancy to inertial forces.

Scattering. In the atmosphere the redirection of light waves due to reflection and diffraction by atmospheric molecules (Rayleigh) and cloud droplets (Mie).

Semi-implicit. A numerical scheme for projecting model equations to a future model timestep. Semi-implicit schemes have the advantage of being more accurate and treating non-linear components of the equations better than other differencing schemes.

Sensitivity. The response of a model to a perturbation. Usually described as a unit of response per unit change.

Solar constant. The amount of radiation from the Sun incident on a surface at the top of the atmosphere perpendicular to the direction of the Sun. Currently taken to be $1370\,\mathrm{W\,m^{-2}}$ and known to be variable! Note that S can denote both $1370\,\mathrm{W\,m^{-2}}$, one quarter of this or the instantaneous top-of-the-atmosphere solar flux at a particular location. Context usually indicates which is meant, but beware confusing algebra.

Spectral. Related to waves and wavelength. Spectral models express the variation of geophysical parameters such as wind velocity in terms of waves. Spectral reflectance refers to the different characteristics of a surface or object at different light wavelengths (red, green, blue, etc.).

Spherical harmonic. For a variable defined on the surface of a sphere the natural method of representation in the frequency domain is by means of functions called spherical harmonics. These can be thought of as the extension to spherical coordinates of the concept of Fourier transformation (*q.v.*).

Stability. A measure of the capacity of a system to resist perturbation. The ability to recover the original position after displacement.

Stability (of the atmosphere). Consider the situation in Figure B.2a where the dashed line shows the critical lapse rate, γ_c. The dotted lines show both stable and unstable temperature profiles. If a parcel of air is displaced from the surface it will rise such that its temperature decreases at a rate given by γ_c. If the environmental lapse rate is stable, then the displaced parcel will be colder (and thus denser) than the surrounding air (Point A) and will sink back. In the unstable case the parcel will be warmer (less dense) than its surroundings (Point B) and will continue to rise.

Statistical significance. A means of trying to determine the reality of either an observed change or a model result. In the most general terms, statistical significance is based on a ratio of the 'change' compared with the normal variability, or 'noise', in the modelled or real climate. Statistical tests are usually considered as a prelude to an interpretation of results based on physical processes.

Stefan–Boltzmann constant. σ, having a value of $5.67 \times 10^{-8}\,\mathrm{W\,m^{-2}\,K^{-4}}$, the constant of proportionality in Stefan's law.

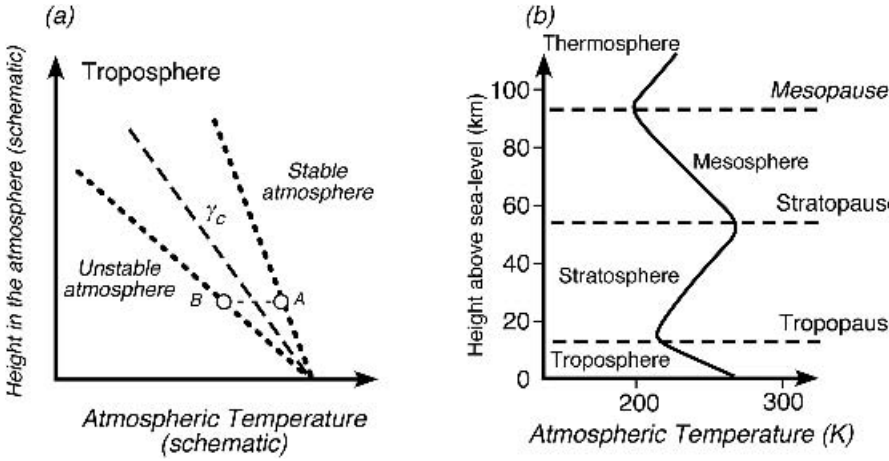

Figure B.2 (a) Stable and unstable tropospheric lapse rates as compared with a predetermined critical lapse rate (γ_c). (b) The four 'regions' of the atmosphere.

Stefan's law. This is the relationship between the amount of energy radiated by a body and its absolute temperature and is given by $E = \sigma T^4$ where E is in $W\,m^{-2}$ and σ is the Stefan–Boltzmann constant.

Stratosphere. The zone of the atmosphere above the troposphere (Figure B.2b). Atmospheric temperature increases with height in the stratosphere due to absorption of radiation by ozone, which is greatest at the stratopause.

Stream function. A description of the amount of volume transport taking place at a particular point (in space) in an ocean or atmospheric model per unit time. It has units of $m^3\,s^{-1}$. In the ocean the term Sverdrup (*q.v.*) is often used where 1 Sverdrup $= 10^6\,m^3\,s^{-1}$.

Student's *t* test. One type of statistical test used by climate modellers to estimate the statistical significance (*q.v.*) of a difference between two quantities. Although often not strictly valid for testing modelled differences, it provides a general identification of the location of important changes which have occurred and thus the basis for cause and effect evaluations.

Sulphate aerosol. When sulphur dioxide is further oxidized, the result is droplets of H_2SO_4. These act to scatter solar radiation back to space and also act as cloud condensation nuclei.

SVAT. A Soil–Vegetation–Atmosphere Transfer scheme. One type of land-surface parameterization scheme, which describes the transfer of energy, moisture and momentum from the land surface to the lower layer of the atmosphere. These models are focused primarily on short-period physics, rather than on chemistry or ecology.

Sverdrup. A measure of water flow rate applied to ocean currents and equal to one million cubic metres per second (1 cubic kilometre per second). Named to honour Harald Ulrik Sverdrup (1888–1957) who played a major role in shaping modern oceanography.

Taylor plot. A two-dimensional plot used in AMIP to compare the performance of a set of models. The plots summarize how well two-dimensional fields from models agree with each other or with observational datasets and are commonly used for assessing how changes in a model affect the performance. The diagram shows three statistics: the correlation coefficient between the observed and simulated field (cosine of the azimuth), the centred root mean square (RMS) difference between the two fields (distance from any point on the diagram to the point on the x-axis marked 'observed'), and the standard deviation of the fields (radial distance).
Thermocline. A region of the ocean column where the vertical temperature gradient is high. It separates a layer of warmer water (which is less dense) from a lower layer of colder water.
Thermodynamics. The science of the movement of heat. Usually concerned with calculations involving fluids.
Thermohaline. Pertaining to heat and salt. The term is usually applied to the deep ocean circulation which is driven by the heat and salt budgets of the ocean. An example of this is the creation of deep water in the North Atlantic where cold saline water, created when sea ice forms, sinks to the bottom. This water flows around the bottom of the ocean and surfaces again in regions of oceanic upwelling.
Timestep. The base unit of temporal resolution in a numerical model.
Transitivity. The phenomenon whereby a system (in this case the climate) evolves from an initial state to another, different, state and stays there.
Transmissivity. The fraction of the radiation, incident upon a body, which passes through it.
Troposphere. Lowest region of the atmosphere (Figure B.2b). In the troposphere, air is well mixed and temperature decreases with height. Clouds and weather systems are confined below its upper boundary, the tropopause, at a global average height of about 10 km.
Truncation. When a function, which is currently represented as a summation of many terms, is reduced in length and complexity by removing a number of small terms.
UNEP. The United Nations Environment Programme.
Validation. The process of determining the truth of a statement or calculation.
Variance. A measure of the spread of a set of results (about a mean). Used in climate modelling as a measure of the variability of the model climate.
Vorticity. The vorticity of a body is twice its angular velocity about the vertical. The Coriolis parameter $f = 2\Omega\sin\phi$ is the vorticity of the Earth. The absolute vorticity is the vorticity of the body plus the vorticity of the Earth at latitude ϕ. The potential vorticity of an air column is the absolute vorticity divided by the height of the column. Potential vorticity is always conserved.
WCRP. The World Climate Research Programme.
Weak Sun–warm early Earth paradox. It is known that the solar constant was 20–30 per cent lower in the Earth's early history. Despite this, the surface temperature has never been as low as would be expected from simple calculations. It is possible that the larger amounts of CO_2 or other greenhouse gases in the early atmos-

phere and different cloud and surface characteristics may have compensated for the lower solar luminosity.

WGNE. The World Climate Research Programme's Working Group on Numerical Experimentation.

Working Groups. The operating components of the IPCC assessments. The responsibility of these groups has changed and continues to change between assessments but the general discipline or theme basis remains as: I, science; II, impacts; III, social, economic and technological responses.

w.r.t. With respect to.

Zenith angle. The angular distance between a point in the sky and the zenith (directly above an observer, usually at the Earth's surface). It is the complement of the elevation angle (*q.v.*).

Appendix C About the Primer CD

The CD that accompanies this book is designed to complement the book. As explained throughout the text, developments in climate modelling are closely coupled to the development of computer technology. Since 1995, when the CD for the second edition was created, the Internet has grown substantially. Climate modellers now routinely share models and model results over the Internet, as well as sharing ideas via discussion groups and web pages. In this edition, we have expanded the list of visualizations and models from that in the second edition, included the figures from the book in a form suitable for lectures or presentations and added a collection of web links to get the reader started on finding out more about climate modelling. We do not claim that the lists are definitive or exhaustive, but we hope they are representative of the material you can find 'out there'.

To access the material on the CD, insert the disk in your CD drive, open the CD and double click on the file index.htm in the top level of the CD. Many of the links on the CD require an active Internet connection and these links are indicated. Links to material not included on the CD will open in a separate window.

The CD has been tested on a range of browsers, but there may be some aspects that do not transfer between browsers. Your experience with the CD will depend on your browser choice, your local browser settings and the software available on your computer. We have found the CD is best viewed with Netscape 7.0 or Internet Explorer 6.0 (or better) on 'Wintel' PC systems, or Safari 1.0.2, Mozilla (tested with 1.8) or Internet Explorer 5.2 (or better) on Macintosh systems. The CD is not compatible with Netscape 4.X.

A Climate Modelling Primer, Third Edition. K. McGuffie and A. Henderson-Sellers.
 ISBN: 0-470-85750-1 (HB); 0-470-85751-X (PB)

Index

A Climate Modelling Primer, Third Edition. K. McGuffie and A. Henderson-Sellers.

ISBN: 0-470-85750-1 (HB); 0-470-85751-X (PB)